TRIGA Reactor Facility

Nuclear Engineering Teaching Laboratory

The University of Texas at Austin

Submitted November 1984

Safety Analysis Report

Table of Contents

List of Tables

List of Figures

ADDENDUM

Chapter 1

INTRODUCTION AND SUMMARY

This report describes the TRIGA* reactor and the University of Texas facility, and provides a safety evaluation which shows that the reactor or facility does not cause undue risk to the health and safety of the public. A TRIGA type reactor was first operated in 1963 on the main campus of The University of Texas at Austin. Subsequent operation experience included safe operation of the facility at steady state thermal power levels of 10 kW and 250 kW, and pulse powers of 250 MW. Safe operation of a TRIGA reactor at the Balcones Research Center of the University of Texas is expected for steady state power levels of 1.0 MW and pulse powers of 1400 MW.

Some values used in this report represent the latest design parameters, or maximum values as a means of evaluating the safety of the system. For this reason, these values may differ from those quoted in other documents or from those that will be measured in the operating reactor system. Safety analysis demonstrates safe operation at power levels as high as 1.5 MW steady state and 8400 MW peak pulse power.

1.1 PRINCIPAL DESIGN CRITERIA

The reactor will be operated in two modes: steady state and pulsing. Reactor power levels in the steady state mode will range up to and include 1 MW(t). Pulsed mode operation will take place by step reactivity insertions with the reactor initially at a power level less than 1 kW. The maximum step reactivity insertion will be 2.1% $\delta k/k$ ($3.00) which will produce a peak reactor power of approximately 1400 MW(t) with a prompt energy release of about 18 MW-sec. A summary of principal design parameters for the reactor is given in Table 1-1.

1. DESIGN HIGHLIGHTS

The reactor will be located in a reactor pool structure. Reactor cooling will be provided by natural circulation of pool water which is cooled and purified in external coolant circuits. Reactor experiment facilities will include a rotary specimen rack, a pneumatic transfer system, core irradiation tubes, and horizontal and vertical beam tubes.

*Manufactured by GA Technologies Inc.

Table 1-1

PRINCIPAL DESIGN PARAMETERS

Reactor type	TRIGA Mark II
Steady state power (maximum)	1 MW
Pulse power (maximum)	2.1% δk/k ($3.00)
Fuel element design	
Fuel-moderator material	U-ZrH(a)
Uranium content	8.5 wt %
Uranium enrichment	19.7% U-235
Shape	Cylindrical
Length of fuel	38 cm (15 in.) overall
Diameter of fuel	3.63 cm (1.43 in.) o.d.
Cladding material	304 stainless steel
Cladding thickness	0.051 cm (0.020 in.)
Number of fuel elements	
Critical core	~64
Operational core	~90
Excess reactivity, maximum	4.9% δk/k
Number of control rods	4
transient	1
safety, shim (fuel followed)	2
regulating (fuel followed)	1
Total reactivity worth of rods	8.7% δk/k
Reactor cooling	Natural convection of pool water

(a) The nominal d/Zr ratio is 1.60, and the maximum value is 1.65.

The inherent safety of this TRIGA reactor has been demonstrated by the extensive experience acquired from similar TRIGA systems throughout the world. Forty-eight TRIGA reactors are now in operation throughout the world and of these 31 are pulsing. TRIGA reactors have more than 450 reactor years of operating experience, over 30,000 pulses, and more than 15,000 fuel element years of operation. The safety arises from a large, prompt negative temperature coefficient that is characteristic of uranium zirconium hydride fuel-moderator elements used in TRIGA systems. As the fuel temperature increases, this coefficient immediately compensates for reactivity insertions. The result is that reactor power excursions are terminated quickly and safely.

The prompt shutdown mechanism has been demonstrated extensively in many thousands of transient tests performed on two prototype TRIGA reactors at the GA Technologies laboratory in San Diego, California, as well as other pulsing TRIGA reactors in operation. These tests included step reactivity insertions as large as 3.5% $\delta k/k$ with resulting peak reactor powers up to 8400 MW(t) on TRIGA cores containing similar fuel elements as are used in this TRIGA reactor.

Because the reactor fuel is similar, the previously cited experience and tests apply to this TRIGA system. As a result it has been possible to use accepted safety analysis techniques applied to other TRIGA facilities to update evaluations with regard to the characteristics of this facility [1-6].

1.3 CONCLUSIONS

Past experience has shown that TRIGA systems can be designed, constructed, and safely operated in the steady state and pulsing modes of operation. This history of safety and the conservative design of the reactor have permitted TRIGA systems to be sited in urban areas using buildings without pressure type containment such as is normally associated with reactors of like power levels.

Results of this safety analysis indicate that the TRIGA Mark II reactor system proposed for construction and operation will pose no health or safety problem to the public when operated in either normal or abnormal conditions.

Abnormal or accident conditions considered in this analysis include:

a. A step insertion of reactivity with the reactor at low and high power levels,

b. Complete and instantaneous loss of coolant water in the reactor pool,

c. And fission product release from fuel element ruptured in air.

The insertion of excess reactivity may represent a normal reactor operating condition, while the loss of pool water is expected to be an abnormal condition. Conservative estimates of doses from fission product releases are made independent of accident scenarios.

In both these postulated conditions, fuel and clad temperatures remain at levels below those required to generate stress conditions which would cause loss of clad integrity. However, the results of a clad failure are analyzed and it is shown that such a failure will not cause excessive radiation exposures.

The loss of pool water has been examined from the standpoint of direct radiation to operating personnel as well as in terms of maintaining fuel integrity.

The effects of argon-41 and nitrogen-16 production during normal operation of the reactor have also been evaluated. Results of these analyses show that production of these radioactive gases will present no hazard to persons in the reactor room or to the general public.

Chapter 1 References

1. "Hazards Report for TRIGA Mark II Pulsing Reactor", General Atomic Division Report GA-1998, February 1961.

2. "Hazards Summary Report for a TRIGA-I Nuclear Reactor", University of Texas Bureau of Engineering Research, October 1961.

3. "Safeguards Analysis Report for TRIGA Reactors using Aluminum-Clad Fuel", General Atomic Division Report GA-7860, March 1967.

4. "Safety Analysis Report for 250 Kilowatt Operation of a TRIGA Mark I Nuclear Reactor", University of Texas, College of Engineering August 1967.

5. "Safety Analysis Report for the TRIGA Mark II Reactor", E-117-478, General Atomic Company, October, 1975.

6. "TRIGA Mark I Safety Analysis Report", University of Texas, January 1981.

Chapter 2

SITE DESCRIPTION

The facility containing the TRIGA reactor will be situated on the east track of the Balcones Research Center [1], a tract of land owned and operated by The University of Texas. The Research Center is located in northern Travis County and the City of Austin about 11.6 kilometers north-northwest of The University of Texas at Austin campus. Figures 2-1 thru 2-4 display the facility locations in relation to surrounding areas. Located near the transition line between hill country and rolling plains, the site is situated about 7.4 kilometers from where the flood controlled Colorado river crosses the transition region and Balcones fault zone. The Balcones Research Center east and west tracts span part of the inactive fault zone. The east tract is within the transition region to rolling plains.

2.1 GENERAL LOCATION AND AREA

Major activities of The University of Texas at Austin, State of Texas government, and City of Austin business district are centered at respective distances of 11.6, 12.6, and 12.9 kilometers to the south-southwest. Distances to air traffic landing facilities in the area are 6.2 kilometers for private aircraft, 9.7 kilometers for commercial aircraft and 20.8 kilometers for military aircraft.

A total area of 1.87 square kilometers is contained within the Research Center east and west tracts of land. The east side of the Center is bounded by a State highway, FM 1325, and the west side is bounded by a Federal highway, US 183. The two tracts are divided by a rail line, formerly the Missouri-Pacific, with 0.93 square kilometers in the east tract and 0.94 square kilometers in the west tract of land. Highway intersections of US 183 with FM 1325 and with Loops 1 and 360 are within two kilometers of the site. Both highway loops are planned for extension into the area associated with the west tract of land [2]. The reactor facility is sited near the center of the northern half of the east tract. Distance from the reactor site to nearest rail line or highway is approximately 250 meters.

Most areas adjacent to the Research Center are developed for mixed commercial and industrial activities including warehouses, manufacturing facilities, small business parks and a few undeveloped areas. Mixed

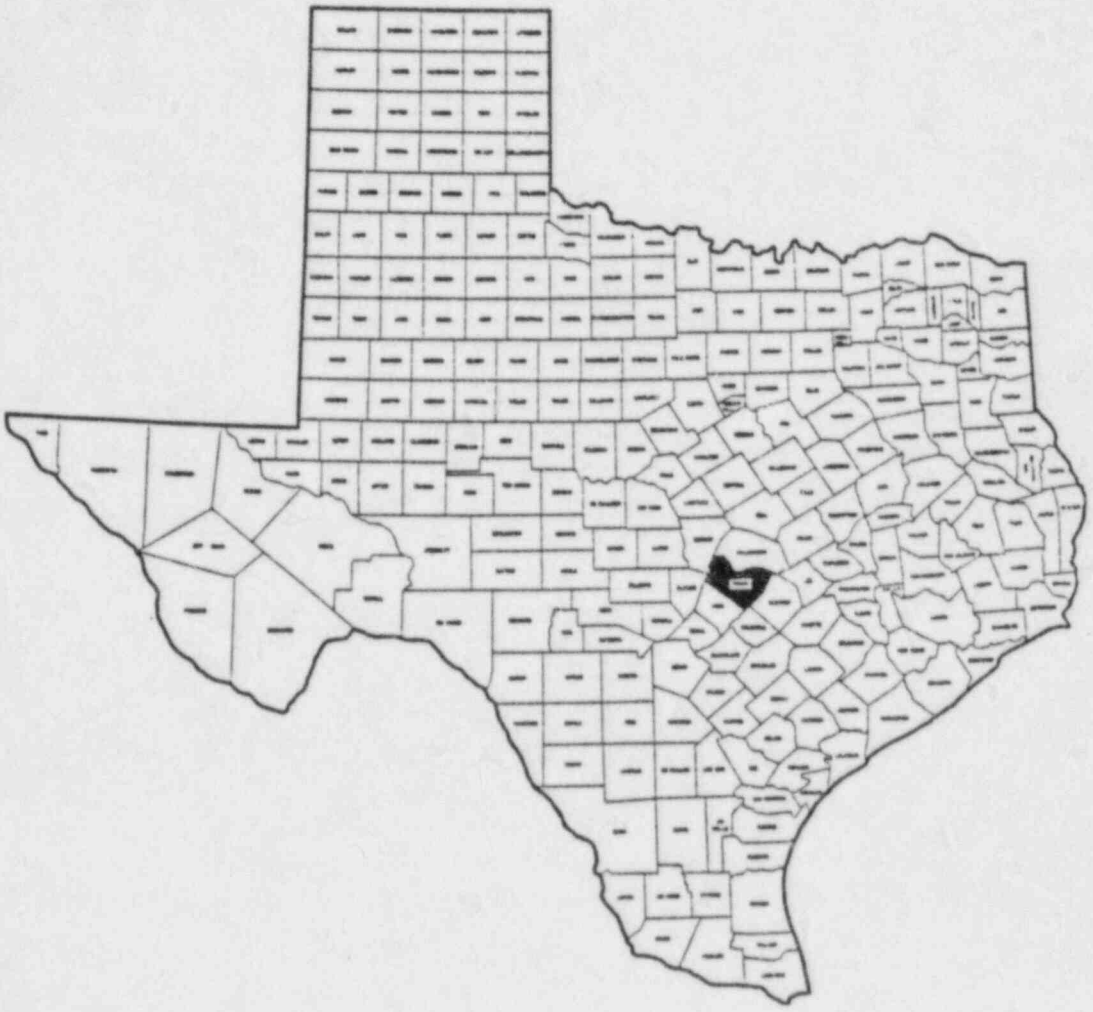

STATE OF TEXAS COUNTIES
Figure 2-1

TRAVIS COUNTY
Figure 2-2

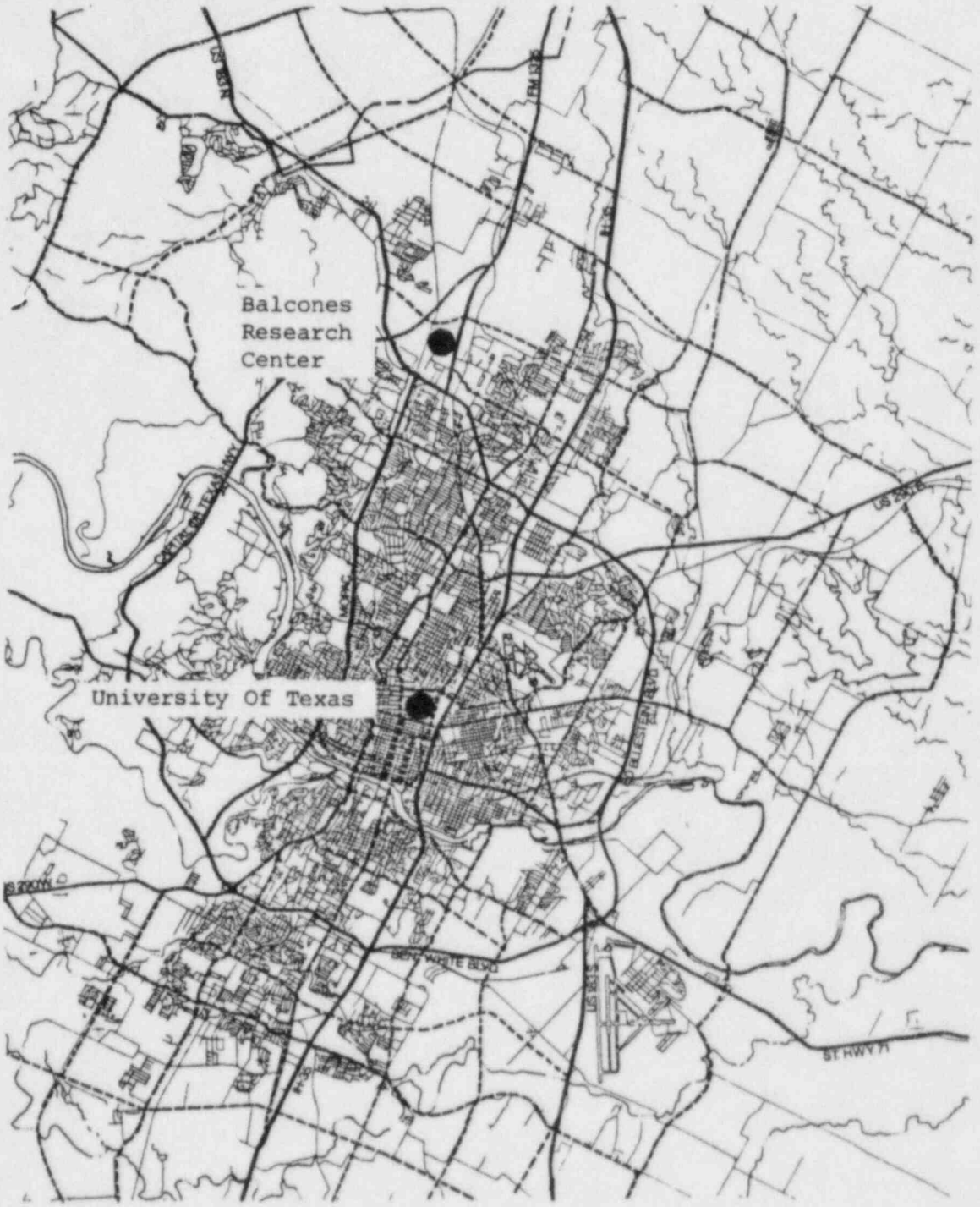

EXPRESSWAYS, FREEWAYS and MAJOR ARTERIALS

——— Expressways and Freeways
- - - - Major Arterials

CITY OF AUSTIN
Figure 2-3

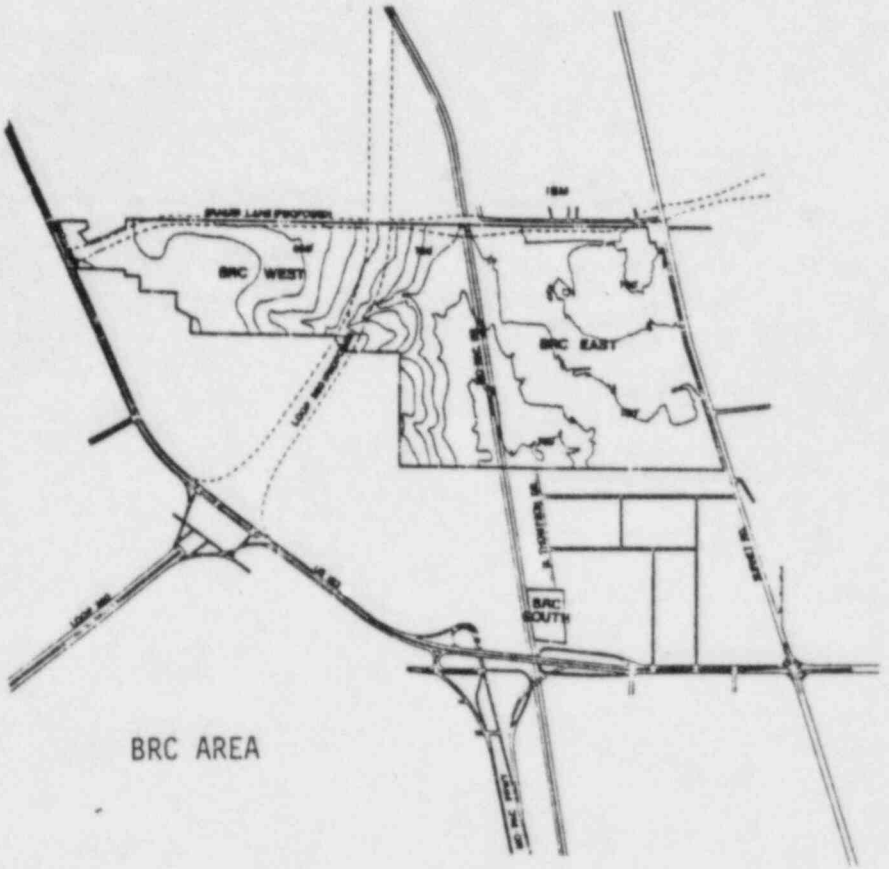

BRC AREA

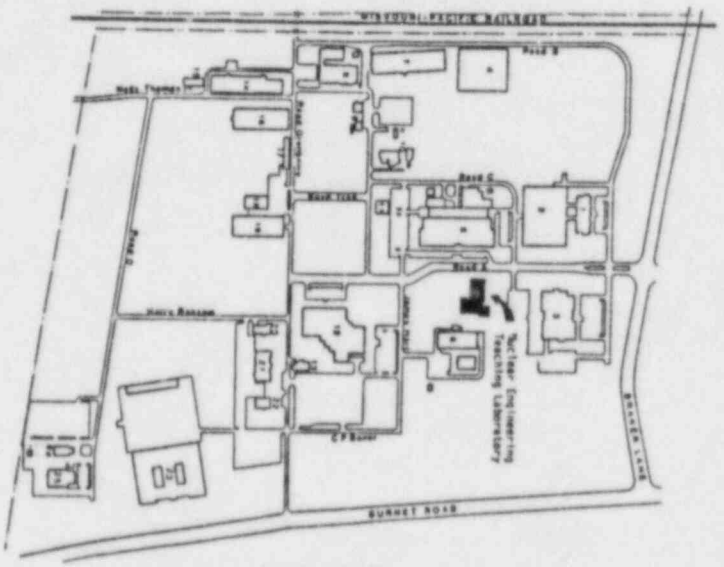

BRC EAST

BALCONES RESEARCH CENTER
Figure 2-4

commercial and industrial areas south and east of the Research Center are bounded by highway US 183, highway FM 1325, and the Texas New Orleans Railroad to the east. Approximately 2.2 square kilometers of land are enclosed by the area. Much of the remaining area to the west of the Research Center is bounded by highway US 183 and the Missouri Pacific Railroad and is not developed. The area is planned for future road right-of-ways and includes the west tract area. Immediately north of the Balcones Research Center east tract is a 2.3 square kilometer complex operated by International Business Machines Corporation. Undeveloped areas around the Research Center are expected to develop as a mixed commercial, industrial, research or office park areas. Residential areas are located beyond adjoining areas around the Balcones Research Center with distances from the reactor facility site of 1.2 kilometers to 2.0 kilometers. Few residential structures for either multifamily or single family units are located within a radius of 1.2 kilometers of the reactor site.

2.2 POPULATION AND EMPLOYMENT

Austin is composed primarily of governmental, business, and professional persons with their families. The city has substantial light industry but practically no heavy industry. Many of the persons in the local labor force are related to activities of the City and its role as a State Capitol or the University and its educational and research programs. Population growth of Travis county between the 1970 and 1980 census was 42%. The substantial growth of the "sun belt" areas, and Austin in particular, is expected to continue throughout the 1980's. Population data of the Travis county area is presented in Table 2-1 with supportive data in Figure 2-5 and Figure 2-6.

The 1980 population census listed the Austin city population at 345,496 and Travis county population at 419,573 with the Austin Standard Metropolitan Statistical Area population at 536,450 [3]. Three counties, Travis, Hays and Williamson, compose the Austin Standard Metropolitan Statistical Area. Population densities in Travis county range from 6.4 persons per 1000 square meters encompassing the main university campus to less than 12 persons per 100 square meters in growth areas north of the research center site. Population census tracts adjacent to the site exhibit densities of 1.2 to 2.0 persons per 1000 square meters.

Approximately 800 persons were involved in activities on the east tract of the Balcones Research Center in 1981 with projected activities at the site to add an estimated 900 to 1000 persons by the late 1980's. On the west tract the Microelectronics and Computer Technology Corporation is

Table 2-1
TRAVIS COUNTY
1980 POPULATION DENSITY DISTRIBUTION

Census Tracts	Acres In City	Acres Out of City	Acres Total	Total Population	Population Density
1.01	800	-	800	3,857	4.8
1.02	1,160	260	1,420	2,176	1.5
2.01	600	-	600	4,744	7.9
2.02	150	-	150	1,008	6.7
2.03	300	-	300	958	3.2
2.04	465	-	465	2,781	6.0
3.01	680	-	680	5,831	8.6
3.02	535	-	535	4,755	8.9
3.03	1,160	-	1,160	2,636	2.3
4.01	565	-	565	3,614	6.4
4.02	395	-	395	3,099	7.8
5.00	320	-	320	4,185	13.0
6.01	260	-	260	6,802	26.2
6.02	375	-	375	7,887	21.0
7.00	435	-	435	1,419	3.3
8.01	325	-	325	1,903	5.9
8.02	430	-	430	3,570	8.3
8.03	365	-	365	2,771	7.6
8.04	250	-	250	2,871	11.0
9.01	230	-	230	2,150	9.3
9.02	740	-	740	6,231	8.4
10.00	575	-	575	5,425	9.4
11.00	690	-	690	1,665	2.4
12.00	825	-	825	3,095	3.8
13.03	455	-	455	2,732	6.0
13.04	465	-	465	3,127	6.7
14.05	800	-	800	6,489	8.1
15.06	780	-	780	6,105	7.8
14.00	870	-	870	5,949	6.8
15.01	860	-	860	5,362	6.2
15.03	880	-	880	3,775	4.3
15.04	660	-	660	4,665	7.1
15.05	550	-	550	4,326	7.9
16.02	740	-	740	3,711	5.0
16.03	650	-	650	3,995	6.1
16.04	870	-	870	3,802	4.4
16.05	520	-	520	3,573	6.9
16.06	140	-	140	911	6.5
17.03	520	1,410	1,930	4,493	2.3
17.04	630	-	630	4,817	7.6
17.05	580	745	1,325	2,789	2.1
17.06	560	15	575	2,375	4.1
17.07	730	-	730	3,899	5.3
17.08	2,170	1,485	3,655	4,586	1.3
17.09	3,700	3,170	6,870	4,148	.6
17.10	430	10,585	11,015	4,077	.4
17.11	1,730	124,400	126,130	5,080	.4
17.12	580	-	580	3,583	6.2
17.13	650	-	650	3,890	6.0
17.14	1,230	2,975	4,205	6,981	1.7
17.15	1,250	18,230	19,480	6,262	.3
17.16	-	61,345	61,345	5,028	.1
17.17	290	54,932	55,222	5,404	.1
18.04	580	-	580	4,695	8.1
18.05	390	-	390	3,335	8.6
18.06	500	-	500	2,874	5.7
Census Tracts	Acres In City	Acres Out of City	Acres Total	Total Population	Population Density
18.07	720	-	720	5,656	7.9
18.08	1,130	-	1,130	7,527	6.7
18.09	610	415	1,025	2,996	2.9
18.10	1,560	10,560	12,120	8,024	.7
18.11	370	-	370	2,274	6.1
18.12	580	-	580	2,450	4.2
18.13	920	-	920	2,813	3.1
18.14	480	715	1,195	6,184	5.2
18.15	590	3,950	4,540	4,235	.9
18.16	100	90,930	91,030	4,998	.1
18.17	620	-	620	3,824	6.2
18.18	640	-	640	5,086	7.9
19.01	780	230	1,010	4,791	4.7
19.02	30	12,760	12,790	2,856	.2
19.03	2,650	7,100	9,750	4,483	.4
19.04	80	3,065	3,145	4,038	1.4
20.01	620	-	620	3,295	4.5
20.02	395	-	395	2,723	6.3
20.03	500	-	500	2,383	5.4
21.03	950	-	950	7,391	7.8
21.04	290	-	290	3,198	11.0
21.05	480	-	480	2,940	6.1
21.06	420	-	420	3,202	7.6
21.07	765	-	765	4,119	5.4
21.08	860	-	860	1,903	2.2
21.09	720	-	720	4,014	5.6
21.10	910	-	910	3,338	3.7
21.11	1,690	-	1,690	4,184	2.5
22.01	470	810	1,280	1,057	.8
22.02	760	2,400	3,160	1,716	.5
22.03	4,320	58,870	65,190	5,160	.1
22.04	410	-	410	1,228	3.0
23.03	110	4,460	4,570	3,680	.8
23.04	385	-	385	4,002	11.0
23.05	300	-	300	5,794	19.3
23.06	1,230	-	1,230	1,003	.8
23.07	540	-	540	3,234	6.0
23.08	805	-	805	3,664	4.6
23.09	2,320	-	2,320	7,130	3.1
23.10	285	3,870	4,155	2,317	.6
24.01	640	-	640	4,786	7.5
24.02	930	-	930	4,593	4.9
24.03	630	-	630	2,583	4.1
24.04	1,060	600	1,660	7,517	4.5
24.05	1,021	1,810	2,831	4,499	1.6
24.06	935	3,380	4,315	7,039	1.6
24.07	-	3,540	3,540	1,782	.5
24.08	1,240	79,610	80,850	9,144	.1
Total In County	79,253	568,427	647,680	418,573	.6
Total In City	79,253	-	-	345,496	4.4

Source: Population figures were taken from the 1980 Census of Population and Housing. Acreage by census tract was compiled by the City of Austin Planning Department.

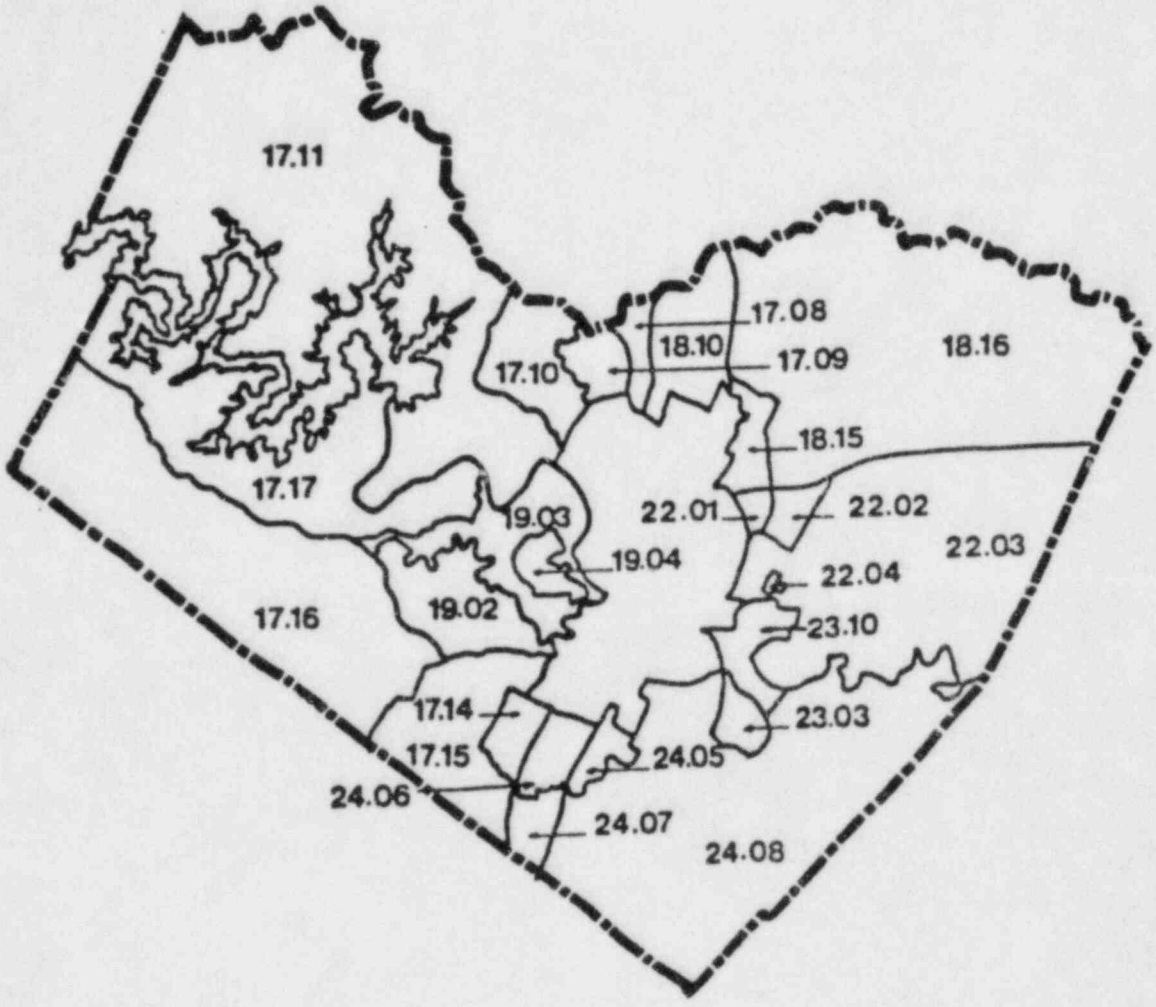

TRAVIS COUNTY 1980 CENSUS TRACT BOUNDARIES
Figure 2-5

CITY OF AUSTIN CENSUS TRACT BOUNDARIES
Figure 2-6

expected to employ 1000 persons by 1985. Facilities north of the Research Center operated by International Business Machines Corporation are expected to employ 6500 persons in 1985.

Research activities at the Balcones Research Center are diverse, consisting of many different research organizations of the university science and engineering colleges. Research organizations located adjacent to the site for the TRIGA reactor are the Center for Energy Studies, Center for Electromechanics, Bureau of Economic Geology and Water Resources Center.

2.3 CLIMATOLOGY

Austin, capital of Texas, is located on the Colorado River where the stream crosses the Balcones Escarpment separating the Texas Hill Country from the Blackland Prairies to the east. Elevations within the City vary from 120 meters to 275 meters above sea level. Native trees include cedar, oak, walnut, mesquite, and pecan.

The climate [4] of Austin is humid subtropical with hot summers. Winters are mild, with below freezing temperatures occurring on an average of less than twenty-five days each year. Rather strong northerly winds, accompanied by sharp drops in temperature, occasionally occur during the winter months in connection with cold fronts, but cold periods are usually of short duration, rarely lasting more than two days. Daytime temperatures in summer are hot, but summer nights are usually pleasant with average daily minima in the low seventies.

Precipitation is fairly evenly distributed throughout the year, with heaviest amounts occurring in late spring. A secondary rainfall peak occurs in September. Precipitation from April through September usually results from thundershowers, with fairly large amounts falling within short periods of time. While thunderstorms and heavy rains have occurred in all months of the year, most of the winter precipitation occurs as light rain. Snow is insignificant as a source of moisture, and usually melts as rapidly as it falls. The City may experience several seasons in succession with no measurable rain fall.

Prevailing winds are southerly throughout the year. Northerly winds accompanying the colder air masses in winter soon shift to southerly as these air masses move out over the Gulf of Mexico.

Climatology data is summarized in Figure 2-7. Typical Austin wind data are presented in Figure 2-8 [5].

CLIMATOLOGICAL DATA

TEMPERATURE (DEGREES FAHRENHEIT)

TEMPERATURE EXTREMES: HIGH 109
LOW -2

SOLAR PATH DIAGRAM

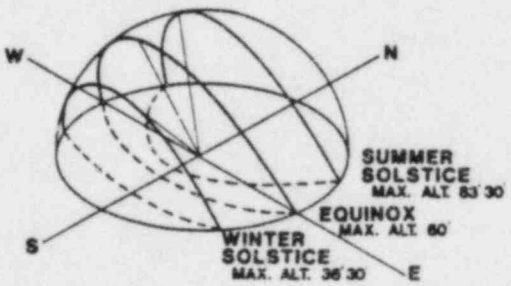

HUMIDITY (AVG. % RELATIVE)

MIDNIGHT: 76
6 A.M.: 84
NOON: 56
6 P.M.: 53

PREVAILING WINDS

SOUTHERLY
AVERAGING 9 MPH

SUNSHINE (% POSSIBLE)

AVERAGE ANNUAL: 61

PRECIPITATION (INCHES)

AVERAGE ANNUAL: 38.1
24 HOUR EXTREME: 19.03

AUSTIN CLIMATOLOGY DATA
Figure 2-7

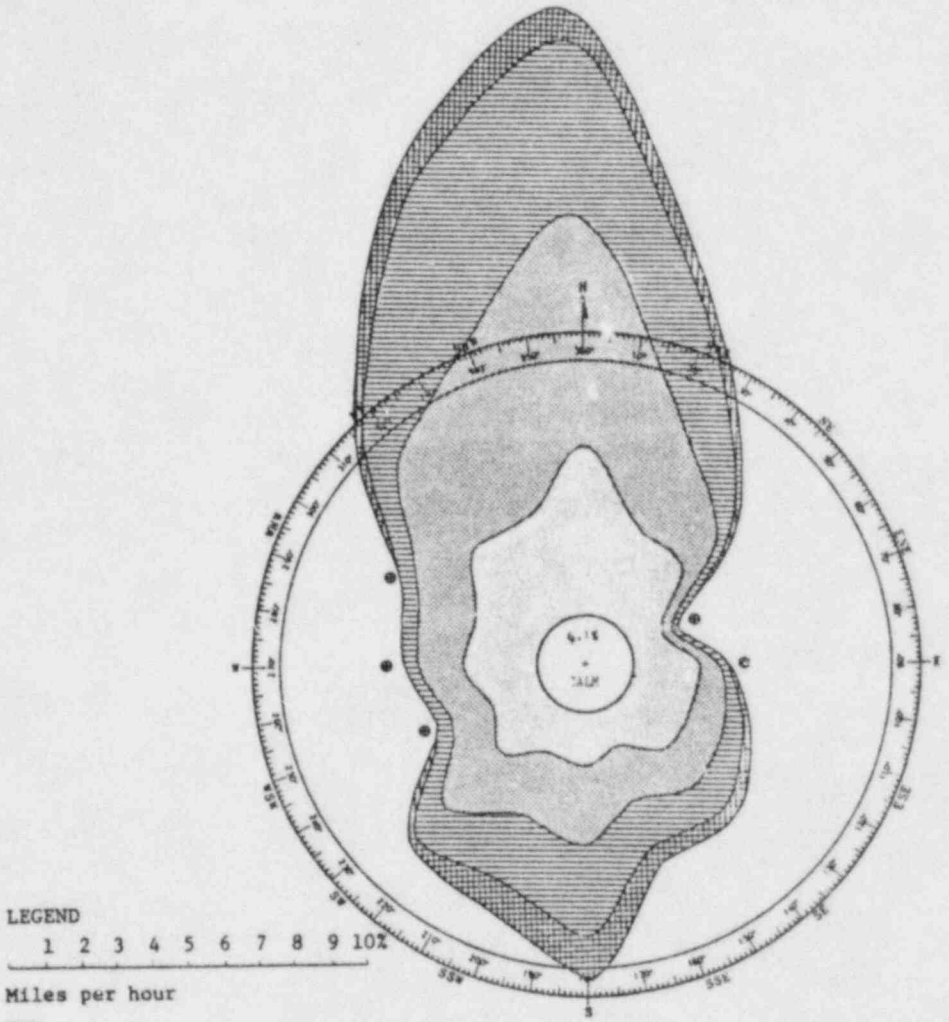

AUSTIN WIND ROSE DATA
Figure 2-8

The average length of the warm season (freeze-free period) is 270 days. Based on data from 1943-1961, the average date of the last occurrence of freezing or below has occurred as late as April 13 (1940), and as early as October 26 (1924). Meteorological data is tabulated in Table 2-2 and Table 2-3 [4].

Destructive winds and damaging hailstorms are infrequent. On rare occasions, dissipating tropical storms effect the City with strong winds and heavy rains. The frequency of tornado type activity is illustrated in Figure 2-9 [6]. Recent tropic storm paths and local sitings of tornadoes and funnel clouds are presented in Figure 2-10 and Figure 2-11 [7,8].

2.4 GEOLOGY

The northwestern half of Travis county is part of the physiographic province of Texas known as the Edwards Plateau. In Travis County, this is a highly dissected plateau with wooden hills rising in some places more than 150 meters above the drainageways. In marked contrast, the southeastern half of the county is gently rolling prairie land which is part of the physiographic province known as the Gulf Coastal Plain. These provinces are separated by the scarp of the Balcones fault zone, which rises 30 to 90 meters above the Coastal Plain. The scarp, however, is not a vertical cliff; it is an indented line of sloping hills leading up from the lower plain to the plateau summit.

The rocks that outcrop in Travis County are primarily of sedimentary origin and of Mesozoic (Cretaceous) and Cenozoic age. They consist largely of limestone, clay, and sand strata which dip southeastward toward the Gulf of Mexico at an angle slightly greater than the slope of the land surface. Therefore, in going from southeast to northwest the outcrops of progressively older formations are encountered, and the rocks lowest in the geologic column have the highest topographic exposure.

At the reactor facility site on the east tract, the geology is of the Austin Group defined as chalk, marly limestone, and limestone with light gray, soft to hard, thin to thick bed, and massive to slightly nodular character. On the west tract, the geology changes to the Edwards Formation of limestone and dolomite with light gray to tan, hard to soft, thin to thick bed, and fine to medium grain character. The separate formations are, respectively, the up and down side of a segment of the Mount Bonnell Fault that passes approximately along the boundary of the east and west Balcones Research Center tracts. Distance to the fault is about 500 meters from the reactor facility site.

Table 2-2
1982 METEOROLOGICAL DATA
FOR AUSTIN TEXAS

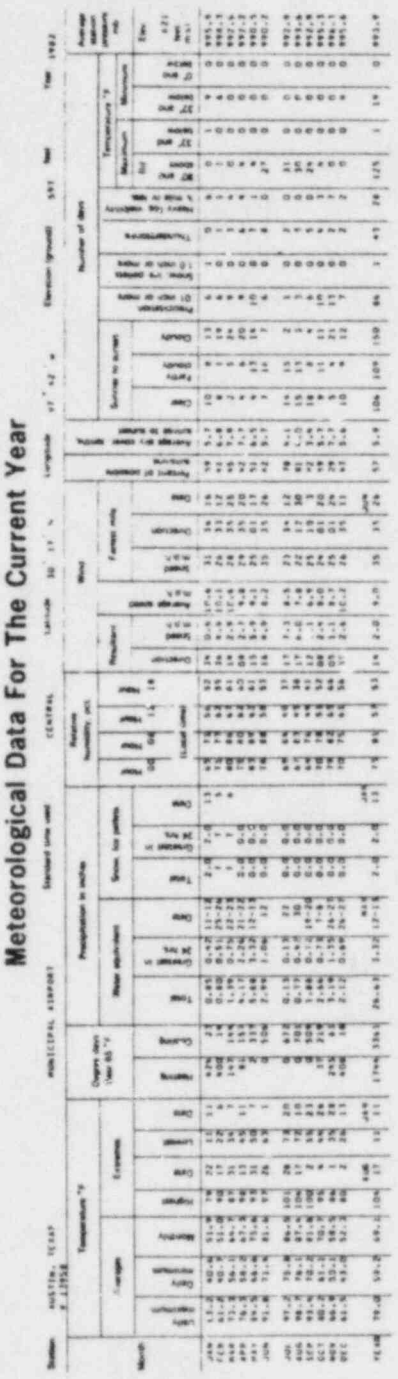

Table 2-3
HISTORICAL METEOROLOGICAL DATA
FOR AUSTIN TEXAS

Average Temperature

Year	Jan	Feb	Mar	Apr	May	June	July	Aug	Sept	Oct	Nov	Dec	Annual
1943	49.4	57.6	51.9	70.4	76.0	81.1	83.4	85.4	76.9	68.3	56.7	49.2	67.5
1944	48.4	55.9	58.6	67.6	71.8	81.0	84.4	84.9	77.6	69.1	59.8	48.0	67.2
1945	50.8	54.8	65.8	66.0	74.3	81.4	83.7	83.6	78.8	67.5	63.2	49.8	68.2
1946	48.6	55.0	62.3	69.8	74.6	79.1	87.2	83.8	76.8	70.8	59.1	54.9	68.2
1947	48.0	47.0	54.6	69.1	74.0	82.7	84.7	83.1	79.7	76.2	56.4	52.8	67.1
1948	43.2	50.7	58.0	71.6	76.2	81.1	84.4	85.8	78.4	69.9	58.2	55.4	69.0
1949	45.1	54.7	60.5	63.9	77.6	81.0	83.9	82.5	78.4	68.6	62.6	54.2	69.0
1950	55.7	56.4	59.1	64.7	76.2	81.3	83.9	83.4	78.5	73.6	59.9	52.7	68.8
1951	50.8	54.4	61.8	67.4	74.9	81.4	86.9	87.6	79.2	71.6	56.9	54.0	68.9
1952	59.1	58.1	58.8	64.3	72.8	81.4	83.5	87.1	77.9	65.5	57.3	50.4	69.2
1953	56.2	53.5	66.1	66.4	74.8	84.9	85.1	84.3	79.5	70.9	57.2	48.5	66.9
1954	52.0	59.5	59.4	72.4	73.4	83.5	86.9	86.6	82.4	72.9	59.9	56.5	70.4
1955	51.6	57.8	62.4	72.9	78.0	77.2	84.9	84.5	82.7	71.9	59.2	52.5	69.4
1956	57.8	55.8	61.8	69.1	78.7	84.4	87.0	85.9	81.7	73.7	57.3	56.6	70.2
1957	50.5	60.9	59.5	66.0	73.5	80.9	86.3	86.0	77.0	65.3	55.9	56.1	68.2
1958	48.7	48.8	59.6	66.3	76.0	83.7	85.1	85.8	79.5	67.5	60.7	48.5	67.0
1959	47.7	52.9	59.9	65.1	77.1	82.6	84.2	83.5	80.1	69.5	52.2	53.7	67.8
1960	49.3	47.9	56.3	69.7	77.5	82.9	84.7	83.1	79.3	71.5	60.7	48.5	67.2
#1961	47.7	54.8	63.7	67.9	76.2	77.6	81.4	81.8	78.2	69.8	56.5	52.2	67.3
1962	45.5	63.4	57.9	67.7	76.6	80.3	85.9	86.8	79.7	73.7	59.6	51.0	68.7
1963	47.6	51.6	64.5	72.9	76.9	82.9	84.9	87.5	82.0	75.1	62.6	45.1	69.1
1964	50.3	48.4	60.7	70.8	76.6	81.7	85.7	86.0	79.9	67.6	62.5	57.2	68.5
1965	53.4	49.4	51.4	73.4	76.7	82.7	84.7	84.3	80.5	66.6	69.1	56.0	68.2
1966	45.3	48.9	60.3	69.1	73.9	79.9	86.7	82.2	78.2	69.6	64.2	51.0	67.2
1967	52.9	51.4	61.3	75.9	77.3	83.3	85.7	82.6	75.2	67.7	59.9	49.4	68.6
1968	47.6	47.2	57.3	68.1	74.2	79.6	82.7	84.1	76.0	72.0	55.9	50.4	66.2
1969	53.6	52.6	[illegible]	69.0	75.1	81.7	86.7	84.9	78.7	68.6	57.9	53.6	67.9
1970	44.0	53.1	59.2	68.7	71.9	79.9	83.9	85.8	78.2	64.7	57.4	58.7	67.1
1971	54.6	54.9	62.1	68.2	76.2	83.7	85.9	81.2	79.1	72.2	60.5	56.4	69.6
1972	53.0	55.7	66.1	73.5	77.5	81.7	83.3	83.1	82.9	70.9	52.8	48.3	68.5
1973	45.8	50.3	63.7	63.1	73.7	79.6	82.8	82.5	79.1	73.1	65.1	52.4	67.4
1974	49.0	56.3	66.5	68.9	77.7	81.1	84.9	81.3	72.3	69.5	56.9	50.7	67.8
1975	53.4	52.2	59.7	67.8	73.7	79.9	82.7	82.4	75.8	70.7	60.4	52.9	67.5
1976	49.5	61.7	67.0	66.0	70.7	79.8	80.7	83.4	78.1	61.7	51.6	48.5	66.7
1977	43.6	54.2	61.3	67.0	75.3	82.2	85.1	86.4	83.4	71.6	61.7	53.6	68.7
1978	40.7	45.0	59.3	69.9	77.3	83.3	86.4	84.8	79.5	69.8	60.6	49.7	67.0
1979	40.4	48.5	61.1	67.0	71.5	79.8	83.1	82.5	77.6	73.5	54.5	53.0	66.2
1980	51.7	52.9	61.4	66.7	75.1	84.6	87.9	86.0	81.7	68.4	57.5	53.7	68.9
1981	50.6	53.6	54.1	69.6	74.6	81.4	84.9	85.5	79.7	72.2	63.7	53.7	69.3
1982	51.9	51.0	[illegible]	67.3	75.6	81.6	86.9	87.4	81.8	70.7	58.9	52.1	69.1
RECORD MEAN	50.0	53.4	60.6	68.0	74.7	81.5	84.2	84.3	79.1	69.9	59.2	51.8	68.1
MAX	69.3	64.1	71.6	78.4	84.7	91.6	94.7	95.1	89.4	85.9	69.6	62.0	79.6
MIN	39.7	42.6	49.4	57.5	64.7	71.4	73.6	73.9	68.7	58.7	48.5	41.5	57.5

Heating Degree Days

AUSTIN, TX

Season	July	Aug	Sept	Oct	Nov	Dec	Jan	Feb	Mar	Apr	May	June	Total
1962-63	0	0	0	20	172	429	657	774	[illegible]	27	4	0	1797
1963-64	0	0	0	0	137	610	451	475	154	20	0	0	1847
1964-65	0	0	0	17	158	415	332	451	367	12	0	0	1770
1965-66	0	0	2	58	76	388	611	449	169	29	11	0	1687
1966-67	0	0	0	31	129	453	446	380	77	0	2	0	1498
1967-68	0	0	7	41	192	471	538	410	265	37	1	0	2068
1968-69	0	0	0	7	294	446	368	365	396	6	1	0	1813
1969-70	0	0	0	49	253	339	[illegible]	130	309	47	10	9	2010
1970-71	0	0	1	75	240	231	326	300	171	52	0	0	1400
1971-72	0	0	1	7	184	271	434	298	66	4	0	0	1262
1972-73	0	0	0	46	375	513	586	405	72	129	1	0	2128
1973-74	0	0	0	9	83	387	496	756	108	36	0	0	1776
1974-75	0	0	5	11	271	441	377	156	239	53	0	0	1719
1975-76	0	0	1	27	204	404	476	158	173	19	1	0	1465
1976-77	0	0	0	170	402	506	719	308	148	20	0	0	2273
1977-78	0	0	0	16	136	354	750	561	225	15	7	0	2064
1978-79	0	3	0	5	186	475	754	465	144	17	10	0	2071
1979-80	0	0	0	16	278	372	425	357	168	47	0	0	1663
1980-81	0	0	1	69	262	361	443	360	172	6	0	0	1677
1981-82	0	0	0	44	86	364	424	400	147	61	2	0	1533
1982-83	0	0	0	37	245	454							

Cooling Degree Days

Year	Jan	Feb	Mar	Apr	May	June	July	Aug	Sept	Oct	Nov	Dec	Total
1969	25	5	8	137	276	474	[illegible]	629	450	386	76	1	2891
1970	6	1	10	165	235	451	589	[illegible]	439	[illegible]	22	43	2744
1971	14	20	46	157	355	577	656	711	436	227	53	13	3100
1972	6	16	111	269	272	519	597	571	529	118	16	3	3107
1973	1	0	36	79	277	407	557	557	467	205	43	4	2653
1974	6	21	140	158	398	467	676	717	329	157	38	6	2751
1975	21	0	47	141	277	454	536	552	429	167	72	22	2436
1976	0	57	85	119	186	457	479	577	401	61	7	0	2418
1977	0	7	18	90	324	527	629	681	572	227	[illegible]	7	3161
1978	5	6	31	167	396	529	[illegible]	621	427	161	60	7	3077
1979	2	7	29	107	216	449	570	569	365	285	29	8	2531
1980	5	11	62	128	322	594	716	659	510	182	55	19	[illegible]
1981	2	23	27	237	304	501	527	641	456	272	54	5	3129
1982	23	19	144	157	317	506	672	701	509	219	61	18	3361

Precipitation

Year	Jan	Feb	Mar	Apr	May	June	July	Aug	Sept	Oct	Nov	Dec	Annual
1943	0.80	0.45	2.58	2.67	5.38	1.27	3.91	0.92	3.31	0.33	1.73	1.42	24.76
1944	5.47	3.89	1.83	0.33	9.23	2.01	0.37	4.47	4.66	0.35	4.55	5.91	47.97
1945	2.83	3.94	4.98	4.11	1.76	5.69	1.61	5.78	2.76	3.00	1.47	2.96	40.87
1946	3.76	2.29	2.77	7.92	6.13	1.34	1.48	1.36	6.00	1.42	7.91	2.71	47.28
1947	3.62	0.43	1.28	7.24	3.55	0.11	2.18	2.12	5.07	0.07	2.07	1.89	31.58
1948	0.97	2.71	1.38	1.69	4.49	1.25	2.29	0.27	1.29	1.78	1.28	1.67	20.98
1949	3.97	2.35	2.24	4.93	3.83	7.57	1.99	2.37	3.77	4.38	0.01	4.09	36.36
1950	0.74	3.79	0.80	7.58	4.19	1.99	0.77	0.59	4.77	0.59	0.03	T	25.79
1951	0.61	2.96	3.73	1.09	3.51	6.19	0.19	2.07	6.45	0.93	1.08	0.34	28.98
1952	0.25	1.77	2.25	5.08	4.06	1.88	0.69	0.00	3.28	T	5.36	3.15	27.71
1953	0.63	1.32	1.73	4.69	1.88	3.59	0.51	2.10	2.98	6.58	0.38	5.29	29.68
1954	1.01	0.29	0.27	1.66	2.86	0.68	0.89	1.15	0.82	0.89	0.35	0.61	11.42
1955	1.87	4.27	0.83	0.75	4.49	2.61	2.02	1.92	1.33	0.09	1.40	1.01	22.56
1956	1.65	1.74	2.26	0.56	3.12	0.99	0.11	1.21	0.09	0.89	2.13	2.76	15.91
1957	0.55	3.14	4.58	9.93	7.38	5.25	1.10	T	6.43	8.79	2.95	1.20	51.30
1958	3.09	6.39	2.55	4.24	3.67	2.89	3.42	0.68	6.89	5.18	0.37	1.15	41.02
1959	0.42	2.37	0.23	4.35	1.66	3.10	1.69	4.80	4.37	5.99	1.95	2.11	34.96
1960	1.07	2.36	1.27	1.01	0.81	4.26	2.41	2.60	1.68	12.31	1.90	4.08	35.82
1961	1.27	4.89	0.67	0.10	1.03	11.47	[illegible]	0.40	3.68	0.91	2.87	0.91	36.47
1962	0.56	0.63	1.19	4.04	1.06	8.21	0.00	4.58	4.75	4.07	0.92	3.47	33.48
1963	0.59	2.81	0.22	3.53	1.32	2.10	0.54	0.88	1.50	0.78	1.37	1.42	17.30
1964	2.57	1.87	1.95	1.47	1.87	7.56	5.69	2.09	6.29	2.79	2.45	0.88	32.47
1965	4.09	5.06	1.30	1.91	9.98	0.89	0.27	1.32	5.46	1.24	2.65	4.28	47.57
1966	1.58	3.23	0.30	3.74	3.13	1.51	0.47	6.21	1.22	0.60	0.11	0.87	25.19
1967	0.29	1.52	1.09	4.44	3.35	*	1.19	3.71	[illegible]	4.55	4.36	3.41	33.54
1968	7.94	1.64	2.09	1.67	8.75	3.10	3.11	0.74	3.42	0.60	4.91	0.55	38.72
1969	0.40	4.19	3.26	5.04	3.25	2.46	0.17	5.78	1.17	2.65	0.79	4.29	33.59
1970	1.61	5.77	2.97	1.36	6.18	5.29	0.66	1.03	3.82	5.27	T	0.11	35.64
1971	0.64	0.69	0.79	1.07	1.37	1.68	1.27	5.69	2.13	3.02	3.02	4.22	24.95
1972	1.88	0.31	*	1.96	7.88	2.27	2.55	2.51	1.55	2.96	2.47	0.53	25.07
1973	3.42	2.05	2.92	3.09	1.10	4.70	2.99	0.06	7.44	11.11	0.58	0.76	40.46
1974	2.74	0.36	1.34	1.79	5.88	0.21	0.61	8.97	1.58	7.49	7.35	2.50	36.21
1975	1.11	2.30	0.60	3.66	6.16	7.07	2.29	2.59	3.62	2.58	0.53	2.09	36.81
1976	1.16	1.11	2.11	6.17	6.05	3.19	4.71	0.80	3.80	5.91	1.78	2.48	41.25
1977	2.25	2.58	2.18	6.09	1.26	1.22	0.21	0.06	3.10	1.19	1.69	0.39	22.16
1978	0.88	1.97	0.69	1.72	5.78	2.98	1.19	1.49	4.64	1.38	5.48	2.09	30.47
1979	2.11	3.58	1.76	2.99	7.29	[illegible]	13.54	2.61	1.40	0.45	0.59	3.40	37.50
1980	0.85	2.37	1.20	2.25	5.43	0.31	0.29	1.18	5.66	1.29	3.41	1.29	27.38
1981	2.61	1.19	3.05	0.81	4.02	14.96	3.38	0.91	2.65	7.24	0.72	0.79	45.71
1982	0.85	0.87	1.38	4.17	5.68	2.99	0.17	0.77	1.88	2.66	3.19	2.12	26.63
RECORD MEAN	2.07	2.40	2.21	3.51	4.33	2.89	2.27	2.17	3.61	3.11	2.39	2.46	33.34

Snowfall

Season	July	Aug	Sept	Oct	Nov	Dec	Jan	Feb	Mar	Apr	May	June	Total
1970-71	0.0	0.0	0.0	0.0	0.0	T	0.0	T	0.0	0.0	0.0	0.0	T
1971-72	0.0	0.0	0.0	0.0	0.0	T	T	0.0	0.0	0.0	0.0	0.0	T
1972-73	0.0	0.0	0.0	0.0	0.0	0.0	0.6	[illegible]	0.0	0.0	0.0	0.0	1.7
1973-74	0.0	0.0	0.0	0.0	0.0	0.0	0.0	[illegible]	0.0	0.0	0.0	0.0	0.0
1974-75	0.0	0.0	0.0	0.0	0.0	0.0	T	T	0.0	0.0	0.0	0.0	T
1975-76	0.0	0.0	0.0	0.0	0.0	0.0	0.0	0.0	0.0	0.0	0.0	0.0	0.0
1976-77	0.0	0.0	0.0	0.0	T	0.0	0.0	T	0.0	0.0	0.0	0.0	T
1977-78	0.0	0.0	0.0	0.0	0.0	0.0	T	T	T	0.0	0.0	0.0	T
1978-79	0.0	0.0	0.0	0.0	0.0	T	T	T	0.0	0.0	0.0	0.0	T
1979-80	0.0	0.0	0.0	0.0	T	0.0	T	T	0.0	0.0	0.0	0.0	T
1980-81	0.0	0.0	0.0	0.0	0.0	0.0	T	T	0.0	0.0	0.0	0.0	[illegible]
1981-82	0.0	0.0	0.0	0.0	0.0	0.0	[illegible]	T	T	0.0	0.0	0.0	[illegible]
1982-83	0.0	0.0	0.0	0.0	0.0	0.0							
RECORD MEAN	0.0	0.0	0.0	0.0	0.1	T	0.5	0.4	T	0.0	0.0	0.0	1.0

# Indicates a station move or relocation of instruments. See Station Location table.

Record mean values above are means through the current year for the period beginning in 1898 for temperature, 1956 for precipitation, and 1942 for snowfall.

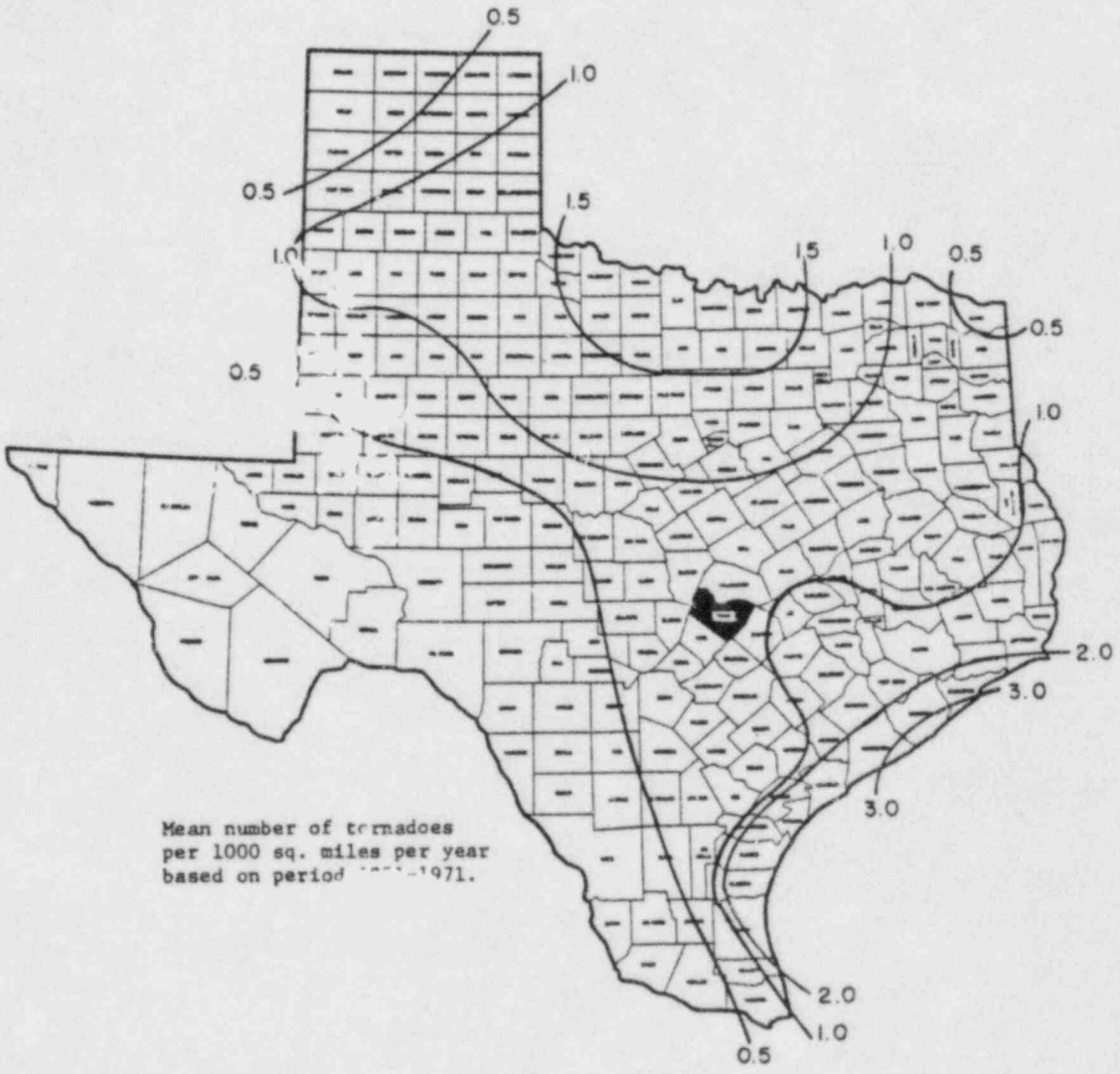

TEXAS TORNADO FREQUENCIES
Figure 2-9

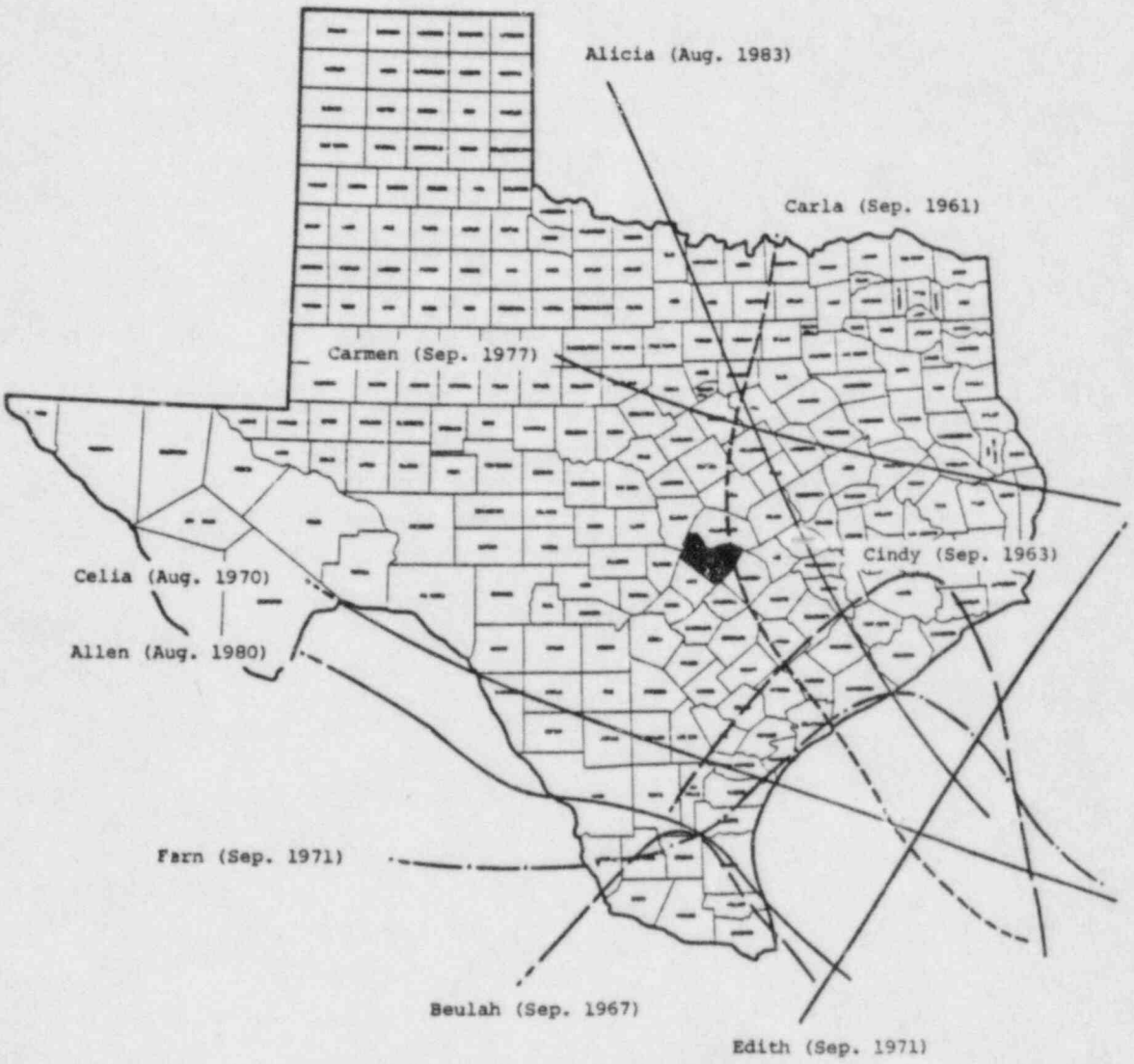

Hurricanes 1960-1983

TEXAS HURRICANE PATHS
Figure 2-10

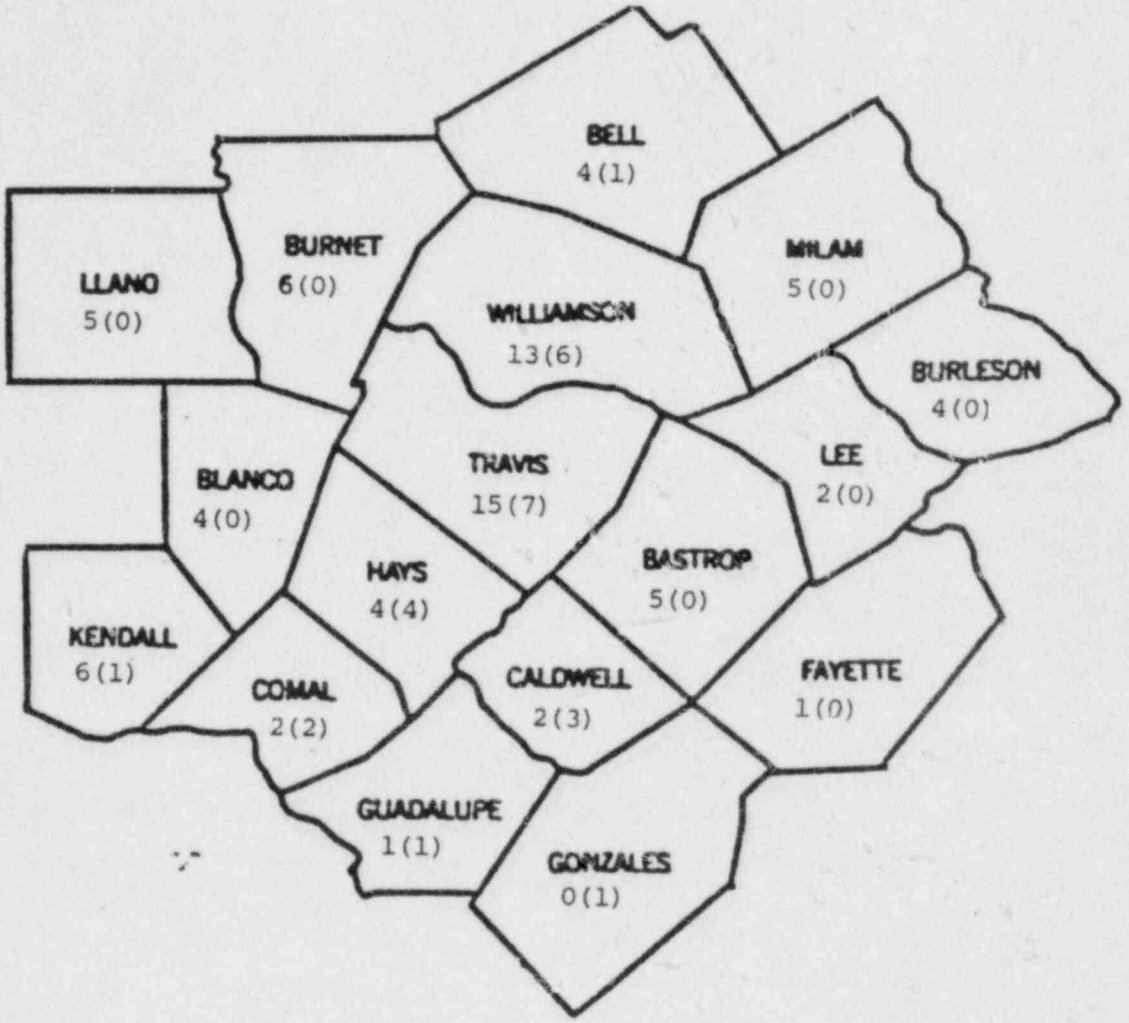

Tornado and funnel cloud occurences in a 50 mile radius of Austin for the years 1975-1983; # Tornados (#Funnel Clouds).

LOCAL FUNNEL CLOUD SITINGS
Figure 2-1i

The Balcones fault zone, which extends from Williamson County to Uvalde County, extends the full length of Travis County on a line passing through Manchaca, Austin, and McNeil. Here the orderly sequence of formations is replaced by an outcrop pattern controlled by the faults, most of which are normal faults with the down-thrown side toward the coast. Most of the movement of the Balcones Fault zone occurred during the Miocene period. Since no movement has been detected during modern times, this fault is no longer considered active [9]. Location of the Balcones Fault zone and formations in the Austin area are depicted in Figure 2-12.

2.5 HYDROLOGY

Almost the entire county is drained by the Colorado River and its tributaries. Lake Travis, which is formed by the Mansfield Dam on the Colorado River, is part of the power, flood-control, water conservation, and recreation project of the Lower Colorado River Authority. Other lakes are also operated by the Authority, such as Town Lake and Lake Austin, and are created by Longhorn and Tom Miller dams, respectively. Low level alluvial deposits of the river are commonly saturated with water at relatively shallow depths. Recharge is primarily from the river and local surface contaminations are easily transmitted to this shallow water table.

Ground water from subsurface formation is found in basal Cretaceous sands referred to as the "Trinity" sands. Elevations of the Trinity aquifer range from depths commonly less than 300 meters east of the Balcones Fault Zone to greater than 450 meters to the west of the zone. East of the Mount Bonnell Fault, dolomite and dolomite limestones provide a source of ground water at shallower depths. Access to the Edwards aquifer ranges from 30 meters to 300 meters with natural springs occurring in areas near the Colorado River. Minor aquifers associated with the Glenn Rose Formation supplies small quantities of water west of the Balcones Fault Zone. Water bearing areas in the formation are at varying depths and literally discontinuous. On the Balcones Research Center east tract, wells drilled for environmental monitoring have produced ground water at depths of less than 15 meters. Figure 2-13 shows the location of the ground water aquifers.

Water supply for the research center and wastewater treatment is provided by the City of Austin. Although wells into the aquifers provide substantial water the city supply is filtered river water. Other area municipalities and organizations utilize aquifer water. Control of private wells is the function of county and state Health

BALCONES FAULT ZONE
Figure 2-12

EDWARDS AQUIFER

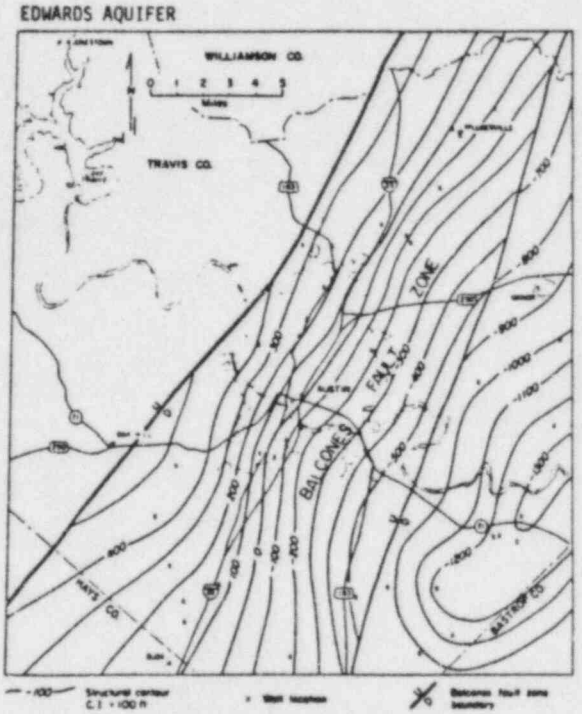

TRINITY AQUIFER

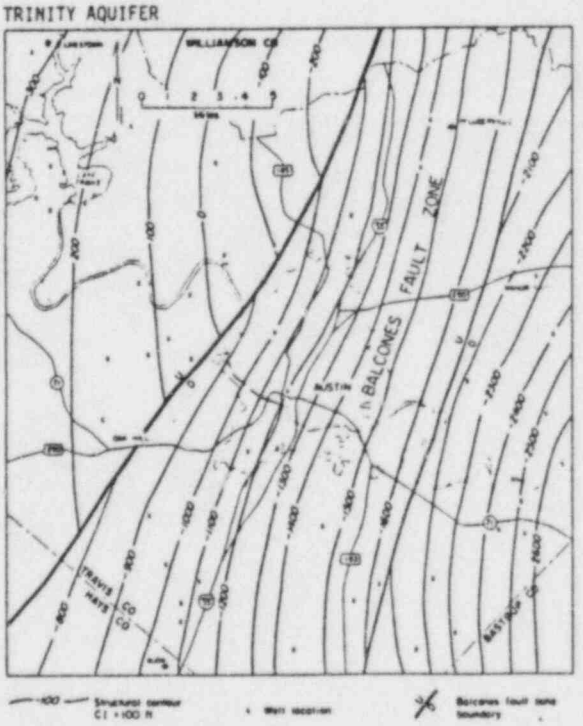

LOCAL WATER AQUIFERS
Figure 2-13

Departments. Gross beta radioactivity of city water has been measured and is reported in Table 2-4.

Table 2-4
GROUND WATER ACTIVITY
(gross beta)

Travis County	6×10^{-9} µCi/ml
Balcones Research Center	8×10^{-9} µCi/ml

2.6 SEISMOLOGY

Thirty three earthquakes of intensity IV or greater have had epicenters in Texas since 1873 [10,11]. The earthquakes were characterized using the Modified Mercalli Scale of 1931. The scale has a range of I thru XII, on which an intensity of I is not felt, an intensity of III is a vibration similar to that due to the passing of lightly loaded trucks, and intensity of VII is noticed by all as shaking trees, waves on ponds, and quivering suspended objects but causes negligible damage to buildings of good design and construction, and an intensity of XII results in practically all works of construction being severely damaged or destroyed. The strongest earthquake, a maximum intensity of VIII, was in western Texas in 1931 and was felt over 1,165,000 square kilometers. Figure 2-14 shows the locations and intensities of all earthquakes in Texas since 1873. Of these, some are known to have been felt in Austin, but no damage has ever occurred to local buildings.

2.7 HISTORICAL

Relocation of the UT TRIGA reactor and related facilities to the Balcones Research Center site is to help accommodate growth of programs both at the University main campus and at the Research Center site. The actual facility location at the Research Center is to replace a concrete and brick lined, 50 meter diameter, tank structure remaining from a magnesium manufacturing plant.

The Balcones Research Center site was operated as a magnesium manufacturing plant by the federal government prior to the University's leasing in 1947 and eventual acquisition. Activities at the site were not fully developed by the early 1980's. University functions or research activities were moved to the site when required accommodations were not available on the main campus. A few functions of the University at the site have resulted in the construction of major facilities suitable for long term use.

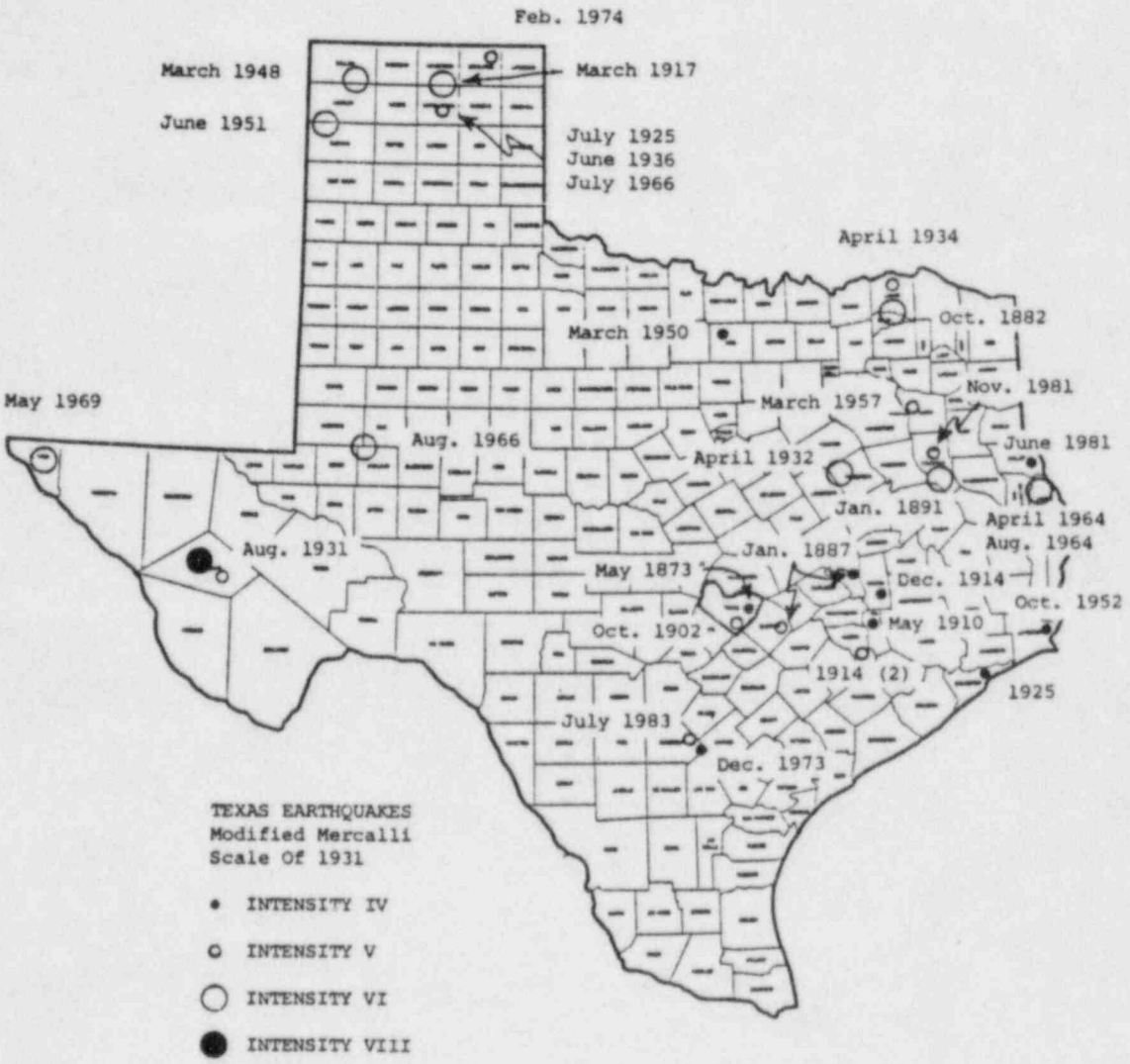

Texas Earthquakes, 1873-1983

TEXAS EARTHQUAKE DATA
Figure 2-14

Other activities at the site have utilized existing structures or other buildings not suited for long term use. In the 1980's, a major program was established to develop the Balcones Research Center site activities. As part of the first phase of development, several major research programs associated with energy and engineering were moved to facilities constructed at the site. Features of the site, before the development activities in the 1980's, are illustrated in Figure 2-15.

Several activities at the Research Center prior to 1980 had been associated with radioactive materials. These activities ranged from the burial of low level radioactive waste materials such as tritium and carbon-14 in the northwest corner of the site, to water transport studies performed in 30 meter diameter tanks adjacent and south of the TRIGA facility site. Isotopes of cesium-137, cesium-134, and cobalt-60 were present in sludge samples of the west tank, and are reported in Table 2-5. Gross beta activity in the samples of the west tank measured 22 microcuries per milliliter (1979).

Table 2-5
TANK SLUDGE SAMPLES

West tank (1979)	22 μCi/ml (gross β)
Cs^{137}	1.3×10^{-3} μCi/ml
Cs^{134}	2.5×10^{-4} μCi/ml
Co^{60}	5.7×10^{-5} μCi/ml

Radioactive materials at the Research Center site are part of the University broad license for radioactive materials which is managed by the University Safety Office and issued by the Texas Department of Health.

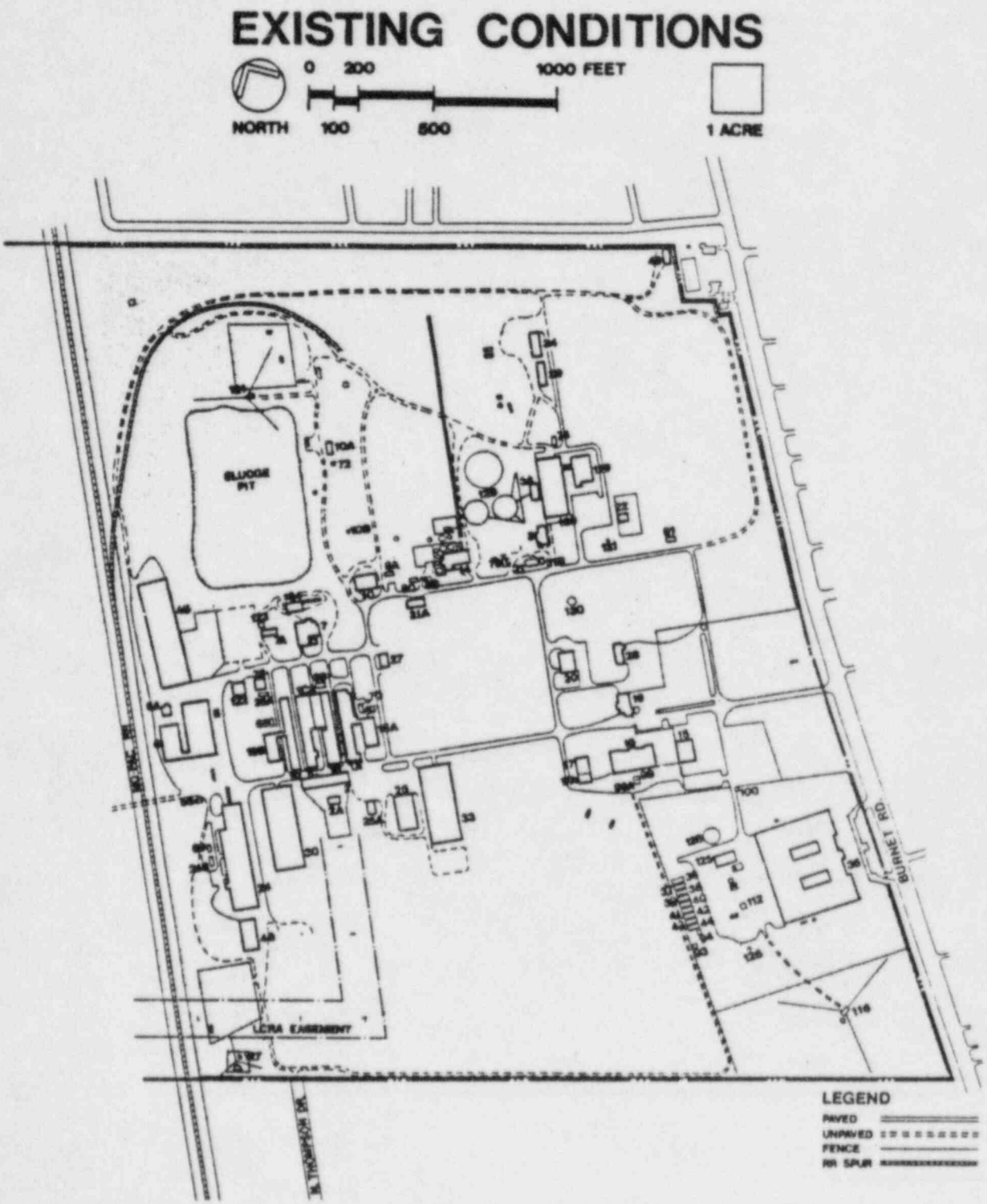

BALCONES RESEARCH CENTER 1980
Figure 2-15

Chapter 2 References

1. "Balcones Research Center Project Analysis", Volume I, The University of Texas, 1981.

2. "Basic Data", City of Austin Planning Department, June 1980.

3. "1980 Census of Population", Department of Commerce, Bureau of Census, City of Austin Planning Department.

4. "Local Climatological Data; Annual Summary with Comparative Data 1982", National Oceanic and Atmospheric Administration, Environmental Data and Information Service, National Climatic Center Asherville, N.C.

5. "Climatography of Texas; Wind Rose-Austin, Texas", National Weather Service, Austin, Texas.

6. "Texas Annual Tornado Density", National Weather Service, Austin, Texas.

7. George W. Bomar, "Texas Weather", 1983.

8. "Storm Data", 1975-1983, National Oceanic and Atmospheric Administration, Environmental Data and Information Service, National Climatic Center, Asherville, N.C.

9. L.E. Garner and K.P. Young, "Environmental Geology of the Austin Area: An Aid to Urban Planning", Report of Investigations No. 86.

10. "Earthquake Information Bulletin," May-June 1977 Vol. 9 No. 3, U.S. Department of the Interior Geological Survey.

11. Steven M. Caulson, "Investigations of Recent and Historical Seismicity in East Texas", Masters Thesis May 1984, University of Texas.

12. "Project Analysis", Vol. 1, Balcones Research Center, The University of Texas at Austin, August 1981.

Chapter 3

TRIGA REACTOR

3.1. DESIGN BASES

The reactor design bases are predicted on the maximum operational capability for the fuel elements and configuration described in this report. The TRIGA reactor system has three major areas which are used to define the reactor design bases:

a. Fuel temperature,

b. Prompt negative temperature coefficient,

c. Reactor power.

Of these three only one, fuel temperature, is a real limitation. A summary is presented below of the conclusions obtained from the reactor design bases described in this section.

Fuel Temperature

The fuel temperature is a limit in both steady-state and pulse mode operation. This limit stems from the out-gassing of hydrogen from U-ZrH (H/Zr ; x) fuel and the subsequent stress produced in the fuel element clad material. The strength of the clad as a function of temperature can set the upper limit on the fuel temperature. Fuel temperature limits of 1150°C (with clad < 500°C) and 970°C (with clad > 500°C) for U-ZrH (H/Zr ; 1.65) have been set to preclude the loss of clad integrity.

Prompt Negative Temperature Coefficient

The basic parameter which provides the TRIGA system with a large safety factor in steady-state operation and under transient conditions is the prompt negative temperature coefficient which is rather constant with temperature (~0.01% δk/k°C), as described later. This coefficient is a function of the fuel composition and core geometry.

Reactor Power

Fuel and clad temperature limit the operation of the reactor. However, it is more convenient to set a power level limit which is based on temperature. The design bases

analysis indicates that operation at up to 1900 kW (with an 85 element core and 120°F inlet water temperature) with natural convective flow will not allow film boiling, and therefore high fuel and clad temperatures which could cause loss of clad integrity could not occur.

3.1.1 Reactor Fuel Temperature

The basic safety limit for the TRIGA reactor system is the fuel temperature; this applies for both the steady-state and pulsed mode of operation.

Two limiting temperatures are of interest, depending on the type of TRIGA fuel used. The TRIGA fuel which is considered low hydride, that with an H/Zr ratio of less than 1.5, has a lower temperature limit than fuel with a higher H/Zr ratio. Figure 3-1 indicates that the higher hydride compositions are single phase and are not subject to the large volume changes associated with the phase transformations at approximately 530°C in the lower hydrides. Also, it has been noted [1] that the higher hydrides lack any significant thermal diffusion of hydrogen. These two facts preclude concomitant volume changes. The important properties of delta phase U-ZrH are given in Table 3-1.

Table 3-1
PHYSICAL PROPERTIES OF DELTA PHASE U-ZrH

Thermal conductivity (93°C - 650°C)	13 Btu/hr-ft^2-°F
Elastic modulus: 20°C	9.1×10^6 psi
650°C	6.0×10^6 psi
Ultimate tensile strength (to 650°C)	24,000 psi
Compressive strength (20°C)	60,000 psi
Compressive yield (20°C)	35,000 psi
Heat of formation (δH_f^o 298°C)	37.72 kcal/g-mole

Among the chemical properties of U-ZrH and ZrH, the reaction rate of the hydride with water is of particular interest. Since the hydriding reaction is exothermic, water will react more readily with zirconium than with zirconium hydride systems. Zirconium is frequently used in contact

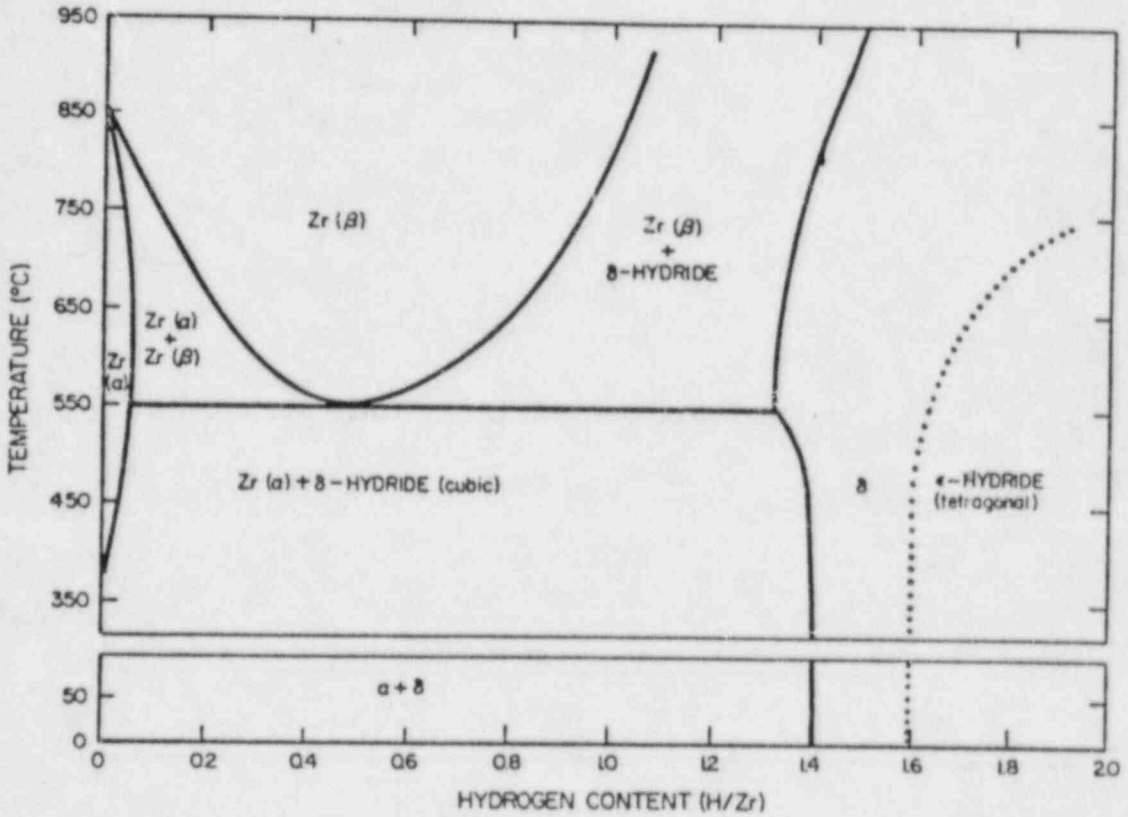

PHASE DIAGRAM OF THE
ZIRCONIUM-HYDROGEN SYSTEM
Figure 3-1

with water in reactors, and the zirconium-water reaction is not a safety hazard. Experiments carried out at GA Technologies show that the zirconium hydride systems have a relatively low chemical reactivity with respect to water and air. These tests have involved the quenching with water of both powders and solid specimens of U-ZrH after heating to as high as 850°C, and of solid U-Zr alloy after heating to as high as 1200°C. Tests have also been made to determine the extent to which fission products are removed from the surfaces of the fuel elements at room temperature. Results prove that, because of the high resistance to leaching, a large fraction of the fission products is retained in even completely unclad U-ZrH fuel.

For the rest of the discussion of fuel temperatures, we will concern ourselves with the higher hydride (H/Zr > 1.5) TRIGA fuel clad with 304 stainless steel 0.020 in. (0.508mm) thick, or a cladding material equivalent in strength at the temperatures discussed.

At room temperature the hydride is like ceramic and shows little ductility. However, at the elevated temperatures of interest for pulsing, the material is found to be more ductile. The effect of very large thermal stress on hydride fuel bodies has been observed in hot cell observations to cause relatively widely spaced cracks which tend to be either radial or normal to the central axis and do not interfere with radial heat flow. Since the segments tend to be orthogonal, their relative positions appear to be quite stable.

The limiting effect of fuel temperature then is the hydrogen gas over pressure. Figure 3-2 relates equilibrium hydrogen pressure over the fuel as a function of temperature for material with three different H/Zr ratios.

The hydrogen gas over pressure is not in itself detrimental but if the stress produced by the gas pressure within the fuel can exceed the ultimate strength of the clad material, a rupture of the fuel clad could occur. While the final conditions of fuel temperature and hydrogen pressure in which such an occurrence could come about are of interest, the mechanisms in obtaining temperatures and pressures of concern are different in the pulsing and steady-state mode of operation, and each mechanism will be discussed independently of the other.

In this discussion it will be assumed that the fuel consists of U-ZrH (H/Zr ; 1.65) with the uranium being 8.5 wt. % and further that the cladding can is 304 stainless steel. The clad thickness is 0.020 in. (0.508 mm) with an inside clad diameter of 1.43 in. (3.63 cm). These fuel parameters have been chosen since they represent the nominal specifications for TRIGA fuel elements. Figure 3-3 shows

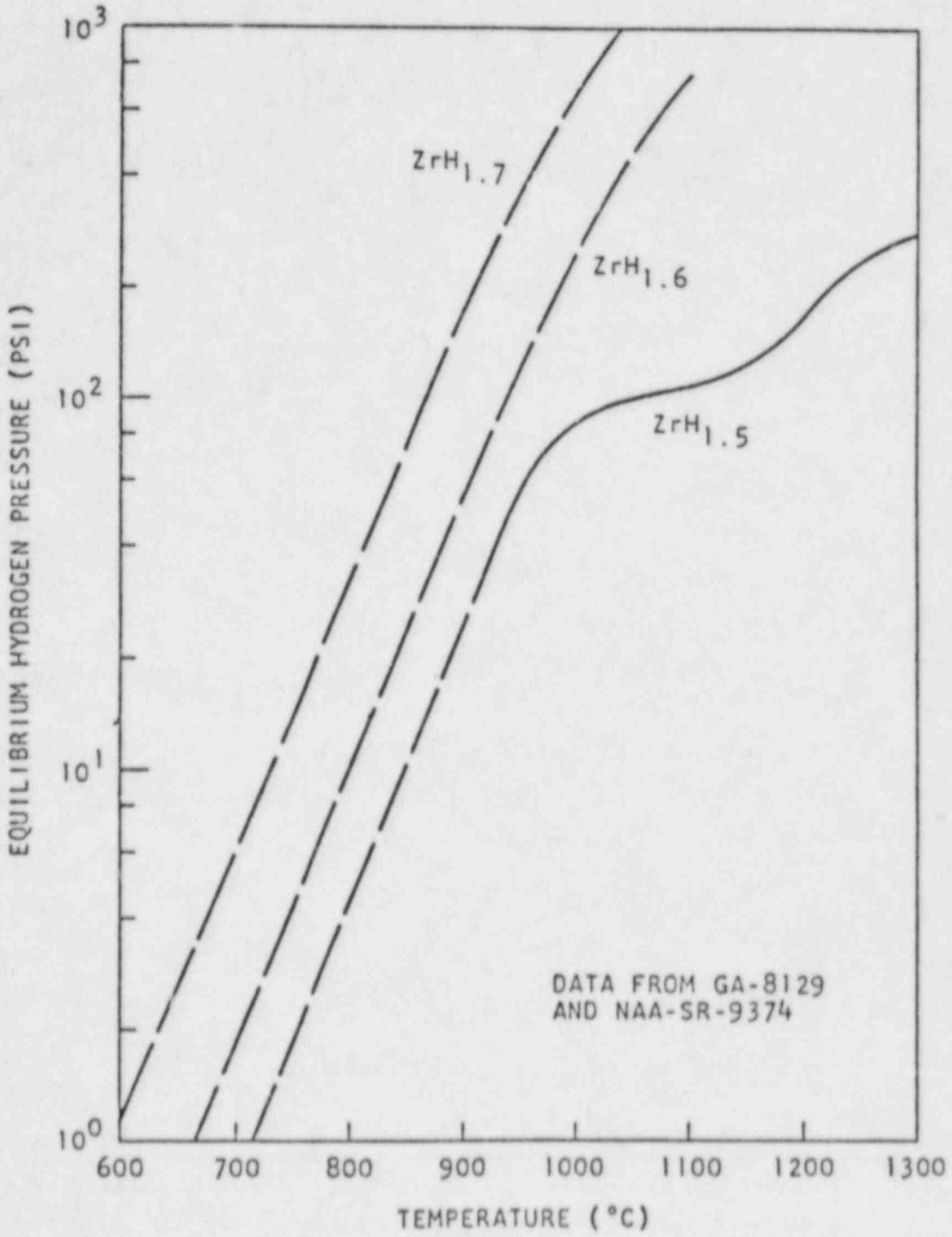

EQUILIBRIUM HYDROGEN PRESSURE
VERSUS TEMPERATURE FOR ZIRCONIUM-HYDROGEN
Figure 3-2

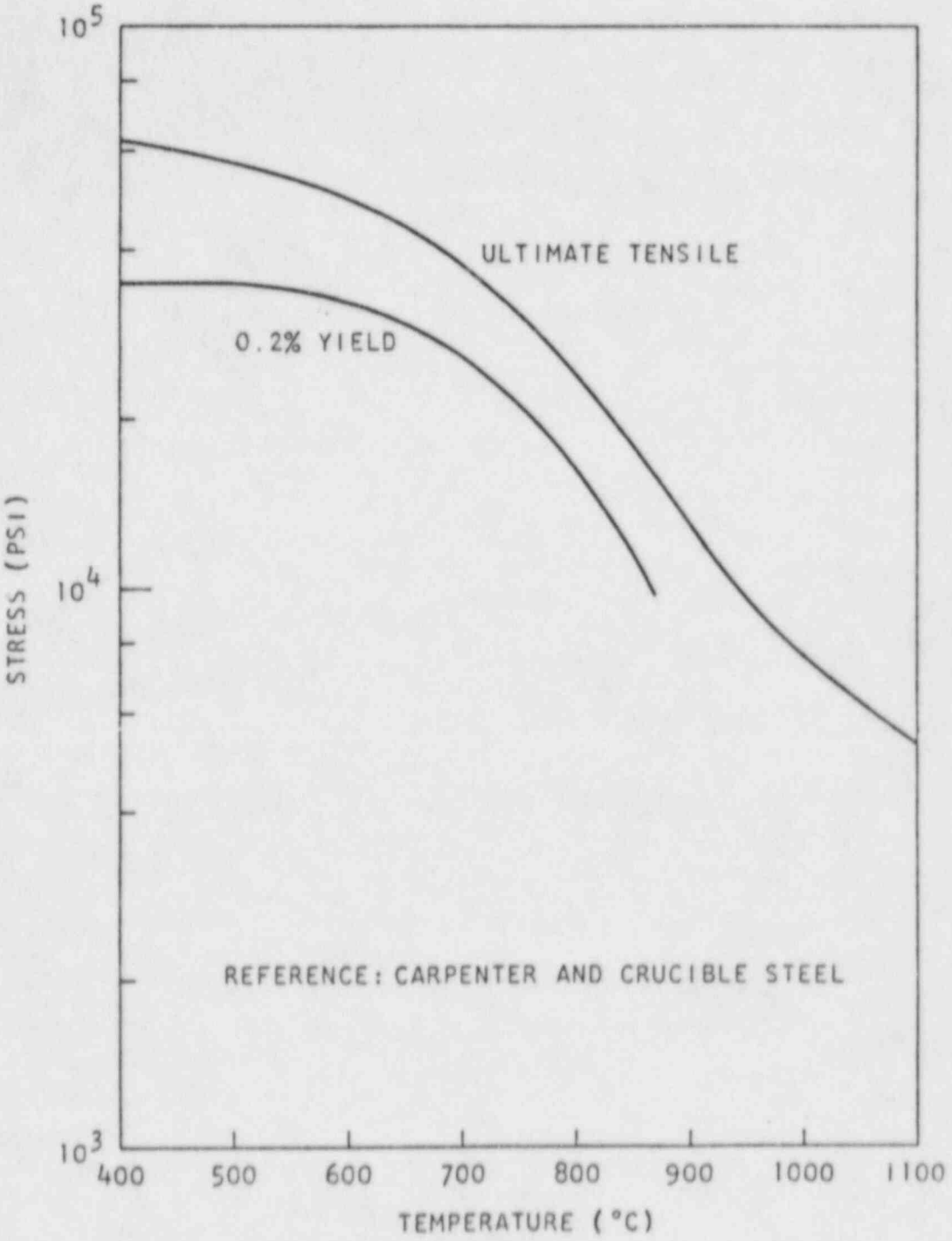

STRENGTH OF TYPE 304 STAINLESS STEEL
AS A FUNCTION OF TEMPERATURE
Figure 3-3

the characteristic of 304 stainless steel with regard to yield and ultimate strengths as a function of temperature.

In determining the stress applied to the cladding from the internal hydrogen gas pressure the equation

$$S = P\, r/t \,, \qquad (1)$$

applies where

S = stress in psi,

P = internal pressure in psi,

r = radius of the cladding can,

t = wall thickness of the clad.

Then for the cladding we have approximately

$$S = 36.7\, P \,, \qquad (2)$$

or the stress applied to the clad is approximately 36.7 times the internal pressure.

It is of interest to relate the strength of the clad material at its operating temperature to the stress applied to the clad from the internal gas pressure associated with the fuel temperature. Figure 3-4 gives information as to the ultimate clad strength as a function of temperature and also describes the stress applied to the clad as a result of hydrogen dissociation for fuel having a H/Zr ratio of 1.65 as a function of temperature.

There are several reasons why the gas pressure should be less for the transient conditions than the equilibrium condition values would predict. For example, the gas diffusion rates are finite; surface cooling is believed to be caused by endothermic gas emission which tends to lower the diffusion constant at the surface; reabsorption takes place concurrently on the cooler hydride surfaces away from the hot spot; there is evidence for a low permeability oxide film on the fuel surface; and some local heat transfer does take place during the pulse time to cause a less than adiabatic true surface temperature.

3.1.1.1 Fuel and Clad Temperature. The following discussion relates the element clad temperature and the maximum fuel temperature during a short time after a pulse.

The radial temperature distribution in the fuel element immediately following a pulse is very similar to the power distribution shown in Figure 3-5. This initial steep thermal gradient at the fuel surface results in some heat

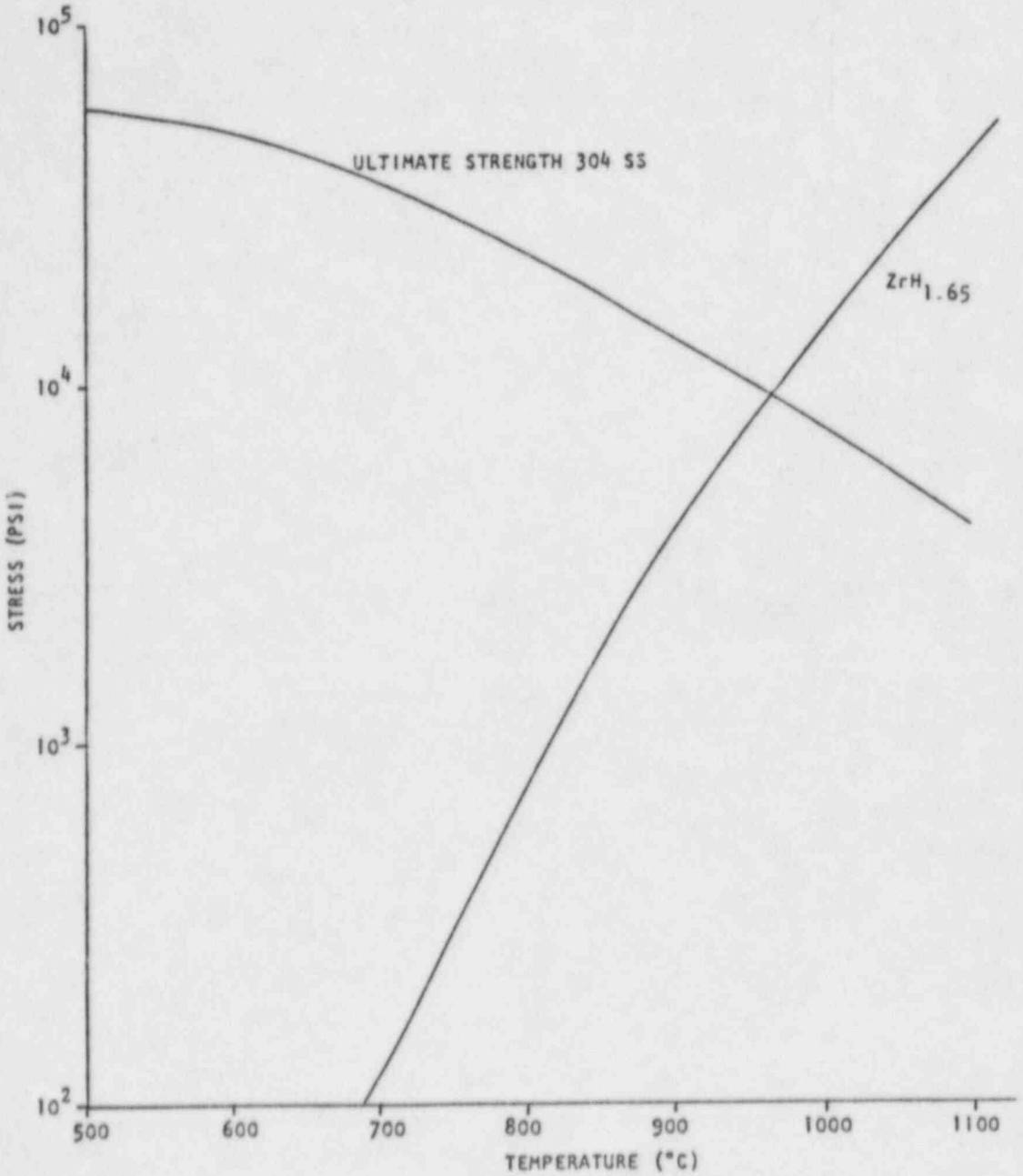

STRENGTH AND APPLIED STRESS AS A FUNCTION OF TEMPERATURE, EQUILIBRIUM HYDROGEN DISSOCIATION PRESSURE
Figure 3-4

transfer during the time of the pulse so that the true peak temperature does not quite reach the adiabatic peak temperature. A large temperature gradient is also impressed upon the clad which can result in a high heat flux from the clad into the water. If the heat flux is sufficiently high, film boiling may occur and form an insulating jacket of steam around the fuel elements permitting the clad temperature to tend to approach the fuel temperature. Evidence has been obtained experimentally which shows that film boiling has occurred occasionally for some fuel elements in the Advanced TRIGA Prototype Reactor located at GA Technologies [2]. The consequence of this film boiling was discoloration of the clad surface.

Thermal transient calculations were made using the RAT computer code. RAT is a 2D transient heat transport code developed to account for fluid flow and temperature dependent material properties. Calculations show that if film boiling occurs after a pulse it may take place either at the time of maximum heat flux from the clad, before the bulk temperature of the coolant has changed appreciably, or it may take place at a much later time when the bulk temperature of the coolant has approached the saturation temperature, resulting in a markedly reduced threshold for film boiling. Data obtained by Johnson et al. [3] for transient heating of ribbons in 100°F water, showed burnout fluxes of 0.9 to 2.0 MBtu/ft^2-hr for e-folding periods from 5 to 90 milliseconds. On the other hand, sufficient bulk heating of the coolant channeled between fuel elements can take place in several tenths of a second to lower the departure from nucleate boiling (DNB) point to approximately 0.4 MBtu/ft^2-hr. It is shown, on the basis of the following analysis, that the second mode is the most likely; i.e., when film boiling occurs it takes place under essentially steady-state conditions at local water temperatures near saturation.

A value for the temperature that may be reached by the clad if film boiling occurs was obtained in the following manner. A transient thermal calculation was performed using the radial and axial power distributions in Figure 3-5 and Figure 3-6, respectively, under the assumption that the thermal resistance at the fuel-clad interface was nonexistent. A boiling heat transfer model, as shown in Figure 3-7, was used in order to obtain an upper limit for the clad temperature rise. the model used the data of McAdams [4] for the subcooled boiling and the work of Sparrow and Cess [5] for the film boiling regime. A conservative estimate was obtained for the minimum heat flux in film boiling by using the correlations of Speigler et al. [6], Zuber [7], and Rohsenow and Choi [8] to find the minimum temperature point at which film boiling could occur. This calculation gave an upper limit of 760°C clad temperature for a peak initial fuel temperature of 1000°C,

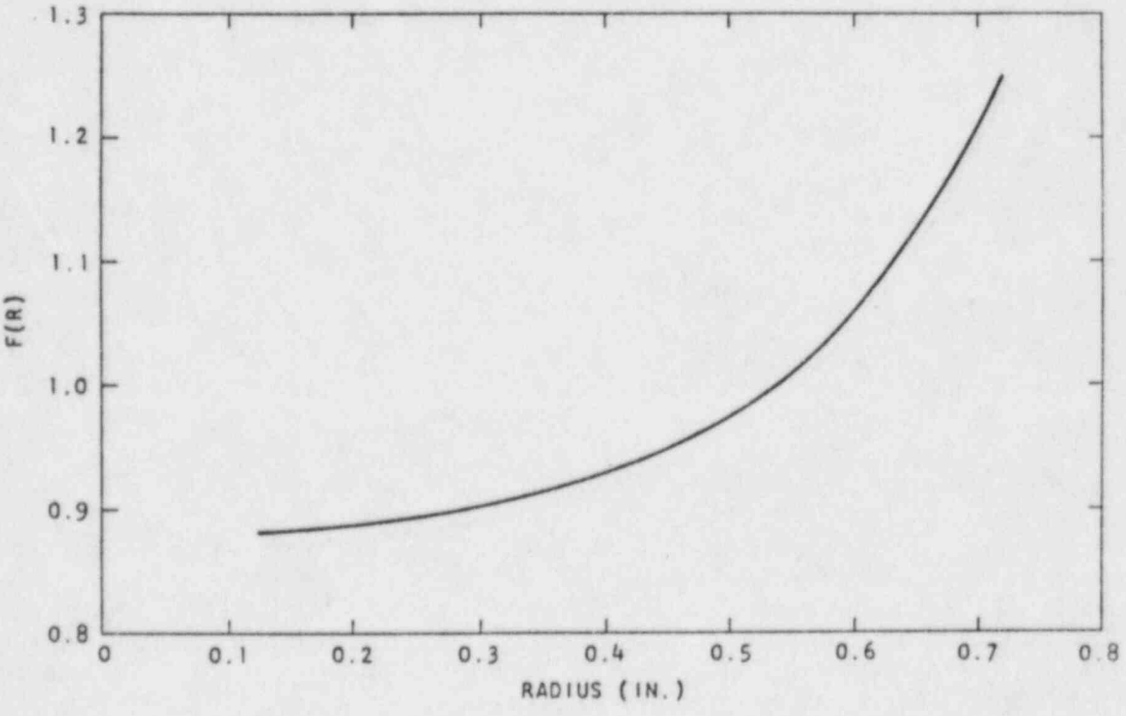

RADIAL POWER DISTRIBUTION IN
THE U-ZrH FUEL ELEMENT
Figure 3-5

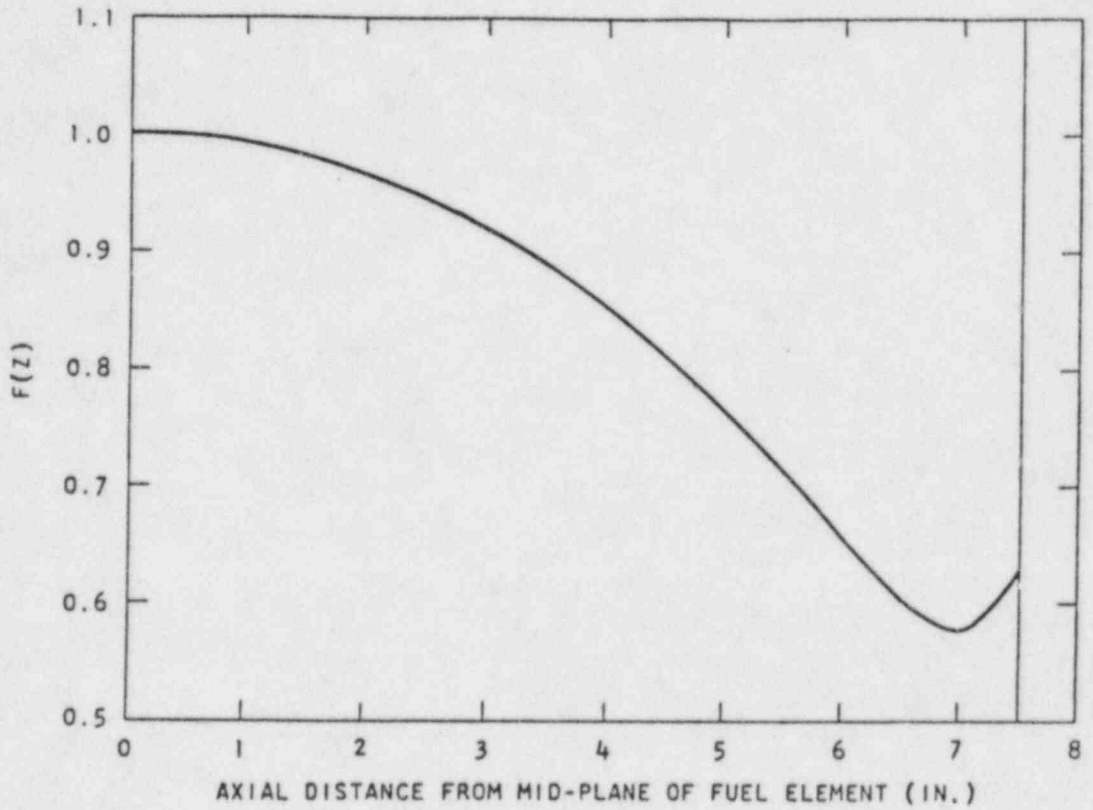

AXIAL POWER DISTRIBUTION IN
THE U-ZrH FUEL ELEMENT
Figure 3-6

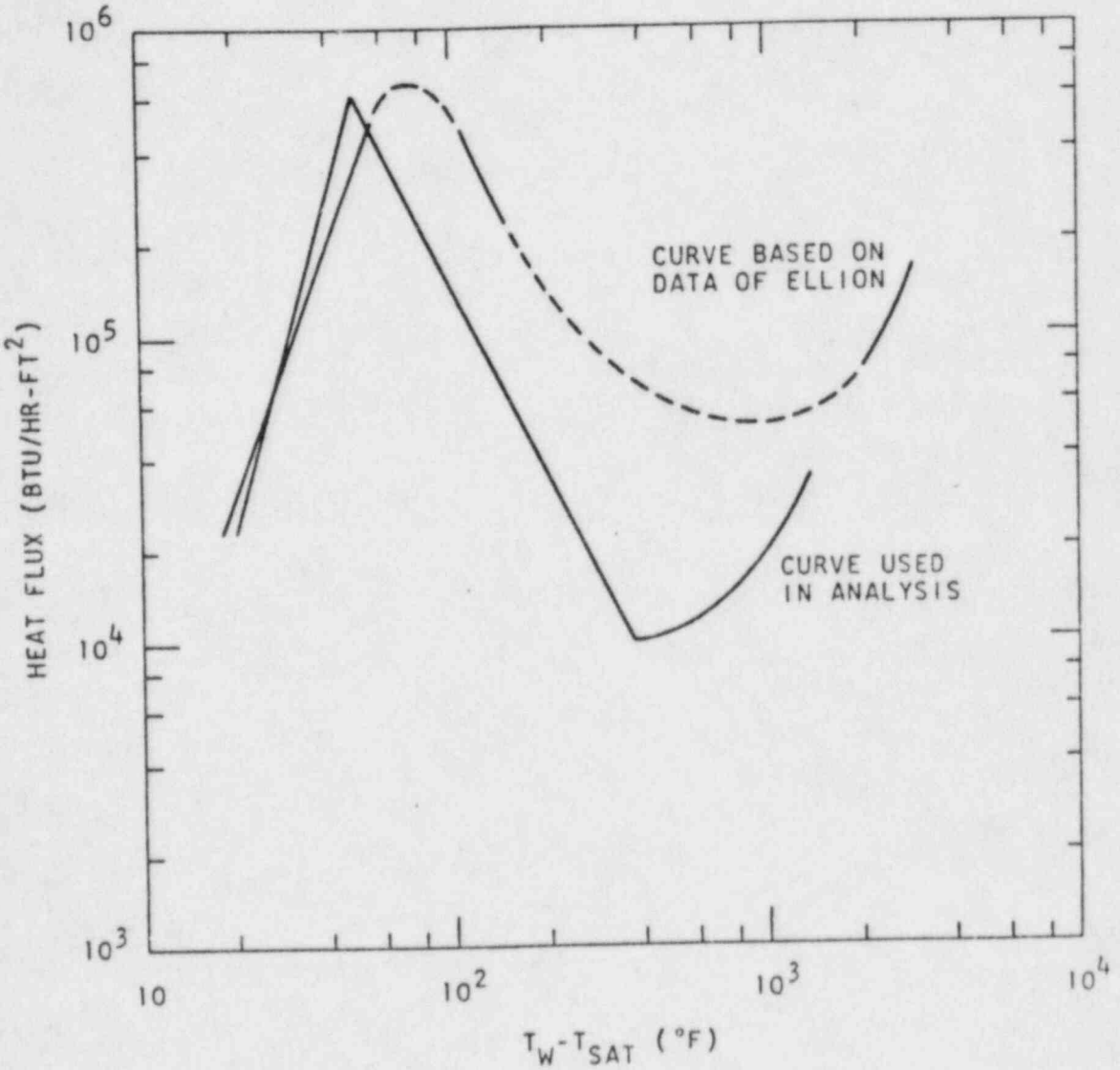

SUBCOOLED BOILING HEAT TRANSFER FOR WATER
Figure 3-7

as shown in Figure 3-8. Fuel temperature distributions for this case are shown in Figure 3-9 and the heat flux into the water from the clad is shown in Figure 3-10. In this limiting case, DNB occurred only 13 milliseconds after the pulse, conservatively calculated assuming a steady-state DNB correlation. Subsequently, experimental transition and film boiling data were found to have been reported by Ellion [9] for water conditions similar to those for the TRIGA system. The Ellion data show the minimum heat flux, used in the limiting calculation described above, was conservative by a factor of 5. An appropriate correction was made which resulted in a more realistic estimate of 470°C as the maximum clad temperature expected if film boiling occurs. This result is in agreement with experimental evidence obtained for clad temperatures of 400°C to 500°C for TRIGA Mark F fuel elements which have been operated under film boiling conditions [10].

The preceding analysis assessing the maximum clad temperatures associated with film boiling assumed no thermal resistance at fuel-clad interface. Measurements of fuel temperatures as a function of steady-state power level provide evidence that after operating at high fuel temperatures, a permanent gap is produced between the fuel body and the clad by fuel expansion. This gap exists at all temperatures below the maximum operating temperature. (See, for example, Figure 16 in Reference 10.) The gap thickness varies with fuel temperature and clad temperature so that cooling of the fuel or overheating of the clad tends to widen the gap and decrease the heat transfer rate. Additional thermal resistance due to oxide and other films on the fuel and clad surfaces is expected. Experimental and theoretical studies of thermal contact resistance have been reported [11-13] which provide insight into the mechanisms involved. They do not, however, permit quantitative prediction of this application because the basic data required for input are presently not fully known. Instead, several transient thermal computations were made using the RAT code. Each of these was made with an assumed value for the effective gap conductance, in order to determine the effective gap coefficient for which departure from nucleate boiling is incipient. These results were then compared with the incipient film boiling conditions of the 1000°C peak fuel temperature case.

For convenience, the calculations were made using the same initial temperature distribution as was used for the preceding calculation. The calculations assumed a coolant flow velocity of 1 ft per second, which is within the range of flow velocities computed for natural convection under various steady-state conditions for these reactors. The calculations did not use a complete boiling curve heat transfer model, but instead, included a convection cooled region (no boiling) and a subcooled nucleate boiling region

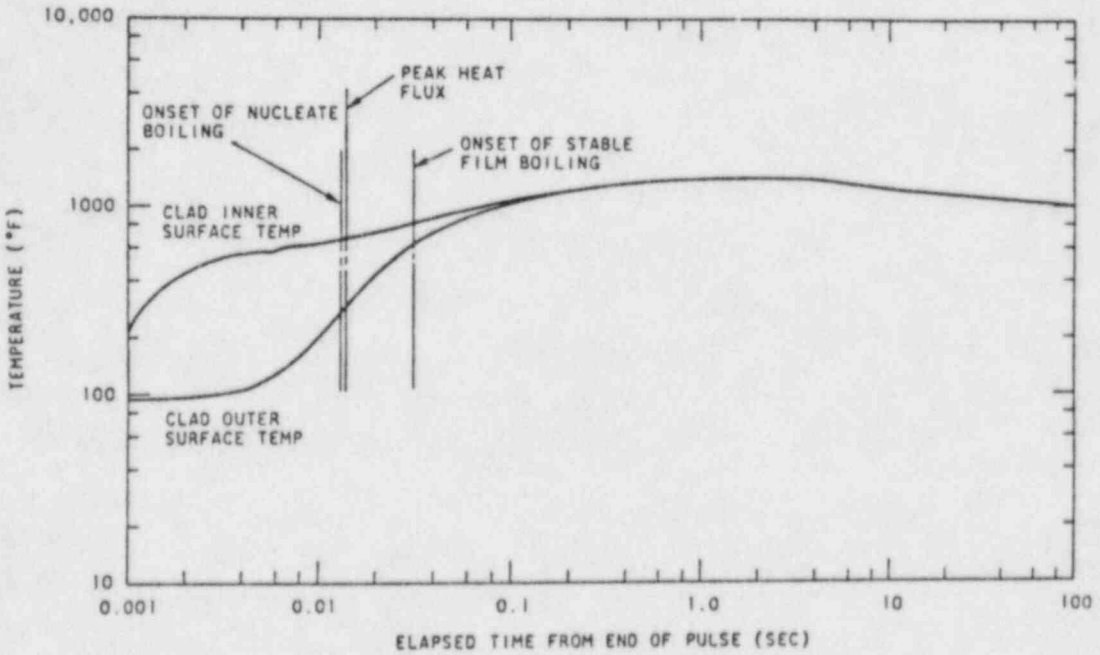

CLAD TEMPERATURE AT MIDPOINT OF
WELL-BONDED FUEL ELEMENT
Figure 3-8

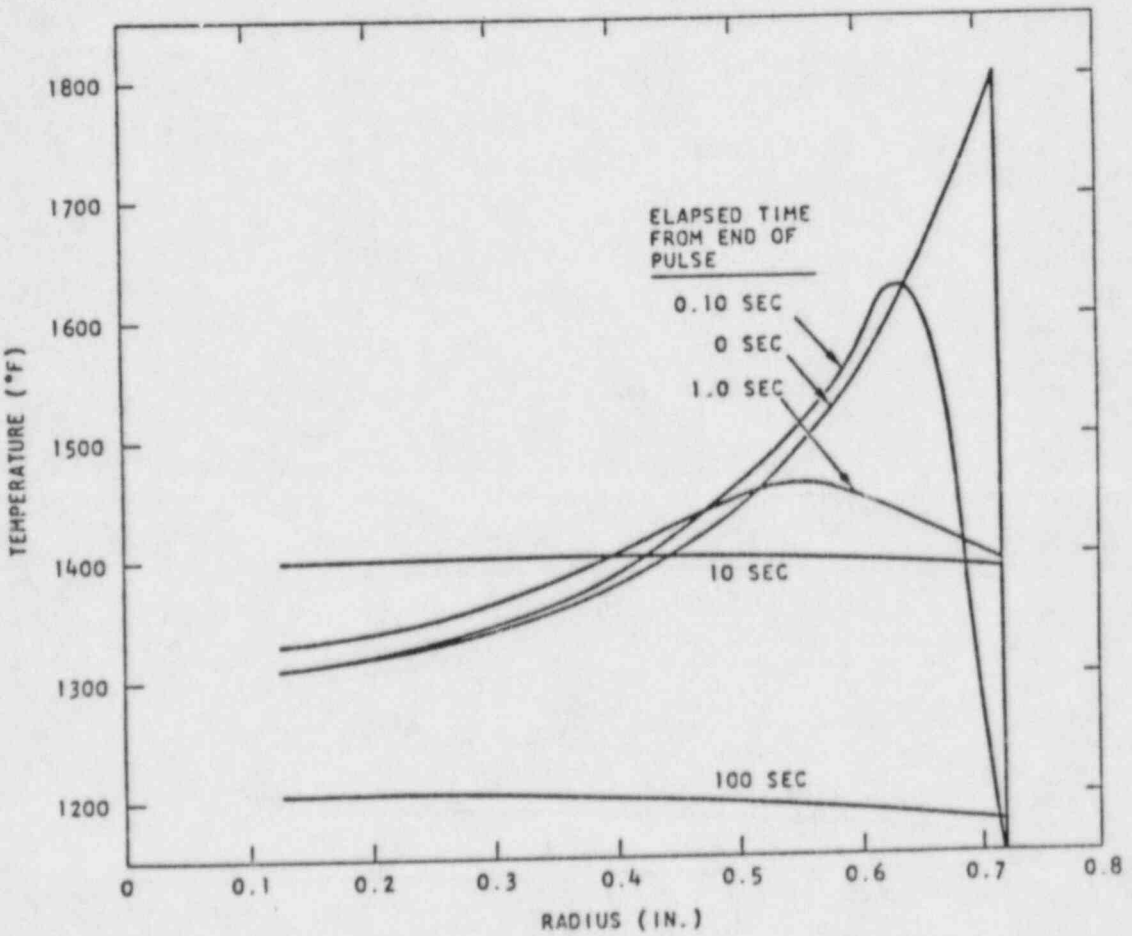

FUEL BODY TEMPERATURES AT MIDPLANE OF WELL-BONDED
FUEL ELEMENT AFTER A PULSE
Figure 3-9

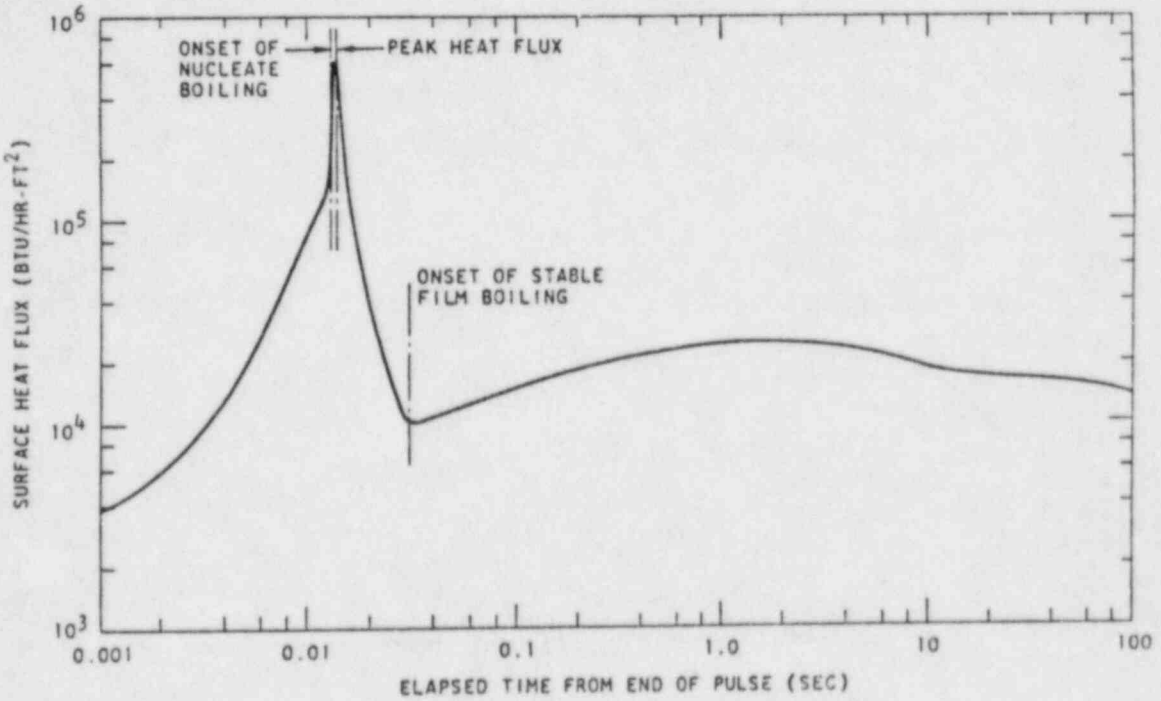

SURFACE HEAT FLUX AT MIDPLANE OF WELL-BONDED
FUEL ELEMENT AFTER A PULSE
Figure 3-10

without employing an upper DNB limit. The results were analyzed by inspection using the extended steady-state correlation of Bernath [14] which has been reported by Spano [15] to give agreement with SPERT II burnout results within the experimental uncertainties in flow rate.

The transient thermal calculations were performed using effective gap conductances of 500, 375, and 250 Btu/hr-ft^2-°F. The resulting wall temperature distributions were inspected to determine the axial wall position and time after the pulse which gave the closest approach between the local computed surface heat flux and the DNB heat flux according to Bernath. The axial distribution of the computed and critical heat fluxes for each of the three cases at the time of closest approach is given in Figures 3-11 thru 3-13. If the minimum approach to DNB is corrected to TRIGA Mark F conditions and cross-plotted, an estimate of the effective gap conductance of 450 Btu/hr-ft^2-°F is obtained for incipient burnout so that the case using 500 is thought to be representative of standard TRIGA fuel.

The surface heat flux at the midplane of the element is shown in Figure 3-14 with gap conductance as a parameter. It may be observed that the maximum heat flux is approximately proportional to the heat transfer coefficient of the gap, and the time lag after the pulse for which the peak occurs is also increased by about the same factor. The closest approach to DNB in these calculations did not necessarily occur at these times and places, however, as indicated on the curves of Figures 3-11 thru 3-13. The initial DNB point occurred near the core outlet for a local heat flux of about 340 kBtu/hr-ft^2-°F according to the more conservative Bernath correlations at a local water temperature approaching saturation.

From the foregoing analysis, a maximum temperature for the clad during a pulse which gives a peak adiabatic fuel temperature for the clad during a pulse which gives a peak adiabatic fuel temperature of 1000°C is conservatively estimated to be 470°C.

As can be seen from Figure 3-3, the ultimate strength of the clad at a temperature of 470°C is 59,000 psi. If the stress produced by the hydrogen over pressure in the can is less than 59,000 psi, the fuel element will not undergo loss of containment. Referring to Figure 3-4, and considering U-ZrH fuel with a peak temperature of 1000°C, one finds the stress on the clad to be 12,600 psi. Further studies show that the hydrogen pressure which would result from a transient for which the peak fuel temperature is 1150°C would not produce a stress in the clad in excess of its ultimate strength. TRIGA fuel with a hydrogen to zirconium ratio of at least 1.65 has been pulsed to temperatures of about 1150°C without damage to the clad [16].

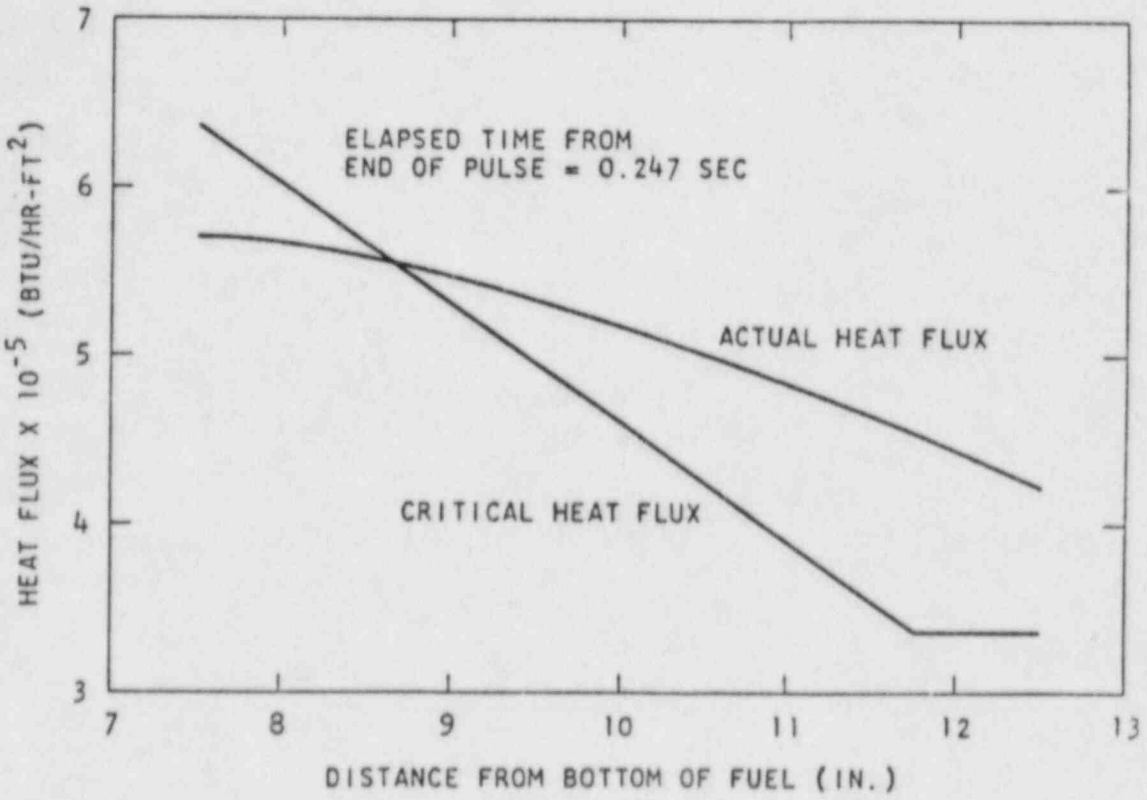

SURFACE HEAT FLUX DISTRIBUTION FOR STANDARD NON-GAPPED (h_{gap}=500) FUEL ELEMENT AFTER A PULSE
Figure 3-11

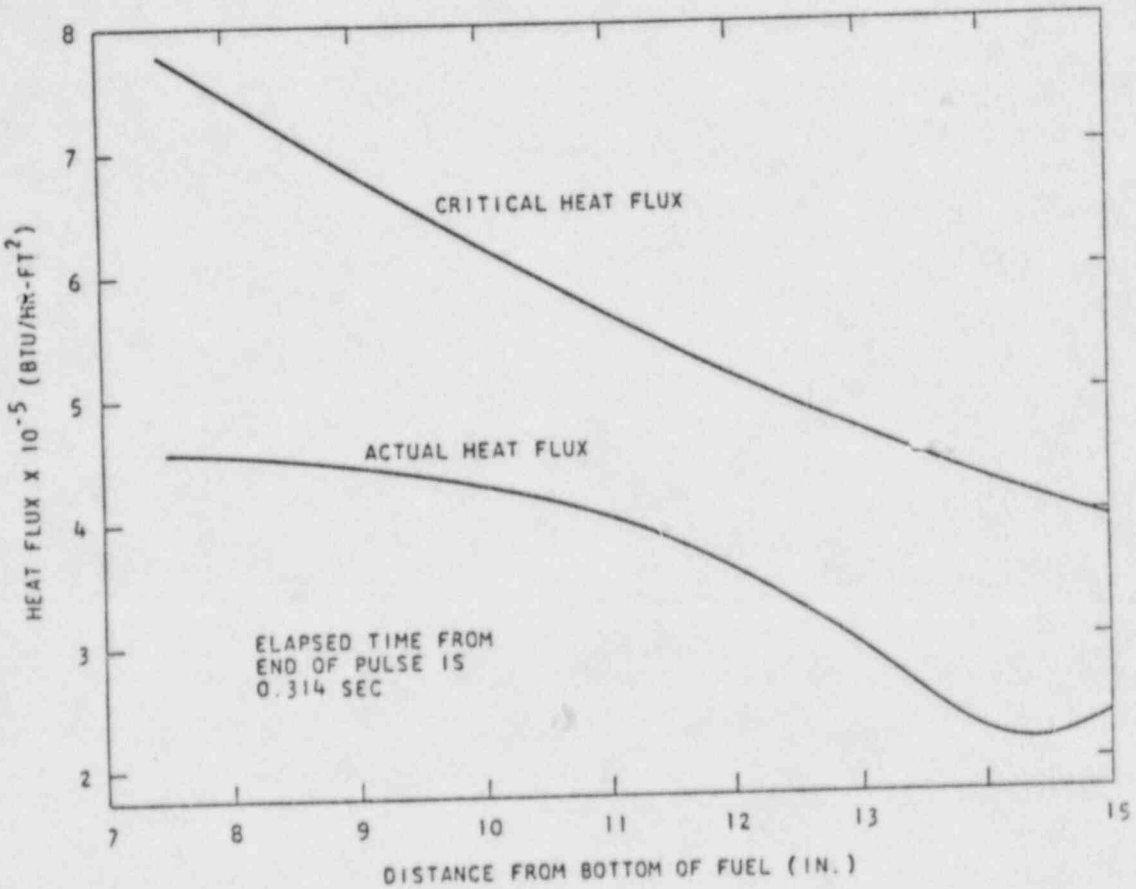

SURFACE HEAT FLUX DISTRIBUTION FOR STANDARD NON-GAPPED (h_{gap}=375) FUEL ELEMENT AFTER A PULSE
Figure 3-12

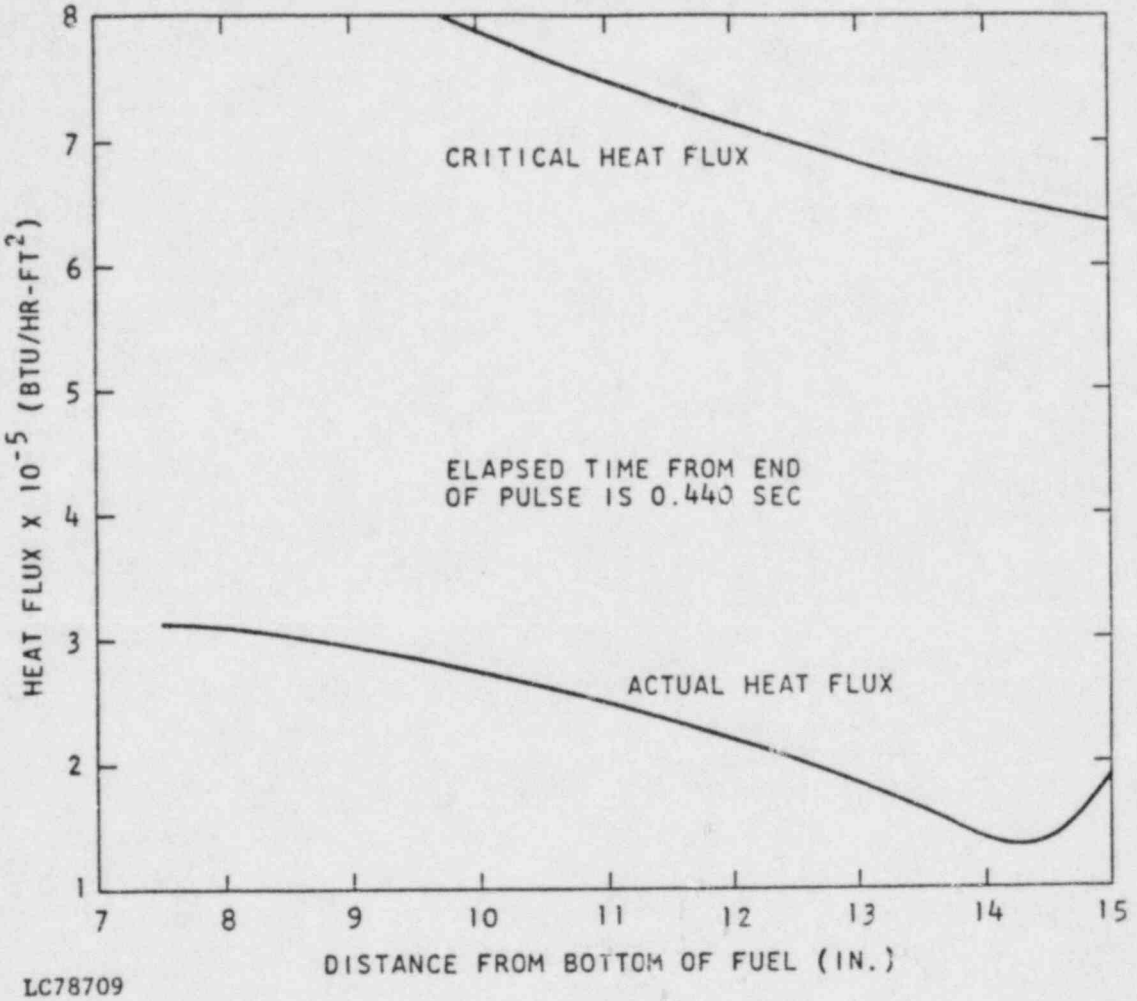

SURFACE HEAT FLUX DISTRIBUTION FOR STANDARD NON-GAPPED (h_{gap}=250) FUEL ELEMENT AFTER A PULSE
Figure 3-13

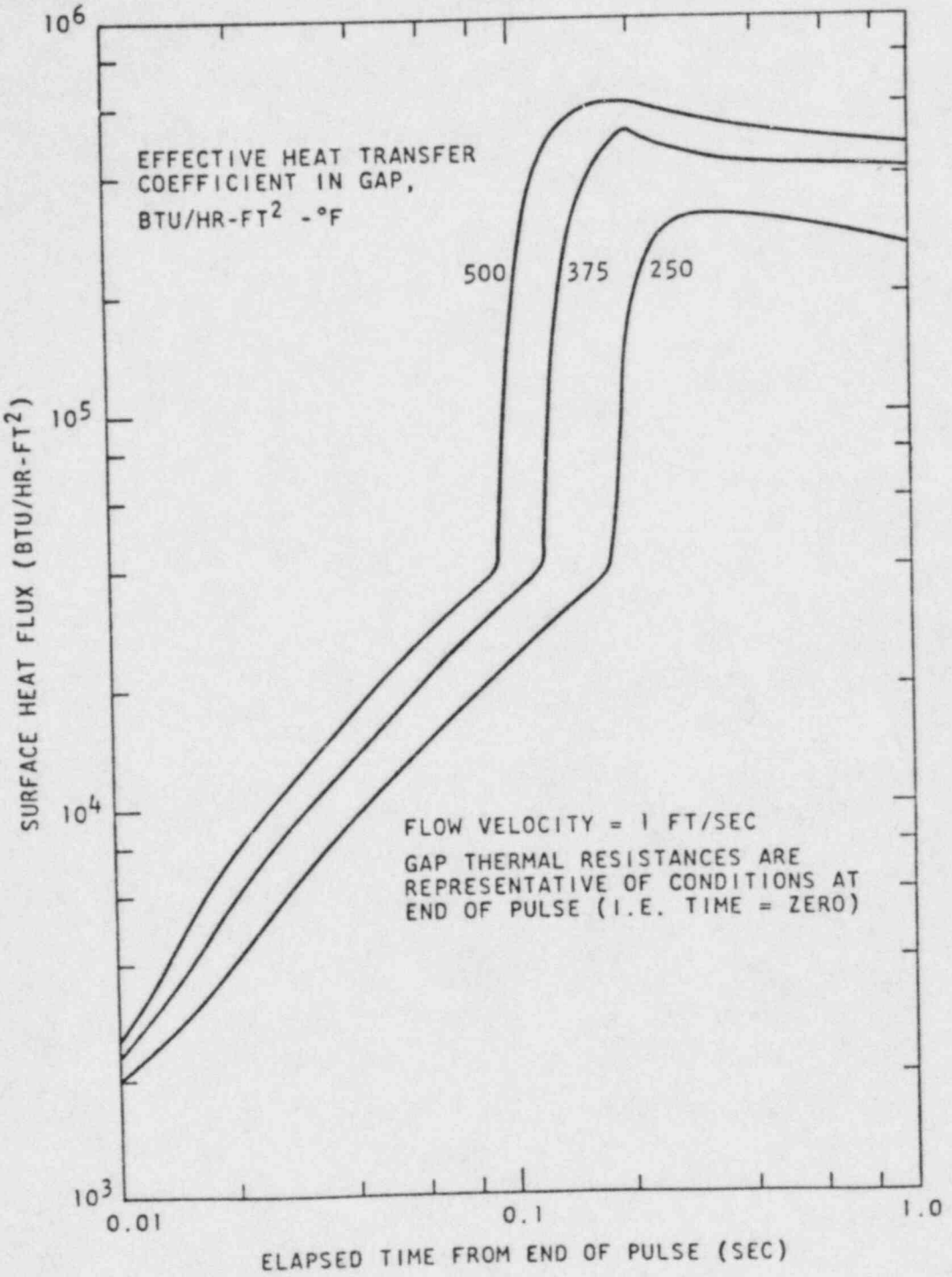

SURFACE HEAT FLUX AT MIDPOINT VERSUS TIME
FOR STANDARD NON-GAPPED FUEL ELEMENT AFTER A PULSE
Figure 3-14

3.1.1.2 Finite Diffusion Rate. To assess the effect of the finite diffusion rate and the rehydriding at the cooler surfaces, the following analysis is presented.

As hydrogen is released from the hot fuel regions, it is taken up in the cooler regions and the equilibrium that is obtained is characteristic of some temperature lower than the maximum. To evaluate this reduced pressure, we will use diffusion theory to calculate the rate at which hydrogen is evolved and reabsorbed at the fuel surface.

Ordinary diffusion theory provides an expression for describing the time dependent loss of gas from a cylinder:

$$\frac{\bar{c} - c_f}{c_i - c_f} = \sum_{n=1}^{\infty} \frac{4}{Z_n^2} \exp - \frac{Z_n^2 \, Dt}{r_0^2} \quad , \qquad (3)$$

where $\bar{c}$, c_i, c_f, = the average, the initial, and the final gas concentration in the cylinder, respectively,

Z_n = the roots of the Equation $J_0(x) = 0$,

D = the diffusion coefficient for the gas in the cylinder,

r_0 = the radius of the cylinder,

t = time.

Setting the term on the right-hand side of Equation 3 equal to κ, one can rewrite Equation 3 as:

$$\bar{c}/c_i = c_f/c_i + (1 - c_f/c_i)\,\kappa \quad , \qquad (4)$$

and the derivative in time is given by

$$\frac{d(\bar{c}/c_i)}{dt} = (1 - c_f/c_i)\,\frac{d\kappa}{dt} \quad . \qquad (5)$$

This represents the fractional release rate of hydrogen from the cylinder, f(t). The derivative of the series in the right-hand side of Equation 3 was approximated by

$$\frac{d\kappa}{dt} = - (7.339e^{-8.34\varepsilon} + 29.88e^{-249\varepsilon})\,\frac{d\varepsilon}{dt} \quad , \qquad (6)$$

where $\varepsilon = Dt/r_0^2$.

The diffusion coefficient for hydrogen in zirconium hydride in which the H/Zr ratio is between 1.56 and 1.86 is given by

$$D = 0.25\ e^{-17800/R(T+273)}\ , \qquad (7)$$

where R = the gas constant and,

T = the zirconium hydride temperature in °C.

Equation 3 describes the escape of gas from a cylinder through diffusion until some final concentration is achieved. Actually, in the closed system considered here, not only does the hydrogen diffuse into the fuel-clad gap, but also it diffuses back into the fuel in the regions of lower fuel temperature. The gas also diffuses through the clad at a rate dependent on the clad temperature. Although this tends to reduce the hydrogen pressure, it is not considered in this analysis. When the diffusion rates are equal, an equilibrium condition will exist. To account for this, Equation 5 was modified by substituting for the concentration ratios the ratio of the hydrogen pressure in the gap to the equilibrium hydrogen pressure, P_h/P_e. Thus,

$$f(t) = \frac{d(c/c_i)}{dt} = (1 - P_h(t)/P_e)\ \frac{d\kappa}{dt}\ , \qquad (8)$$

where $P_h(t)$ = the hydrogen pressure, a function of time and

P_e = the equilibrium hydrogen pressure over the zirconium hydride which is a function of the fuel temperature.

The rate of change of the internal hydrogen pressure, in psi, inside the fuel element cladding is

$$\frac{dP_h}{dt} = \frac{14.7\ f(t)\ N_h}{6.02 \times 10^{23}}\ \frac{22.4}{V_g}\ \frac{T+273}{273}\ , \qquad (9)$$

where N_h = the number of molecules of H_2 in the fuel,

T = the gas temperature (°C),

f(t) = the fractional loss rate from Equation 8,

V_g = the free volume inside the fuel clad (liters).

As the atom density of hydrogen in ZrH (H/Zr ; 1.65) is about 0.1 moles and the fuel volume is 400 cubic cm., N_h is 19.9 moles (H_2). The free volume is assumed to consist of a cylindrical volume, at the top of the element, 1/8-in. high with a diameter of 1.43 in. for a total of 3.3 cubic cm. Also, the temperature of the hydrogen in the gap was assumed to be the temperature of the clad. The effect of changing

these two assumptions was tested by calculations in which the gap volume was decreased by 90% and the temperature of the hydrogen in the gap was set up equal to the maximum fuel temperature. Neither of these changes resulted in maximum pressures different from those based on the original assumptions although the initial rate of pressure increase was greater. For these conditions

$$P_h = 7.29 \times 10^3 \, (T + 273) \int f(t)\, dt \, . \qquad (10)$$

The fuel temperature used in Equation 7 to evaluate the diffusion coefficient is expressed as

$$\begin{aligned} T(z) &= T_0 \quad ; \; t < 0 \quad , \\ T(z) &= T_0 + (T_m - T_0) \cos [2.45(z-0.5)] \quad ; \; t \geq 0 \quad , \end{aligned} \qquad (11)$$

where T_m = the peak fuel temperature (°C),

T_0 = the clad temperature (°C),

z = the axial distance expressed as a fraction of the fuel length,

t = the time after step increase in power.

It was assumed that the fuel temperature was invariant with radius. The hydrogen pressure over the zirconium hydride surface when equilibrium prevails is strongly temperature dependent as shown in Figure 3-2 and, for ZrH (H/Zr ; 1.65), can be expressed by

$$P_e = 2.07 \times 10^9 \; e^{-1.974 \times 10^4/(T+273)} \, . \qquad (12)$$

The coefficients have been derived from data developed by Johnson. The rate at which hydrogen is released or reabsorbed takes the form

$$g(t,z) = \frac{[P_e(z) - P_h(t)]}{P_e(z)} \; f(t,z) \quad , \qquad (13)$$

where $f(t,z)$ = the derivative given in Equation 8 with respect to time evaluated at the axial position z,

$P_h(t)$ = the hydrogen pressure in the gap at time t,

$P_e(z)$ = the equilibrium hydrogen pressure at the ZrH temperature at position z.

The internal hydrogen pressure is then

$$P_h(t) = 7.29 \times 10^3 \, (T_0 + 273) \int_0^t \int_0^l \dot{g}(t,z) \, dz \, dt. \quad (14)$$

This Equation was approximated by

$$P_h(t_i) = 7.29 \times 10^3 \, (T_0 + 273) \times \sum_{i=i}^{n} \sum_{j=1}^{m} \left[1 - \frac{P_H(t_{i-1})}{P_E(z_j)}\right] \times f(t_i, z_j) \, \delta z \, \delta t \quad , \quad (14)$$

where the internal summation is over the fuel element length increments and the external summation is over time.

For the case in which the maximum fuel temperature is 1150°C, the equilibrium hydrogen pressure in ZrH (H/Zr ; 1.65) is 2000 psi. Calculations indicate, however, that the internal pressure increases to a peak at about 0.3 sec, at which time the pressure is about one-fifth of the equilibrium value or abut 400 psi. After this time, the pressure slowly decreases as the hydrogen continues to be redistributed along the length of the element from the hot regions to the cooler regions.

Calculations have also been made for step increases in power to peak fuel temperatures greater than 1150°C. Over a 200°C range, the time to the peak pressure and the fraction of the equilibrium pressure value achieved were approximately the same as for the 1150°C case. Thus, if the clad remains below about 500°C, the internal pressure that would produce the yield stress in the clad (35,000 psi) is about 1000 psi and the corresponding equilibrium hydrogen pressure corresponds to a maximum fuel temperature of about 1250°C in ZrH (H/Zr ; 1.65). Similarly, an internal pressure of 1600 psi would produce a stress equal to the ultimate clad strength (over 59,000 psi). This corresponds to an equilibrium hydrogen pressure of 5 x 1600 or 8000 psi and a fuel temperature of about 1300°C.

Measurements of hydrogen pressure in TRIGA fuel elements during steady-state operation have not been made. However, measurements have been made during transient operations and compared with the results of an analysis similar to that described here. These measurements indicated that in a pulse in which the maximum temperature in the fuel was greater than 1000°C the maximum pressure was only about 6% of the equilibrium value evaluated at the peak temperature. Calculations of the pressure resulting from such a pulse using the methods described above gave calculated pressure values about three times greater than the measured values.

An instantaneous increase in fuel temperature will produce the most severe pressure conditions. When a peak fuel temperature of 1150°C is reached by increasing the power over a finite period of time, the resulting pressure will be no greater than that for the step change in power analyzed above. As the temperature rise times become long compared with the diffusion time of hydrogen, the pressure will become increasingly less than for the case of a step change in power. The reason for this is that the pressure in the clad element results from the hot fuel dehydriding faster than the cooler fuel rehydrides (takes up the excess hydrogen to reach an equilibrium with the hydrogen over pressure in the can). The slower the rise to peak temperature, the lower the pressure because of the additional time available for rehydriding.

3.1.1.3 Summary. The foregoing analysis gives a strong indication that the clad will not be ruptured if fuel temperatures are never greater than in the range of 1200°C to 1250°C, providing that the clad temperature is less than about 500°C. However, a conservative safety limit of 1150°C has been chosen for this condition. As a result, at this safety limit temperature the pressure is about a factor of 4 lower than would be necessary for clad failure. This factor of 4 is more than adequate to account for uncertainties in clad strength and manufacturing tolerances.

Under any condition in which the clad temperature increases above 500°C, the temperature safety limit must be decreased as the clad material loses strength at elevated temperatures. To establish this limit, it is assumed that the fuel and the clad are at the same temperature. There are no conceivable circumstances that could give rise to a situation in which the clad temperatures was higher than the fuel temperature.

In Figure 3-4 there is plotted the stress imposed on the clad by the equilibrium hydrogen pressure as a function of the fuel temperature, again assuming a clad radius of 0.73 in. and a thickness of 0.02 in. Also shown is the ultimate strength of 304 stainless steel at the same temperatures. The use of these data for establishing the safety limit is justified as

a. the method used to measure ultimate strength requires the imposition of the stress over a longer time than would be imposed for accident conditions,

b. the stress is not applied biaxially in the ultimate strength measurements as it is in the fuel clad.

The point at which the two curves in Figure 3-4 intersect is the safety limit, that is, 970°C. At that temperature the

equilibrium hydrogen pressure would impose a stress on the clad equal to the ultimate strength of the clad.

The same argument about the redistribution of the hydrogen within the fuel presented earlier is valid for this case also. In addition, at elevated temperatures the clad becomes quite permeable to hydrogen. Thus, not only will hydrogen redistribute itself within the fuel to reduce the pressure, but also some hydrogen will escape from the system entirely.

The use of the ultimate strength of the clad material in the establishment of the safety limit under these conditions is justified because of the transient nature of such accidents. Although the high clad temperatures imply sharply reduced heat transfer rates to the surroundings (and consequently longer cooling times), only slight reductions in the fuel temperature are necessary to reduce the stress sharply. A 50°C decrease in temperature from 970°C to 920°C will reduce the stress by a factor of 2.

As a safety limit, the peak adiabatic fuel temperature to be allowed during transient conditions is considered to be 1150°C for $U\text{-}ZrH_{1.65}$.

3.1.2. Prompt Negative Temperature Coefficient

The basic parameter which allows the TRIGA reactor system to operate safely with large step insertions of reactivity is the prompt negative temperature coefficient associated with the TRIGA fuel and core design. This temperature coefficient (α) also allows a greater freedom in steady-state operation as the effect of accidental reactivity changes occurring from the experimental devices in the core is greatly reduced.

GA Technologies, the designer of the reactor, has developed techniques to calculate the temperature coefficient accurately and therefore predict the transient behavior of the reactor. This temperature coefficient arises primarily from a change in the disadvantage factor resulting from the heating of the uranium zirconium hydride fuel-moderator elements. The coefficient is prompt because the fuel is intimately mixed with a large portion of the moderator and thus fuel and solid moderator temperatures rise simultaneously. A quantitative calculation of the temperature coefficient requires a knowledge of the energy dependent distribution of thermal neutron flux in the reactor.

The basic physical processes which occur when the fuel-moderator elements are heated can be described as follows: the rise in temperature of the hydride increases the probability that a thermal neutron in the fuel element

will gain energy from an excited state of an oscillating hydrogen atom in the lattice. As the neutrons gain energy from the ZrH, their mean free path is increased appreciably. This is shown qualitatively in Figure 3-15. Since the average chord length in the fuel element is comparable with a mean free path, the probability of escape from the fuel element before capture is increased. In the water the neutrons are rapidly rethermalized so that the capture and escape probabilities are relatively insensitive to the energy with which the neutron enters the water. The heating of the moderator mixed with the fuel thus causes the spectrum to harden more in the fuel than in the water. As a result, there is a temperature dependent disadvantage factor for the unit cell in the core which decreases the ratio of absorptions in the fuel to total cell absorptions as the fuel element temperature is increased. This brings about a shift in the core neutron balance, giving a loss of reactivity.

The temperature coefficient then, depends on spatial variations of the thermal neutron spectrum over distances of the order of a mean free path with large changes of mean free path occurring because of the energy change in a single collision. A quantitative description of these processes requires a knowledge of the differential slow neutron energy transfer cross section in water and zirconium hydride, the energy dependence of the transport cross section of hydrogen as bound in water and zirconium hydride, the energy dependence of the capture and fission cross sections of all relevant materials, and a multigroup transport theory reactor description which allows for the coupling of groups by speeding up as well as by slowing down.

3.1.2.1. Codes Used for Calculations. Calculational work on the temperature coefficient made use of a group of codes developed by GA Technologies: GGC-3 [17], GAZE-2 [18], and GAMBLE-5 [19], as well as DTF-IV [20], an S_n multigroup transport code written at Los Alamos. Neutron cross sections for energies above thermal (>1 eV) were generated by the GGC-3 code. In this code, fine group cross sections (~100 groups), stored on tape for all commonly used isotopes, are averaged over a space independent flux derived by solution of the B_1 equations for each discrete reactor region composition. This code and its related cross-section library predict the age of each of the common moderating materials to within a few percent of the experimentally determined values and use the resonance integral work of Adler, Hinman, and Nordheim [21] to generate cross sections for resonance materials which are properly averaged over the region spectrum.

Thermal cross sections were obtained in essentially the same manner using the GGC-3 code. However, scattering kernels were used to describe properly the interactions of

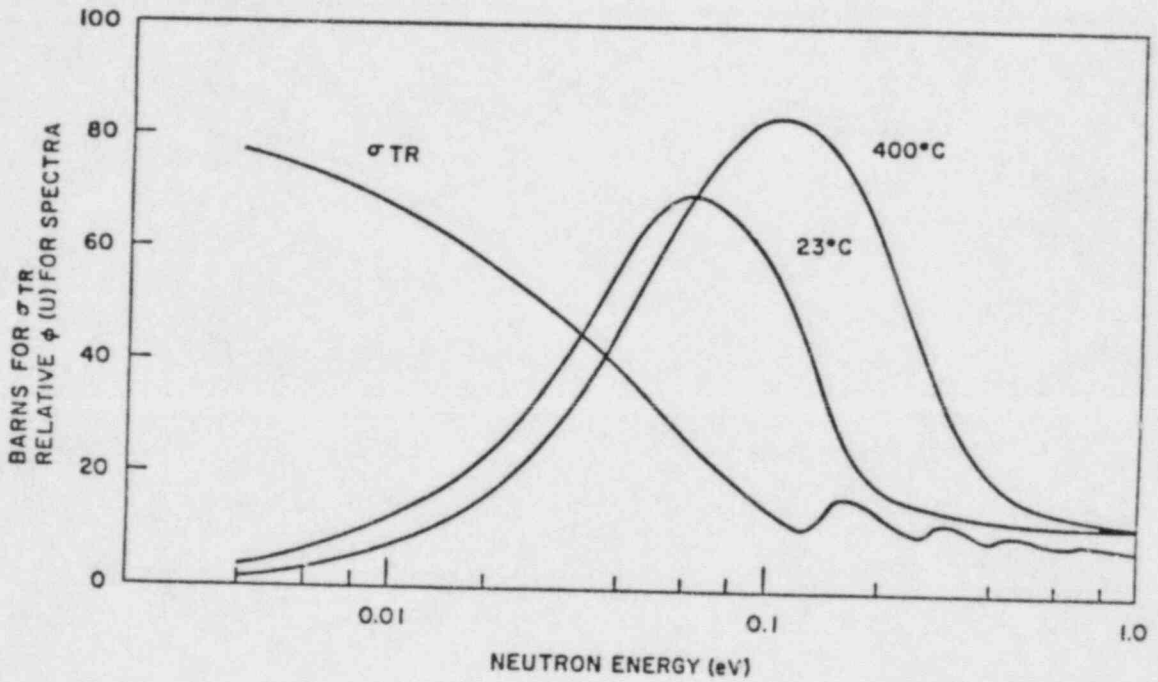

3-32

TRANSPORT CROSS SECTION FOR HYDROGEN
IN ZrH AND AVERAGE NEUTRON SPECTRA IN FUEL ELEMENT
Figure 3-15

the neutrons with the chemically bound moderator atoms. The bound hydrogen kernels used for hydrogen in the water were generated by the THERMIDOR code [22] using thermalization work of Nelkin [23]. Early thermalization work by McReynolds et al [24] on zirconium hydride has been greatly extended at GA Technologies [25], and work by Parks resulted in the SUMMIT [26] code, which was used to generate the kernels for hydrogen as bound in ZrH. These scattering models have been used to predict adequately the water and hydride (temperature dependent) spectra as measured at the GA Technologies linear accelerator as shown in Figure 3-16 and Figure 3-17 [27].

3.1.2.2. ZrH Model. Qualitatively, the scattering of slow neutrons by zirconium hydride can be described by a model in which the hydrogen atom motion is treated as an isotropic harmonic oscillator with energy transfer quantized in multiples of ~0.14 eV. More precisely, the SUMMIT model uses a frequency spectrum with two branches, one for the optical modes for energy transfer with the bound proton, and the other for the acoustical modes for energy transfer with the lattice as a whole. The optical modes are represented as a broad frequency band centered at 0.14 eV, and whose width is adjusted to fit the cross section data of Woods et al. [28]. The low frequency acoustical modes are assumed to have a Debye spectrum with a cutoff of 0.02 eV and a weight determined by an effective mass of 360.

This structure then allows a neutron to slow down by the transition in energy units of ~0.14 eV as long as its energy is above 0.14 eV. Below 0.14 eV the neutron can still lose energy by the inefficient process of exciting acoustic Debye type modes in which the hydrogen atoms move in phase with the zirconium atoms, which in turn move in phase with one another. These modes therefore, correspond to the motion of a group of atoms whose mass is much greater than that of hydrogen, and indeed even greater than the mass of zirconium. Because of the large effective mass, these modes are very inefficient for thermalizing neutrons, but for neutron energies below 0.14 eV they provide the only mechanism for neutron slowing down within the ZrH. (In a TRIGA core, the water also provides for neutron thermalization below 0.14 eV.) In addition, in the ZrH it is possible for a neutron to gain one or more energy units of ~0.14 eV in one or several scatterings, from excited Einstein oscillators. Since the number of excited oscillators present in a ZrH lattice increases with temperature, this process of neutron speeding up is strongly temperature dependent and plays an important role in the behavior of ZrH moderated reactors.

3.1.2.3. Calculations. Calculations of the temperature coefficient were done in the following steps:

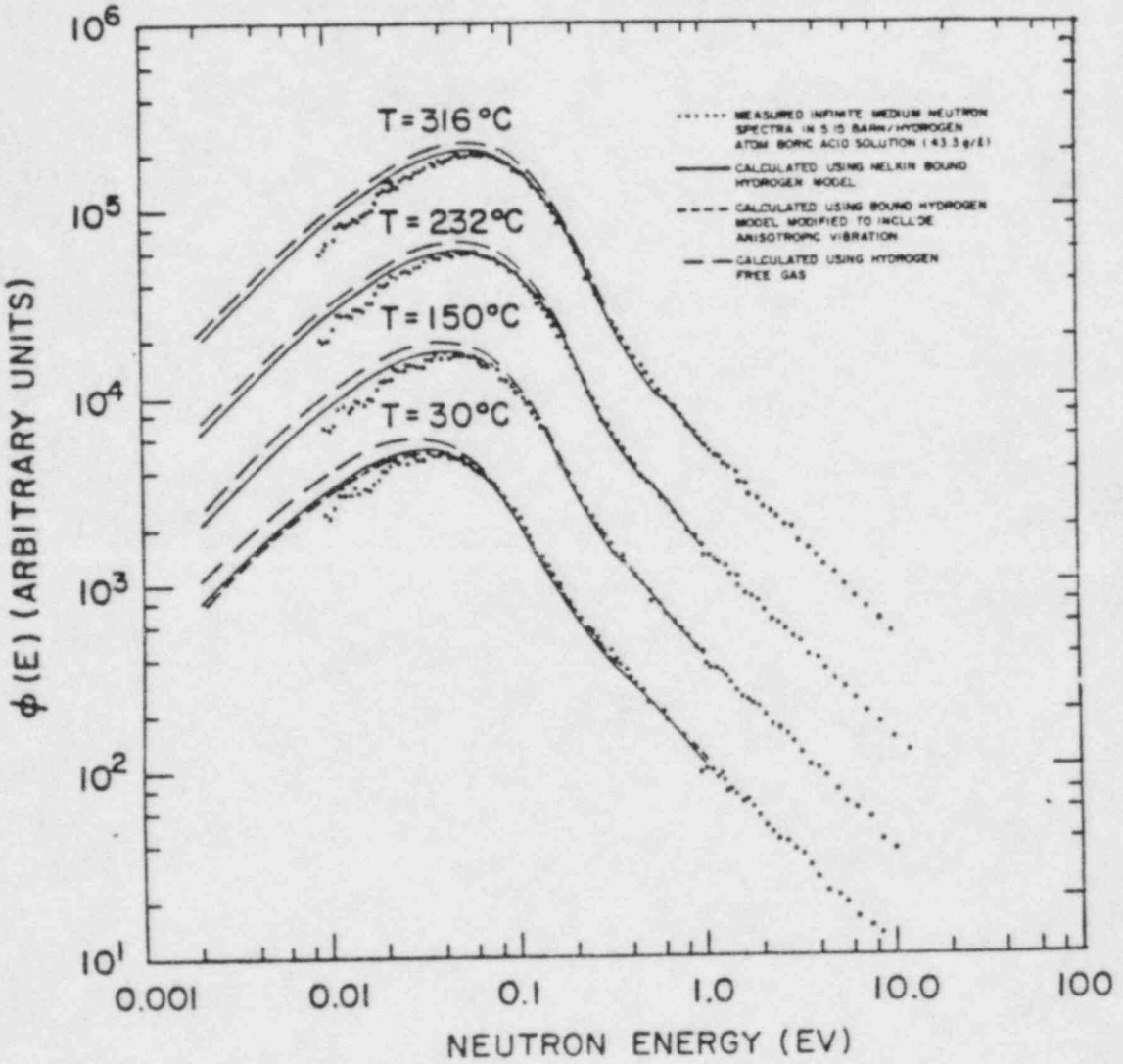

A COMPARISON OF NEUTRON SPECTRA
BETWEEN EXPERIMENTS AND SEVERAL HYDROGEN MODELS
Figure 3-16

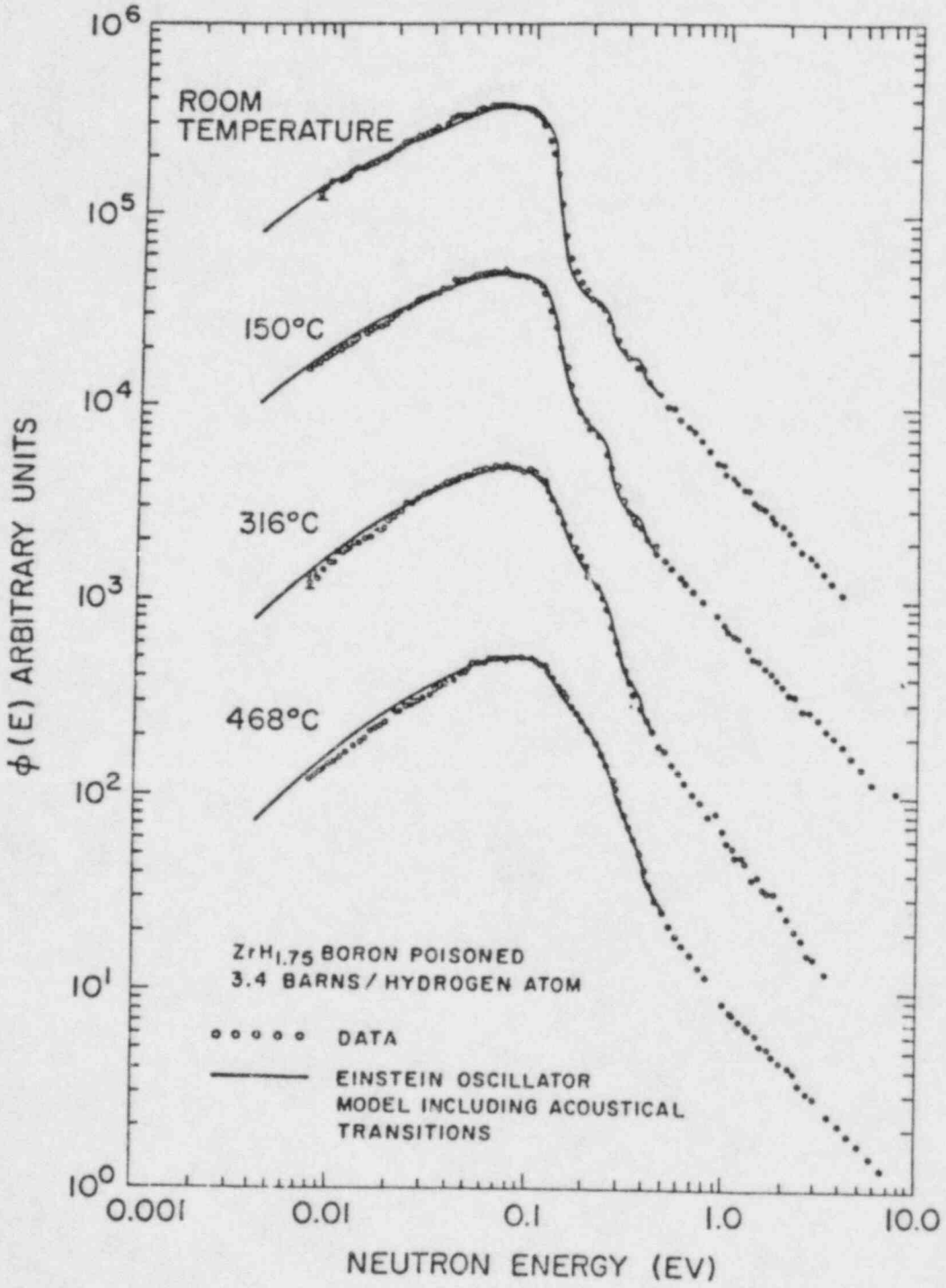

EFFECT OF TEMPERATURE VARIATION ON
ZIRCONIUM HYDRIDE NEUTRON SPECTRA
Figure 3-17

a. Multigroup cross sections were generated by the GGC-3 code for a homogenized unit cell. Separate cross-section sets were generated for each fuel element temperature by use of the temperature dependent hydride kernels and Doppler broadening of the U-238 resonance integral to reflect the proper temperature. Water at room temperature was used for all prompt coefficient calculations.

b. A value for k_∞ was computed for each fuel element temperature by transport cell calculations, using the P_1 approximation. Comparisons have shown S_4 and S_8 results to be nearly identical. Group dependent disadvantage factors were calculated for each cell region (fuel, clad, and water) where the disadvantage factor is defined as the ratio: ϕ_g^r / ϕ_g^c (region/cell).

c. The thermal group disadvantage factors were used as input for a second GGC-3 calculation where cross sections for a homogenized core were generated which gave the same neutron balance as the thermal group portion of the discrete cell calculation.

d. The cross sections for an equivalent homogenized core were used in a full reactor calculation to determine the contribution to the temperature coefficient due to the increased leakage of thermal neutrons into the reflector with increasing hydride temperature. This calculation still requires several thermal groups, but transport effects are no longer of major concern. Thus, reactivity calculations as a function of fuel element temperature have been done on the entire reactor with the use of diffusion theory codes.

Results from the above calculations indicate that more than 50% of the temperature coefficient for a standard TRIGA core comes from the temperature-dependent disadvantage factor or "cell effect", and ~20% each from Doppler broadening of the U-238 resonances and temperature dependent leakage from the core. These effects produce a temperature coefficient of ~-0.01%/°C, which is rather constant with temperature. The temperature coefficient is shown in Figure 3-18 for the high-hydride core of this TRIGA.

3.1.3. Steady-State Reactor Power

The following evaluation has been made for a TRIGA system operating with cooling from natural convection flow around the fuel elements. This analysis investigates the limits to which such a system may be operated.

The analysis was conducted by considering the hydraulic characteristics of the flow channel from which the heat rejection rate is maximum. The geometrical data from this channel are given in Table 3-2. All symbols in Equation 16 through 45 are defined in the list of nomenclature in Section 3.1.3.9.

Table 3-2
HYDRAULIC FLOW PARAMETERS

Flow area (ft^2/elem.)	0.00580
Wetted perimeter (ft/elem.)	0.3861
Hydraulic diameter (ft)	0.0601
Fuel element diameter (ft)	0.1229
Fuel surface area (ft^2)	0.4826

The heat generation rate in the fuel element is distributed axially in a cosine distribution chopped at the end such that the peak-to-average ratio is 1.25. The number of fuel elements in the core is assumed for 1 MW operation, but the departure from nucleate boiling (DNB) ratio is conservatively evaluated on the basis of 85 elements.

The driving force is supplied by the buoyance of the heated water in the core. Countering this force are the contraction and expansion losses at the entrance and exits to the channel, and the acceleration and potential energy losses and friction losses in the cooling channel itself.

Figure 3-19 illustrates schematically the natural convection system established by the fuel elements bounding one flow channel in the core. The system shown is general and does not represent any specific configuration. Steady-state flow is governed by the Equation

$$\delta p_i + \delta p_e + \delta p_l + \delta p_u + \sum_{j=1}^{n} wp_j = z_t / v_o \quad , \qquad (16)$$

where the left-hand member represents the pressure drops through the flow channel due to entrance, exit, friction, acceleration, and gravity losses and the right-hand member represents the driving pressure due to the static head in the pool. The pressure drops through the flow channel are

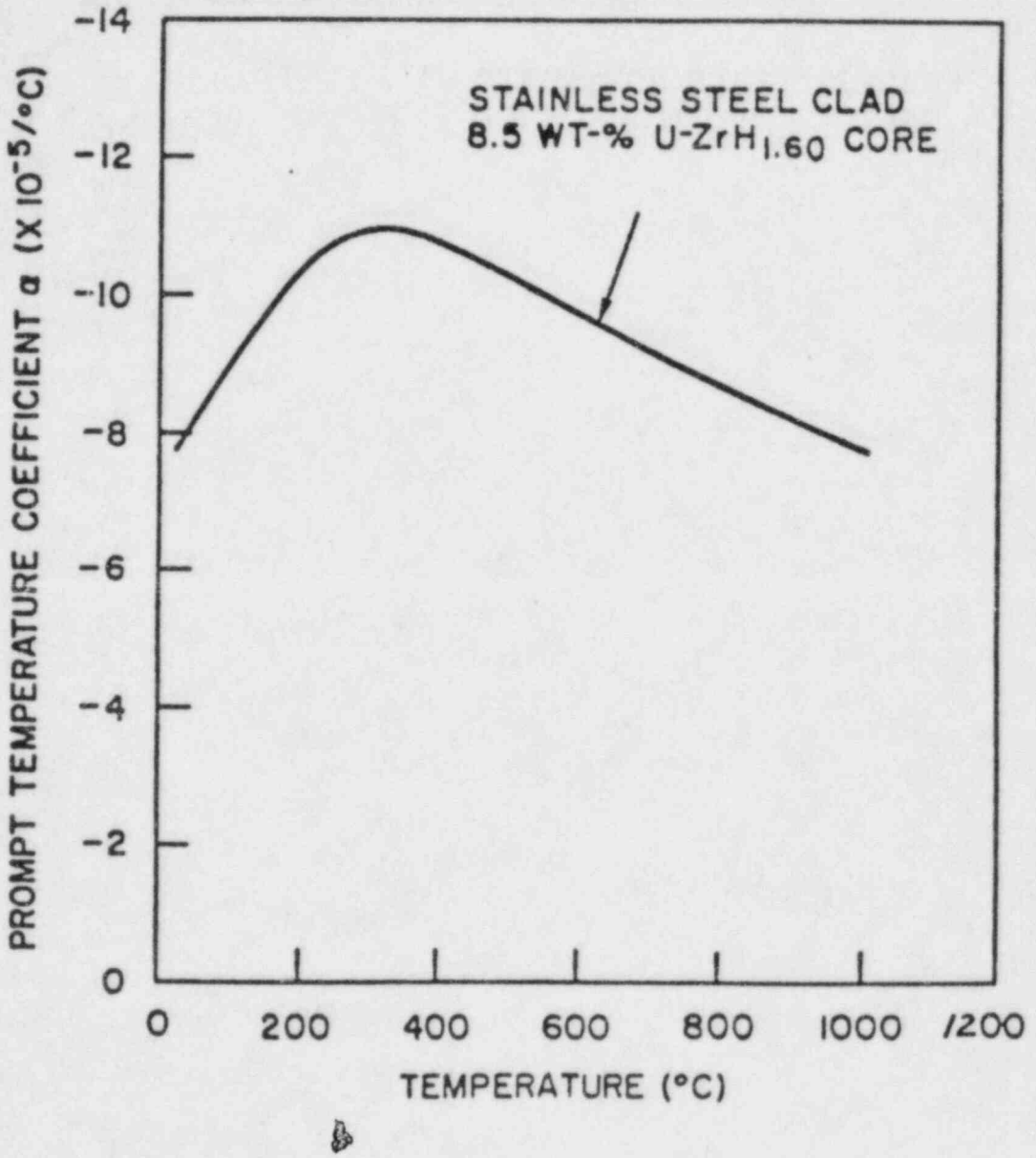

PROMPT NEGATIVE TEMPERATURE COEFFICIENT
VERSUS AVERAGE FUEL TEMPERATURE FOR TRIGA
Figure 3-18

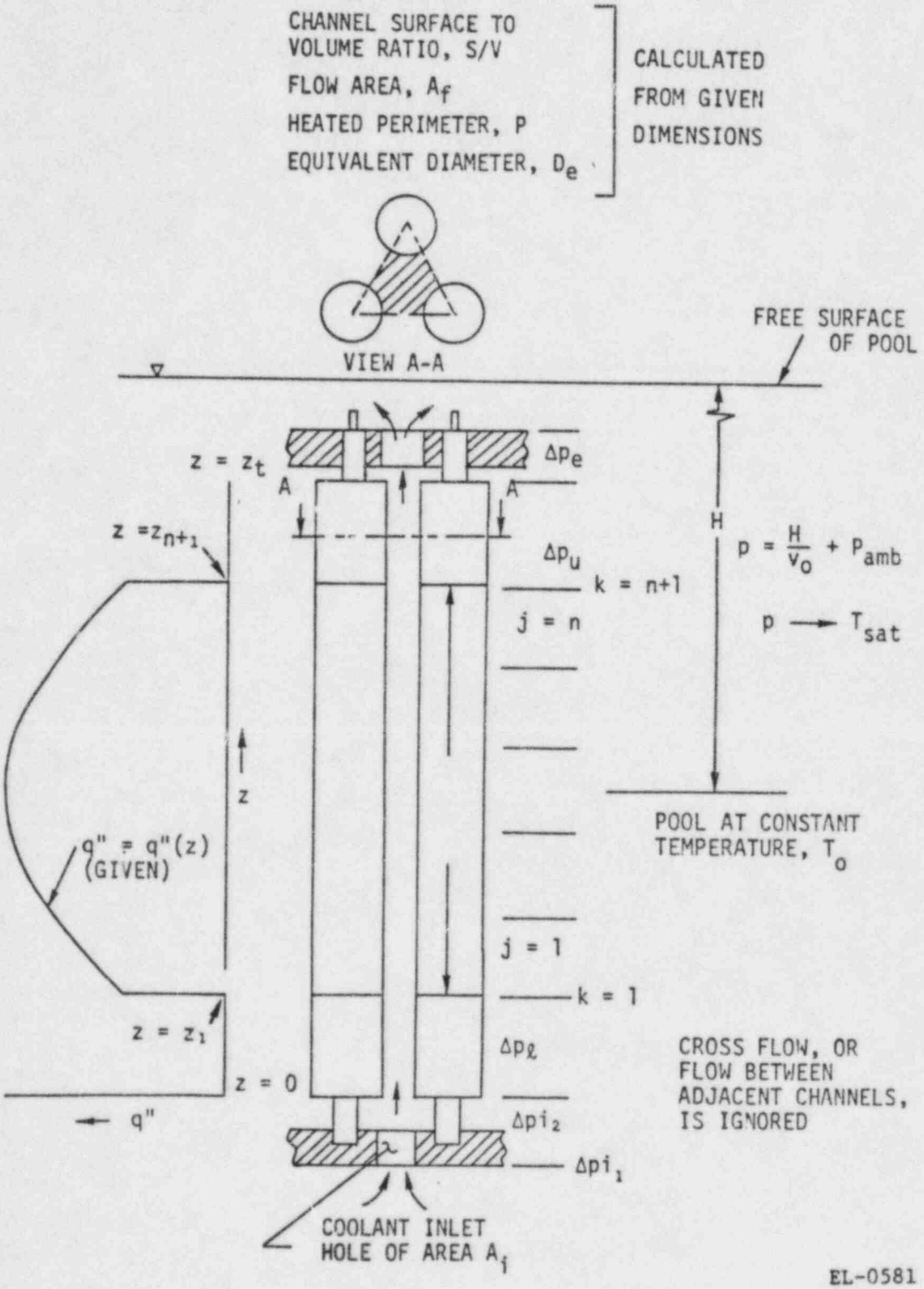

GENERAL FUEL ELEMENT CONFIGURATION FOR SINGLE COOLANT CHANNEL IN THE TRIGA
Figure 3-19

dependent on the flow rate while the available static driving pressure is fixed for a known core height and pool temperature. The analysis, therefore, becomes an iterative one in which the left-hand side of Equation 16 is evaluated on the basis of an assumed flow rate and compared with the known right-hand side until equality is achieved. The method has been programmed for digital computer solution. The methods of evaluating each of the δp terms in Equation 16 for known power distribution and flow geometry and assumed flow rates are discussed below.

3.1.3.1. Entrance Loss, δp_i. The entrance loss, δp_i, may be evaluated in the usual way as a fraction of the velocity head in the lower grid plate hole:

$$\delta p_i = \frac{k_{i_1} + k_{i_2} v_o}{2g A_i^2} (NW)^2 , \qquad (17)$$

where N = the number of channels which receive their flow from a single hole in the lower grid plate,

k_{i_1} = the loss factor for the entrance to the hole in the lower grid plate. For even slight rounding of the entrance, k_{i1} will be no greater than 0.30,

k_{i_2} = the loss factor covering transfer of the flow from the hole in the lower grid plate to the coolant channels. In most cases this can be satisfactorily approximated as a sudden expansion using $k_{i2} = 1.0$.

3.1.3.2. Exit Loss, δp_e. The exit loss is expressed in terms of a coefficient K_e which is the fraction of the velocity head in the flow channel which is not recovered:

$$\delta p_e = \frac{K_e v_{n+1}}{2gA_f^2} W^2 . \qquad (18)$$

The term v_{n+1} is the specific volume at the highest axial station along the heated length of the core. It is evaluated from the temperature T_{n+1} which is obtained from an overall heat balance:

$$T_{n+1} = q_t/WC + T_o , \qquad (19)$$

where $q_t = P \int_{z_1}^{z_{n+1}} q''(z)\, dz$.

3.1.3.3. Loss Through Portion of Channel Adjacent to Lower Reflector, δp_1. The flow is isothermal at the bulk pool temperature so that

$$\delta p_1 = \frac{f_m v_o \delta z_1}{2g D_e A_f^2} W^2 + \frac{\delta z_1}{v_o} . \quad (20)$$

f_m is evaluated from the Moody chart (assuming smooth surface) on the basis of a Reynolds number which is

$$R_e = \frac{D_e v_o}{A_f \nu_o} W . \quad (21)$$

3.1.3.4. Loss Through Portion of Channel Adjacent to Upper Reflector, δp_u. The flow is isothermal at T_{n+1} where T_{n+1} is determined by Equation 19 :

$$\delta p_u = \frac{f_m v_n \delta z_u}{2g De Af^2} W^2 + \frac{\delta z_u}{vn} . \quad (22)$$

f_m is again evaluated from the Moody chart, assuming smooth surface, on the basis of a Reynolds number which is

$$R_e = \frac{D_e v_n}{A_f \nu_n} W . \quad (23)$$

3.1.3.5. Loss Through Each Increment of the Channel Adjacent to the Fueled Portion of the Elements, δp_i. For the present, let us assume that the entire heated portion of the channel is in subcooled boiling. This implies that the wall temperatures calculated from subcooled boiling correlations are lower than those calculated for convection alone and that the liquid is below its saturation temperature at all locations. The pressure drop through an increment is given by

$$\delta p_{n-(n+1)} = \underbrace{\frac{v_{m_{k+1}} - v_{m_k}}{g A_f^2} W^2}_{\text{(acceleration)}} + \underbrace{\frac{f_{b_j} v_{m_j} \delta z}{2g A_f^2 D} W^2}_{\text{(friction)}} + \underbrace{\frac{\delta z}{v_{m_j}}}_{\text{(gravity)}} \quad (24)$$

3.1.3.6. Acceleration Term. v_m denotes the mean specific volume and is larger than the liquid specific volume, because of the vapor voidage:

$$v_m = v/(1-\alpha) . \quad (25)$$

α is the void fraction or the fraction of a channel cross section which is occupied by vapor. α may be calculated from the vapor volume (cubic in. vapor/square in. heating

surface) and the flow channel geometry. Denoting the vapor volume as ξ,

$$\alpha = \xi \ (S/V) \tag{26}$$

where S/V is the surface to volume ratio of the coolant channel. The parameter ξ, is dependent on the surface heat flux, the subcooling of liquid and the velocity of the liquid. It can be evaluated only by experiment. Data given by Jordan and Leppert [29] were used to estimate ξ; these data are plotted in Figures 3-20 and 3-21. Most of this represents a flow velocity of 4 ft/sec and appears to be the only available data applicable under the thermal conditions encountered in TRIGA type reactors. Extrapolations from these data are made for flow velocities different from 4 ft/sec. The extrapolations were based on a small amount of data given for flow velocities other than 4 ft/sec. The liquid temperature at a station, T_k, may be calculated from

$$T_k = \frac{P \int_{z_1}^{z_k} q''(z)dZ}{WC} + T_o \ . \tag{27}$$

Therefore, one finds ξ (Figure 3-21) from $T_{sat} - T_k$ and q_k'', where T_{sat} and q_k'' are known.

Since $\alpha_k = \xi_k \ (S/V)$

and v_k is a function of T_k, v_m may be evaluated from Equation 25.

3.1.3.7. Friction Term. v_{m_j} denotes a linear average of the mean specific volumes at the upper and lower boundaries of an increment. The approximate mean value is assumed to apply over the entire increment so that

$$v_{m_j} = \frac{v_{m_k} + v_{m_{k+1}}}{2} \ . \tag{28}$$

A friction factor f_{bj} is applied locally to calculate the friction pressure drop over the increment in subcooled boiling. Jordan and Leppert develop the correlation

$$f_b = 8 \ S_t = \frac{8 \ h_b}{\rho \ CV} = \frac{8 \ q''}{\rho \ CV \ (T_w - T)} \tag{29}$$

and provide experimental verification near atmospheric pressure in the range $0.0015 < S_t < 0.0050$. This is simply an extension of Reynolds' analogy to the case of subcooled boiling. The Equation of continuity is used to write Equation 29 as

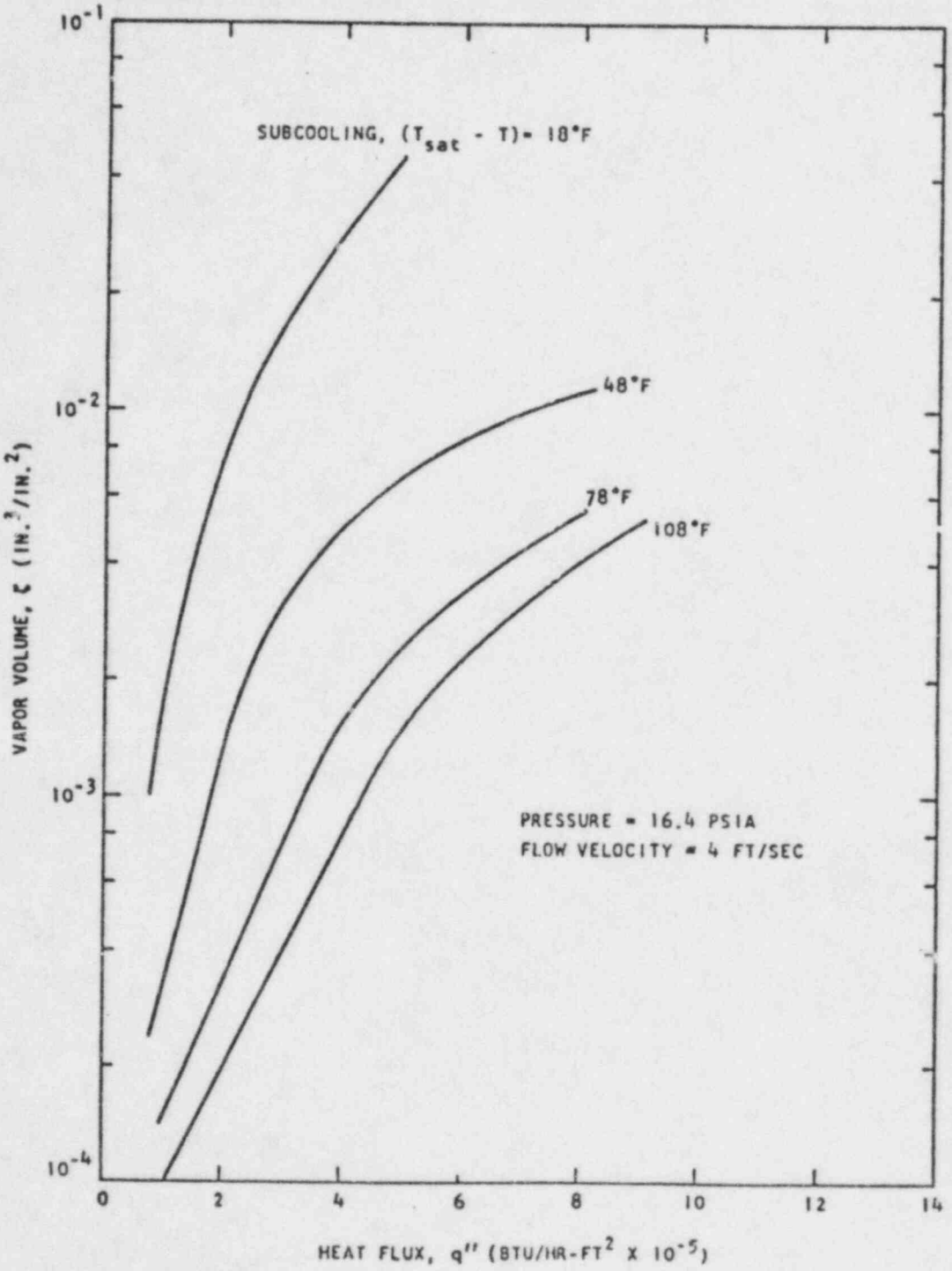

EXPERIMENTALLY DETERMINED VAPOR VOLUMES FOR
SUBCOOLED BOILING IN A NARROW VERTICAL ANNULUS
Figure 3-20

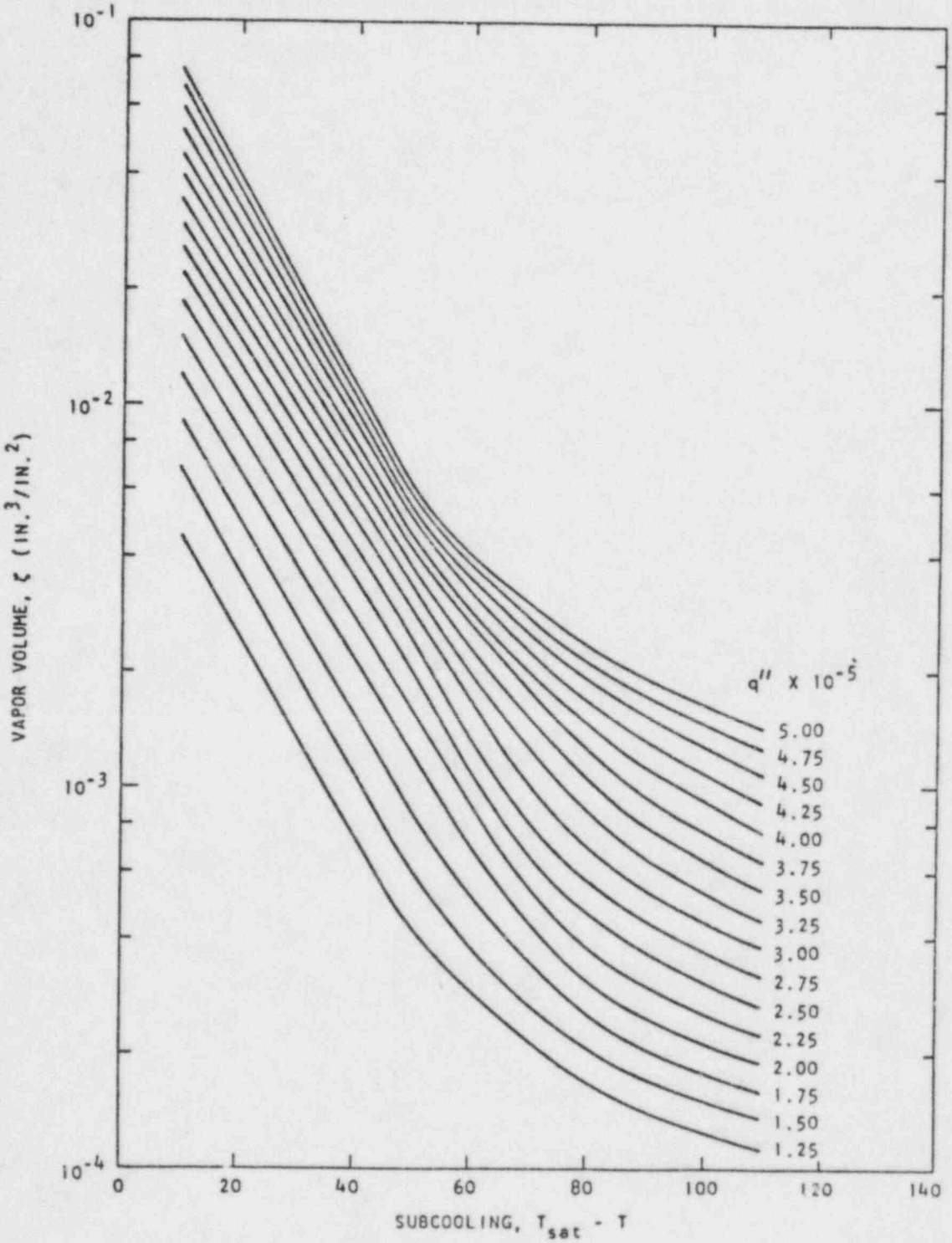

CROSS PLOT OF Figure 3-20 USED IN CALCULATIONS
Figure 3-21

$$f_b = \frac{8\ q''\ A_f}{WC\ (T_w - T)} \qquad (30)$$

which may be evaluated if T_w is known. For subcooled boiling, the heat transfer is usually defined by an experimentally determined correlation of q" vs $(T_w - T_{sat})$ which has been obtained over a given range of flow velocity and pressure. McAdams [30] gives such a correlation for pressures between 2 and 6 atmospheres and flow velocities between 1 and 12 ft/sec. This correlation will be used to determine T_w for use in Equation 30.

Approximate mean values are assumed to apply over the entire increment so that

$$f_{b_j} = 1/2\ \frac{8\ A_f}{WC}\ \left[\ \frac{q''_k}{T_{wk} - T_k} + \frac{q''_{k+1}}{T_{Wk+1} - T_{k+1}}\ \right]\ , \qquad (31)$$

$$\text{and } T_w - T_{sat_j} = \frac{\Phi(q''_k) + \Phi(q''_{k+1})}{2}\ ,$$

where $\Phi(q'')$ is the correlation of McAdams previously cited.

3.1.3.8. Gravity Term. The gravity term is evaluated from v_j calcuated from Equation 28.

As implied in Section 3.1.3.5., each increment must be checked to determine whether heat is being transferred by subcooled boiling or by convection. T_w is evaluated at the lower boundary of the increment on the basis of both the correlation from McAdams for subcooled boiling and a standard correlation for convection (Dittus-Boelter). If the T_w calculated from convection correlations is less than that obtained for subcooled boiling, boiling is assumed not to be present in the increment. Equation 24 still applies, but since there is no boiling and hence no vapor void, v_m becomes v and f_b becomes f_m.

In the foregoing analysis an assumption was made that all of the vapor formed on the surface of the fuel element detaches and adds to the fluid buoyancy. This is not a conservative assumption. The position where vapor bubbles first leave the heated surface is obtained from two considerations; first, the balance of the forces exerted on the vapor bubble while it is in contact with the wall (buoyancy, surface tension, and friction), and, second, the temperature distribution in the single phase liquid away from the walls.

Determinitation of the buoyance forces resulting from the formation and subsequent detachment of vapor bubbles is complicated by the difficulty in predicting the point at which the vapor detaches, and the fraction of that vapor

which subsequently condenses. The problem was simplified by making use of an analysis performed by Levy [31] to determine the position at which the vapor detaches from the wall, assuming that at that point all of the vapor detaches and, finally, that there is no recombination of the vapor with subcooled fluid.

According to Levy the position at which the vapor leaves the surface is obtained from considering the balance of forces exerted on the vapor bubble while it is in contact with the wall, and the temperature distribution in the single phase liquid away from the wall.

The forces acting on the bubble in the vertical direction consist of a buoyant force, F_B; a frictional force, F_F; exerted by the liquid on the bubble; and a vertical component of the surface tension force, F_S.

The buoyant force, F_B, is given by

$$F_B = \frac{C_B \, r_B^3 \, (\rho_L - \rho_v) g}{g_c} \quad , \tag{32}$$

where r_B is the bubble radius, CB is a proportionality constant, ρ_L and ρ_v are the liquid and vapor density, g is the acceleration due to gravity and g_c is a conversion ratio from lb-force to lb-mass. The frictional force, F_F, is related to the liquid frictional pressure drop per unit length, $(-dp/dz)_F$. The pressure differential across the bubble is proportional to the pressure differential times the bubble radius and it acts across an area proportional to the square of the bubble radius. Relating the pressure differential to the wall shear stress τ_w by

$$-(dp/dz)_F = 4 \, \tau_w / D_H \quad , \tag{33}$$

there results for F_F:

$$F_F = C_F \frac{\tau_w}{D_H} r_B^3 \quad , \tag{34}$$

where C_F is a constant of proportionality and D_H is the hydraulic diameter (four times the cross-sectional area divided by the wetted perimeter). The surface tension force, F_S, is given by

$$F_S = C_S \, r_B \, \sigma \quad , \tag{35}$$

where C_S is a proportionality constant and σ is the surface tension. Assuming upward flow the balance of these forces results in the following solutions for the bubble radius:

$$r_B = \left[\frac{C_S \sigma}{C_B \frac{g}{g_c} (\rho_L - \rho_v) + C_F \frac{\tau_w}{D_H}} \right]^{1/2} \quad (36)$$

Assuming that the distance from the wall to the tip of the bubble is proportional to the bubble radius, a non-dimensional distance corresponding to this real distance can be given by

$$Y_B = C \frac{(\sigma g_c D_H - \rho_L)^{1/2}}{\mu_L} \left[1 + C' \frac{g}{g_c} \frac{(\rho_L - \rho_v) D_H}{\tau_w}\right]^{-1/2} \quad (37)$$

where C and C' are appropriate constants. For those cases where the fluid forces are considerably greater than the buoyant forces this expression reduces to

$$Y_B = C (\sigma g_c D_H - \rho_L)^{1/2} 1/\mu_L \quad . \quad (38)$$

For the bubble to detach, the fluid temperature at the tip of the bubble must exceed the saturation temperature by an amount such that the pressure differential acting across the interface at the tip of the bubble balances the surface tension forces at the same position. By using the Clausius-Clapeyron solution of this pressure differential one finds that the fluid temperature-saturation temperature difference can be assumed to be zero.

The temperature at the tip of the bubble can also be specified from existing solutions for the fluid temperature distribution. Thus, if the flow is assumed to be turbulent, and using the solution proposed by Martinelli, we have

$$T_w - T_B = \theta P_r Y_B \; ; \qquad 0 \leq Y_B \leq 5 \quad (39)$$

$$= 50 \{Pr + \ln [1 + Pr (Y_B/5 - 1)]\} \; ; \qquad 5 \leq Y_B \leq 30$$

$$= 50 \{Pr + \ln [1 + 5 Pr] + 0.5 \ln [Y_B/30]\} \; ; \quad Y_B > 30.$$

The parameter θ is a non-dimensional term defined through the heat flux and liquid specific heat, that is,

$$\theta = \frac{q/A}{\rho_L C_{pL} (\tau_w g_c/\rho_L)^{1/2}} \quad . \quad (40)$$

Levy obtained values for the constants C and C' by correlation with available experimental data. Using the accepted heat-transfer relation from Dittus-Boelter, one obtains

$$hD_H/k_L = 0.023 (WD_H/\mu_L)^{0.8} (Pr)^{0.4} \quad . \quad (41)$$

Calculating the friction factor from

$$f = 0.0055\{1 + [20{,}000(\varepsilon/D_H) + 10^6/(WD_H/\mu_L)]^{1/3}\}, \quad (42)$$

we are able to find the wall shear stress from

$$\tau_w = (f/8)\ (W^2/\rho_L\ g_c) \quad , \quad (43)$$

The correlation with experiment yielded values for the constants of

$$C = 0.015 \quad , \quad (44)$$

$$C' = 0 \quad .$$

Finally, from the definition of the heat transfer coefficient, one obtains

$$T_w - T = q''/h \quad , \quad (45)$$

and setting the bubble tip temperature, T_B, equal to the saturation temperature, T_{sat}, we can express the relationship between the saturation temperature, the wall temperature, and the fluid temperature at which the bubble would detach from the wall by

$$(T_w - T_{sat})/(T_w - T) = 0.023\ (WD_H/\mu_L)^{-0.2}\ (Pr)^{-0.6}(f/8)^{-0.5}\ \Omega, \quad (46)$$

where $\Omega = Pr\ Y_B$; $0 < Y_B < 5$

$= 5\ \{Pr + \ln\ [1 + Pr\ (0.2\ Y_B - 1)]\}$; $5 \leq Y_B < 30$

$= 5\ \{Pr + \ln\ (1 + 5Pr) + 0.5\ \ln\ (Y_B/30)\}$; $Y_B \geq 30.$

The solution of the force balance equation with void detachment was accomplished by iterating on the void detachment point to find where the right and left sides of Equation 46 were equal. The point at which the void was assumed to seperate from the surface was taken as the point at which equality obtained.

The peak heat flux, that is, the heat flux at which there is a departure from nucleate boiling and the transition to film boiling begins, was determined by two correlations. The first, given by McAdams [32], indicates that the peak heat flux is a function of the fluid velocity and the fluid only. The second correlation is due to Bernath [33]. It encompasses a wider range of variables over which the correlation was made and it takes into account the effect of different flow geometries. It generally gives a lower value for the peak heat flux and is the value used here for determining the minimum DNB ratio, that is, the minimum ratio of the local allowable heat flux

to the actual heat flux. In general, the McAdams correlation gives a DNB ratio 50% to 80% higher than the Bernath correlation.

Figure 3-22 shows the results of this analysis. Here we have plotted the maximum channel heat flux for which the DNB ratio is 1, with bulk pool water temperature as a parameter. It is assumed that all the vapor above the detachment point seperates from the heated surface. From the figure it can be seen that with the design cooling water temperature at the core inlet (120°F) the maximum heat flux is 325 kBTU/hr-ft^2. For a 85 element core with an overall peak-to-average power density ratio of 2.0, this heat flux corresponds to a maximum reactor power of 1900 kW.

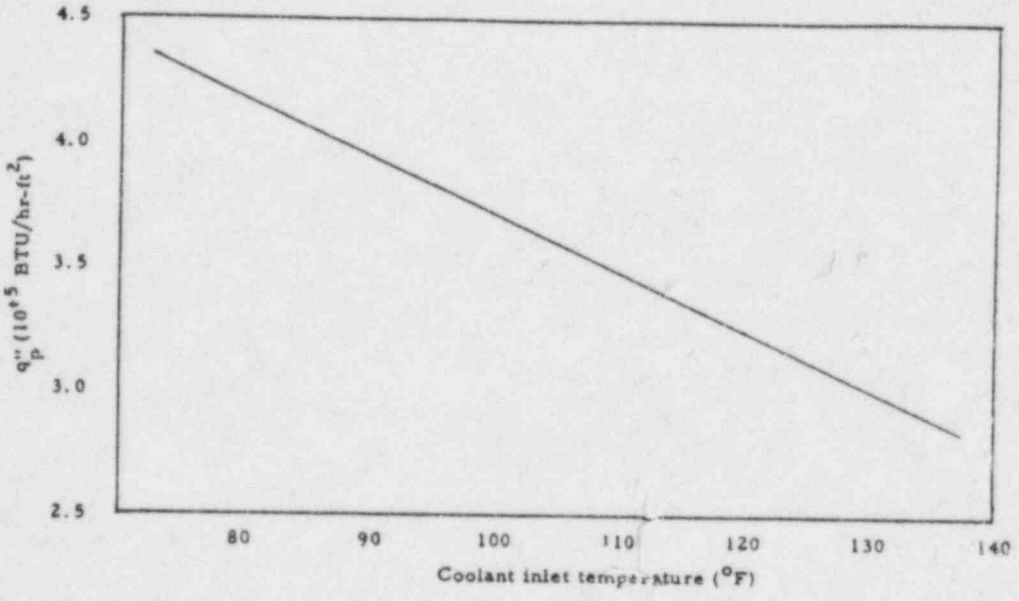

PLOT FOR WHICH DNB RATIO IS 1.0 OF
MAXIMUM HEAT FLUX VERSUS COOLANT TEMPERATURE
Figure 3-22

3.1.3.9. Nomenclature

A	cross-sectional area, ft^2
A_f	channel free flow area, ft^2
C	coolant specific heat, Btu/lb-°F
d	diameter, in.
D_e	channel equivalent diameter, ft
D_H	hydraulic diameter, ft
f_b	friction factor with subcooled boiling, dimensionless
f_m	friction factor without boiling, dimensionless
F	forces acting on vapor bubble
g	constant, 4.18×10^8 ft/hr^2
h_b	heat transfer coefficient with subcooled boiling, Btu/hr-ft^2 -°F
H	distance from midplane of heated channel to free surface of pool, ft
K	pressure loss factor at channel inlet or exit, dimensionless
n	number of equal axial increments into which heated length of core is subdivided
N	Number of channels which receive their flow from a single opening in the lower grid plate
p	absolute pressure, lb/ft^2
P	heated perimeter of channel, ft
Pr	Prandtl number
δp	pressure loss, lb/ft^2
q	heat load, Btu/hr
q_t	total heat load to channel, Btu/hr
q"	heat flux, Btu/hr-ft^2
q_p"	peak or "burnout" heat flux, Btu/hr-ft^2
r_B	bubble radius

R_e	Reynolds number, dimensionless
S/V	channel surface to volume ratio, in.$^{-1}$
T	coolant temperature, °F
T_{sat}	coolant saturation temperature, °F
v	specific volume, ft^3/lb
V	flow velocity, ft/hr
W	mass flow rate, lb/hr
Y	non-dimensional radius
z	axial coordinate in channel, ft
z_t	total length of channel, ft
δz	length of a calculation increment in the channel, ft
μ	dynamic viscosity, ft-lb/hr
α	void fraction or fraction of a channel cross section which is occupied by vapor, dimensionless
σ	surface tension, lb/ft
ξ	vapor volume, or volume of vapor produced per unit area of heated surface, cubic in./square in.
ν	kinematic viscosity, ft^2/hr
τ	shear stress, lb/ft^2
ρ	density, lb/ft^3
ε/D_e	relative roughness

Subscripts

e	conditions at channel exit
i	conditions at channel entrance or inlet
l	conditions in portion of channel adjacent to lower reflector
m	conditions averaged over the liquid and vapor phases
o	bulk pool conditions
u	conditions in portions of channel adjacent to upper reflector
j	axial increment index
k	axial station index
w	conditions at cladding outer surface
v	vapor
L	liquid

3.2. NUCLEAR DESIGN AND EVALUATION

The characteristics and operating parameters of this reactor have been calculated and extrapolated using experience and data obtained from existing TRIGA reactors as bench marks in evaluating the calculated data. There are several TRIGA systems with essentially the same core and reflector relationship as this TRIGA so the values presented here are felt to be accurate to within 5% but, of course, are influenced by specific core configuration details as well as operational details.

Table 3-3 summarizes the typical Mark II TRIGA reactor parameters for a core containing high-hydride, stainless steel clad fuel elements.

Table 3-3
TYPICAL TRIGA CORE NUCLEAR PARAMETERS

Fuel elements	SS-clad U-$ZrH_{1.6}$
Cold clean critical loading	~64 elements ~2.5 kg U-235
Operational loading	~90 elements ~3.4 kg U-235
ℓ Prompt neutron lifetime	41 μsec
β Effective delayed neutron frction	0.0070
α Prompt negative temperature coefficient	~1.0×10^{-4} $\delta k/k°C$
T_f Average fuel temperature (1MW)	260°C
T_w Average water temperature (1MW)	64°C

3.2.1. Reactivity Effects

The reactivity associated with the control rod is of interest both in the shutdown margin and in calculations of possible abnormal conditions related to reactivity accidents. Table 3-4 gives approximate reactivity values associated with a total control rod travel of 15 in. (38.1 cm), the full travel in the core.

Table 3-4
ESTIMATED CONTROL ROD NET WORTH

	diameter in. (cm)	δk/k %
C ring - transient	1.25 (3.18)	2.1
C ring - shim	1.35 (3.43)	2.6
D ring - safety	1.35 (3.43)	2.0
D ring - regulating	1.35 (3.43)	2.0

The maximum reactivity insertion rate is that associated with the transient rod which can be fully removed from the core in 0.1 sec producing an average reactivity insertion rate of 21% δk/k-sec.

The total reactivity worth of the control system is about 8.7%. With a core excess reactivity of 4.9%, the shutdown margin with all rods down is about 3.8% and with the most reactive rod stuck out is about 1%.

The reactivity worth of the fuel elements is dependent on their position within the core. Table 3-5 indicates the values that are expected in this installation.

Table 3-5
ESTIMATED FUEL ELEMENT REACTIVITY WORTH COMPARED WITH WATER AS A FUNCTION OF POSITION IN CORE

Core Position	Worth (% δk/k) SS Clad $U\text{-}ZrH_{1.6}$	Number of Fuel Positions
B ring	1.07	6
C ring	0.85	12
D ring	0.54	18
E ring	0.36	24
F ring	0.25	30
G ring	0.19	36

Because of the prompt negative temperature coefficient a significant amount of reactivity is needed to overcome temperature and allow the reactor to operate at the higher power levels in steady-state operation. Figure 3-23 shows the relationship of reactor power level and associated reactivity loss to achieve a given power level. Figure 3-24 relates fuel temperature to a given steady-state reactor power level.

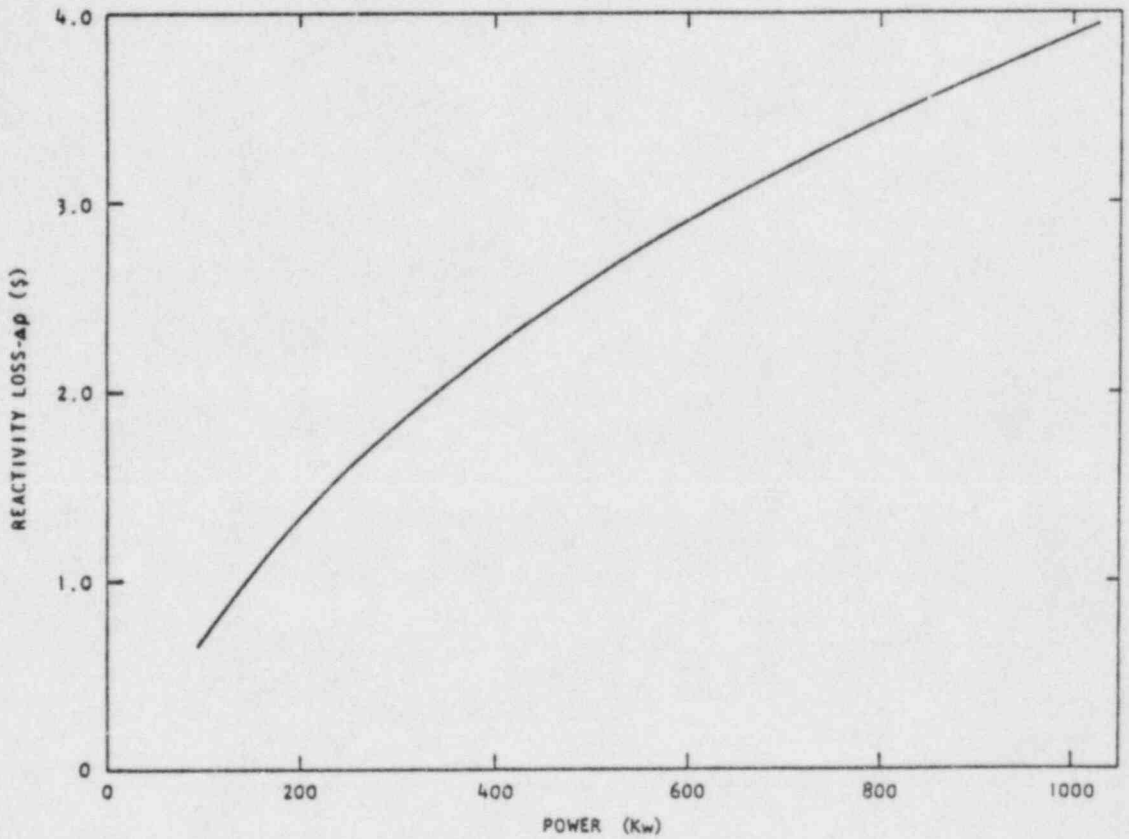

ESTIMATED REACTIVITY LOSS VERSUS POWER
Figure 3-23

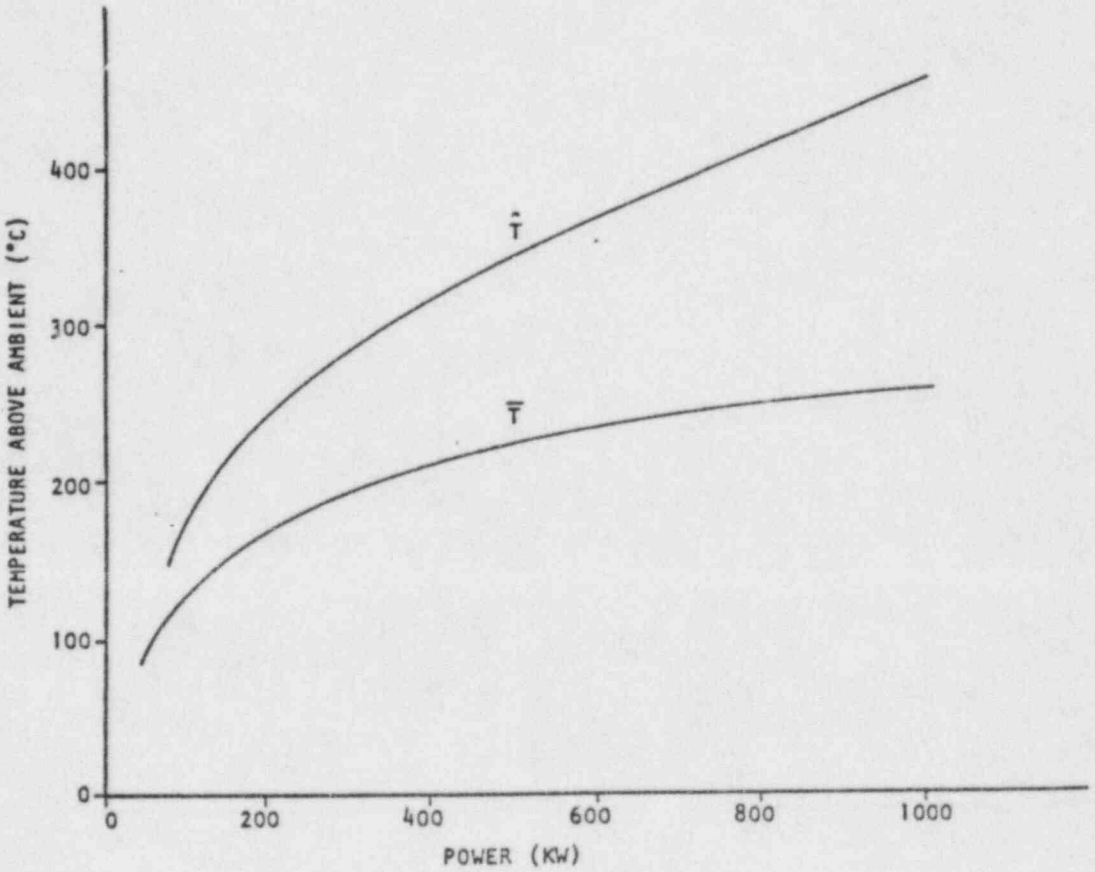

ESTIMATED MAXIMUM B RING AND
AVERAGE CORE TEMPERATURE VERSUS POWER
Figure 3-24

The reactivity effects associated with the insertion and removal of experiments in or around the core are difficult to predict; however, Table 3-6 is supplied to provide a guide to the magnitude of the reactivity effects associated with the introduction of experiments in the reactor core.

Table 3-6
EXPECTED REACTIVITY EFFECTS ASSOCIATED WITH EXPERIMENTAL FACILITIES

	Worth (% δk/k)
Central thimble, fuel vs H_2O	+0.90
Central thimble, void vs H_2O	-0.15
Pneumatic transfer tube, (G ring) void vs H_2O	-0.10
Rotary specimen rack, void vs H_2O	-0.20

3.2.2. Evaluation of Nuclear Design

The TRIGA reactor system is well-known for its conservative design. The stability of this reactor type has been proven both through calculations as well as through tests performed with the many TRIGA reactors in operation throughout the world. The stability of the TRIGA type reactor stems from the prompt negative temperature coefficient associated with the U-ZrH_x fuel in conjunction with a suitable neutron thermalizing material. This TRIGA will have the stability that has been demonstrated on other TRIGA systems over the years.

A review of the reactivity worths associated with the reactor core indicates that no single item listed can produce a step reactivity insertion greater than that offered by routine pulse operation. In the pulsed mode of operation the results of a step insertion of $3.00 are far below those attributed to test pulses on the advanced TRIGA prototype reactor in which 3.5% δk/k was inserted in a step as is shown in Table 3-7.

Therefore before experimental facilities are used, the worth of the experiment should be carefully evaluated. If the experiment is worth more than $3.00, a special safety analysis should be prepared.

Table 3-7
COMPARISON OF REACTIVITY INSERTION EFFECTS

	Pulse Resulting from Insertion of Maximum Excess Reactivity in This TRIGA	Max Pulse Tested on SS-Clad, High Hydride Fueled TRIGA types
Reactivity insertion, $	3.00	5.00
Steady-State power before pulse, kW	<1	<1
Peak power, MW	~1400	~8400
Total energy release, MW-sec	~18	~54
Period, msec	~3.1	~1.4
Max fuel temperature, °C	~540	~1050
Pulse width, msec	~11	~5.5

The possibility of a reactivity accident which could produce reactor powers and fuel temperatures attributed to a $4.00 step insertion has been considered and evaluated in the accident analysis section of this report. It is concluded from this analysis that the peak and average fuel temperatures resulting from this accident are well below the temperatures indicated as safety limits described in the reactor design bases of this document. It is further concluded that the integrity of the fuel containment will not be jeopardized and no adverse effects to the reactor system or personnel will arise from the advent of such an accident.

3.3 THERMAL AND HYDRAULIC DESIGN

This TRIGA reactor will be operated with natural convective cooling by reactor pool water. This method of heat dissipation is more than adequate for the power level of the reactor; i.e. 1000 kW(t). That is,the thermal and hydraulic design of the reactor is well within the safety limits required to assure fuel integrity.

3.3.1. Design Bases

The thermal and hydraulic design for this TRIGA is based on assuring that fuel integrity is maintained during steady-state and pulsed mode operation as well as during those abnormal conditions which might be postulated for reactor operation. During steady-state operation fuel integrity is maintained by limiting reactor powers to values which assure that the fuel cladding can transfer heat from the fuel to the reactor coolant without reaching fuel-clad temperatures that could result in clad rupture. If these temperature conditions were exceeded, the maximum local heat flux in the core would be greater than the heat flux at which there is a departure from the nucleate boiling regime and consequently film blanketing of the fuel. This heat flux safety limit is a function of the inlet coolant temperature. Figure 3-22 summarizes the results of the thermal and hydraulic analysis for steady-state operation of the TRIGA. In the figure critical heat flux for departure from nucleate boiling is plotted as a function of the coolant inlet temperature. The maximum power density in a TRIGA core is found by multiplying the average power density by a radial peak-to-average power generation ratio of 1.6 and an axial value of 1.25.

The correlation used to determine the heat flux at which there is a departure from nucleate boiling is from Bernath [33]. This correlation encompasses a wider range of experimental data than the usual correlations, e.g., the correlation due to McAdams, and, generally gives a lower value for the DNB ratio than the other correlations.

During pulsing operation the limiting thermal-hydraulic condition is the fuel temperature and the corresponding H_2 overpressure beyond which clad rupture may occur. As indicated in Section 3.1, coolant temperature is not a limiting condition in pulsing since heating conditions are essentially adiabatic and significant transfer of heat energy to the coolant does not occur until after peak fuel-clad temperatures occur.

The safety limit on fuel temperature occuring in the pulse mode of operation is 1150°C. This temperature will give an internal equilibrium hydrogen pressure (U-ZrH fuel, H/Zr; 1.6) less than that which would produce a stress equivalent to the ultimate strength of the clad at a temperature of 680°C. This clad temperature is higher than would actually occur and therefore conservative even in the case of a pulse producing a peak adiabatic fuel temperature of 1150°C.

Table 3-8 lists the pertinent heat transfer and hydraulic parameters for the TRIGA operating at 1000 kW.

These data were taken from the results of calculations described in Section 3.1.

Table 3-8
1000 kW(t) TRIGA HEAT TRANSFER AND HYDRAULIC PARAMETERS

Number of fuel elements	90
Diameter	1.475 in.
Length (heated)	15.0 in.
Flow area	0.522 ft^2
Wetted perimeter	34.75 ft
Hydraulic diameter	0.0601 ft
Heat transfer surface	43.44 ft^2
Inlet coolant temperature	120°F (48.9°C)
Exit coolant temperature (average)	174°F (78.9°C)
Coolant mass flow	63,700 lb/hr
Average flow velocity	0.55 ft/sec
Average fuel temperature	500°F (260°C)
Maximum wall temperature	280°F (138°C)
Maximum fuel temperature	842°F (450°C)
Average heat flux	78,600 Btu/hr-ft^2
Maximum heat flux	157,100 Btu/hr-ft^2
Minimum DNB ratio	2.0

3.3.2. Thermal and Hydraulic Design Evaluation

The validity and safety of the TRIGA thermal-hydraulic design is established in Section 3.1. In that section it is shown that design-basis conditions evaluated for TRIGA reactors using stainless steel clad U-ZrH (H/Zr;1.6) fuel elements provide a generous safety margin for this TRIGA. These general evaluations are supported by extensive experience in operation of TRIGA cores at equivalent fuel temperatures and reactor power levels. No adverse results are reported from operation of TRIGA cores at fuel temperatures and power levels greater than this design.

3.4. MECHANICAL DESIGN AND EVALUATION

3.4.1. General Description

The TRIGA Mark II reactor core assembly is located near the bottom of a elongated cylindrical aluminum tank surrounded by a reinforced concrete structure. A typical installation is shown in Figure 3-25. The standard reactor tank is a welded aluminum vessel with 1/4-in.-thick walls, a diameter of approximately 2 meters, and a depth of approximately 7.6 meters. The tank is all-welded for water tightness. The integrity of the weld joints is verified by radiographic testing, dye penetrant checking, and leak testing. The outside of the tank is coated for corrosion protection.

An aluminum angle used for mounting the ion chambers, fuel storage racks, underwater lights, and other equipment, is located around the top of the tank. Demineralized water in the tank is provided such that approximately 6.4 meters of shielding water above the core. The core is shielded radially by a minimum of 2.91 meters of ordinary concrete with a density of 2.4 g/cm^3 (or 2.43 meters of concrete with a density of 2.88 gm/cc), ~45cm. (1.5 ft) of water, 25.9 cm. (10.2 in.) of graphite reflector and 5.1 cm. (2 in.) of lead (see Figure 3-26).

3.4.2. Reflector Assembly

The reflector is a ring-shaped block of graphite that surrounds the core radially. The graphite is 10.2 inches (25.91 cm.) thick radially, with an inside diameter of 21-5/8 inches (54.93 cm.) and a height of 21-13/16 inches (54.40 cm.) The graphite is protected from water penetration by a leak-tight welded aluminum can.

A "well" in the top of the graphite reflector is provided for the rotary specimen rack. This well is also aluminum-lined, the lining being an integral part of the aluminum reflector can. The rotary specimen rack is a self-contained unit and does not penetrate the sealed reflector at any point.

The graphite, and outer surface of the aluminum can are pierced by an aluminum tube which forms the inner section of beam ports that penetrate the reflector. The reflector penetrating beam tubes are connected by stainless steel couplings to the corresponding beam tube section fabricated as part of the reactor tank stucture.

The reflector assembly rests on an aluminum platform at the bottom of the tank, and provides the support for the two grid plates and the safety plate. Four lugs are provided for lifting the assembly.

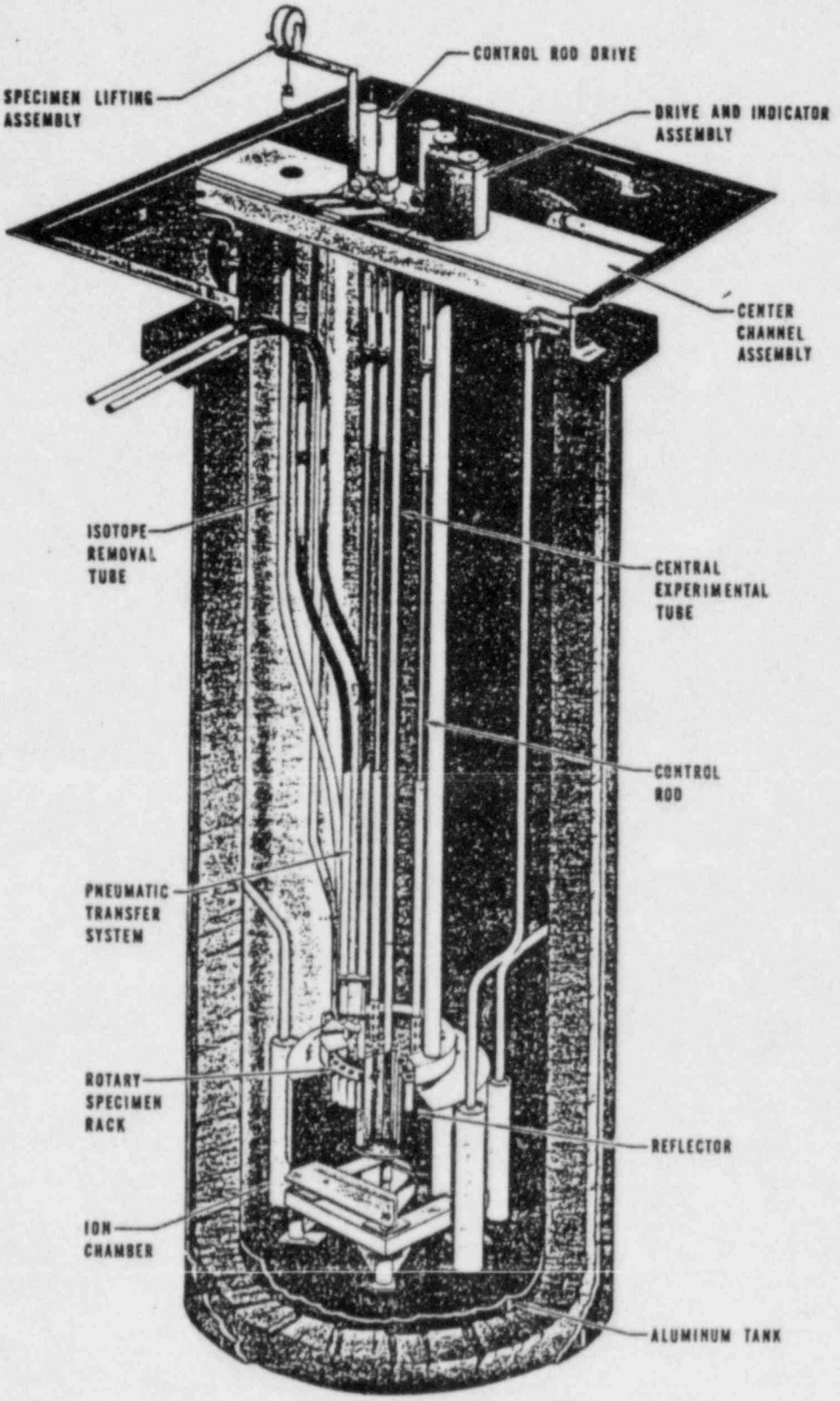

TYPICAL MARK I TRIGA REACTOR
Figure 3-25

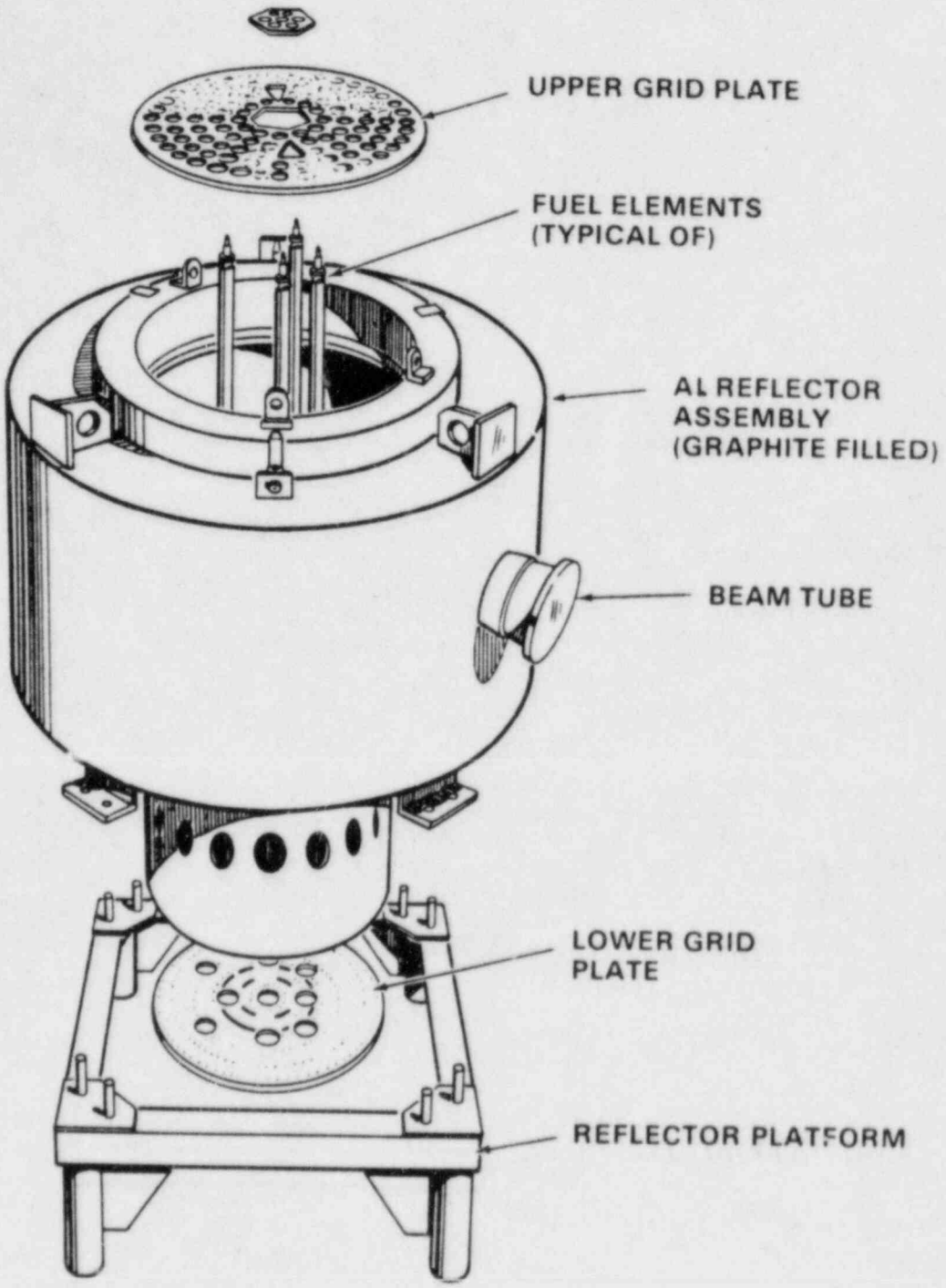

REACTOR, REFLECTOR AND SHIELDING
Figure 3-26

3.4.3. Grid Plates

The top grid plate is an aluminum plate 5/8 inches (1.59 cm.) thick (3/8 inches, 0.95 cm., thick in the central region) that provides accurate lateral positioning for the core components. The plate is supported by a ring welded to the top inside surface of the reflector container and is anodized to resist wear and corrosion.

One hundred twenty six (126) holes, 1.505 inches (3.823 cm.) are drilled into the top grid plate in six circular bands around a central hole to locate the fuel-moderator and graphite dummy elements, the control rods and guide tubes, and the pneumatic transfer tube. (See Figure 3-27.) An equivalent diameter center hole accomodates the central thimble. Small holes at various positions in the top grid plate permit insertion of foils into the core to obtain flux data.

A hexagonal section can be removed from the center of the upper grid plate for the insertion of specimens up to 4.4 inches (11.18 cm.) in diameter into the region of highest flux; this requires prior relocation of the six fuel elements from the B ring to the outer portion of the core and removal of the central thimble. This removable section will not be used initially; a seperate license amendment will be obtained prior to its use.

Two generally triangular-shaped sections are cut out of the upper grid plate. Each encompasses two F and one G ring holes. When fuel elements are placed in these locations, their lateral support is provided by a special fixture. When the fuel elements and support are removed, there is room for inserting specimens up to 2.4 inches (6.1 cm.) in diameter.

The differential area between the fitting at the top of the fuel elements and the round holes in the top grid plate permits passage of cooling water through the plate.

The bottom grid plate is an aluminum plate 3/4 inch (1.91 cm.) thick which supports the entire weight of the core and provides accurate spacing between the fuel-moderator elements. Six pads welded to a ring which is, in turn, welded to the reflector container support the bottom grid plate.

Holes in the bottom grid plate are aligned with fuel element holes in the top grid plate. They are countersunk to receive the adaptor end of the fuel-moderator elements and the adaptor end of the pneumatic transfer tube.

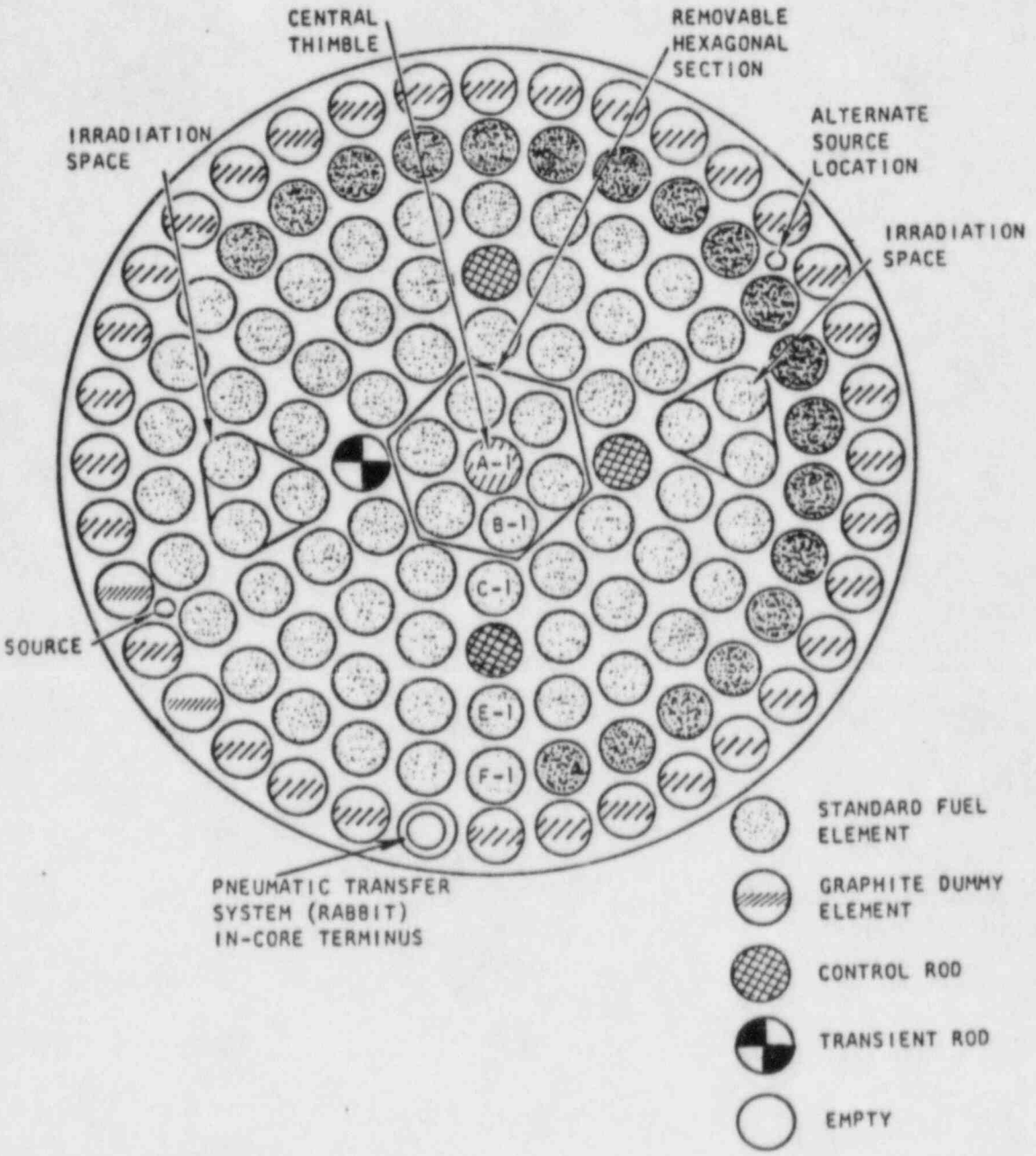

CORE ARRANGEMENT
Figure 3-27

3.4.4. Safety Plate

The safety plate is provided to preclude the possibility of control rods falling out of the core. It is a 1/2 inch (1.27 cm.) thick plate of aluminum welded to the extension of the inner reflector liner and placed about 16 inches below the bottom grid plate.

A central hole of 1.505 inches (3.823 cm.) in diameter in the lower grid serves as a clearance hole for the central thimble. Eight additional 1.505-inch (3.823 cm.) diameter holes are aligned with upper grid plate holes to provide passage of fuel-follower control rods. Those holes in the bottom grid plate not occupied by control rod followers are plugged with removable fuel element adaptors that rest on the safety plate. These fuel element adaptors are solid aluminum cylinders 1.5 inches (3.81 cm.) in diameter by 17 inches (43.18 cm.) long. At the lower end is a fitting that is accomodated by a hole in the safety plate. The upper end of the cylinder is flush with the upper surface of the bottom grid plate when the adaptor is in place. This end of the adaptor has a hole similar to that in the bottom grid plate for accepting the fuel element lower end fitting. With the adaptor in place, a position formerly occupied by a control rod with a fuel follower will now accept a standard fuel element. The adaptor can be removed with a special handling tool.

3.4.5. Fuel-Moderator Elements

The active part of each fuel-moderator element, shown in Figure 3-28, is approximately 1.43 in. (3.63 cm.) in diameter and 15 in. long (38.1 cm.). The fuel is a solid, homogeneous mixture of uranium-zirconium hydride alloy containing about 8.5% by weight of uranium enriched to 20% U-235. The hydrogen-to-zirconium atom ratio is about 1.6. To facilitate hydriding, a small hole is drilled through the center of the active fuel section and a zirconium rod is inserted in this hole after hydriding is complete.

Each element is clad with a 0.020 in. thick (.508 mm.) stainless steel can, and all closures are made by heliarc welding. Two sections of graphite are inserted in the can, one above and one below the fuel, to serve as top and bottom reflectors for the core. Stainless steel end fixtures are attached to both ends of the can, making the overall length of the fuel-moderator element 28.8 in. (73.2 cm.).

The lower end fixture supports the fuel-moderator element on the bottom grid plate. The upper end fixture consists of a knob for attachment of the fuel-handling tool and a triangular spacer, which permits cooling water to flow through the upper grid plate. The total weight of a fully-loaded fuel element is about 3.18 kg. (7 lb).

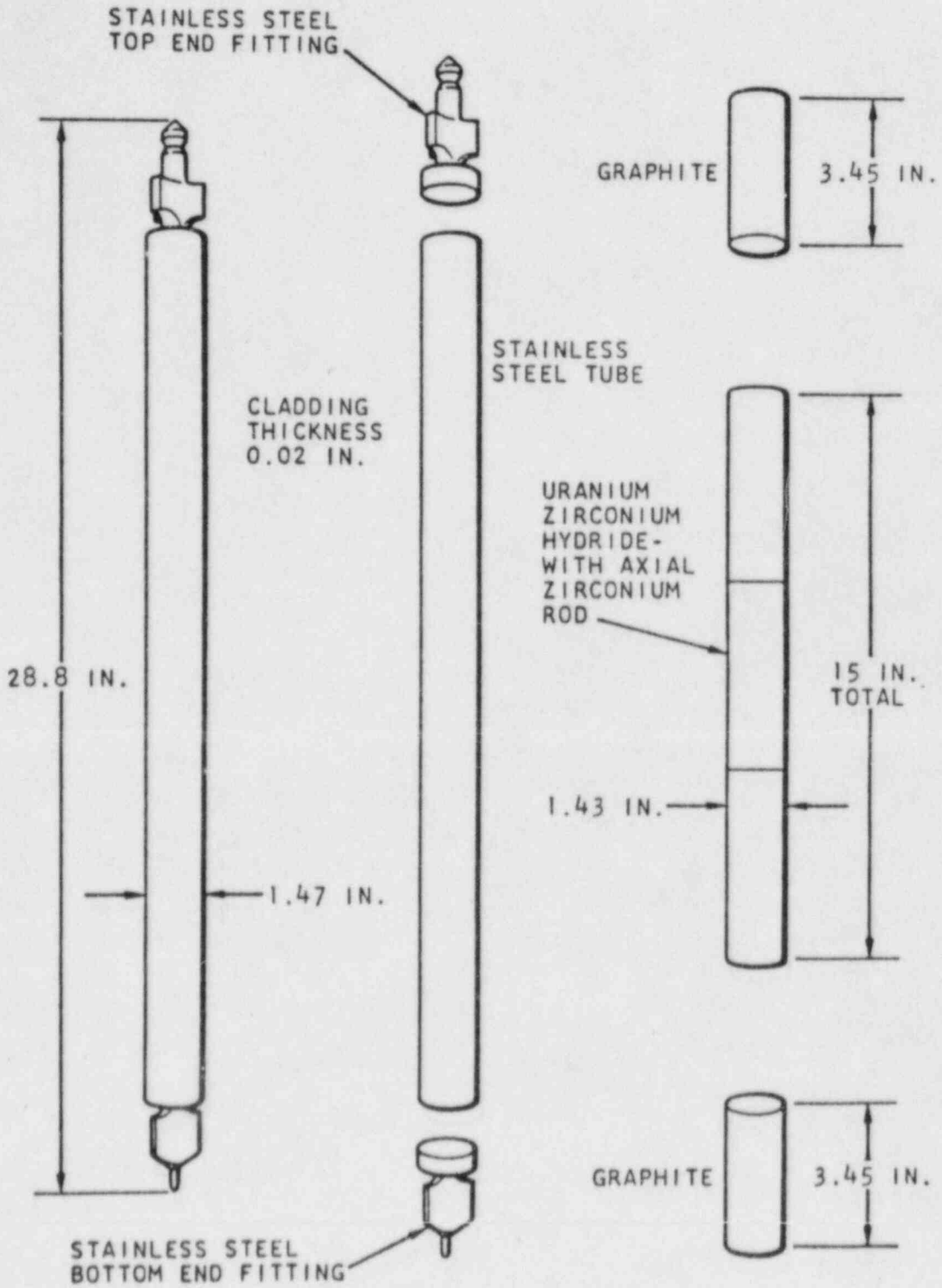

TRIGA STAINLESS STEEL CLAD
FUEL ELEMENT WITH END FITTINGS
Figure 3-28

An instrumented fuel-moderator element will have three thermocouples embedded in the fuel. As shown in Figure 3-29, the sensing tips of the fuel element thermocouples are located about 0.3 in. (0.76 cm.) from the vertical centerline.

The thermocouple leadout wires pass through a seal in the upper end fixture. A leadout tube provides a watertight conduit carrying the leadout wires above the water surface in the reactor pool. Thermocouple specifications are listed in Table 3-9. In other respects the instrumented fuel-moderator element is identical to the standard element.

Most of the fuel for the initial core loading will consist of elements with burnups of a fraction of a MW-day to several MW-days. It is anticipated that an initial core loading of about 94 fuel elements, including instrumented elements, and fuel followed control rods, will produce a cold, clean excess reactivity of ~4.9% δk/k. Table 3-10 gives a summary of the fuel element specifications.

3.4.5.1. Evaluation of Fuel Element Design. General Atomic has acquired extensive experience in the fabrication and operation of high hydride, stainless steel clad fuel elements. As shown in other sections of this report, the stresses associated with the fuel and cladding temperatures in all modes of operation, normal and abnormal, are within the safety limits described in the Reactor Design Bases.

It is concluded that the chemical stability of U-$ZrH_{1.6}$ fuel-moderator material does not impose a safety limit on reactor operation (see Section 3.1.1).

Dimensional stability of the overall fuel element has been excellent in the TRIGA reactors in operation. Analysis of the heat removal from elements that touch owing to transverse bending shows that the contact will not result in hot spots that damage the fuel.

Tests have been conducted on TRIGA fuel elements to determine the strength of the fuel element clad when subjected to internal pressure. At room temperature the clads ruptured at about 2050 psig. This corresponds to a hoop stress at rupture of about 72,000 psi which compares favorably with the minimum expected value for 304 stainless steel.

3.4.6. Neutron Source and Holder

A 2 or 3 curie americiam beryllium neutron source will be used for startup. The neutron source holder is made of aluminum, is cylindrical in shape, and has a cavity to hold the source. The source holder can be installed in any vacant fuel or graphite element location. A shoulder at the

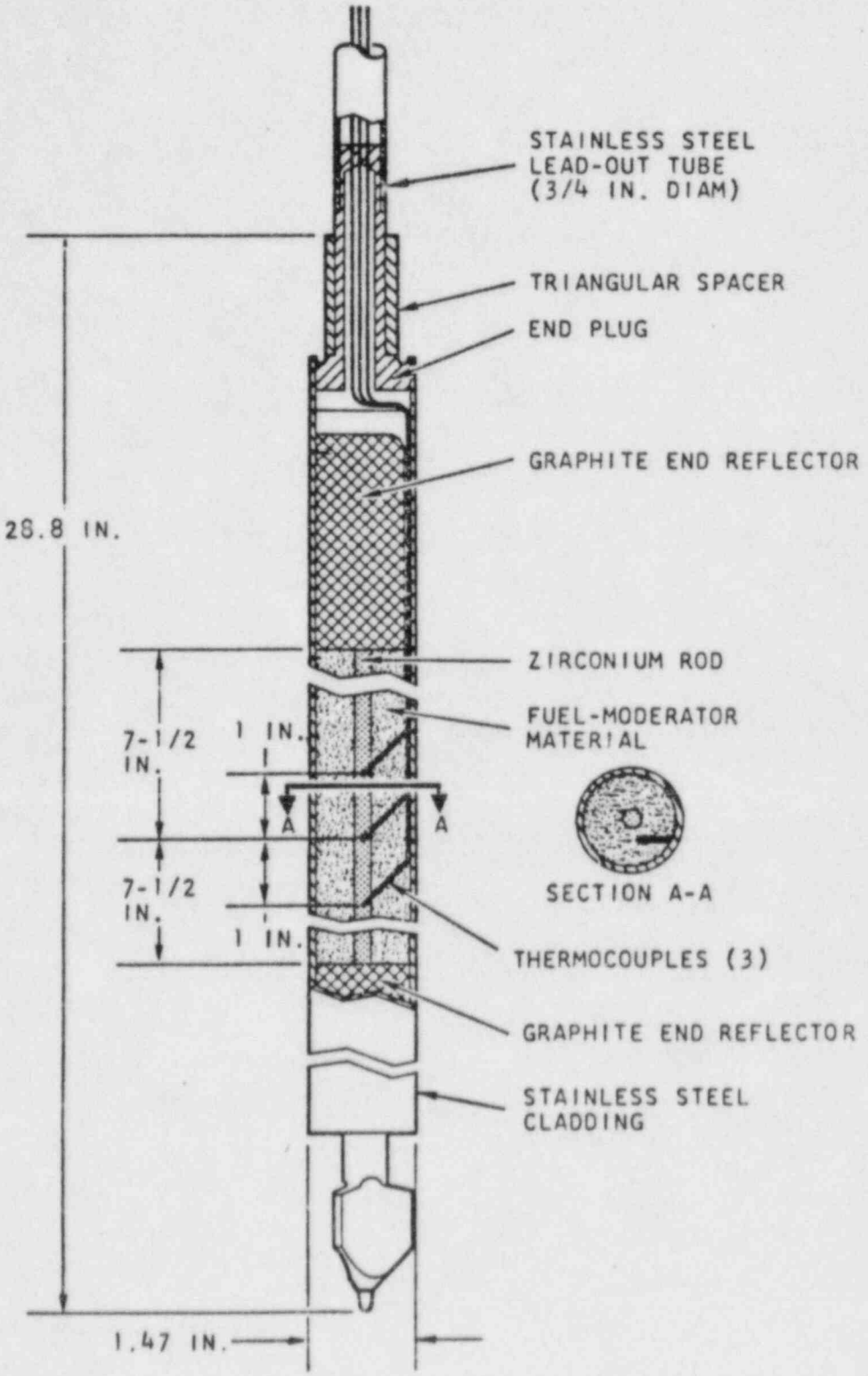

INSTRUMENTED FUEL ELEMENT
Figure 3-29

Table 3-9
THERMOCOUPLE SPECIFICATIONS

Type	Chromel-alumel
Wire diameter	0.005 in.
Resistance	24.08 ohms/double foot at 68°F
Junction	Grounded
Sheath material	Stainless steel
Sheath diameter	0.040 in.
Insulation	MgO
Lead-out wire	
Material	Chromel-alumel
Size	20 AWG
Color code	Chromel - yellow (positive) Alumel - red (negative)
Resistance	0.59 ohms/double foot at 75°F

Table 3-10
SUMMARY OF FUEL ELEMENT SPECIFICATIONS

	Nominal Value	
Fuel-Moderator Material		
H/Zr ratio	1.6	
Uranium content	8.5 wt %	
Enrichment (U-235)	19.7 ±0.2	
Diameter	1.43 in.	
Length	15 in.	
Graphite End Reflectors	Upper	Lower
Porosity	20%	20%
Diameter	1.43 in.	1.43 in.
Length	3.44 in.	3.47 in.
Cladding		
Material	Type 304 SS	
Wall thickness	0.020 in.	
Length	22.10 in.	
End Fixtures and Spacer	Type 304 SS	
Overall Element		
Outside diameter	1.47 in.	
Length	28.37 in.	
Weight	7 lb	

upper end of the holder supports the assembly on the upper grid plate, the rod itself, which contains the source, extending down into the core region. The neutron source is contained in a cavity in the lower portion of the rod assembly at the horizontal centerline of the core. This cylindrical cavity is 0.981 in. (2.492 cm.) in diameter and approximately 3 in. (7.62 cm.) deep. The upper and lower portions are screwed together. A soft aluminum ring provides sealing against water leakage into the cavity. Since the upper end fixture of the source holder is similar to that of the fuel element, the source holder can be installed or removed with the fuel handling tool. In addition, the upper end fixture has a small hole through which one end of a stainless steel wire may be inserted to facilitate handling operation from the top of the tank.

3.4.7. Graphite Dummy Elements

Graphite dummy elements may be used to fill grid positions not filled by the fuel-moderator elements or other core compounds. They are of the same general dimensions and construction as the fuel-moderator elements, but are filled entirely with graphite and are clad with aluminum.

3.4.8. Control System Design

The reactor uses four control rods:

a. A safety rod
b. A shim rod
c. A transient rod
d. A regulatory rod

The regulating, shim and safety rods are sealed 304 stainless steel tubes approximately 109 cm (43 in.) long by 3.43 cm (1.35 in.) in diameter in which the uppermost 16.5 cm (6.5 in.) section is an air void and the next 38.1 cm (15 in.) is the neutron absorber (boron carbide in solid form). Immediately below the neutron absorber is a fuel follower section consisting of 38.1 cm (15 in.) of U-$ZrH_{1.6}$ fuel. The bottom section of the rod is 16.5 cm (6.5 in.) air void.

The regulating, safety, and shim rods pass through and are guided by 3.81 cm. (1.5 in.) diameter holes in the top and bottom grid plates. A typical control rod with fuel follower is shown in the withdrawn and inserted postions in Figure 3-30.

The safety-transient rod is a sealed, 93.35 cm. (36.75 in.) long by 3.18 cm. (1.25 in.) diameter tube containing solid boron carbide as a neutron absorber. Below the absorber is an air filled follower section. The absorber section is 38.1 cm. (15 in.) long and the follwer is 53.02

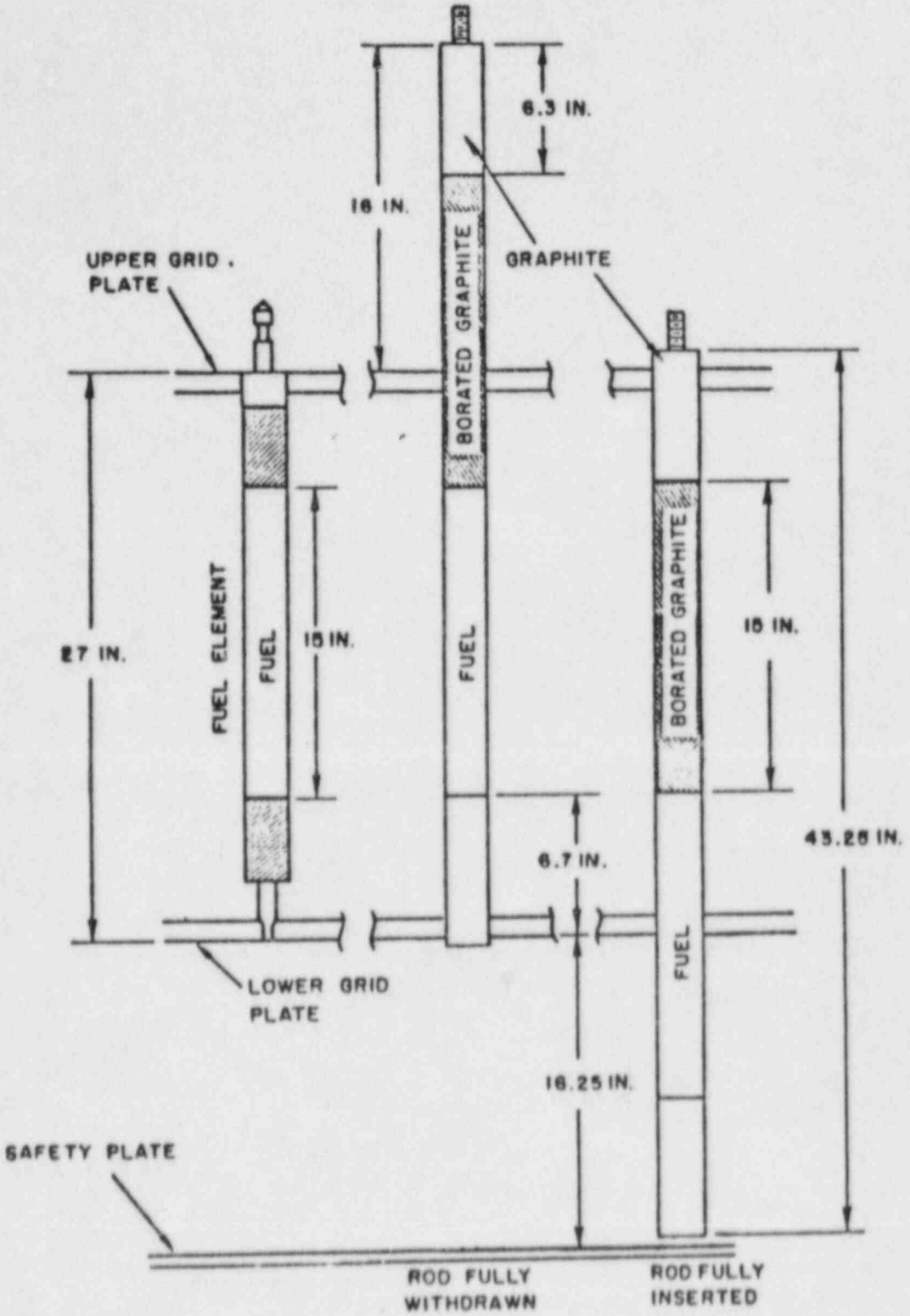

FUEL FOLLOWED CONTROL ROD
Figure 3-30

cm. (20.88 in.) long. The transient rod passes through the core in a perforated aluminum guide tube. The tube recieves its support from the safety plate and its lateral positioning from both grid plates. It extends approximately 25.4 cm. (10 in.) above the top grid plate. Water passage through the tube is provided by a large number of holes distributed evenly over its length. A locking device is built into the lower end of the assembly.

The control rods are connected to their individual drive units by screwing the upper end of the rod into a control rod drive assembly connecting rod. Vertical travel of each rod is approximately 38.1 cm. (15 in.). Reactivity worths and core positions for each rod are summarized in the section on nuclear design. A summary of other control rod design parameters is given in Table 3-11.

Table 3-11
SUMMARY OF CONTROL ROD DESIGN PARAMETERS

	Transient	Safety Shim and Regulating
Cladding		
Material	Al	Type 304 SS
OD	3.18 cm (1.25 in.)	3.43 cm (1.35 in.)
Length	93.35 cm (36.75 in.)	109.5 cm (43.13 in.)
Wall thickness	0.071 cm (0.028 in.)	0.051 cm (1.35 in.)
Absorber		
Material	Boron Carbide (solid form)	
OD	3.02 cm (1.19 in.)	3.32 cm (1.31 in.)
Length	38.1 cm (15 in.)	36.20 cm (14.25 in.)
Follower		
Material	Air	$U\text{-}ZrH_{1.6}$
OD	3.18 cm (1.25 in.)	3.34 cm (1.31 in.)
Length	53.02 cm (20.88 in.)	38.1 cm (15 in.)

3.4.8.1. Control Rod Drive Assemblies. The control rod drive assemblies for the safety, shim and regulating rods are mounted on a bridge assembly over the pool and consist of a motor and reduction gear driving a rack-and-pinion

as indicated in Figure 3-31. A helipot connected to the pinion generates the position indication. Each control rod drive has a tube that extends to a dashpot below the surface of the water. The control rod assembly is connected to the rack through an electromagnet and armature. In the event of a power failure or scram signals, the control rod magnets are de-energized and the rods fall into the core. The time required for a rod to drop into the core from the full-out position is about 1 second. The rod drive motor is non-synchronous, single-phase, and instantly reversible, and will insert or withdraw the control rod at a rate of approximately 11.5 in./min. (0.5 cm/sec) for the safety and shim. A regulating rod drive withdraws the control rod at a rate of 24.0 in./min (1.02 cm/sec.). A key-locked switch on the control console power supply prevents unauthorized operation of all control rod drives. Electrical dynamic and static braking on the motor are used for fast stops.

Limit switches mounted on the drive assembly actuate circuits which indicate the following:

a. The "up" and "down" positions of the magnet

b. The "down" position of the rod

c. The magnet in contact with the rod

3.4.8.2. Transient Rod Drive Assembly. The safety transient control rod on pulsing TRIGA Mark II reactors is operated with a pneumatic rod drive (see Figures 3-32 and 3-33). Operation of the transient rod drive is controlled from the reactor console.

The transient rod drive is mounted on a steel frame that bolts to the bridge. Any value from zero to a maximum of 15 in. (38.1 cm.) of rod may be withdrawn from the core; administrative control is exercised to restrict its travel so as not to exceed the maximum licensed step insertion of reactivity ($3.00 or 2.1% δk/k).

The transient rod drive is a single-acting pneumatic cylinder with its piston attached to the transient rod through a connecting rod assembly. The piston rod passes through an air seal at the lower end of the cylinder. Compressed air is supplied to the lower end of the cylinder from an accumulator tank when a three-way solenoid valve located in the piping between the accumulator and cylinder is energized. The compressed air drives the piston upward in the cylinder and causes the rapid withdrawal of the transient rod from the core. As the piston rises, the air trapped above it is pushed out through vents at the upper end of the cylinder. At the end of its travel, the piston strikes the anvil of an oil-filled hydraulic shock absorber, which has a spring return, and which decelerates the piston

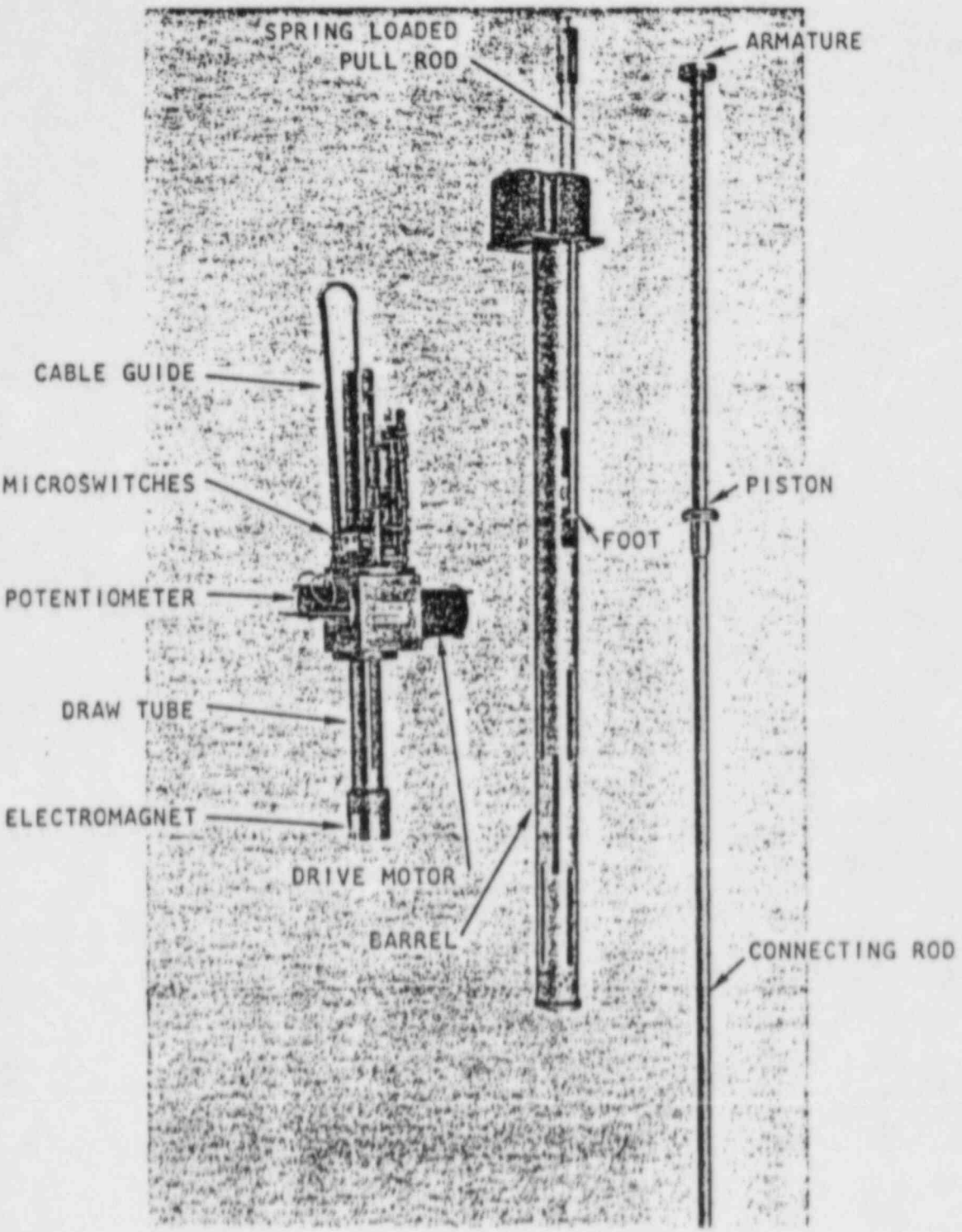

RACK AND PINION CONTROL ROD DRIVE
Figure 3-31

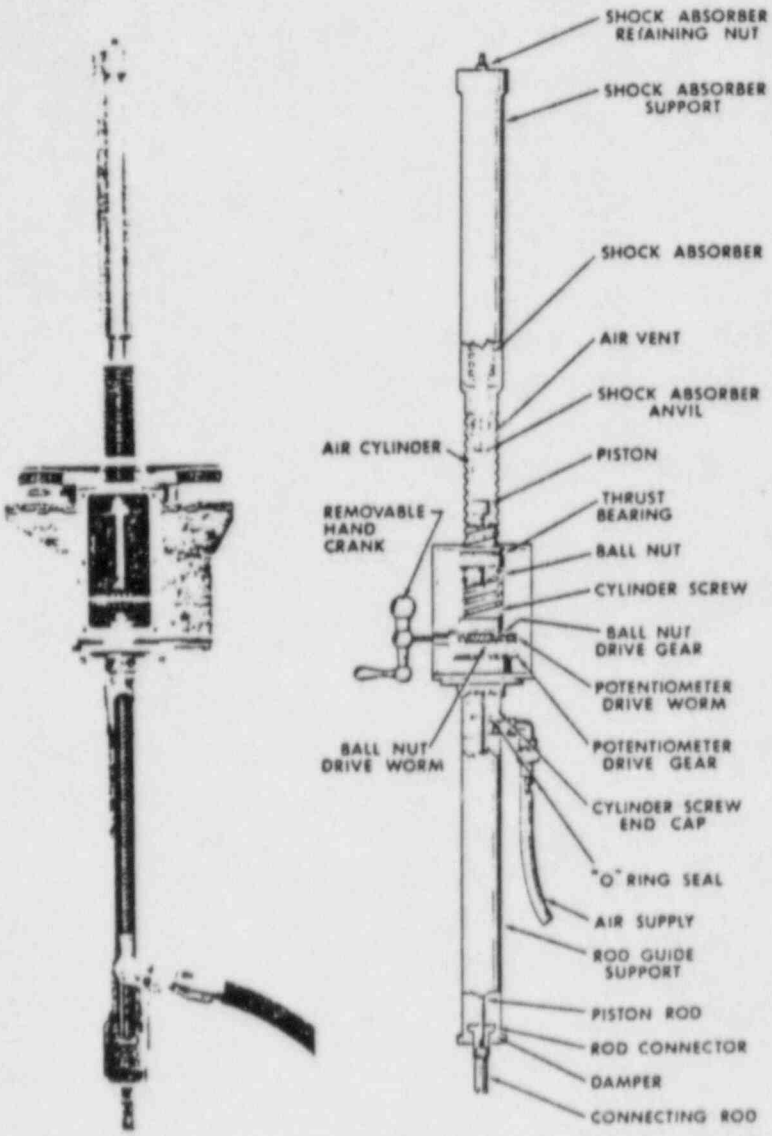

ADJUSTABLE TRANSIENT ROD
Figure 3-32

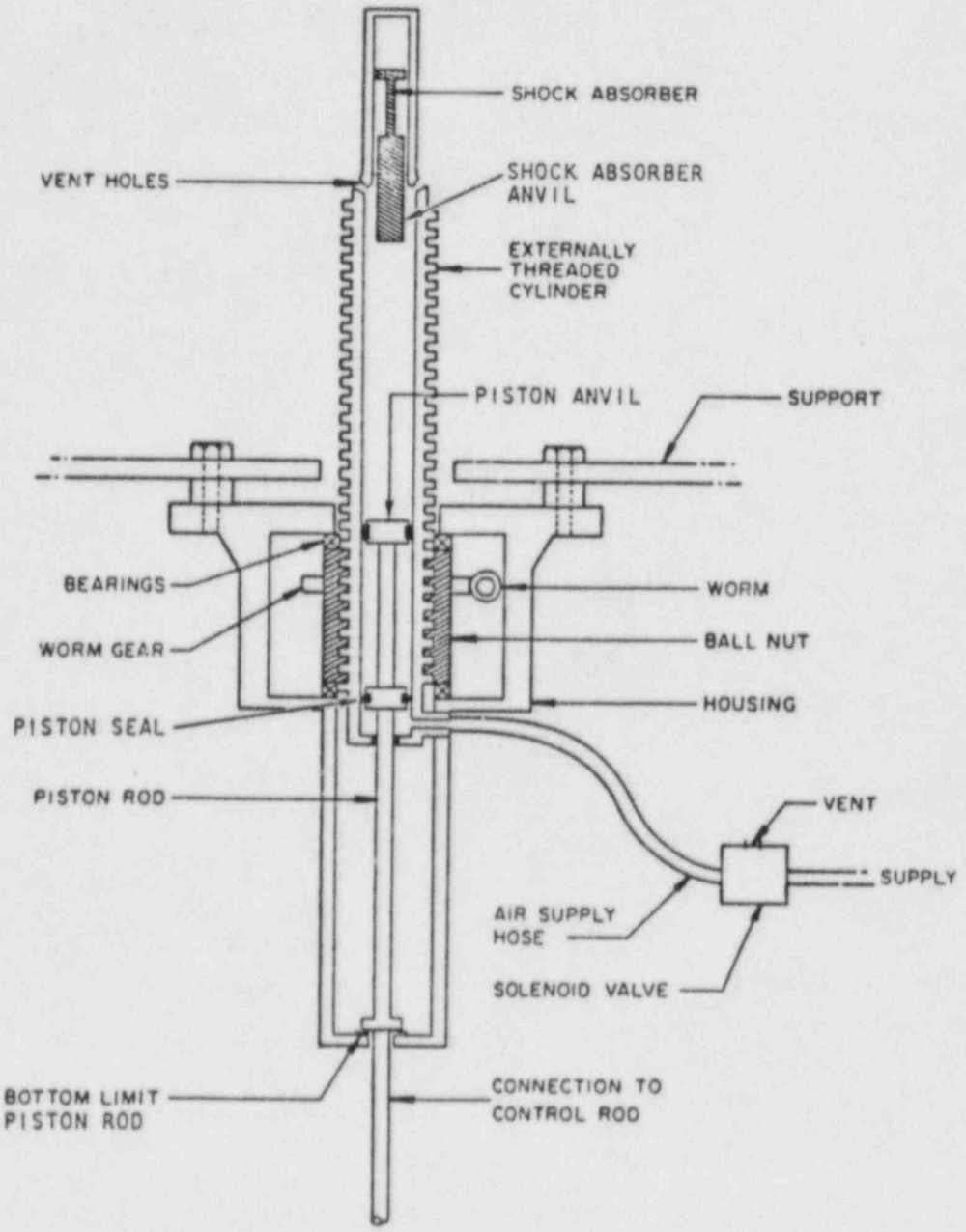

TRANSIENT ROD OPERATIONAL SCHEMATIC
Figure 3-33

at a controlled rate over its last 2 in. (5 cm.) of travel. When the solenoid is de-energized, the valve cuts off the compressed air supply and exhausts the pressure in the cylinder, thus allowing the piston to drop by gravity to its original position and restore the transient rod to its fully inserted position in the reactor core.

The extent of transient rod withdrawal from the core during a pulse is determined by raising or lowering the cylinder, thereby controlling the distance the piston travels.

The cylinder has external threads running most of its length, which engage a series of ball bearings contained in a ball-nut mounted in the drive housing. As the ball-nut is rotated by a worm gear, the cylinder moves up or down depending on the direction of worm gear rotation. A mechanical indicator is driven by the worm shaft. The distance the transient rod will be ejected from the reactor core is determined by the position of the cylinder and the mechanical indicator. The pneumatic cylinder position is controlled by a crank inserted at the rod drive. The crank is inserted into the drive only when position changes are to be made.

Attached to and extending downward from the transient rod drive housing is the rod guide support, which serves several purposes. The air inlet connection near the bottom of the cylinder projects through a slot in the rod guide and prevents the cylinder from rotating. Attached to the lower end of the piston rod is a flanged connector that is attached to the connecting rod assembly that moves the transient rod. The flanged connector stops the downward movement of the transient rod when the connector strikes the damp pad at the bottom of the rod guide support. A microswitch is mounted on the outside of the guide tube with its actuating lever extending inward through a slot. When the transient rod is fully inserted in the reactor core, the flange connector engages the actuating lever of the microswitch and indicates on the instrument console that the rod is in the core.

In the case of the transient rod a scram signal de-energizes the solenoid valve which supplies the air required to hold the rod in a withdrawn position and the rod drops into the core from the full out position in about 1 second.

3.4.8.3. Evaluation of Control Rod System. The reactivity worth and speed of travel for the control rods are adequate to allow complete control of the reactor system during operation from a shutdown condition to full power. The scram times for the rods are quite adequate since the TRIGA system does not rely on speed of control as being

paramount to the safety of the reactor. The inherent shutdown mechanism of the TRIGA prevents unsafe excursions and the control system is used only for the planned shutdown of the reactor and to control the power level in steady-state operation.

3.4.9. Experimental and Irradiation Facilities

The experimental and irradiation facilities of the TRIGA Mark II reactor are extensive and versatile. Physical access and observation of the core are possible at all times through the vertical water shield. Experimental tubes can easily be installed in the core region to provide facilities for high-level irradiations or in-core experiments. Areas outside the core and reflector are available for larger experiment equipment or facilities.

3.4.9.1 Central Thimble. The reactor is equipped with a central thimble for access to the point of maximum flux in the core. The central thimble consists of an aluminum tube that fits through the center hole of the top and bottom grid plates. Dimensions of the tube are 1.5 in. o.d. (3.81 cm.) and 1.33 in. i.d. (3.38 cm.). Holes in the tube assure that it is normally filled with water. Water is expelled from the tube by compressed air. Experiments with the central thimble include irradiations of small samples and the exposure of aterials to a collimated beam of neutrons or gamma rays.

3.4.9.2 Rotary Specimen Rack. A rotary, multiple-position (40) specimen rack located in a well in the top of the graphite reflector provides for the large scale production of radioisotopes and for the activation and irradiation of mutilpe samples. All positions in this rack are exposed to neutron fluxes of comparable intensity. Specimen positions are 1.25 in. (3.18 cm.) in diameter by 10.80 in. (27.4 cm.) in depth. Samples are loaded from the top of the reactor through a water-tight tube into the rotary rack using a specimen lifting device or pneumatic pressure for insertion and removal of samples from the sample rack positions. The rotary specimen rack can be turned from the top of the reactor by manual operation or by a motor drive.

3.4.9.3 Pneumatic Specimen Tube. A pneumatic transfer system permits applications with short-lived radioisotopes. The in-core terminus of this system is normally located in the outer ring of fuel element positions, a region of high neutron flux. The sample container (rabbit) is conveyed to a receiver-sender station via 1.25 in. o.d. (3.18 cm.) aluminum tubing. Effective space in the specimen transfer capsules is 0.68 in. (1.7 cm.) diameter by 4.5 in. (11.4 cm.) height. An optional transfer box may be employed to

permit the sample to be sent and received from up to three different receiver-sender stations.

3.4.9.4 Beam Tube Facilities. The beam ports provide tubular penetrations through the concrete shield and reactor tank water, making beams of neutrons (or gamma radiation) available for experiments. The beam ports also provide an irradiation facility for large sample specimens in a region close to the core. Beam port diameters near the core are 6 in. (15.2 cm.).

There are five beam ports divided into two categories as follows:

a. Tangential beam ports. Two beam ports are oriented tangential to the reactor core, penetrate the graphite reflector, the coolant water, and the concrete shield. A hole is drilled in the graphite tangential to the outer edge of the core. One beam port terminates at the tangential point to the core. The other beam tubes extend both directions from the reflector and out opposite sides of the reactor shield.

b. Radial beam ports. There are two radial beam ports, each which penetrate the concrete shield structure and the coolant water. One radial port terminates at the outer edge of the reflector. The second radial port also terminates at the outer edge of the reflector. However, a hole drilled in the graphite reflector extends the effective source of the radiations to the reactor core region.

A step is incorporated into each beam port to prevent radiation streaming through the gap between the beam tube and shielding plug. The inner section of each beam port is an aluminum pipe 6 in. (15.2 cm) in diameter; the outer section is a steel pipe 8 in. (20.3 cm) in diameter. A "shadow" shield is incorporated in the concrete structure around the step in each beam port. This shield, which is constructed of 4-in. (10.2-cm)-thick steel plate, reduces the amount of radiation passing through the concrete when the beam port is in use. Special shielding reduces the radiation outside the concrete to a safe level when the beam port is not in use. The shielding is provided in four sections as follows:

a. An inner shield plug.

b. An outer shield plug.

c. A lead-filled shutter.

d. A lead-filled door.

The inner shield plug consists of 40 in. (1.02 m) of graphite backed with a 0.125-in. (0.32-cm) sheet of boral and 5 in. (12.7 cm) of lead sandwiched between two 1.25-in. (3.2-cm)-thick steel plates. The graphite is 6 in. (15.2 cm) in diameter. Three rollers are provided to facilitate the insertion and removal of the inner shield plugs. To help guide the innermost plug over the step in the beam tube during insertion, the inner end of the plug is cone-shaped. A threaded hole is provided in the outer end of the plug for attaching the beam tube plug-handling tool.

The outer shield plug is polyethylene and is 8 in. (20.3 cm) in diameter and 43 in. (1.09 m) long. A handle on the outer end of this plug is provided for manual handling. The plug weighs about 45 lb (20 kg). The plug is equipped with an electrical circuit consisting of a position switch mounted in the front of the plug and an electrical connector at the rear of the plug. The switch can be actuated only by the inner plug when the inner plug is installed in the beam tube.

The connector is inserted in an outlet box mounted in the beam to complete the circuit to the control console. Lights on the console for each beam tube indicate when the plugs are inserted.

The lead-filled shutter and lead-lined door provide limited gamma shielding when the plugs are removed. The shutter is contained in a rectangular steel housing recessed in the outer surface of the concrete shield. The shutter is ~10 in. (25.4 cm) in diameter and 9.5 in. (24.1 cm) thick. It is operated by a removable push rod on the face of the shield structure and can be moved even with the shutter housing door closed. In the open position, a section of the shutte consisting of an 8-in. (20.3-cm) pipe is aligned with the beam port and the outer shield center plug to facilitate insertion or removal of the beam plugs. The shutter housing is equipped with a steel cover plate lined with 1.25 in. (3.2 cm) of lead for additional shielding. The cover plate is bolted in place and equipped with a rubber gasket. A removable lead-lined center plug provides easy access to the beam port. The plug can be bolted shut so that the seal would prevent loss of shielding water if the beam tube should develop a serious leak.

3.5. SAFETY SETTINGS IN RELATION TO SAFETY LIMITS

As has been indicated, fuel temperatures are the main safety considerations in the operation of the TRIGA system. The temperature of the fuel may be controlled by setting limits on other operating parameters. The operating parameters of interest for TRIGA are:

a. Maximum licensed steady-state power level

b. Fuel temperature measured by thermocouple

c. Maximum reactivity worth of transient rod

d. Core inlet coolant water temperature.

The safety settings as listed in Table 3-12 are such that in all operation, normal and abnormal, the safety limits indicated in the reactor design bases will not be exceeded.

Table 3-12
TRIGA SAFETY SETTINGS

Parameter Limited	Safety Setting	Function
Maximum power level steady-state	1100 kW(t)	Reactor scram
Maximum fuel temperature measured	500°C	Reactor scram

Administative limitations are imposed for the transient rod and coolant water temperature as follows:

a. Maximum worth of transient insertion of 2.28% δk/k

b. Core inlet water temperature of 48.9°C.

These safety settings are conservative in the sense that if they are adhered to, the consequence of normal or abnormal operation would be fuel and clad temperatures well below the safety limits indicated in the reactor design bases. Because of the conservatism in these safety settings, it is reasonable that at some later date less restrictive safety system settings could be assigned in conjunction with the upgrading of the reactor to operate at higher steady-state power levels or in the pulsing mode, while still using the same fuel and core configuration.

Chapter 3 References

1. Merten, U., et al., "Thermal Migration of Hydrogen in Uranium-Zirconium Alloys", General Dynamics, General Atomic Division Report GA-3618, 1962.

2. Coffer, C. O., et al., "Research in Improved TRIGA Reactor Performance, Final Report", General Dynamics, General Atomic Division Report GA-5786, 1964.

3. Johnson, H. A., et al., "Temperature Variation, Heat Transfer, and Void Volume Development in the Transient Atmosphere Boiling of Water", SAN-1001, University of California, Berkeley, 1961.

4. McAdams, W. H., Heat Transmission, 3rd ed, McGraw-Hill Book Co., New York, 1954.

5. Sparrow, E. M. and R. D. Cess, "The Effect of Subcooled Liquid on Film Boiling", Heat Transfer, 84, 149-156 (1962).

6. Speigler, P., et al., "Onset of Stable Film Boiling and the Foam Limit", Int. J. Heat and Mass Transfer, 6, 987-989 (1963).

7. Zuber, W., "Hydrodynamic Aspects of Boiling Heat Transfer", AEC Report AECV-4439, TIS, ORNL, 1959.

8. Rohsenow, W., and H. Choi, Heat, Mass and Momentum Transfer, Prentice-Hall, 1961, pp. 231-232.

9. Ellion, M. E., "A Study of the Mechanism of Boiling Heat Transfer", Jet Propulsion Laboratory Memo. No. 20-88, 1954.

10. Coffer, C. O., et al., " Characteristics of Large Reactivity Insertions in a High Performance TRIGA U-ZrH Core", General Dynamics, General Atomic Division Report GA-6216, 1965.

11. Fenech, H., and W. Rosenow, "Thermal Conductance of Metallic Surfaces in Contact", USAEC NYO-2130, 1959.

12. Graff, W. J.", Thermal Conductance Across Metal Joints", Machine Design, Sept. 15, 1960, pp. 166-172.

13. Fenech, H., and J. J. Henry, "An analysis of a Thermal Contact Resistance", Trans. Am. Nucl. Soc. 5, 476 (1962).

14. Bernath, L., "A Theory of Local Boiling Burnout and Its Application to Existing Data", Heat Transfer - Chemical Engineering Progress Symposium Series, Storrs,

18. Lenihan, S. R., "GAZE-2: A One-Dimensional, Multigroup, Neutron Diffusion Theory Code for the IBM-7090", General Dynamics, General Atomic Division Report GA-3152, 1962.

19. Dorsey, J. P., and R. Froehlich, "GAMBLE-5 - A Program for the Solution of the Multigroup Neutron-Diffusion Equations in Two Dimensions, with Arbitrary Group Scattering, for the UNIVAC-1108 Computer", Gulf General Atomic Report GA-8188, 1967.

20. Lathrop, D. K., "DTF-IV, A FORTRAN-IV Program for Solving the Multigroup Transport Equation with Anisotropic Scatterings", USAEC Report LA-3373, Los Alamos Scientific Laboratory, New Mexico, 1965.

21. Adler, F. T., G. W. Hinman, and L. W. Nordheim, "The Quantitative Evaluation of Resonance Integrals", in Proc. 2nd Intern. Conf. Peaceful Uses At. Energy (A/CONF. 15/P/1983), Geneva, International Atomic Energy Agency, 1958.

22. Brown, H. D., Jr., Gulf General Atomic Inc., "THERMIDOR - A FORTRAN II Code for Calculating the Nelkin Scattering Kernel for Bound Hydrogen (A Modification of Robespierre)", unpublished data.

23. Nelkin, M. S., "Scattering of Slow Neutrons by Water", Phys. Rev. 119, 741-746 (1960).

24. McReynolds, A. W., et al., "Neutron Thermalization by Chemically-Bound Hydrogen and Carbon", in Proc. 2nd Intern. Conf. Peaceful Uses At. Energy (A/CONF. 15/P/1540), Geneva, International Atomic Energy Agency, 1958.

25. Whittemore, W. L., "Neutron Interactions in Zirconium Hydride", USAEC Report GA-4490 (Rev.), General Dynamics, General Atomic Division, 1964.

26. Bell, J., "SUMMIT: An IBM-7090 Program for the Computation of Crystalline Scattering Kernels", USAEC Report, General Dynamics, General Atomic Division Report GA-2492, 1962.

27. Beyster, J. R., et al., "Neutron Thermalization in Zirconium Hydride", USAEC Report, General Dynamics, General Atomic Division Report GA-4581, 1963.

28. Woods, A. D. B., et al., "Energy Distribution of Neutrons Scattered from Graphite, Light and Heavy Water, Ice, Zirconium Hydride, Lithium Hydride, Sodium Hydride, and Ammonium Chloride, by the Beryllium Detector Method", in Proc. Symp. Inelastic Scattering of Neutrons in Solids and Liquids, Vienna, Austria, Oct. 11-14, International Atomic Energy Agency, 1960.

29. Jordan, D. P. and G. Leppert, "Pressure Drop and Vapor Volume with Subcooled Nucleate Boiling", Int. J. Heat Mass Trans. 5, 751-761 (1962).

30. McAdams, op. cit., pp. 390-392.

31. Levy, S., "Forced Convection Subcooled Boiling-Prediction of Vapor Volumetric Fraction", Int. J. Heat Mass Trans. 10, 961-965 (1967).

32. McAdams, op. cit., p. 392.

33. Bernath, op. cit., pp. 95-116

Chapter 4

INSTRUMENTATION AND CONTROL SYSTEM

Design of the instrumentation and control system is intended for new TRIGA reactor facilities and replacement of old reactor consoles. Completion and verification of the design will occur in a GA Technologies reactor facility before installation at The University of Texas at Austin. An active evaluation by the University is intended of the GA instrument and control console for the TRIGA as part of the original installation of the console by the vendor.

4.1 DESIGN BASES

A new Instrumentation and Control System (ICS) [1] for the TRIGA reactor is a computer-based design incorporating the use of a GA-developed, multi-function, NM-1000 digital neutron monitor channels. Two complete NM-1000 systems provide redundant safety channels (percent power with scram), wide-range log power (below source level to full power), period, and multi-range linear power (source level to full power). The control system logic is contained in a separate control system computer (CSC) with color graphics display which is the interface between the operator and the reactor. While information from the NM-1000 channels is processed and displayed by the CSC, each NM-1000 safety channel is independent, has its own output displays and connects directly to the safety system scram circuit.

The NM-1000 digital neutron monitor channels were developed for the nuclear power industry and are fully qualified for use in the demanding and restrictive conditions of a nuclear power generating plant. Their design is based on a special GA-designed, high sensitivity fission chamber, and low noise ultra-fast pulse amplifier.

The control system computer manages all control rod movements, accounting for such things as interlocks and choice of particular operating modes. The CSC also processes and displays information on control rod positions, power level, fuel and water temperature and can display pulse characteristics and forced flow system parameters. Many other functions can also be performed by the CSC, such as calibrating control rods, and monitoring reactor usage. A computer-based control system has many advantages over an analog system in terms of speed, accuracy and reliability, and the ability for self-calibration, improved diagnostics, graphic displays and logging of vital information.

4.1.1 NM-1000 Safety and Neutron Monitor Channel

The NM-1000 nuclear channels have multi-function capability to provide safety (scram) action as well as neutron monitoring over a wide power range from a single detector. The selectable functions are:

a. Percent power with scram.

b. Wide-range log power.

c. Power rate of change.

d. Multi-range linear power.

For the TRIGA ICS, one NM-1000 system is designated to provide the wide-range log power function and the percent power safety channel with scram (linear power level from 1 to 125%). The wide-range log power function is a digital version of the patented GA 10-decade log power system to cover the reactor power range from below surface level to 150% power and provide a period signal. For the log power function, the chamber signal from startup (pulse counting) range through the Campbelling (root mean square [RMS] signal processing) range covers in excess of 10-decades of power level. The self-contained microprocessor combines these signals and derives the power rate of change (period) through the full range of power. The microprocessor automatically tests the system to ensure that the upper decades are operable while the reactor is operating in the lower decades and vice versa when the reactor is at high power.

The second NM-1000 system provides the multi-range linear power range data as well as the percent power safety channel with scram. For the multi-range function, the NM-1000 utilizes the same signal source as for the log function. However, instead of the microprocessor converting the signal into a log function, it converts it into 10 linear power ranges. This feature provides for a more precise reading of linear power level over the entire range of reactor power. The same self-checking features are included for the log function. The multi-range ranging function is either auto-ranged or slaved to a position switch on the operator's console via the control system computer.

Each NM-1000 system is contained in two NEMA (National Electrical Manufacturers Assoc.) enclosures, one for the amplifier and one for the processor assemblies. The amplifier assembly contains modular plug-in subassemblies for pulse preamplifier electronics, bandpass filter and RMS electronics, signal conditioning circuits, low voltage power supplies, detector high voltage power supply and digital

diagnostics and communication electronics. The processor assembly is made up of modular plug-in subassemblies for communication electronics (between amplifier and processor), the microprocessor, a control/display module, low voltage power supplies, isolated 4 to 20 mA outputs, and isolated alarm outputs. Outputs are Class 1E as specified by IEEE 323-1974. Communication between the amplifier and processor assemblies is via 2 twisted pair shielded cables. The amplifier/microprocessor circuit design employs the latest concepts in automatic on-line self diagnostics and calibration verification. Detection of unacceptable circuit performances is automatically alarmed.

The neutron detector uses the standard 0.2 counts/sec per nv fission chamber that has provided reliable service in the past. It has, however, been improved by additional shielding to provide a greater signal to noise ratio. The low noise construction of the chamber assembly allows the system to respond to a low reactor shutdown level which is subject to being masked by noise. An illustration of the neutron channel operating ranges is shown in Figure 4-1.

4.1.2 CSC and Control Console

A conceptual layout of the control console is shown in Figure 4-2. The control console contains the several components needed by the operator for reactor control. Included are:

a. Reactor control panel.

b. Control system computer (CSC).

c. Color CRT monitor.

d. Power and temperature meter panel.

e. Two disc drives, printer and terminal.

Functions of the control panel are represented in Figure 4-3 and are presented as:

a. Key switch for rod magnet power.

b. Digital rod position indicators.

c. Rod control switches and annunciators.

d. Reactor operating mode switches.

e. External switch annunciators (such as beam port open-close, reactor bay access etc.).

As previously mentioned, the power and period information from the NM-1000 channels is processed and

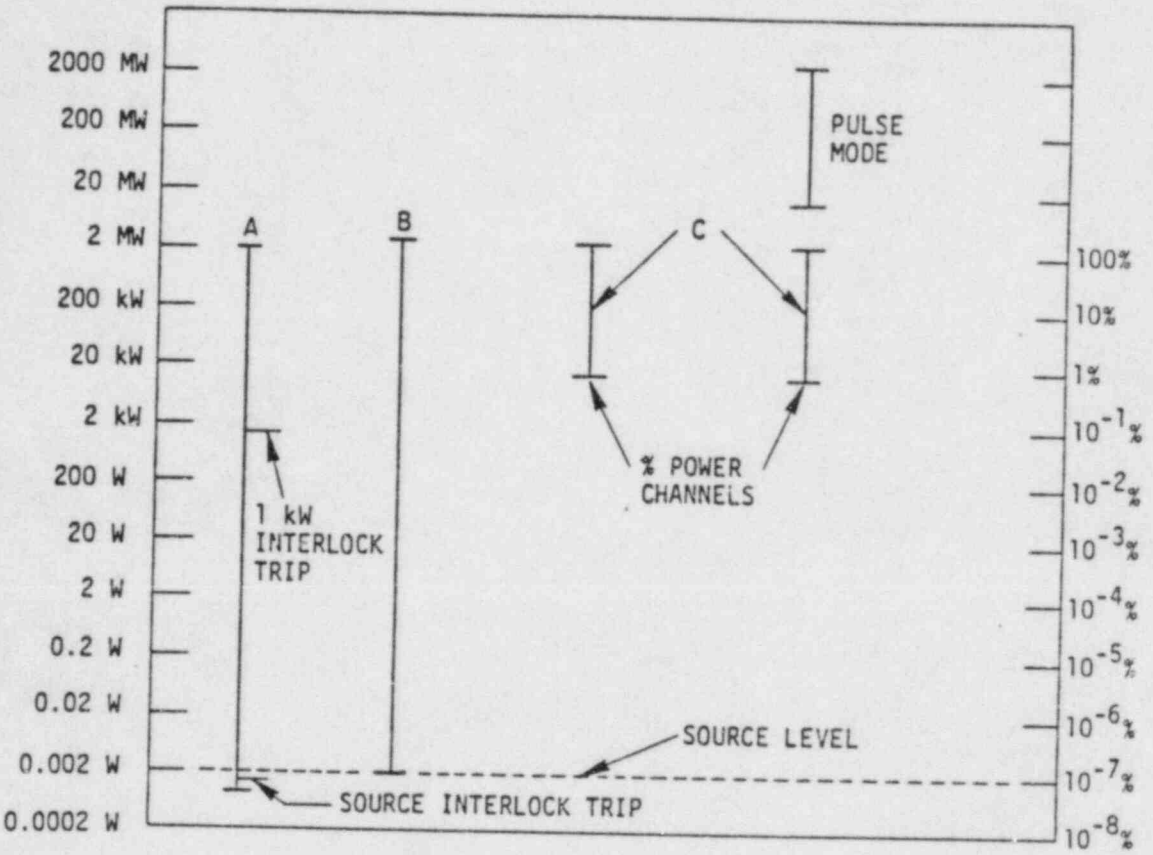

A = Wide Range Log Channel
B = Wide Range Linear Channel
C = Manual, Automatic, and Squarewave Modes

EL-0350B

NEUTRON CHANNEL OPERATING RANGES
Figure 4-1

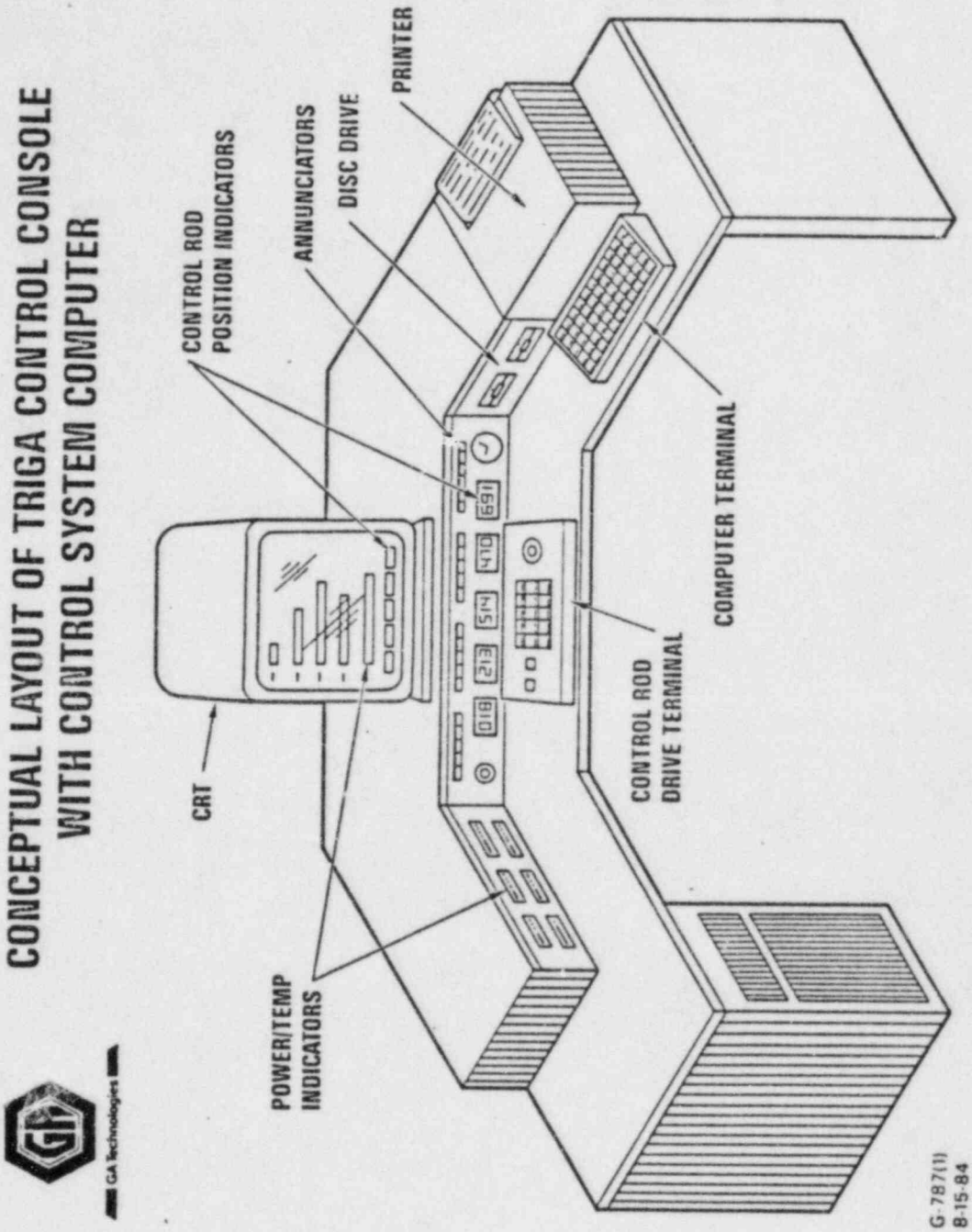

LAYOUT OF THE REACTOR CONTROL CONSOLE
Figure 4-2

GA Technologies

TRIGA CONTROL CONSOLE PANELS

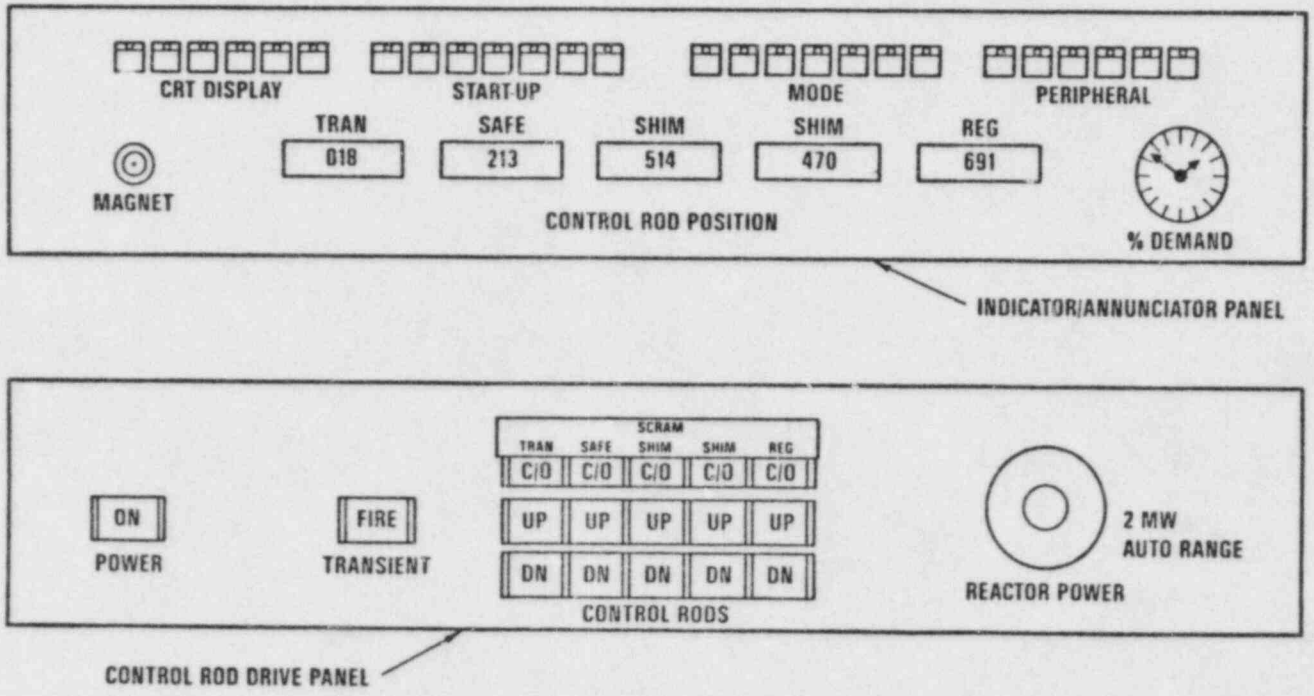

G-835(3)
8-15-84

CONSOLE CONTROL PANELS
Figure 4-3

displayed by the CSC. However, each NM-1000 safety system is independent, has its own output displays and connects directly to the control system scram circuit. Thus, both percent power channels, wide-range log power, period and multi-range linear power have their output displayed on meters as well as on the color CRT. This is also true of fuel temperature and control rod position indication.

The control system computer (CSC) provides all of the logic functions needed to control the reactor and augments the safety system by monitoring for undesirable operating characteristics. It displays reactor operational information in a color format on a CRT monitor for ease of comprehension and on demand will display secondary information concerning the operation of the reactor auxiliary systems. Essentially all of the control system logic contained in previous TRIGA reactor control systems is incorporated into the CSC. However, instead of utilizing electronic circuits and electrical relay circuits, the logic is programmed into the computer. The availability of the computer allows great versatility and flexibility in operationally related activities aside from the direct control of rod movements. Many other functions can also be performed by the CSC, such as calibrating control rods, monitoring reactor usage and locating individual fuel element positions and burnup, isotope irradiation data, etc.

The control system logic regulates control rod movements are based upon the operating mode selected and the reactor operating characteristics that are constantly monitored, such as power and fuel temperature.

4.1.3 Reactor Operating Modes

There are four operating modes: the basic modes - manual, automatic, square-wave and pulse - that operate with natural convection cooling. Four additional modes are available with operation logic for forced flow cooling.

The manual and automatic modes are steady-state reactor conditions; the square-wave and pulse modes are the conditions implied by their names. The natural convection mode provides cooling without operation of a primary cooling pump. This mode has a lower maximum power level than the forced-flow mode, which uses primary coolant pumps.

The manual and automatic reactor control modes are used for reactor operation from source level to 100% power. These two modes are used for manual reactor startup, change in power level, and steady-state operation. The square-wave operation allows the power level to be raised quickly to a desired power level. The pulse mode generates high-power levels for very short periods of time. High power and low power pulse mode options are available.

Manual rod control is accomplished by the lighted push buttons on the rod control panel. The top row of annunciators, when illuminated, indicates magnet contact with the armature and magnet current. Depressing any one of the CONT/ON push buttons will interrupt the current to that magnet and extinguish the magnet current ON indicator. If the rod is above the down limit, the rod will fall back into the core and the CONT light will remain extinguished until the magnet is driven to the down limit where it again contacts the armature.

When illuminated, the annunciators in the middle row indicate the upper (UP) limit position, and the bottom row annunciators indicate the lower (DOWN) limit position of the rods. Depressing the indicators causes the control rod to move in the direction indicated. Several interlocks prevent the movement of the rods in the UP direction such as:

a. Scrams not reset.

b. Magnet not coupled to armature.

c. Source level below minimum count.

d. Two UP switches depressed at the same time.

e. Mode switch in one of the pulse positions.

f. Mode switch in AUTOMATIC position (regulation rod only).

There is no interlock inhibiting the DOWN direction of the control rods except in the case of the regulating rod while in the AUTOMATIC mode.

Automatic power control can be obtained by switching from manual operation to automatic operation. All the instrumentation, safety, and interlock circuitry described above applies and is in operation in this mode. However, the regulating rod is now controlled automatically in response to a power level and period signal. Reactor power level is compared with the demand level set by the operator and is used to bring the reactor power to the demand level on a fixed preset period. The purpose of this feature is to maintain automatically the preset power level during long-term power runs. Options are available to maintain power by movement of a single rod or by bank operation of the rods. Under bank operation, rods can be controlled by equal position (all rod positions equal) or by set position (rods move as a bank from pre-established positions).

In square-wave operation, the reactor is first brought to criticality below 1 kW, leaving the transient rod partially in the core. All of the steady-state

instrumentation is in operation. The transient rod is ejected from the core by means of the transient rod FIRE push button. When the power level reaches the demand level, it is maintained much the same as in the automatic mode except that two rods are used to maintain power after the pulse rod is ejected.

Reactor control in the pulsing mode consists of establishing criticality at a flux level below 1 kW in the steady-state mode. This is accomplished by the use of the motor-driven control rods, leaving the transient rod either fully or partially inserted. One of the two pulse mode selector switches is then depressed (selected to give an on-scale reading for the peak power level of the pulse to be produced). The MODE SELECTOR switch automatically connects the gamma pulsing chamber to monitor and record peak flux (nv) and energy release (nvt). Pulsing can be initiated from either the critical or sub-critical reactor state.

4.1.4 Reactor Scram System

A reactor protective action interrupts the magnet current and results in the immediate insertion of all rods under any of the following:

a. One out of two high neutron fluxes on safety channels.

b. High fuel temperature.

c. High-voltage failure on either or both safety channels.

d. Manual scram.

e. Peak neutron flux (pulse mode).

f. Minimum period (available for use as desired).

g. External safety switches (as required).

h. Water level (forced flow systems).

i. Coolant flow (forced flow systems).

j. Coolant temperature (forced flow systems).

For systems designed for long-term, high power steady-state operation, three safety channels are used with a 2 out of 3 logic, allowing one channel to be out of service without requiring reactor shutdown.

All scram conditions are automatically indicated on the CRT monitor and by the annunciators. A manual scram will also insert the control rods and may be used for a normal fast shutdown of the reactor. On the external switch panel, a bank of annunciators is available for additional auxiliary scrams or alarms.

Upper limit power scrams are set and actuated within the NM-1000 safety system. Upper limit temperature scrams are set at the temperature transmitters. However, lower level, operational scrams for power and temperature can be reset within the CSC prior to reactor startup. These lower level, operational scrams are actuated within the CSC logic.

4.1.5 Logic Functions

A control system logic diagram is shown in Figure 4-4. Each NM-1000 system receives its input from a low noise fission chamber mounted adjacent to the reactor core. For the log power function, the chamber signal is processed to indicate reactor power from below source level to 150% power (in excess of 10-decades) and period. The system also derives the percent power safety signal of 1% to 125% of power. The microprocessor compares the percent power output against a pre-determined scram level, as set by an on-board microterminal, which when exceeded, causes an opto-isolated relay to change state. For the functions used in second NM-1000, the microprocessor converts the signal source into 10 linear ranges for the multi-range linear power and derives a redundant percent power safety signal of 1% to 125% of power. The same level comparator and self checking features are included.

The fuel temperature transmitters are accurate, highly stable units which convert the 0-1000°C fuel temperature into a 4-10 mA output signal. A level comparator is included which provides scram capability through an isolated contact state change when the preset level is exceeded.

The water temperature transmitters are standard Resistance Temperature Detector (RTD) transmitters which convert the 0 to 100°C temperature into a 4-20 mA signal. The transmitters have a self-contained power supply.

A gamma chamber provides the signal for peak power (nv) and energy release (nvt) in the pulse mode. The nv/nvt amplifier provides the high impedance interface, high voltage and calibration circuits for the pulsing detector.

The control rod interface accepts the digital commands from the data acquisition and control system (DAC) to operate the control rod motors. It contains the opto-isolation circuits which send the up-down limits and loss of contact signals to the control rod logic system. An

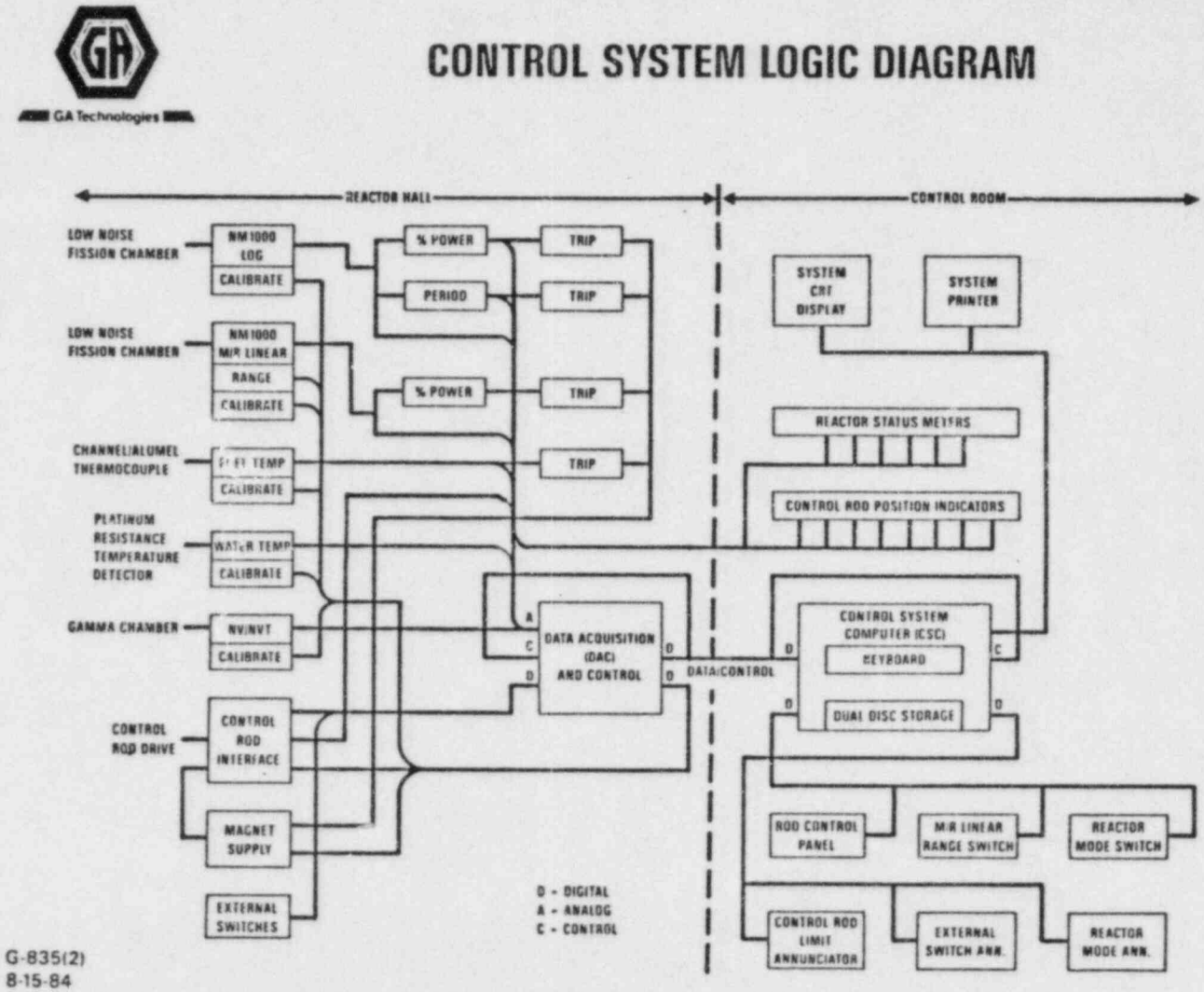

LOGIC DIAGRAM FOR CONTROL SYSTEM
Figure 4-4

excitation power supply provides a stable reference voltage for the rod position indicator system.

The magnet supply furnishes the required 200 mA needed for the rod magnets to hold control rods in contact with the armature. An opto-isolator detects the absence of magnet current to each drive magnet.

The external switches are provided with terminal strips to terminate and connect various switches to the DAC chassis (beam port open-close, etc.)

All of the analog signals are routed to the DAC chassis. However, the prime reactor operating signals are also sent directly to the control room. These signals include log power, period, percent power (2), fuel temperature (2), and all of the control rod position indicators.

The DAC system converts the analog signals to a digital equivalent for transmitting along with the digital signals to the CSC in the control room. The DAC chassis receives control instructions from the CSC, via the communication link, which in turn moves the control rods as requested by the operator and causes the individual subsystems to go to the calibrate mode when commanded by the system or operator.

4.1.6 Mechanical Hardware

The typical reactor installation will be contained in seven NEMA enclosure junction boxes, normally installed in the reactor hall, and the reactor operator console components installed in the reactor control room. Figure 4-5 indicates the placement of the hardware items.

The control console consists of the components needed by the operator for reactor control. These components include rod control switches and annunciators. the digital rod position indicators, on-line reactor status meters (power and temperature), the control system computer (CSC), reactor operating mode switch panel, color CRT monitor, printer, disc drives (2) and external switch annunciators (beam port open-close, reactor access, etc.).

Enclosures 1 and 3 each contain NM-1000 high and low voltage power supplies, a pulse pre-amp with discriminator, an RMS Campbell convertor and a communications module.

Enclosures 2 contains the NM-1000 microprocessor selected to provide the 10-decade log signal from the information provided by the circuits in enclosure 1. The information processed by the microprocessor is 10-decades of log power, rate of power change (period), linear percent

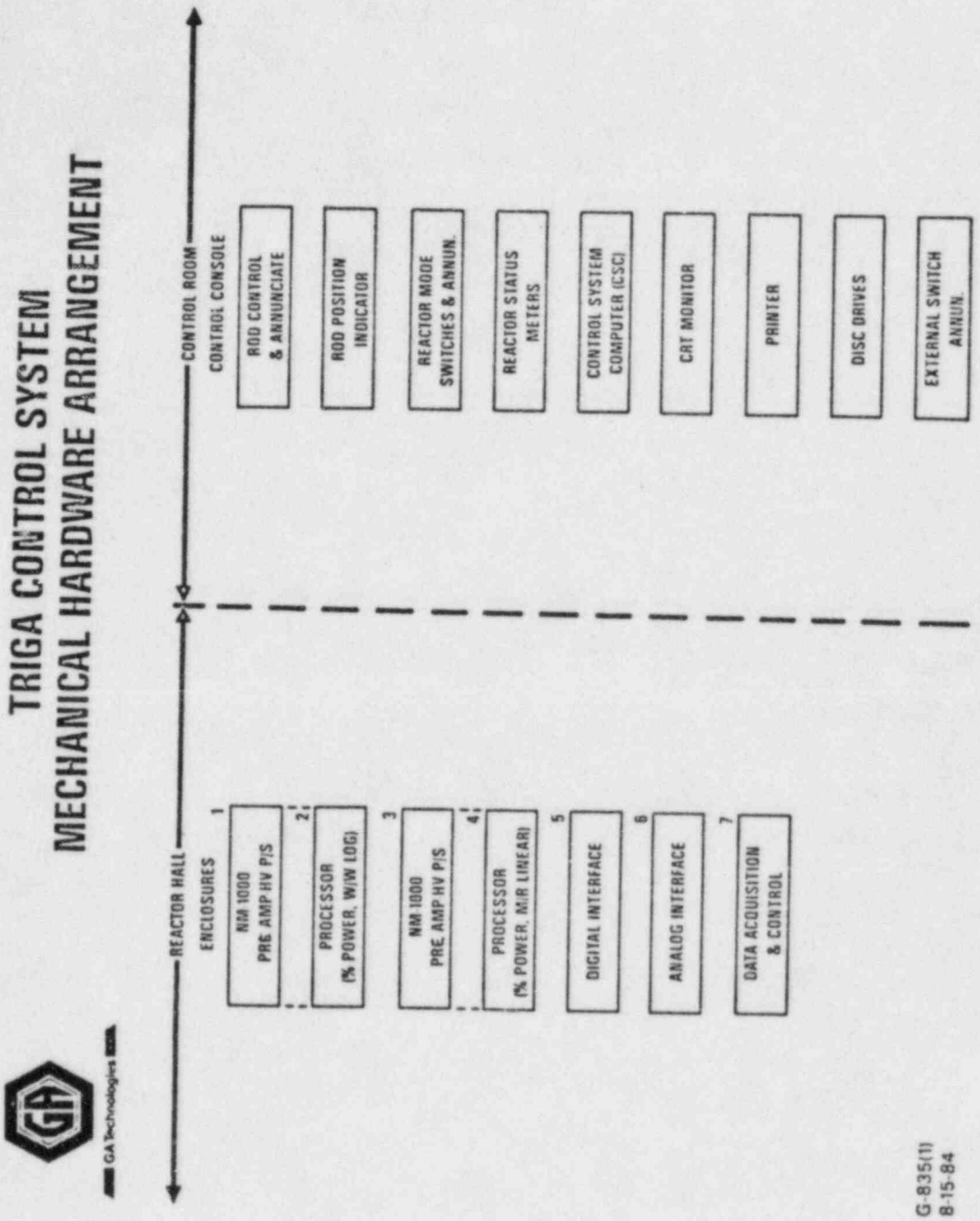

LOCATION OF CONTROL SYSTEM COMPONENTS
Figure 4-5

power from 1 to 125%, level trips from the log and linear percent power, calibrate and failure signals.

Enclosure 4 contains the NM-1000 microprocessor selected to provide the multi-range linear function from the information provided by the circuits in enclosure 3. In addition to the multi-range function, a linear percent power signal of 1 to 125% power is developed along with a trip level and associated calibrate and failure circuits.

Enclosure 5 houses the terminal strips which interface the digital signals of the DAC with the rod drives and external switches (such as beam port open-close). The magnet power supply is also mounted in enclosure 5 to facilitate easy access to the rod drive magnets. Opto-isolators provide the sensor inputs for a loss of magnet contact, magnet current and the up-down limit switches.

Enclosure 6 provides the analog interface where modular electronic sub-systems convert the various primary inputs into a 4-20 mA signal loop. The sub-systems contain their own power supplies and comparators for providing the required level trips. Calibrate circuits in each sub-system respond to the CSC requests for a specific input value as a check on system performance.

Enclosure 7 contains the DAC sub-assemblies and the communications loop to the CSC located in the control room. The digital and analog sub-assemblies contain calibration circuits which respond to periodic or programmed calibration requests from the CSC to verify proper operation and validity of the information being handled.

4.2 Design Evaluation

The TRIGA reactor console has developed through the successful operation of many installed facilities throughout the world. Design of the new ICS unit incorporates similar basic logic functions proven effective in prior designs. Incorporation of digital electronic techniques in the design to replace analogue circuits is justified by improved performance. Functional self-checks, circiut calibrations, and automated data logging are implemented effectively and efficiently.

Installation and verification of the original design is planned for a reactor operated by the ICS manufacturer, GA Technologies. Subsequent installation of the ICS unit at The University of Texas facility is planned with appropriate design changes, inclusion of facility specific parameters, and completion of an acceptance evaluation.

References Chapter 4

1. GA Technologies, private communications.

Chapter 5

REACTOR COOLANT SYSTEM

TRIGA is designed for operation with cooling provided by natural convective flow of demineralized water in the reactor pool. The suitability of this type of cooling at the power levels for this TRIGA has been demonstrated by numerous TRIGA installations throughout the world.

The primary functions of the coolant system are:

a. to dissipate heat generated in the reactor,

b. to provide vertical shielding above the core for radiation shielding.

Heat dissipation is satisfied by natural convective flow of pool water through the reactor core and forced circulation of the pool water through an external heat exchanger. The pool coolant volume is composed of approximately 38.6 cubic meters in a 2x3 meter oval pool with a vertical depth of 7.4 meters. A vertical shield is provided by about 6.4 meters of water above the reactor core.

Other functions provided by the coolant system are:

a. minimize corrosion of all reactor components, particularly the fuel elements,

b. maintain a minimal level of radioactivity in the reactor pool water and

c. maintain optical clarity of pool water.

These three functions are accomplished by a purification system that is included as a part of the coolant system.

5.1 DESIGN BASES

The design basis for the reactor coolant system is predicated on its primary function, reactor cooling. Other coolant system functions establish the design bases for the purification circuit.

5.1.1 Reactor Core Heat Removal

To assure adequate reactor cooling, the effectiveness of natural convective cooling has been evaluated with respect to the peak heat flux which may be achieved in the reactor. This evaluation then establishes the maximum heat flux beyond which fuel element cladding integrity cannot be assured.

Based on these evaluations, which were discussed in Chapter 3, it is concluded that for steady-state operation the coolant inlet temperature and maximum heat flux at which fuel clad integrity is no longer assured is determined by the curve relating heat flux and coolant temperature for the hottest coolant channel. The maximum design temperature of the coolant system, coolant inlet temperature, is 120°F (48.9°C). The maximum allowable peak heat flux at this temperature is 325 kBtu/hr-ft^2 (103 watts/cm^2) corresponding to a power level of 1900 kW for an 85 element core (see Chapter 3). Since the maximum licensed power level is 110% of design or 1100 kW, the resulting maximum heat flux will be 188 kBtu/hr-ft^2 (59.4 watts/cm^2) which is well below the value at which clad integrity may be questioned.

5.1.2 Reactor Pool Heat Removal

Supplemental cooling of the reactor pool is required for continuous operation at the rated power level. A heat rate of 22.3°C/hour is expected with the reactor operated at 1000 kW. Heat removal from the pool is provided by heat exchange with a chilled water supply. The chilled water supply is operated by the University for cooling of Research Center buildings and equipment. Chilling capacity is provided by multiple 1200 ton (4220 kW) units. At reactor rated power the heat removal capacity required is represented by about 25% of the chilling system capacity of one unit. A tube and shell heat exchanger is installed for heat removal from the reactor pool to the available chilled water system.

5.1.3 Heat Exchanger Design Basis

Heat exchanger capacity is designed for a stable operating temperature of the reactor pool at or below the coolant design temperature, 120°F (48.9°C) for convective reactor core cooling. The stable temperature is maintained by a heat exchanger capacity equivalent to the reactor core thermal output capacity. Other heat losses such as evaporation, or heat gains such as the pump, are considered negligible.

Heat transfer is defined by

$$q = U A \delta T_m \qquad (1)$$

where U = overall heat transfer coefficient (watt/m^2-°C)

A = surface area for heat transfer (m^2)

δT_m = true mean temperature difference (°C)

For a tube and shell heat exchanger the overall heat transfer coefficient is composed of three terms, the convective heat transfer from the fluid in the tubes to the tube walls, the conductive heat transfer thru the tube wall, and the convective heat transfer from the outside tube wall to the fluid in the shell of the heat exchanger. Based on the outside tube area for heat transfer, the overall heat transfer coefficient is defined as [1]

$$U_c = \frac{A_o}{A_i h_i} + \frac{A_o \ln (r_o/r_i)}{2\pi k l} + \frac{1}{h_o} \qquad (2)$$

where A_o = total outside tube area (m^2)

A_i = total inside tube area (m^2)

r_i = tube inside radius (m)

r_o = tube outside radius (m)

h_i = convective heat transfer coefficient between fluid in tubes and tube wall (w/m^2-°C)

h_o = convective heat transfer coefficient between fluid in shell and tube wall (w/m^2-°C)

k = conductive heat transfer coefficient in the tube wall (w/m^2 ·°C)

l = total tube length in heat exchanger (m)

A correction is applied for fouling of heat exchanger caused by buildup of various deposits. The overall heat transfer coefficient for a fouled heat exchanger is determined by

$$U_f = \frac{1}{R_f + 1/U_c} \qquad (3)$$

where R_f is the fouling factor, (non-dimensional)

The convective heat transfer coefficient is defined as

$$h = \frac{Nu\ k}{d} \qquad (4)$$

where Nu = Nusselt Number

k = thermal conductivity of the fluid evaluated at the appropriate average temperature (w/m · °C)

d = tube diameter or applicable hydraulic diameter (m)

The complicated nature of turbulent flow heat transfer is described by a Nusselt number determined by experimental correlation with the Reynolds and Prandtl Numbers. Dittus and Boelter [2] recommend the following relation for fully developed turbulent flow in tubes:

$$Nu_t = 0.023\ Re^{0.8}\ Pr^n \qquad (5)$$

where parameters are measured inside the tubes

Re = Reynolds Number based on tube diameter

Pr = Prandtl Number at average fluid temperature

n = 0.4 for heating

n = 0.3 for cooling

The relation for the shell side of a baffled cross flow heat exchanger is suggested by Colburn [3] as follows:

$$Nu_s = 0.33\ Re^{0.6}\ Pr^{0.33} \qquad (6)$$

where parameters are measured outside the tubes and

Re = Reynolds number based on tube outside diameter and velocity at minimum shell cross sectional area

Pr = Prandtl Number at average fluid temperature.

The product terms, A δTm, are defined consistent with the definition of U and heat exchanger design. The total cross sectional area of the tubes is represented by the heat transfer area, A, as specified by the heat transfer coefficient, U. The true mean temperature difference, δTm, is related to the heat exchanger type by a correction factor, F, and a log mean temperature difference, LMTD. The correlation relates a simple single pass heat exchanger with more complex multiple pass baffled units. A relation is defined by

$$\delta T_m = F * LMTD \qquad (7)$$

where F = correction factor [4,5]

$$LMTD = (T_a - T_b)/\ln(T_a/T_b) \qquad (8)$$

$T_a = (T_{inlet} - T_{outlet})$; tube side,

$T_b = (T_{outlet} - T_{inlet})$; shell side.

5.1.4 Water Purification Bases

The functions of corrosion control, radioactivity control, and optical clarity of the coolant water are provided by filtration and ion exchange. Control of the water purity is performed by analysis of the water conductivity. Measurements of water conductivity as low as 2.0 micromho per centimeter (or resistance of 1 megaohm per centimeter) are maintained by filtration and ion exchange. The conductivity is reduced further by control of materials exposed to the reactor coolant, dust settling to the pool surface, and occasional cleaning of pool surfaces. Experience has shown that conductivities of 5.0 μmho/cm are sufficient to maintain acceptable limits on corrosion plus good quality for water optical quality and removal of activation products in the water.

5.2 SYSTEM DESIGN

Principle components of the coolant system are the aluminum reactor pool tank, the external cooling loop consisting of heat exchanger and pump, and purification loop consisting of filter, resin bed and pump. Most of the total coolant volume is represented by the approximately 38.6 cubic meters of water in the reactor pool. A typical flow diagram for the system is shown in Figure 4-1.

5.2.1 Coolant System

Suction of water from the pool is provided by inlets that extend no more than 2 meters below the top of the reactor tank. The suction intake is composed of a bulk flow inlet for most of the intake volume and a limited volume flow inlet for water surface skimming. The coolant water is drawn through the coolant pump and forced through the heat exchanger. Return of cooled water to the reactor pool is provided by a discharge outlet above the reactor core or an outlet near the tank bottom. A diffused water jet is created at the outlet by a nozzle above the reactor core. Delay and diffusion of the reactor core convective coolant column is enhanced by the action of the coolant discharge nozzle.

Accidental siphoning of reactor pool water is prevented by the presence of suction breaks on both suction and discharge lines of the coolant system. Siphon breaks are created by holes located in the lines approximately half a meter below the normal water level.

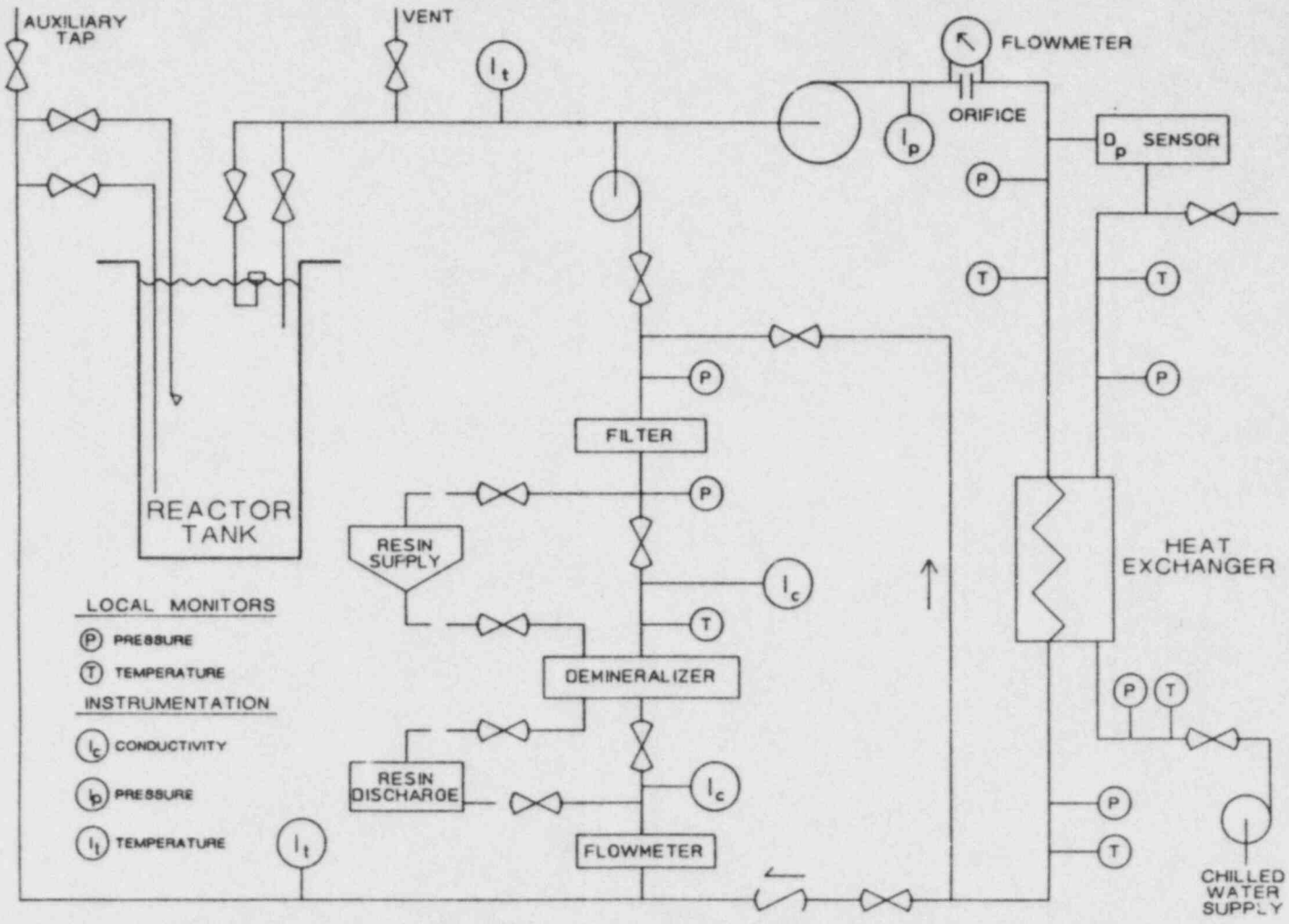

WATER COOLANT & PURIFICATION SYSTEMS

COOLANT AND PURIFICATION SYSTEM LAYOUT
Figure 5-1

The heat exchanger and pump, the major components of the cooling system, are located at about the same vertical level as the reactor core. Valves are provided in the coolant loop for control and isolation of the cooling system function. Specifications of cooling system components are listed in Table 5-1. A positive pressure difference of 1psi (7kilopascals) between the shell side outlet and tube side inlet of the heat exchanger is designed to prevent leakage of primary pool coolant into the secondary chilled water system.

Table 5.1
REACTOR COOLANT SYSTEM DESIGN
SUMMARY

Reactor Tank		
Material	Al plate (6061)	
Thickness	1/4in. (0.635 cm)	
Volume (maximum)	10525 gal. (39.85 m^3)	
Coolant Lines	Aluminum (6061)	
Valves	Aluminum	
Diameter	3in. (7.62 cm)	
Coolant Pump		
Type	Centrifugal	
Material	Stainless steel	
Capacity	375 gpm (23.6 liter/sec)	
Heat Exchanger		
Type	Shell and tube	
Materials: shell	Carbon steel	
tubes	304 stainless steel	
Heat Duty	1000 kW	
Flowrate: tubes	225 gpm (23.6 liters/sec)	
shell	375 gpm (14.2 liters/sec)	
Typical Parameters:		
Tube inlet	100°F	40 psia
Tube outlet	68°F	30 psia
Shell inlet	45°F	65 psia
Shell outlet	67°F	45 psia

5.2.2 Purification System

A purification loop is integrated into the cooling system. The loop bypasses the heat exchanger and is located at about the same vertical location as the heat exchanger. A portion of the cooling system flow, less than 10 gal/min

(0.6 liters/sec), is diverted through the purification loop during operation of the cooling system. A small purification loop pump is operated when the cooling system is not in operation to allow continuous removal of suspended particulates and soluble ions from the water coolant. Water suction and discharge is accomplished by the same lines that are used by the cooling system. The purification system is operated either independently or in conjunction with the cooling system.

Purification functions of the loop are generated by two components, a filter for removal of suspended materials and a resin bed for removal of soluble elements. Typical filtration is provided with 25 micron filters. Typical ion exchange is provided by .085 cubic meters of mixed cation and anion resin. Water purity is measured by conductivity cells at the inlet and outlet of the resin beds. Purification loop flow rate is indicated by a flow meter so that flow rate through the resin bed is controlled.

5.2.3 Water System Instrumentation

Several monitoring sensors are installed to allow remote readout of water system parameters in the reactor control room. Other system parameters are indicated by local monitoring devices. Parameter monitoring points are illustrated in Figure 4-1. The parameters that are considered part of the water system instrumentation system are presented in Figure 4-2.

Indication of the reactor pool status is determined by two sensors located in the pool. Pool level and bulk pool temperature sensors in the pool are monitored in the control room. An annunciator and alarm indication are generated by high or low pool levels and by high pool temperatures.

Measurements of cooling system function are indicated by two temperature probes, one on the pool suction line and one on the pool discharge line. Both temperatures are observed on the bulk pool temperature meter by actuation of a momentary contact switch. Typical temperature probes used are resistance temperature detectors (RTD's).

Water quality is determined from two conductivity cells in the purification loop. The cells are located on inlet and outlet lines of the demineralizer with readouts located in the control room. Conductivity cells are designed with platinum electrodes shielded by glass. A Wheatstone bridge circuit in the control room is connected to the cells by a switch for selecting inlet or outlet conductivity. The circuit is composed of a rectified power supply, one stage amplifier, temperature compensation and electric tuning eye.

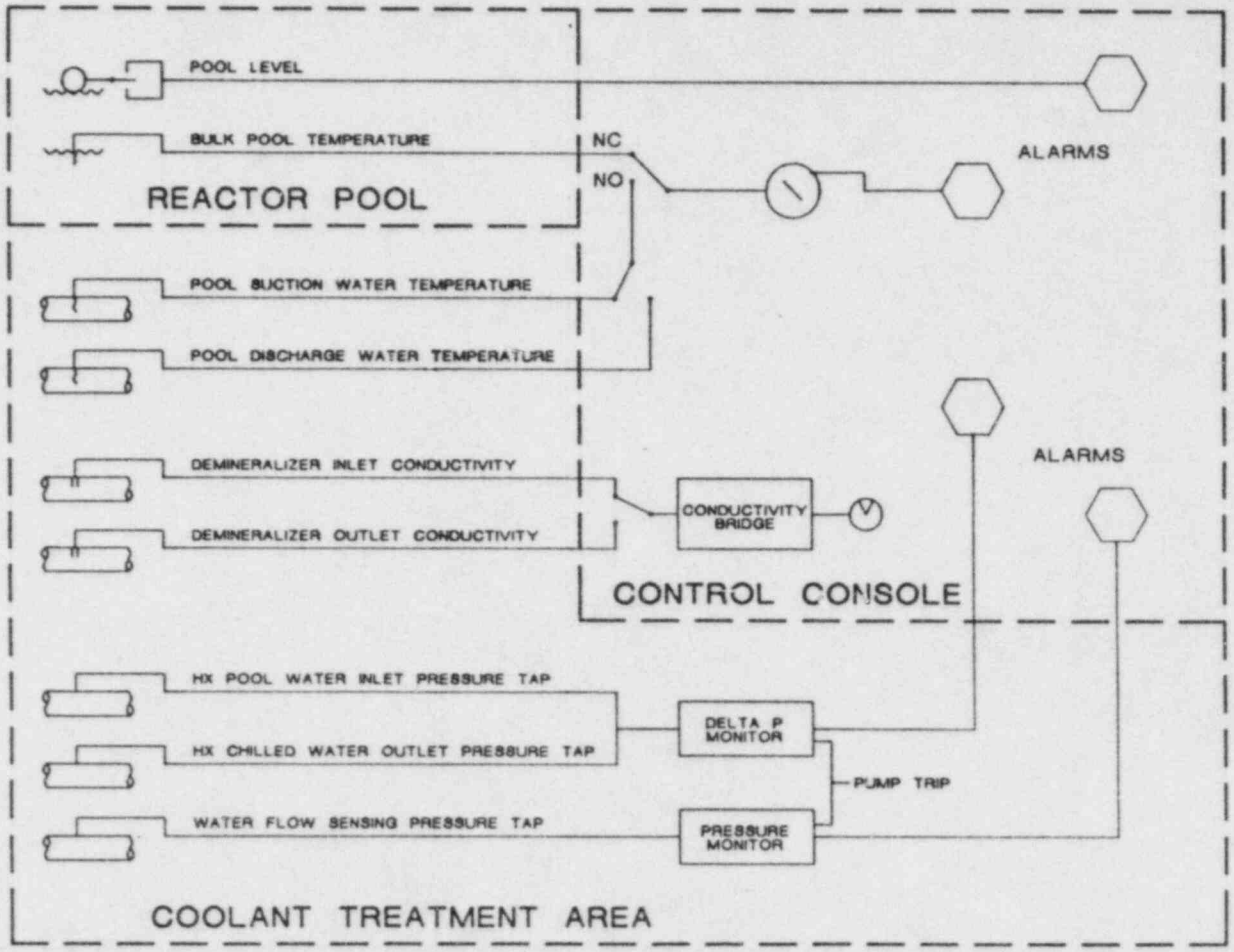

POOL WATER MONITORING SYSTEM

WATER SYSTEM INSTRUMENTATION
Figure 5-2

Heat exchanger operation and coolant flow indication in the coolant room is generated from two pressure measurements. One pressure sensor in the coolant line is installed for indication of coolant flow. A pressure monitor is provided with a trip to stop the coolant pump on loss of flow pressure. An alarm indication from the pressure loss caused by flow loss is transmitted to the reactor control room. A second pressure measurement of the pressure difference between the high pressure point on the heat exchanger tube side and low pressure point on the heat exchanger shell side is made with a pump trip provided on loss of positive differential pressure. The differential pressure is designed for a difference substantially greater than 7 kilopascals (1 lb/sq.in.). Alarm indication of loss of pressure differential is provided in the reactor control room.

Several water system parameters are measured by local pressure or temperature sensors in the system lines. Both temperature and pressure probe are located on the inlet and outlet lines of the pool water side and chilled water side of the heat exchanger. A local indication of flow in the coolant loop is provided by the pressure drop across an orifice in the flow path. Purification loop flow is measured by an in line flow meter. Water pressure before and after the filter in the purification loop is measured for indication of filter condition.

5.3 WATER SYSTEM DESIGN EVALUATION

The water system including the reactor pool and the external cooling and purification loops have similar design features as used in many other operating TRIGA facilities. The demonstrated capability and integrity of this system provides assurance that the coolant system will perform its function properly and safely.

Availability of pool water for cooling and vertical shielding is assured by designing the system with siphon breaks on suction lines and discharge lines within 2 meters of the normal pool level. Greater losses of pool water are extremely improbable, although they could conceivably be initiated by rupture of the reactor tank. As shown in the loss of pool water accident analysis, even with complete loss of pool water fuel clad integrity is not threatened.

Adequacy of reactor cooling is assured by the large amount of cooling capacity inherent in the reactor pool volume as well as the capacity of the external cooling circuit which can dissipate heat at a rate equivalent to 1000 kW steady-state operation. If the available heat exchanger capacity is diminished to 900 kW and the initial pool temperature is 100°F, the reactor can be operated for

more than 5 hours before the bulk pool temperature reaches 120°F. The actual time would be considerably longer since as the bulk pool temperature increases the heat exchanger heat removal capacity increases. Without external cooling or other heat loss the bulk pool temperature will rise approximately 22.3°C after one hour of operation at a steady-state power level of 1000 kW(t).

Heat removal capacity and thus pool heat rate is specified by analysis of a six baffle tube and shell heat exchanger. At a flow rate of 250 gal/min (15.75 liters/sec) of chilled water at 45°F (7.22°C) a heat removal rate of 1050 kW is expected. The presence of fouling in the heat exchanger is considered minimal based on the purity of the two heat exchanger fluids. Capacity is reduced to 890 kW for a fouling factor of .0004. The heat transfer and hydraulic parameters used are shown in Table 4-2.

Experience with this purification equipment in other TRIGA systems has shown that coolant conductivity can be easily maintained at levels of less than five micromhos per centimeter using the materials contained in the coolant system design. Furthermore, this experience has shown that no apparent corrosion of fuel clad or other components will occur if the conductivity of the water does not exceed five micromhos per centimeter when averaged over a 30-day period.

Control of radioactivity in the coolant is provided by the purification system. Should radioactivity be released from a clad leak or rupture of an experiment, detection of the release would be signaled by the continuous air monitor or by the reactor room area monitors. Based on coolant transport time calculations in the safety analysis section, these monitors should register an increase in coolant radioactivity within approximately 60 seconds of the time of radioactivity release. The transport time is estimated from the time for the coolant exposed in the core to reach the surface of the water where the continuous air monitor will detect a release of radioactivity from the pool water. An alternate indication of radioactive release is provided if a water activity monitor is installed or by a GM detector area monitor.

Table 5-2
HEAT EXCHANGER HEAT TRANSFER AND HYDRAULIC PARAMETERS

Tubes:	
Outside Diameter	0.750 inch (1.91 cm.)
Wall Thickness	0.049 inch (0.124 cm.)
Thermal Conductivity	8.21 Btu/hr, ft. °F
Flow Area:	
Tube Side	8.0 in^2 (51.6 cm^2)
Shell Side	33.7 in^2 (217 cm^2)
Heat Transfer Surface	341 ft^2 (31.7 m^2)
Average Prandtl Number	
Tube	5.69
Shell	9.07
Reynolds Number	
Tube	6.33×10^4
Shell	1.80×10^4
Corrective Heat Transfer Coefficients	
Inside Tubes	1755 Btu/hr ft^2°F (9966 w/m^2°C)
Outside Tubes	1316 Btu/hr ft^2°F
LMTD	22.7 °F (12.6°C)
Corrective Factor F	0.83
Average Kinematic Viscosity	
Tube	0.9×10^{-5} ft^2/sec (8.36×10^{-7} m^2/sec)
Shell	1.35×10^{-5} ft^2/sec (1.25×10^{-6} m^2/sec)

Chapter 5 References

1. Holman, J.P., "Heat Transfer", McGraw-Hill, Fourth Edition, 1976, pp 386-321.

2. Dittus, F.W. and Boelter, L.M.K., "Univ. California (Berkley) Pub. Eng.", vol. 2, pp 443, 1930.

3. Colburn, A.P. , "A Method of Correlating Forced Convection Heat Transfer Data and Comparison with Fluid Friction", Trans. AIChE vol. 29, pp 174-210, 1933.

4. Bowman, R.A., Mueller, A.C., and Nagle, W.M., "Mean Temperature Difference in Design", Trans. ASME, vol. 62 (1940), pp 283-294.

5. Tubular Exchanger Manufacturers Association, "Standards TEMA/3rd Ed.", New York, 1952.

6. Kreith, F., "Principles of Heat Transfer", Third ed., 1976, pp 557-560.

Chapter 6

FACILITY DESIGN

The TRIGA Mark II reactor is located in a special laboratory bay of an engineering laboratory building. Most of the building design is determined by criteria that are not necessarily directly related to the reactor. However, several design features are incorporated to assure safe facility operation and effective utilization of facility equipment.

Structural engineering design of the building is specified by standard University procedures developed from the Uniform Building Code and State of Texas Building Code. All elements are designed for seismic activities specified for Zone 0 conditions. The provisions of the Life Safety Code and National Fire Protection Code are included in building features.

The building site is located above a rock subsurface composed of limestone that will accommodate substantial loads(1690 kg/m^2). Building foundation is composed of poured concrete piers with concrete slab on compacted fill. Building superstructure is constructed of reinforced concrete for columns, beams, floors and roof. Exterior structure walls ae fabricated of precast concrete slabs.

Building orientation, floor plans, and a section of the reactor bay area are shown in Figures 6-1 thru 6-5. Total floor space of the facility is approximately 1675 square meters.

Areas of the building include office space, general laboratory areas, specialized laboratory areas, support areas and the reactor facility. Some operations of the reactor are supported by specific features or functions of areas not within the reactor bay and control area. Shop areas for mechanical or electrical work and laboratories for radiological measurements are operated within the building for activities of both the reactor operation and education, or applications in nuclear engineering.

6.1 DESIGN BASES

The design of a structure to contain the TRIGA reactor depends on the protection requirements for the fuel elements and the control of exposures to radioactive materials. Fuel elements and other special nuclear materials are protected

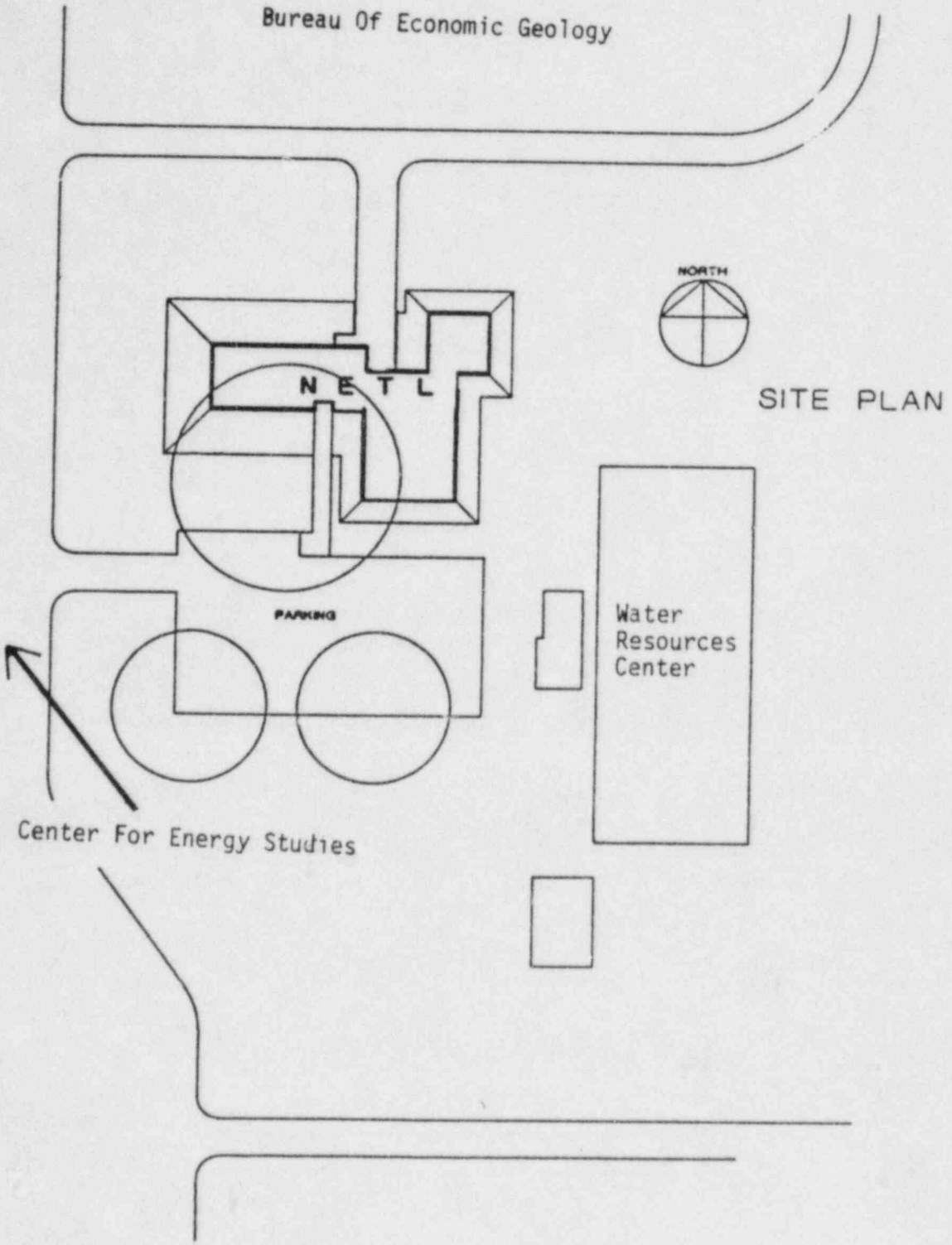

NETL SITE PLAN FOR
BALCONES RESEARCH CENTER
Figure 6-1

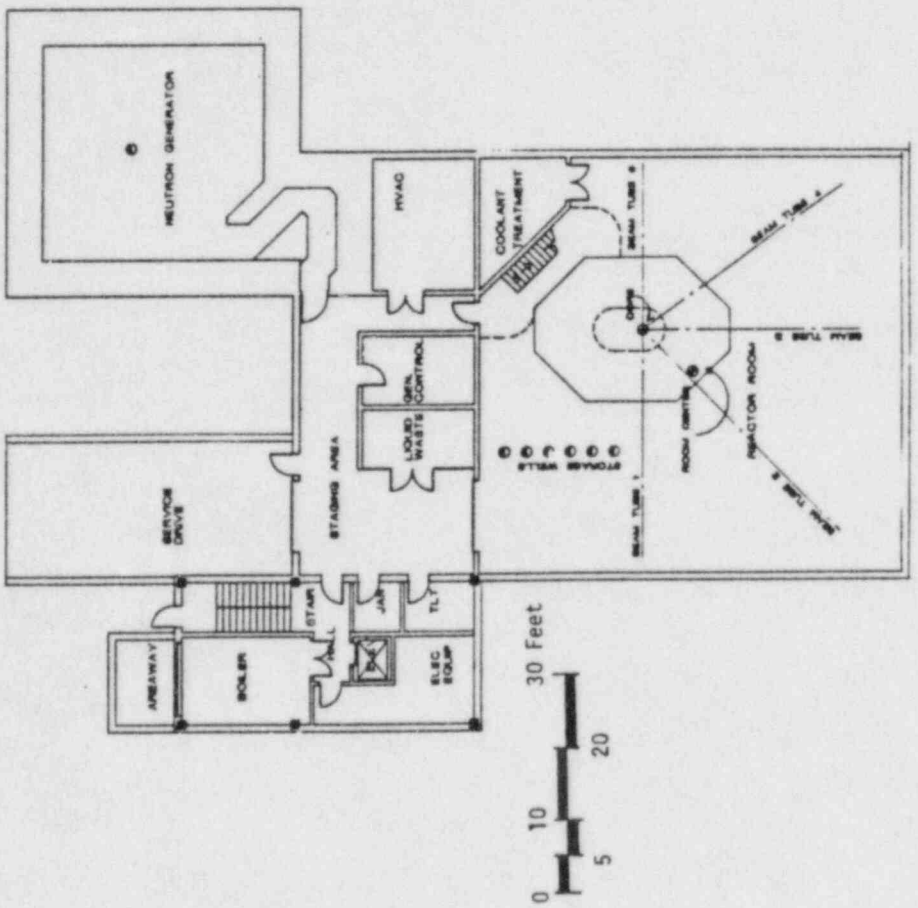

NETL BUILDING FIRST LEVEL
Figure 6-2

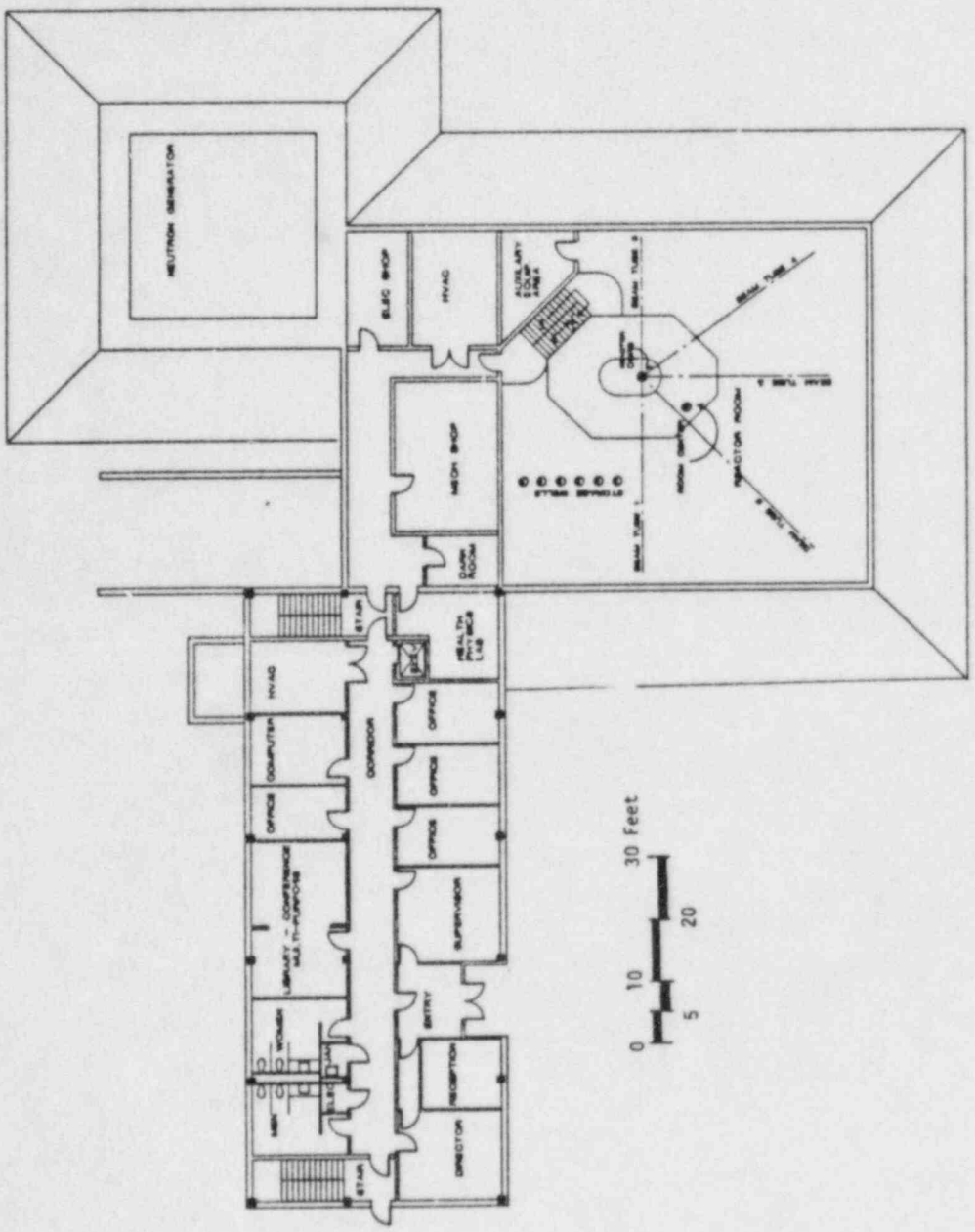

NETL BUILDING SECOND LEVEL
Figure 6-3

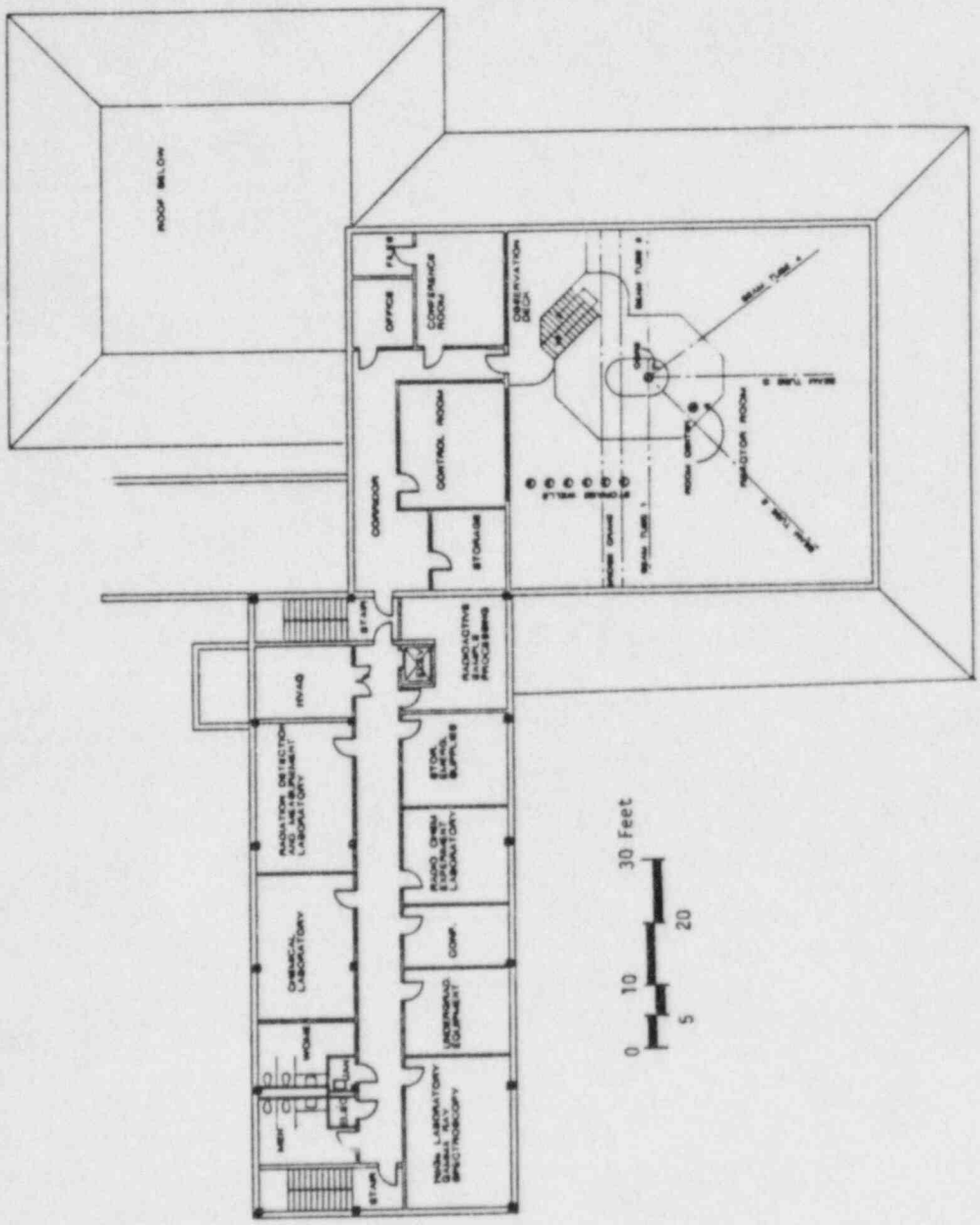

NETL BUILDING THIRD LEVEL
Figure 6-4

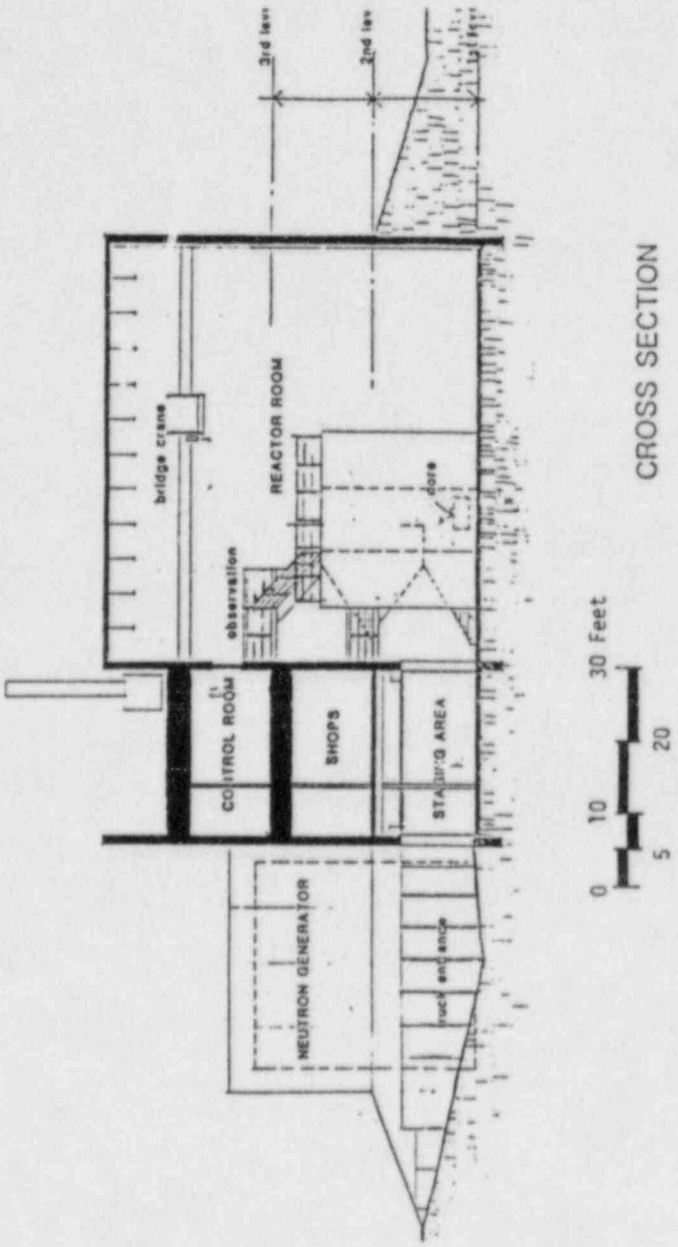

CROSS SECTION OF REACTOR FACILITY AREA
Figure 6-5

by physical containment and surveillance. The physical containment will also control the release of radioactive materials during routine operation or potential accident conditions. Release of airborne radioactivity consists mostly of air activation products from routine operation or fission product materials from a non-routine fuel element failure. Liquid and solid radioactive material are also controlled to assure compliance with appropriate release criteria standards. Other potential releases may be associated with specific types of experiments that require special equipment to provide sufficient control of material releases. The reactor room containment is designed to control the exposure of operation personnel and the public from radioactive material or its release caused by reactor operation. Release criterion are based on Title 10 Chapter 20 of the U.S. Code of Federal Regulations [1].

6.2 REACTOR BAY AND CONTROL AREA

Reactor tank, shield and primary experiment facilities are located in a reactor bay area that is roughly 18.3 meters on each side. A total of 4575 cubic meters of volume is enclosed in the reactor bay above the 335 square meters of floor space. Support of reactor operation and of reactor experiment activities is provided by a control area located adjacent to the reactor bay. Space in the control area is divided into a conference room, office, control room and entry way. Total control area (7.3 by 18.3 m) is 134 square meters of floor space and roughly 489 cubic meters of air space. The floor level of the reactor bay is one level below the office and laboratory areas located on levels two and three of the building.

6.2.1 Physical Design

Design of the TRIGA reactor facility area is specified by constraints on the function of the architecture design, access control for security, radiological control for safety and applicable building code standards.

All access points to the reactor bay are located inside the engineering building and enter from the north side. The remaining three sides of the reactor bay area are enclosed by exterior walls. Both emergency exits and equipment bay doors on the first level open into the adjacent area within the building from which building exits are accessible. Adjacent areas on the north side of the reactor bay provide some laboratory support functions in conjunction with other building support functions. On the third level from the reactor floor the adjacent area to the reactor bay is supplemented by the control room area, conference area operation office, and routine entry point. The third level entry way is provided for access to the control area from

the laboratory building and access to the reactor bay from the control area. Access at the third level is to the top of the reactor shield structure. A stair structure is attached to the reacor shield with a supplementary access point to the reactor bay on the second level.

Design of access points and interior walls are specified for security control, fire control, and ventilation control. Penetrations, besides the doors, into the reactor bay and control areas are limited in size and are sealed to limit air leakage. Details of the reactor bay area are presented in Figure 6-6. A 5-ton bridge crane is installed in the reactor bay for movement of shield structures, heavy equipment and fuel transport loading.

6.2.2 Ventilation Design

Ventilation design is specified to isolate the reactor bay area in the event a radioactive release is detected in the reactor area. The ventilation system is designed to maintain a negative pressure within the reactor bay with respect to the building exterior and other building areas when the high volume system is operating. During normal operation ventilation is exhausted through a roof stack. Isolation of the room is initiated by a signal from the detection of high radiation levels by an air particulate monitor. Isolation is achieved by air control dampers and leakage prevention material at doors and other room penetration points.

Schematics of the ventilation system for he reactor bay area and a diagram of the ventilation control system sensors and controls are provided in Figure 6-7.

An auxiliary low volume room air purge is configured for supplemental movement of air in the reactor bay. The purge system is designed for the potential installation of High Efficiency Air Particulate. Operation of the purge system is controlled by an air activity sampler with the air exhausted t the roof stack. Routine operation of the purge system is d signed for ventilation of the radioactive gases from the laboratory. A schematic of the auxiliary ventilation system is shown in Figure 6-8.

6.2.3 Reactor Shield Structure

Reactor tank and shield design are specified to provide a reliable containment for the reactor coolant and an effective shield for reactor radiations. Shield thickness is determined by radiological exposure constraints with a goal of 1 mrem/hr specified for most accessible areas of the shield. Radiation doses above the shield and at selected locations are expected to exceed the design goal.

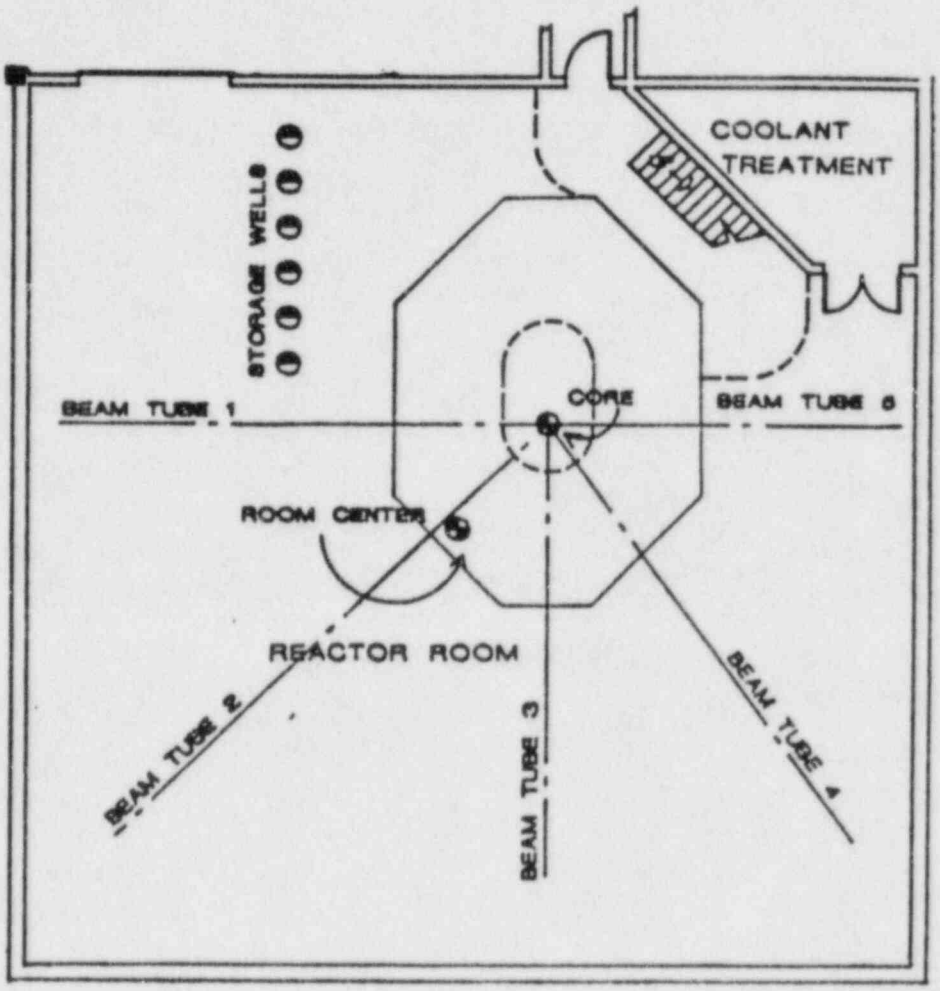

REACTOR BAY AREA
Figure 6-6

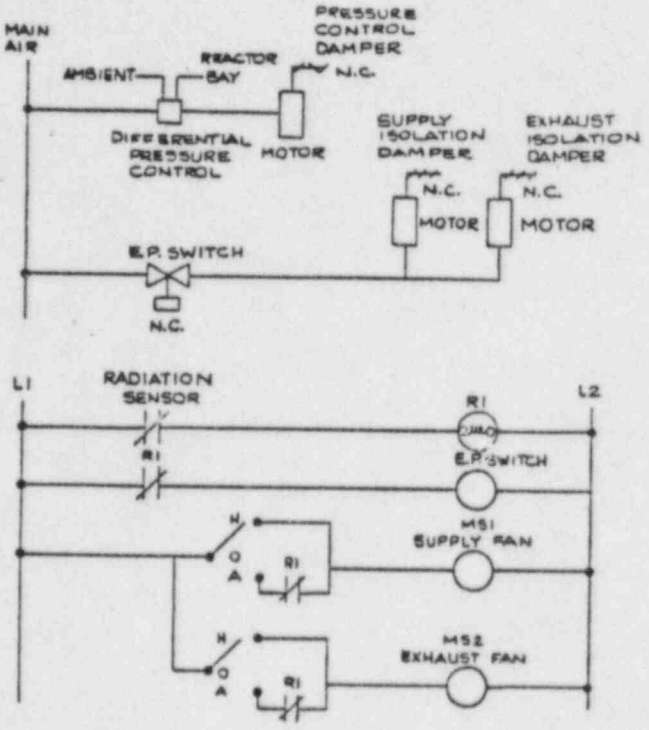

MAIN EXHAUST , ETC.

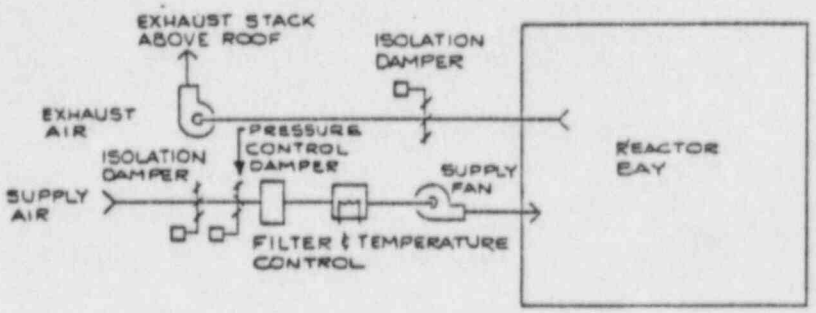

MAIN AIR SUPPLY SYSTEM

REACTOR BAY AIR VENTILATION SYSTEM
Figure 6-7

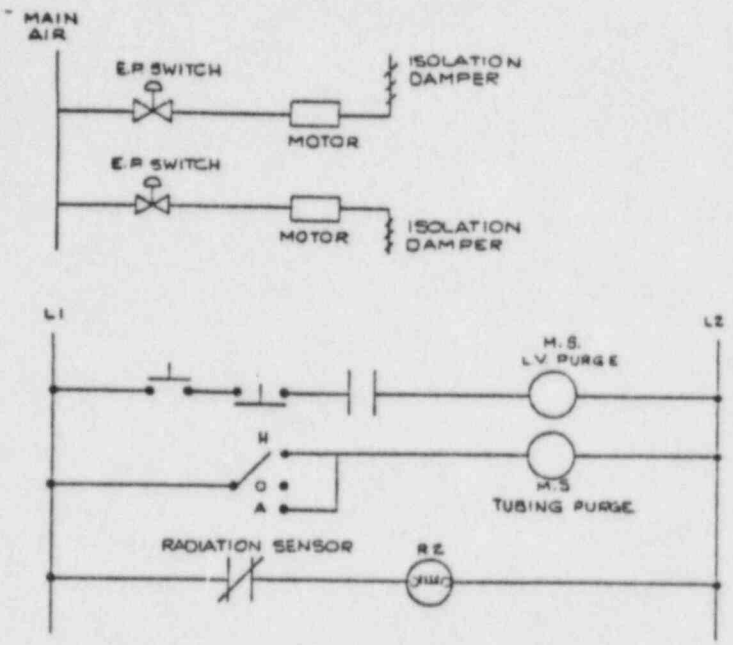

AUXILIARY AIR SCHEMATICS

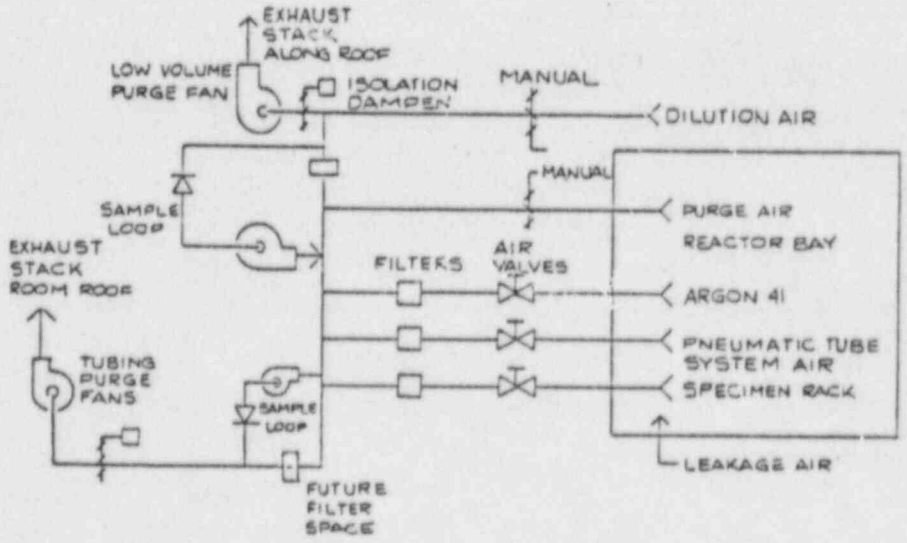

AUXILIARY AIR EXHAUST SYSTEM

REACTOR BAY AUXILIARY EXHAUST SYSTEM
Figure 6-8

Composition and design of the shield are also analyzed for structural properties such as seismic response.

Special features of the shield such as beam tubes, are designed with beam plugs sliding lead shutters, bolted cover plates and gasket seal for protection against reactor radiation and coolant leakage when the tubes are not in use. Other shield penetrations are designed for appropriate radiation shielding. Features of the shield structure are illustrated in Figure 6-9.

6.3 SUPPORT FACILITIES

6.3.1 Radioactive Waste Control

Gaseous radioactive effluents from the operation of the rotary specimen rack and pneumatic irradiation tube are filtered with HEPA filters and vented through the auxiliary ventilation system. Argon-41 from reactor beam tubes is vented via a collection manifold that also exhausts to the auxiliary ventilation system.

A system for retention of liquid radioactive waste is installed on the first level of the building. An area separated by a chain link enclosure from the building loading area is provided for liquid waste storage tanks and solid waste storage barrels. The area is designated for temporary storage of materials of low radioactivity and is not expected to require shielding. Temporary shield block will be installed as required.

Liquid waste from the sink and shower of the Sample Handling Laboratory and drains from the reactor shield, reactor bay and liquid waste storage area are connected to a 1000 gallon retention tank in a pit exterior to the building. A sample line, dilution line and discharge line are connected to the retention tank. Discharge from the tank is accomplished by a pump with gate valves to route the discharge to supplemental storage or sanitary sewer.

Schematics of the gaseous and liquid radioactive effluent handling systems are presented in Figure 6-10. Solid radioactive wastes are segregated for disposal and transport to an approved radioactive waste burial facility.

6.3.2 Sample Handling Laboratory

A sample handling laboratory is situated adjacent to the reactor facility on the third level for the processing of radioactive samples and materials. Access ports via air or gas transfer tubes are installed to move samples between the reactor area and the Sample Handling Laboratory. Two separate sample transfer systems are provided, one for the

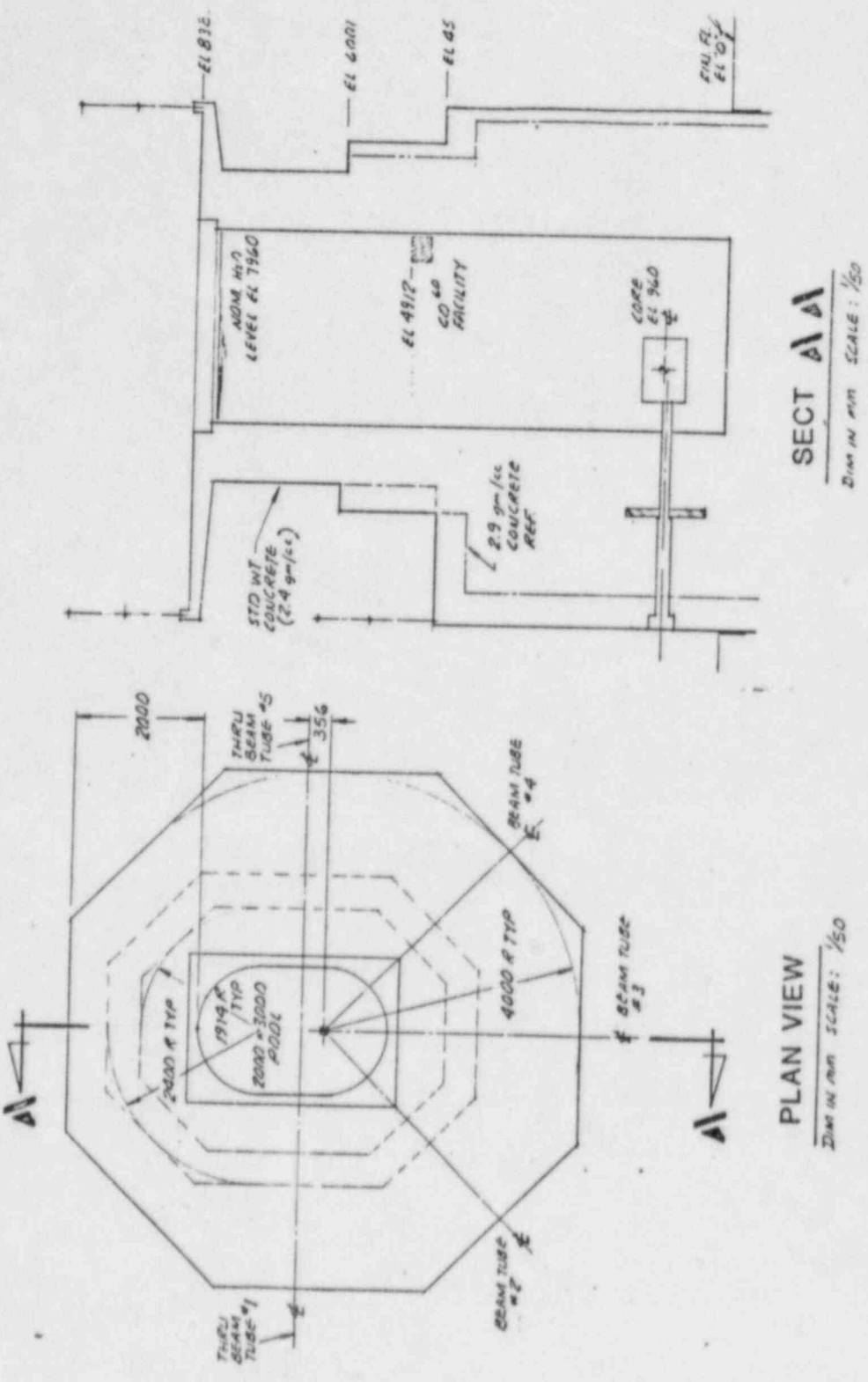

REACTOR SHIELD STRUCTURE
Figure 6-9

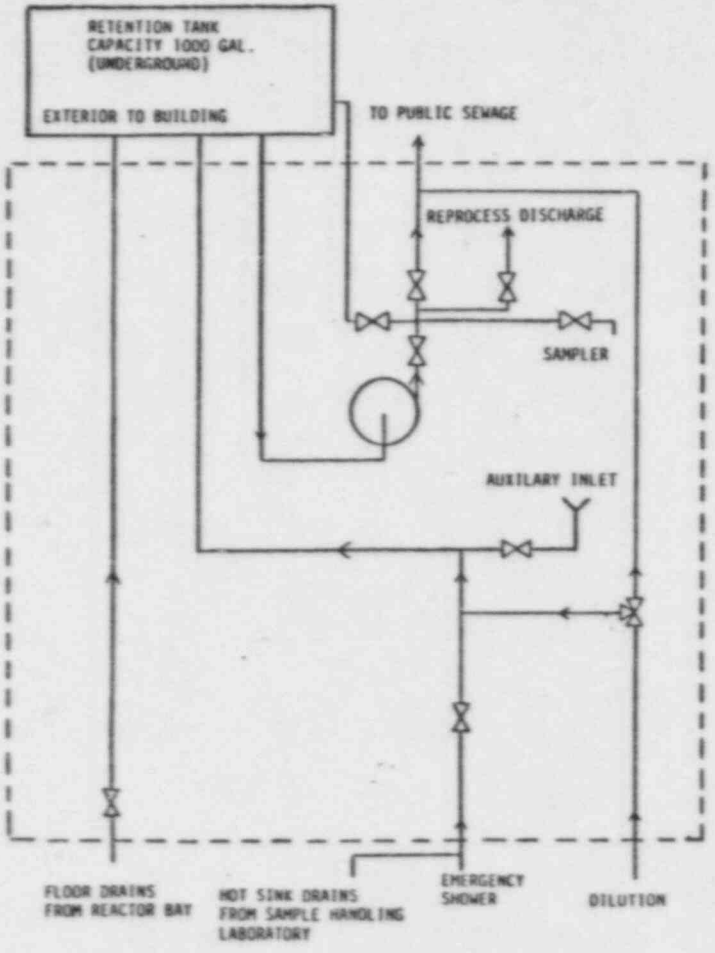

LIQUID WASTE HANDLING SYSTEM SCHEMATIC DIAGRAM

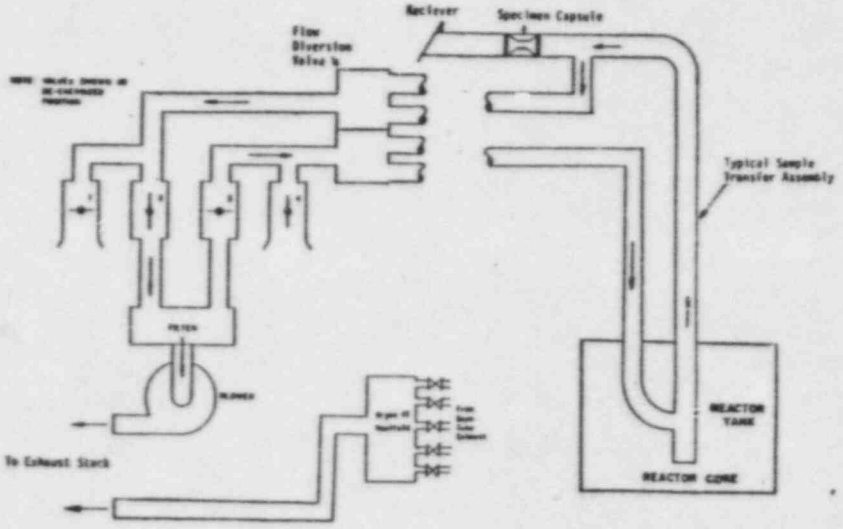

Argon 41 Gaseous Discharge System

pneumatic tube irradiation facility and one for loading the rotary specimen rack facility.

A hood for handling radioactive materials, a sink for disposal of radioactive liquids and a safety shower for decontamination are installed in the Sample Handling Laboratory.

6.3.3 Health Physics Laboratory

A Health Physics Laboratory is situated adjacent to the reactor facility on the second level. Radiation counting systems for evaluation of radiation exposure or contamination, are maintained in the Health Physics Laboratory. Equipment such as a thermoluminescent reader and an alpha-beta proportional counter are maintained in the laboratory. Other equipment and supplies operated or stored in the Laboratory are as portable radiation monitors, coveralls, gloves and related items.

6.3.4 Other Laboratories

Neutron activation of samples is supported by a Chemistry Laboratory for special sample preparations and a Gamma Ray Spectroscopy Laboratory for evaluation of sample irradiations. Student instruction and research areas with radiation counting systems are located in the Radiation Detection and Measurement Laboratory, and a Undergraduate Equipment Laboratory. Supplemental activities are planned for the Radiochemistry Experiment Laboratory.

A major experimental facility of the engineering laboratory is included in the shielded Neutron Measurement Laboratory. The area is a cubical area roughly 9 meters on a side with 1.2 meter thick concrete walls. A control room is located near the measurement area for the control of accelerator generated neutrons and acquisition of experimental data.

6.3.5 Support Areas

Several areas adjacent to the reactor bay on the first level and the second levels are intended for support of some reactor functions such as air ventilation and repair or assembly areas for mechanical and electronic equipment. A staging area on the first level is designed for heavy equipment access to both the reactor bay and the building.

6.4 SPECIAL EXPERIMENTAL FACILITIES

6.4.1 Reactor Core Facilities

Reactor core experiment facilities are designed for replacement of either single fuel element positions or a special multielement position. Access to the core peak flux is provided by a central thimble. The wet central thimble is designed to allow insertion of an encapsulated sample into the core center or extraction of a vertical neutron beam from the core center. Two experiment facilities are located in single element positions in the reactor core for insertion of samples into the reactor neutron flux. A pneumatic terminal is provided for short irradiations of small samples and a dry tube is provided for long period irradiations of small samples.

Experiments with reactor characteristics are demonstrated by a reactivity oscillator apparatus. The oscillator is fabricated with rotating absorbers that are inserted in a single element position.

Multielement experiment locations in the reactor are positioned in the cor center or near the core reflector interface. Fabrication of experiments for the multielement positions are projected for future facility development.

6.4.2 Beam Tube Facilities

Access to horizontal neutron beams is created by five beam tubes penetrating the reactor shield structure. All beam tubes are 6 inch diameter tubes originating at or in the reactor reflector. One tangential beam tube is composed of a penetration in the reactor reflector assembly with extensions through both sides of the reactor shield. A second tangential beam tube penetrates and terminates in the reactor reflector. The two remaining tubes are oriented radial to the reactor core.

6.4.3 Cobalt-60 Irradiation Facility

A cobalt-60 irradiator consisting of 156 pencil size sources is installed in the reactor coolant pool. Each source is contained in a space 0.5 inches diameter and 11.25 inches length. Sources are doubly encapsulated with inner aluminum clad and outer stainless steel clad. The source pencils are arranged in a double staggered, circumferential array with an inside radius of 10.5 inches and outside radius of 12.5 inches (Figure 6-11a). The total source strength when installed was 9260 Curies. A shelf suspended in the pool at the end opposite to the reactor location holds the cobalt-60 irradiation facility below 10 feet of water. Access to the facility is provided by water tight canisters or dry irradiation tubes. Two canisters with 0.625 inch wall thickness, 5.0 inch radius and 11.5 inch height and several 2 inch diameter vertical beam tubes provide exposure volumes for routine experimentation.

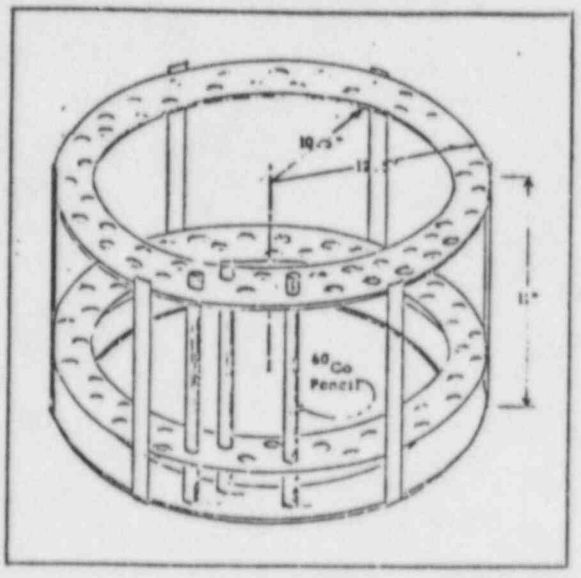

^{60}Co Irradiator Fixture

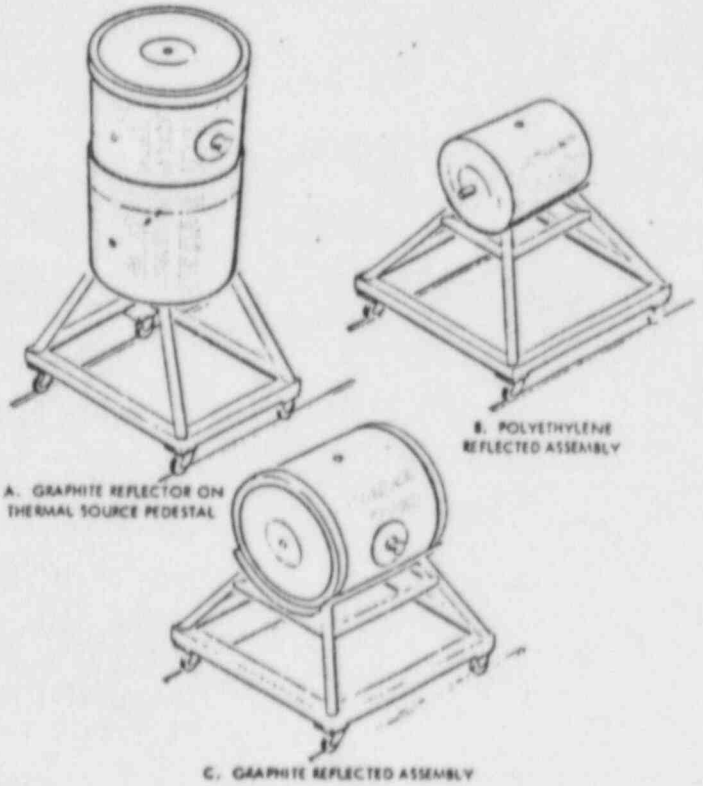

SPECIAL EXPERIMENT FACILITIES
Figure 6-11

6.4.4 Subcritical Reactor and Moderators

Cylindrical assemblies of graphite and polyethylene are utilized for student laboratory experiments with neutron sources and a subcritical uranium-235 reactor assembly. The plutonium beryllium neutron sources and uranium dioxide used in the polyethylene subcritical assembly may be stored and used in the room containing the reactor but are licensed separately from the reactor. The subcritical core and moderator assemblies are products of Lockheed Nuclear Products (Figure 6-11b).

The subcritical polyethylene core is a cylinder 10 inches in diameter and 14 inches long. Reflector assemblies can be assembled with or without the fueled core. Dimensions of the cylindrical reflector assemblies are 30 inch diameter by 34 inch length for the graphite moderator and 22 inch diameter by 25 inch length for the polyethylene moderator. An additional graphite moderator cylinder 30.5 inches high by 24 inch diameter is available for neutron source moderation.

6.4.5 14 MeV Neutron Generator

A small accelerator is designed for the production of D-T reaction neutrons for research measurements and activation experiments. Application areas of the source of neutrons are proposed in neutron dosimetry, neutron activation, and neutron interactions for analysis of related research problems.

6.5 CONTAINMENT DESIGN EVALUATION

Containment evaluation depends on the quantity of airborne radioactivity release possible from the air and water that are in the region of the reactor during operation. Calculation, measurement, and experience of similar research reactors support the evaluation. Evaluation is limited to routine effluents and should be supplemented for experiment conditions that present specific release problems. Analysis of fission product releases are treated in another chapter. The most significant radiological effluents of the reactor are argon-41 and nitrogen-16.

Measurement and experience of other facilities have shown that for a facility of this type the most significant routine radiological contributions are caused by argon-41 generated by the exposure of air in experimental facilities and by nitrogen-16 transported in the coolant from the reactor core region. Argon-41, a noble gas, is contained for decay or eventually released to the atmosphere for

decay. Nitrogen-16, a dissolved gas, is contained in the coolant and generally is dissipated by radioactive decay in the coolant.

6.5.1 Release of Argon-41 and Nitrogen-16 from Pool Water

Argon-41 is produced in the reactor pool as a result of the (n,γ) reaction with argon-40 dissolved in the pool water. Most of this argon-41 remains in solution but some of it is transferred to the reactor room air at the pool surface. Calculations of the argon released from the pool surface estiate a concentration in the room of 1.6×10^{-6} μCi/cc with the reactor operating at 1000 kW.

The nitrogen-16 produced through the (n,p) reaction with the oxygen in the water molecule has a very short half-life (7 sec) so only a very small fraction of that produced in the core will find its way to the pool surface. The principal radiological effect of the nitrogen-16 is as a contributor to the radiation level at the pool surface. Calculations of the nitrogen-16 transported to the pool surface estimate radiation dose rates of between 16 to 400 mrem/hour with the reactor operating at 1000 kW.

6.5.1.1 Argon-41 Activity in Reactor Room.

The argon-41 activity in the reactor pool water results from irradiation of the air dissolved in the water. The following calculations were performed to evaluate the rate at which argon-41 escapes from the reactor pool water into the reactor room. The calculations show that the argon-41 decays while in the water. The changes in argon-41 concentration in the core region, in the pool water external to the reactor, and in the air of the reactor room, are calculated using the variables as defined below:

N atomic density (atoms/cm^3)

λ decay constant (sec^{-1}), 1.06×10^{-4}

σ absorption cross section (cm^2), 0.61 b

q volume flow rate, reactor room exhaust (cm^3/sec)

V volume of region (cm^3)

ρ density (gm/cm^3)

A_f channel free flow area (cm^2)

ℓ channel length (cm)

w mass flow rate (gm/sec)

$\bar{v}$ volume flow rate through the core (cm^3/sec)

$\bar{\Phi}$ average thermal neutron flux in the core (n/cm^2-sec)

The volume flow rate through the core is

$$\bar{v} = \frac{w}{\rho} = \frac{8000 \text{ g/sec}}{1 \text{ g/cm}^3} = 8.0 \times 10^3 \text{ cm}^3/\text{sec} \qquad (1)$$

From the flw channel volume, $A_f \ell_c$, the exposure time in the core is

$$t = V/\bar{v} = A_f \ell_c / \bar{v} = \frac{485.0 \times 38.1}{8.0 \times 10^3} = 2.3 \text{ sec} \qquad (2)$$

It remains to find the atom density N for dissolved argon-40 in the reactor pool water.

According to Henry's law for gases in contact with liquids the equilibrium concentration in the liquid is proportional to the partial pressure of the gas. The saturated concentration of argon in water at one atmosphere of standard air is given in Table 6-1.

Table 6-1
SATURATED ARGON CONCENTRATION IN WATER [1]

Temperature (°C)	S(atoms A-40/cm^3 H_2O)
10	1.14×10^{16}
20	0.94×10^{16}
30	0.79×10^{16}
40	0.69×10^{16}
50	0.62×10^{16}
60	0.56×10^{16}
70	0.52×10^{16}
80	0.48×10^{16}

The argon-40 concentration (N) in the water at the core inlet temperature (38°C) is

$$N = 7.1 \times 10^{15} \text{ atoms/cm}^3 \quad . \qquad (3)$$

The concentration of argon is 5.3×10^{15} atoms/cm^3 at 67.8°C, the core exit water temperature.

The argon-41 density in water (at equilibrium) at the exit from the core is given by

$$A_\infty = A_o e^{-\lambda t} + N \sigma \Phi \left(1 - e^{-\lambda t} \right) \quad , \qquad (4)$$

and at the entrance

$$A_o = A_\infty e^{-\lambda T} \quad , \qquad (5)$$

where t is the exposure time in the core (2.3 sec), and T is the cycle time in the pool.

The average out-of-core cycle time T is given by

$$T = \frac{V_p}{\bar{v}} = \frac{3.86 \times 10^7 \text{ cm}^3}{8.0 \times 10^3 \text{ cm}^3/\text{sec}} = 4.83 \times 10^3 \text{ sec} \quad , \qquad (6)$$

where V_p is the pool volume and $\bar{v}$ is, again, the volume flow rate through the core. The solution to this set of equations is

$$A_\infty = N \sigma \Phi \frac{1 - e^{-\lambda t}}{1 - e^{-\lambda (t + T)}} \quad . \qquad (7)$$

Substituting the values from above one obtains

$$A_\infty = (7.1 \times 10^{25}) (0.61 \times 10^{-24}) (1.2 \times 10^{13}) \frac{1 - \exp\left[-(1.06 \times 10^{-4}) (2.3)\right]}{1 - \exp\left[-(1.06 \times 10^{-4}) 4.83 \times 10^3)\right]}$$

$$A = 31.6 \text{ dps/cm}^3 \quad ,$$

and $N_{41} = 31.6 / 1.06 \times 10^{-4} = 2.98 \times 10^5$ acoms/cm^3 .

One source of argon-41 in the room results from the reduced solubility of argon in water as the temperature increases. Considering the expected temperature rise of the water passing through the core, an immediate release of about 25% of the argon-41 made could be expected during passage. Some of this argon-41 might be redissolved as it is transported into cooler water, but since the cooler water is in equilibrium with the air above, it is nearly saturated with argon and will not absorb all of the argon released. Measurements of argon-41 in the water as a function of height above the core indicate that approximately 60% of the release argon-41 is reabsorbed.

A combination of the two sources of argon-41 mentioned above will give the upper limit of the fraction of total argon atoms that can leave the water per second.

Assuming that the 10% (i.e., 40% of 25%) of the argon-41 comes out of solution, remains undissolved after leaving the core, and escapes to the air, this source would be

$$S_1 = 0.10\ N_{41}\ \bar{v}$$

$$= 0.10 \times 2.98 \times 10^5 \text{ atoms/cm}^3 \times 8.0 \times 10^3 \text{ cm}^3/\text{sec}$$

$$= 2.38 \times 10^8 \text{ atoms/sec}$$

The tendency of the balance of the argon activity in the pool to escape to the air owing to its proximity to the water-air boundary will constitute the additional source of argon-41 at the water surface.

Estimates of the surface exchange coefficient β (i.e., the gas in a unit volume that is exchanged at the surface per unit time per unit surface area) for argon vary considerably. One method of arriving at a value for this parameter is through the diffusion coefficient of the gas in water. The mean square distance traversed by a molecule is

$$\langle \delta X \rangle^2 = 2Dt \quad , \tag{8}$$

where D = diffusion coefficient (cm^2/sec),

t = time (sec).

The exchange coefficient is assumed to be evaluated for 1 sec. as

$$\beta = (\langle \delta X \rangle^2)^{1/2}/_t = (2D/t)^{1/2} \quad . \tag{9}$$

The diffusion coefficient at 40°C is about 1.1×10^{-5} cm^2/sec, and, if one assumes that only one-half of the argon atoms within one diffusion length of the surface escape,

$$\beta = 1/2 \ (2 \times 1.1 \times 10^{-5})^{1/2} = 2.35 \times 10^{-3} \text{ cm/sec}$$

Measurements have been made of the argon-41 activity in a TRIGA Mark III reactor pool and from the data acquired from these measurements it was possible to construct a value for the surface exchange coefficient. This value at 40°C is about 2.9×10^{-4} cm/sec.

Values for the surface exchange coefficient have been reported by Dorsey [3] for air, O^2, and N^2. The values for these three gases are all about equal. Assuming argon

behaves as do these gases, a value is obtained of 5.7×10^{-3} cm/sec for β.

In this analysis the largest of the three values was used for the surface exchange coefficient, i.e. 5.7×10^{-3} cm/sec.

The rate at which argon atoms are transferred across the water-air interface is determined by

$$S_2 = 0.93\ \beta N_{41} A_S \qquad (10)$$

$$= 0.93 \times 5.7 \times 10^{-3} \times 2.98 \times 10^{5} \times 5.05 \times 10^{4}$$

$$= 7.98 \times 10^{7} \text{ atoms/sec} \quad ,$$

where A_S is the surface area of the pool (5.05×10^{4} cm^2).

The total transfer rate of argon-41 nuclei to the reactor room is

$$S^{41} = S_1 + S_2 = 2.38 \times 10^{8} + 7.98 \times 10^{7} \qquad (11)$$

$$= 3.18 \times 10^{8} \text{ nuclei/sec} \quad .$$

Air is removed at the rate of q cm^3/sec from air-filled volumes from which the accumulation of argon-41 as a function of operating time is given by

$$\frac{dN^{41}}{dt} = S^{41}/V - (\lambda^{41} + q/V)N^{41} \quad , \qquad (12)$$

where S is the source of radioactive atoms released to the air.

Integrating from $N^{41} = 0$ at $t = 0$, one obtains,

$$N^{41}(t) = \frac{S^{41}/V}{\lambda^{41} + q/V} (1 - [\exp-(\lambda^{41} + q/V)t]) \qquad (13)$$

For prolonged reactor operation at a steady power level in which

$$t >> 1/(\lambda^{41} + q/V) \quad ,$$

the source term and removal rates of argon-41 are in equilibrium, in which case

$$N^{41} = \frac{S^{41}/V}{\lambda^{41} + q/V} \text{ atoms/cm}^3 \quad . \qquad (14)$$

The argon-41 concentration in the reactor room and building exhaust air

$$N_R = \frac{S/V_R}{\lambda + q/V_R} = \frac{S}{\lambda V_R + q} \qquad (15)$$

$$= \frac{3.18 \times 10^8}{1.06 \times 10^{-4} \times 4.12 \times 10^9 + 1.14 \times 10^5} = 578 \text{ at./cm}^3$$

where the effective room volume is 4.12×10^9 cm^3 and a room air exhaust rate assumes that the air exchange rate is two per hour and that the effective room volume is 90% of 4575 cubic meters. This corresponds to an activity concentration in the room of

$$A = \frac{\lambda N}{C} = \frac{1.06 \times 10^{-4} \times 578}{3.7 \times 10^4} = 1.65 \times 10^{-6} \ \mu Ci/cm^3. \qquad (16)$$

The actual effect of argon-41 releases from the reactor pool would be substantially less than those estimated as a result of the various conservative estimates in the calculation. Among the major conservative assumptions are the transfer amounts of argon from the pool surface, period of full power operation, release rates and volumes.

6.5.1.2 Nitrogen-16 Activity in Reactor Room.

The cross-section threshold for the oxygen-16 (n,p) nitrogen-16 reactions is 9.4 MeV; however, the minimum energy of the incident neutrons must be about 10.2 MeV because of center of mass corrections. This high threshold limits the production of nitrogen-16 since only about 0.1% of all fission neutrons have an energy in excess of 10 MeV. Moreover, a single hydrogen scattering event will reduce the energy of these high-energy neutrons to below the threshold. The effective cross-section of oxygen-16 (n,p) nitrogen-16 reaction averaged over the TRIGA spectrum is 0.021 millibarns. This value agrees well with the value obtained from integrating the effective cross section over the fission spectrum.

The concentration of nitrogen-16 atoms per cm^3 of water as it leaves the reactor core is given by

$$N_2 = \frac{N_1 \sigma_1 \Phi_v}{\lambda_2} \left(1 - e^{-\lambda_2 t} \right) , \qquad (17)$$

where

N_2 = nitrogen-16 atoms per cm^3 of water,

Φ_v = neutron flux = 1.0×10^{13} n/cm^2-sec, (0.6 - 15 MeV),

N_1 = oxygen atoms per cm^3 of water = 3.3×10^{22} $\#/cm^3$,

σ_1 = (n,p) cross section of oxygen = 2.1×10^{-29} cm^2

(averaged over 0.6 - 15 MeV),

λ_2 = nitrogen-16 decay constant = 9.35×10^{-2} sec^{-1},

t = average time of exposure in reactor.

The average exposure time in the core (2.3 sec), was derived in the discussion on argon activity. Solving for N_2 in the equation above, one obtains

$$N_2 = 7.41 \times 10^7 \left(1 - e^{-9.35 \times 10^{-2} \times 2.3}\right) \quad (18)$$
$$= 1.43 \times 10^7 \text{ atoms/cm}^3$$

as the density of nitrogen-16 in the water leaving the core.

If it is assumed that the water continues to flow at the same velocity to the surface, a distance of ~640 cm, the transit time from core to surface is

$$t_{rise} = \frac{640}{16.8} = 38.1 \text{ sec} \quad , \quad (19)$$

where the flow velocity, 16.8 cm/sec (Table 3-7), was given in the discussion on heat transfer.

This assumption is quite conservative as energy losses from the fluid stream resulting from turbulent mixing will reduce the velocity significantly. Furthermore, delays in transit time resulting from operation of the diffuser pump are sizeable. Measurements made of the dose rates at the pool surface of several TRIGA reactors show that the operation of the diffuser pump reduces the nitrogen-16 contribution to the surface dose rate by an order of magnitude of more depending on the size of the pool.

In 38 seconds the nitrogen-16 decays to 2.86×10^{-2} times the value of the activity leaving the core. Thus the concentration of nitrogen-16 atoms that reach the region near the surface of the pool is estimated at about 410,000 atoms/cm^3 per cubic centimeter.

Only a small proportion of the nitrogen-16 atoms present near the pool surface are transferred into the air of the reactor room. When a nitrogen-16 atom is formed, it appears as a recoil atom with various degrees of ionization. For high-purity water (approximately 2 μmho) practically all of the nitrogen-16 combines with oxygen and hydrogen atoms of the water. Most of it combines in an anion form, which has a tendency to remain in the water [4]. It is assumed that at least one-half of all ions formed are anions. Because of its 7.1-sec half-life, the nitrogen-16 decays before reaching a uniform concentration in the tank water. The activity will be dispersed over the surface area of the pool and much of it will decay during the lateral movement.

For the purpose of the analysis it is postulated that the water-bearing nitrogen-16 rises from the core to the surface and then spreads across a disk source with an equivalent radius of 125 cm. For a constant velocity of 16.8 cm/sec the cycle time for distributing the nitrogen-16 over the pool surface would be

$$t_s = 125 \text{ cm}/16.8 \text{ cm/sec} = 7.4 \text{ sec} \quad . \tag{20}$$

The average concentration during this time is

$$\bar{N} = 1/t_s \int_o^{t_s} N_o e^{-\lambda t} \, dt \quad , \tag{21}$$

$$= \frac{N_o}{\lambda t_s} (1 - e^{-\lambda t_s}) = \frac{4.10 \times 10^5}{9.35 \times 10^{-2}} (1 - e^{-0.69})/7.4$$

$$= 3.0 \times 10^5 \text{ atoms/cm}^3$$

The interest from the point of safety is then the number of nitrogen-16 atoms escaping into the air from the diffusing source above the core. The number escaping to the air would be about is estimated from the escape velocity, 0.009 cm/sec, from Dorsey [5] as

$$(3.0 \times 10^5 \text{ atoms/cc}) (0.9 \times 10^{-2} \text{ cm/sec})$$

$$= 2700 \text{ atoms/cm}^2\text{-sec} \quad .$$

In the room, the activity is affected by dilution, ventilation, and decay. Thus the rate of accumulation of nitrogen-16 in the room as a whole is given by

$$\frac{d(VN^{16})}{dt} = S - (\lambda^N + q/V) \, VN^{16} \quad , \tag{22}$$

where S = number of nitrogen-16 atoms entering the room from the pool per secopd, $(2700) (5.05 \times 10^4) = 1.36 \times 10^8$ atoms/sec,

V = volume of the reactor room, 4.12×10^9 cm^3, (effective),

q = volume flow rate, 2.29×10^6 cm^3/sec, (reactor room exhaust).

For saturation conditions

$$VN^{16} = \frac{S}{(\lambda^N + q/V)} = \frac{1.36 \times 10^8}{9.35 \times 10^{-2} + 2.3 \times 10^{-5}} \tag{23}$$

$$= 1.4 \times 10^9 \text{ nuclei}$$

This corresponds to an activity concentration of 8.8×10^{-7} μCi/cc.

The gamma dose rate from nitrogen-16 of this concentration in the air is

$$D = \frac{3.7 \times 10^4 \frac{\text{photons}}{\text{sec-}\mu\text{Ci}} \times 8.8 \times 10^{-7} \frac{\mu\text{Ci}}{\text{cm}^3} \times 1000 \text{ cm}}{2 \times 1.6 \times 10^5 \text{ (photons/sec-cm2/rad-hr)}}$$

$$= 1.0 \times 10^{-4} \text{ rad/hr} = 100 \text{ μrad/hr} \quad ,$$

when the effective radius of the room, taken to be a hemisphere with a volume of 4120 cubic meters is 10 m.

The thickness of the layer of nitrogen-16 bearing water is

$$h = \frac{v_1 t_s}{A_s} = \frac{8.0 \times 10^3 \times 7.4}{5.05 \times 10^4} = 1.17 \text{ cm} \quad , \qquad (24)$$

where the volume flow rate 8.0×10^3 cm^3/sec was given in the discussion on heat transfer.

The dose rate at the pool surface arising from the nitrogen-16 near the surface is

$$D = \frac{\lambda \bar{N}}{2\mu K} [1 - E_2(\mu h)] \quad , \qquad (25)$$

where μ = attenuation coefficient for 6 MeV photons in water (0.0275 cm^{-1}).

K = 1.6×10^5 photons/cm^2-sec per rad/hr flux to dose rate conversion factor,

E_2 = second exponential integral.

This yields, approximately,

D = 400 mr/hr .

This value is larger than those extrapolated from measurements made on other TRIGA reactors. Transport times from the reactor core to the pool surface in excess of those estimated will lower the calculated dose substantially. A delay time twice as long as 38 sec. will generate a calculated dose rate twenty-five times less.

6.5.2 Activation of Air in the Experimental Facilities

In the TRIGA reactor installation, the following experimental facilities contain air: rotary specimen rack, pneumatic transfer tube, and neutron beam tubes. Of the

radioisotopes produced in these air cavities, argon-41 (with half-life of 110 min.) is the most significant with respect to airborne radioactivity hazards. Nitrogen 16 (7.11 sec. half-life) and oxygen-19 (26.9 sec. half-life) are considerably less significant. Estimated releases of argon-41 from reactor operations indicate an upper limit for the release exposure as 190 μrad/hr. Actual values are expected to be less than 1/50 of the estimated value.

The saturated activity of argon-41 in an experimental cavity is calculated from

$$A = N^{41}\lambda^{41} = \frac{\lambda^{41} S}{C(\lambda^{41} + q/V)} \ \mu Ci/cm^3 \quad , \qquad (26)$$

where $C = 3.7 \times 10^4$ disintegrations/sec per μCi,

$S = \phi\Sigma_a$ n/cm^3-sec.

$\Sigma_a = 1.59 \times 10^{-7}$ cm^{-1}.

The effective air volumes of several experimental facilities are listed in Table 6-2. Also given are conservatively high estimatesof the average thermal neutron fluxes for 1000 kW operation.

Table 6-2
VOLUMES AND THERMAL FLUXES OF FACILITIES

Region	Effective Air Volume (cm^3)	Average Thermal Flux at 1000 kW (n/cm^2-sec) x 10^{12}
Central thimble	5.3×10^3	21.6
Rotary specimen rack	3.3×10^4	6.5
Pneumatic tube	1.6×10^3	6.5
Tangential beam ports	3.0×10^5	0.1
Radial beam ports	1.8×10^5	0.1

For volume exhaust rates where the decay constant is negligible, such that

$$\lambda^{41} << q/V \quad , \qquad (27)$$

the activity released from each volume is given by

$$A^{41}q_i = \lambda^{41} (\phi\Sigma_a)_i V_i/C \ \mu Ci/sec \ . \qquad (28)$$

With a flow rate of 4.75×10^3 cm^3/sec this condition is achieved for a volume of approximately 0.45 cubic meters. Total volume of air cavities without any experiments in place is about 0.5 cubic meters. The total activity calculated for the air leaving the experimental facilities is therefore, 176 μCi/sec.

It should be emphasized that the air activation and subsequent release activity are predicted for vacant beam ports and conservative neutron fluxes. Actual release rates depend on the particular configuration of experiments and the air exchange rate in each facility.

The release of argon-41 from the facility is diluted by the ventilation exhaust rate, assumed to represent two air changes per hour, and averaged for a 5 day, 8 hour operation schedule at full power. The release concentration from the pool averaged for one year is,

$$.24 \ (1.65 \times 10^{-6}) = 3.96 \times 10^{-7} \ \mu Ci/cm^3.$$

Only 20% of the experiment facility argon-41 is assumed to exhause since experiments will replace some or most of the exposed air.

$$176 \ (.20) \ (.24)/2.29 \times 10^6 = 3.7 \times 10^{-6} \ \mu Ci/cm^3.$$

Total estimated release is 4.1×10^{-6} μCi/cm^3.

The whole body gamma ray dose rate to a person immersed in a semi-infinite cloud of radioactive gases can be approximated by

$$D = 900 \ EA_D \qquad (29)$$

where E = the photon energy, 1.3 Mev

A_D = effective exposure concentration, Ci/m^3.

The concentration downwind from the point at which the activity is discharged from the building is

$$A_D = Aq \ \psi(x), \qquad (30)$$

where ψ = the dilution factor at the distance x, (sec/m^3),

A = activity concentration in the discharge (Ci/m^3),

q = the building exhaust rates (m^3/sec).

If it is assumed that the discharge is at the roof line, the dilution factor in the lee of the building (x=0), is given [6] by:

$$\psi(0) = 1/csu \quad , \tag{31}$$

where c = a constant (0.5),

s = building cross-sectional area normal to the wind direction (m^2),

u = wind velocity (m/sec).

A minimum cross-sectional area is assumed of 234 m^2 (60 x 42 ft) and, for a wind velocity of 1 m/sec,

$$\psi(0) = 1/(0.5 \times 1. \times 234) = 8.5 \times 10^{-3} \text{ sec/m}^3 \ . \tag{32}$$

The averaged dose rate at the exhaust stack is

$$D = 900 \times 1.3 \ (4.1 \times 10^{-6}) = 4.8 \times 10^{-3} \text{ rads/hr},$$

an average of 4.8 mrad/hr in the stack or

$$D = 4.8 \times 10^{-2} \ (8.5 \times 10^{-3}) = 4.1 \times 10^{-5} \text{ rads/hr},$$

an average of 41 μrad/hr at ground level.

Actual dose values for argon-41 release will be substantially lower. It is expected that release values will be less than 4.8 μrad/hr which is equivalent to 10 mrad/yr. Lower neutron fluxes, smaller air volumes, shorter operation times and larger dilution factors will assure that releases are below the estimated values.

Chapter 6 References

1. Code of Federal Regulations, Chapter 10 part 20, U.S. Government Printing Office, 1982.

2. Dorsey, N.E., Properties of Ordinary Water-Substance, Reinhold Publishing Corp., New York p. 537.

3. Ibid., p. 554.

4. Mittl, R.L., and M.H. Theys, "N-16 Concentration in EBWR," Nucleonics p. 81 (1961).

5. Dorsey, N.E., op cit., p. 554.

6. Slade, D.H., (ed.), "Meteorology and Atomic Energy," USAEC Reactor Develop. and Tech. Div. Report TID-24190, DFSTI, Springfield, Virginia, 1968.

Chapter 7

SAFETY ANALYSIS

In this section an analysis of abnormal operating conditions will be made with conclusions concerning the effects on safety to the reactor, the public, and the operations personnel, as a consequence of any abnormal operations.

The abnormal conditions that will be analyzed are.

a. Reactivity accident

b. Loss of reactor coolant

c. Fission product release from clad rupture

7.1 REACTIVITY ACCIDENT

7.1.1 Summary

Rapid insertion of reactivity into a TRIGA reactor is a designed feature of the fuel performance [1]. Thus, most plausible reactivity accidents do not subject the fuel to conditions more severe than normal operating situations. Postulated accidents for other undetermined scenarios also are predicted not to exceed fuel element safety conditions.

The standard TRIGA fuel element of U-ZrH (H/Zr; 1.6) is composed of a stable gamma phase ZrH that does not undergo a phase transition at temperatures less than about 1250°C [2]. Pulsing limits for fuel elements clad in stainless steel are set by the hydrogen equilibrium pressure within the fuel element. This pressure is a function of temperature and must not exceed the rupture stress of the fuel element cladding. For the stainless steel cladding (0.02 inch thick), the rupture pressure has been measured to be 1800 psi at 100°C. The fuel temperature at which the equilibrium hydrogen pressure will be 1800 psi is about 1150°C. The average and peak fuel temperatures at 1.5 Mw steady-state operation are about 220°C and 400°C, occurring well below the limit. The average and peak fuel temperatures occurring after a 2.8% reactivity insertion at respective power levels of 1 kW and 880 kW are also less than 1150°C. Values of 376°C and 843°C are predicted for a low power insertion and values of 460°C and 795°C are calculated for a high power insertion.

Two reactivity accident scenarios are presented. The first is the insertion of 2.8% reactivity at zero power by the sudden removal of the maximum worth control rod. The second is the sudden removal of the same 2.8% reactivity with the reactor operating at a power level equivalent to the balance of the core excess reactivity. It is unlikely that movement of reactor fuel or experiments would lead to the postulated accidents. Movements of control rods for the first case are controlled administratively while movements of control rods for the second case are prevented by control circuit design. Provided the total worth of reactor experiments are limited to $3.00 no experiment movement could generate the postulated accident.

Pulse powers predicted from kinectics formulations based on the Fuchs-Nordheim-Scalletar model are displayed in Figure 7-1. Pulse shape, energy and temperature for $3 and $4 pulse insertions are shown.

7.1.2 Analysis of 2.8% insertion at 1 kW.

A rapid insertion of excess reactivity in the reactor system is postulated. The method of inserting this reactivity is through the rapid removal of a control rod. This reactivity insertion is the most serious that could occur. It is also the normal pulsing condition and the analysis is presented here as a point of information since it is not actually an accident condition.

The sequence of events leading to the postulated reactivity accident is:

a. The reactor is just critical at some low power level (less than 1 kW).

b. Upward force is applied to a high worth control rod causing it to be ejected from the core and to introduce an excess reactivity of $4.00.

The consequences of the above sequence of events are:

a. Reactor power is increased to a maximum power of approximately 4220 MW.

b. A maximum energy release of approximately 36 MW-sec is reached when the maximum fuel temperature of 843°C is reached.

c. Stresses are predicted in the stainless steel cladding of approximately 2940 psi. These pressures are caused by expansion of the air and fission product gases and the hydrogen release from the fuel material. Neither of the preceding stress values will cause cladding rupture.

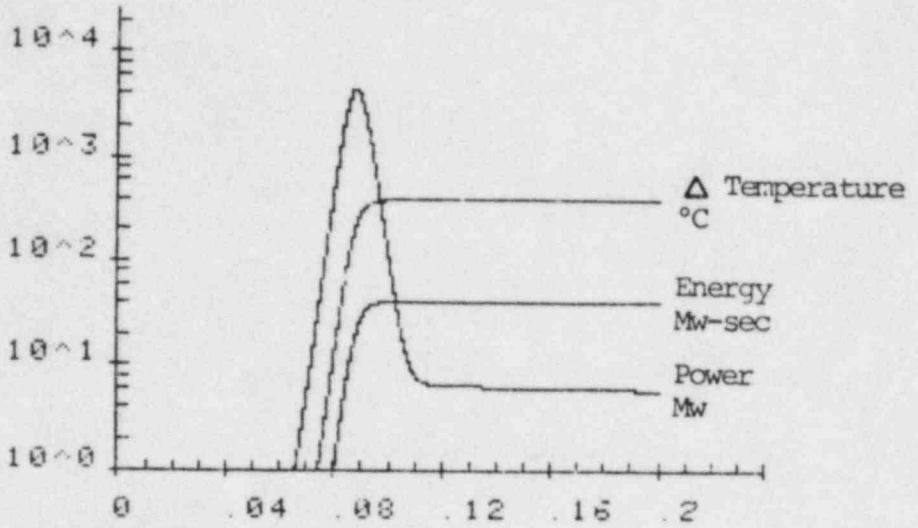

$4 Pulse
Initial Power 1 Kw

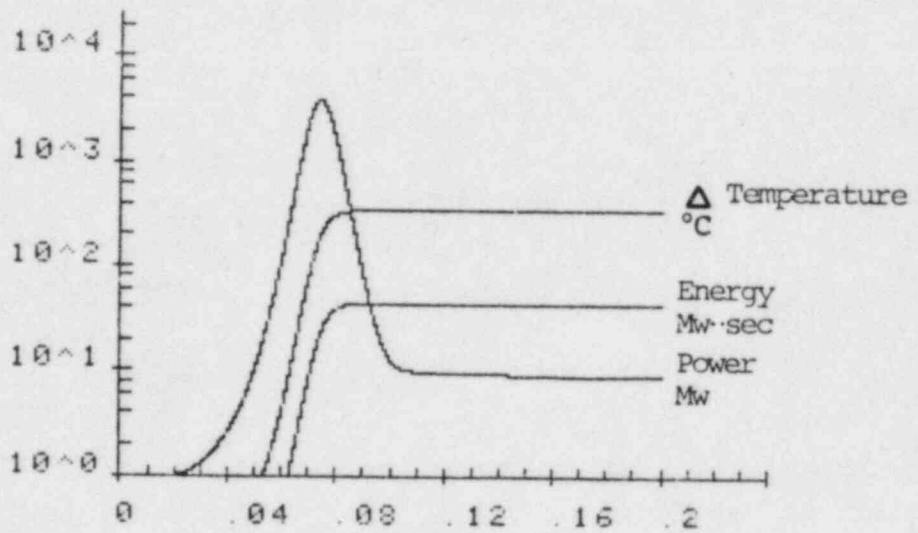

$4 Pulse
Initial Power 880 Kw

CALCULATED PULSE SHAPE, ENERGY
AND TEMPERATURE
Figure 7-1

The analysis of this accident is conservative in a number of ways, some of which have been indicated in the reactor design bases (Chapter 3). For example, the equilibrium pressure of hydrogen over the fuel is not achieved during a pulse or step insertion of reactivity.

It was assumed that the reactor is just critical at a low power level with a fuel and coolant temperature of 25°C. Additional input parameters are summarized in Table 7.1.

Table 7-1
REACTIVITY TRANSIENT INPUT PARAMETERS

Reactivity insertion, $	4.0
Temperature coefficient, prompt (δk/k)/°C	-1.1×10^{-4}
Delayed neutron fraction β, %	0.70
Neutron lifetime ℓ, μsec	41
Heat capacity C_p, watt-sec/element	$817 + 1.6\ T_{fuel}$

The computations leading to these conclusions are determined by the following lumped parameter analysis. The Fuchs-Nordheim model for reactor dynamics yields the coupled set of differential equations:

$$\ell\ \delta P/\delta t = (\delta k - \alpha T)\ P \qquad (1)$$

$$C\ \delta T/\delta t = P - P_0 \quad , \qquad (2)$$

with $$C = C_0 + C_1 T \qquad (3)$$

where ℓ = Prompt neutron lifetime, sec.

P = Power level, (P_0 initial power), watts.

δk = Reactivity above prompt critical, $\delta k/k - \beta$.

α = Magnitude of the negative temperature coefficient, $°C^{-1}$.

T = Temperature (avg. over fuel) above the equilibrium temperature at P_0, °C.

C = Heat capacity of the fuel in the core, w-sec/°C.

C_0 = Heat capacity at the equilibrium temperature corresponding to P_0, w-sec/°C.

C_1 = Rate of change of heat capacity with temperature, w-sec/°C^2.

The above lumped parameter system neglects heat transfer and delayed neutron effects and averages space and neutron energy variations so that all coefficients are assumed constant. Combining equations

$$\frac{dP}{dT} = \frac{(\delta k - \alpha T)\ (C_0 + C_1)\ P}{\ell\ (P - P_0)} \qquad (4)$$

Integrating, using the condition that T = 0 when P = P_0, yields

$$\ell\ \{(P-P_0) - P_0\ \ln(P/P_0)\} =$$

$$T\ \{\delta k C_0 - (\alpha C_0 - C_1 \delta k)T/2 - \alpha C_1 T^2/3)\} \qquad (5)$$

Maximum (or minimum) temperatures occur when the pulse initiates and after culmination of the pulse such that

$$P - P_0 = 0 \ ,$$

$$P = P_0 \ ,$$

and then,

$$T\ \{\delta k C_0 - (\alpha C_0 - C_1 \delta k)T/2 - \alpha C_1 T^2/3)\} = 0 \ . \qquad (6)$$

The roots of this equation are

$$T_a = -3/8\ (\sigma - 1)\ \{1 + [1 + 16/3\ \sigma/(\sigma - 1)^2]^{1/2}\}\ T_f \qquad (7)$$

where $\sigma = \alpha C_0 / \delta k C_1$,

$T_f = 2\ \delta k/\alpha$,

and the positive sign is taken for the square root if $\sigma < 1$.

From the fuel heat capacity the core heat capacity with 90 elements is

$$C_0 = 817 + 1.6\ T_s \text{ w-sec/°C-element} \qquad (8)$$

$$= 857 \text{ w-sec/°C-element} \times 90 \text{ elements/core}$$

$$= 7.71 \times 10^4 \text{ w-sec/°C} \ .$$

For the insertion of \$4.00 of reactivity a value of δk equal to 0.021 = (\$4.00 - \$1.00) (0.7%/\$).

$$\sigma = \frac{1.1 \times 10^{-4}}{2.1 \times 10^{-2}} (857/1.6) = 2.81 \quad (9)$$

and $T_f = 2\ (2.1 \times 10^{-2})/1.1 \times 10^{-4} = 382°C$. (10)

Thus

$$T_a = -3/8\ (2.81 - 1)$$
$$\{1 - [1 + 16/3\ 2.81/(2.81 - 1)^2]^{1/2}\}\ T_f \quad (11)$$
$$= 0.92\ T_f = 351°C \ .$$

Therefore, at the conclusion of the pulse the average fuel temperature will be

$$T_{ss} = 352 + 25 = 376°C \ . \quad (12)$$

To determine the maximum temperature in the hottest fuel element, the average energy release is determined and then multiplied by the peak power ratio to obtain the maximum energy release in the center element. The peak power ratio includes radial, axial and element peaking factors. Then one returns to the energy versus temperature equation to determine the maximum temperature.

Let E equal the energy necessary to raise the average core temperature from the temperature at the initial power level to the temperature at the final power level. Then

$$E = \int_0^{T_a} C\ dT = \int_0^{T_a} [\ C_0 + C_1\ T\ ]dT \quad (13)$$

$$E = C_0\ T_a + C_1\ T_a^{\,2}/2 \quad (14)$$

$$E = 3.57 \times 10^7 \text{ watt-sec}$$

For a peak-to-average power ratio of 2.2 and an element peaking factor of 1.4 the energy release of the element producing the peak power is 3.1E or 110 Mw-sec. A peak temperature is calculated by substituting this energy into the previous equation and solving for the temperature.

$$T_p = -C_0/C_1 + [(C_0/C_1)^2 + 2(3.1E/C_1)]^{1/2} \quad (15)$$

$$T_p = 818°C$$

with

$$T_{ss} = 818 + 25 = 843°C \ .$$

During the time of peak fuel temperature, the stress on the clad from the pressure produced by the expansion of air

and fission product gases and the hydroge. released from the fuel is less than the strength of the clad material and therefore there is no loss of clad integrity.

The partial pressure exerted by gases is

$$P_t = N_t \frac{RT}{V} \qquad (16)$$

where initially the volume, V, is taken as a 1/8-in. space between the fuel and reflector end piece. This result is conservative since the porosity of the graphite reflector of 20% is neglected.

The volume then is

$$V = \pi r^2 h = \pi(1.80)^2\ 0.317 = 3.23\ cm^3 \quad . \qquad (17)$$

The partial pressure of the air in the element is

$$P_{air} = \frac{RT}{2.24} \times 10^3 = 4.46 \times 10^{-5}\ RT \quad . \qquad (18)$$

Calculation of the fission product gases in a fuel element is determined by burnup. For an element operated at three times the 4.5 MW-days discussed in Section 7.2, a total of 0.016 moles of stable and radioactive gases are produced. If the release fraction is taken as .0015% as discussed in Section 7.3, then

$$N_{fp} = \frac{3.22 \times 10^{21}}{6.02 \times 10^{23}} (1.5 \times 10^{-5}) = 2.4 \times 10^{-7}\ \text{moles.} \qquad (19)$$

From this, one obtains,

$$P_{fp} = 7.45 \times 10^{-8}\ RT \quad . \qquad (20)$$

The total pressure exerted by the air and fission products is

$$P_1 = (4.46 + 0.007) \times 10^{-5}\ RT = 4.47 \times 10^{-5}\ RT \qquad (21)$$

$$P_1 = P_{air} \quad .$$

Also we have

$$P_{air} = 14.7 \frac{T}{237}\ psi \quad . \qquad (22)$$

As an upper limit, assuming an air temperature equal to the peak fuel temperature of 843°C or 1116°K , one obtains

$$P_1 = (14.7) \frac{1116}{273} = 60.1\ psi \quad . \qquad (23)$$

The equilibrium hydrogen pressure over ZrH (H/Zr; 1.6) at 843°C is 20 psi. The total internal pressure then is

$$P_t = P_h + P_l = 80 \text{ psi} \quad . \tag{24}$$

Assuming no expansion of the clad, the stress produced in the clad by this pressure is

$$S = \frac{r}{t} P_t = \frac{0.735}{0.020} P_t = 36.75 P_t \tag{25}$$

$$= (36.75)\ (80) = 2940 \text{ psi.}$$

For a reactivity insertion of $4.00, the clad surface temperature would be approximately equal to the saturation temperature of the water which is 113°C at a pressure of 23.4 psia. At this temperature, the ultimate tensile strength for type 304 stainless steel is greater than 60,000 psi with a yield stress of approximately 36,000 psi. Comparing this strength with the stress applied to the cladding during the reactivity insertion, it is seen that the strength of the material far exceeds the stress which would be produced. Therefore there would be no loss of clad integrity or damage to the fuel as a result of the reactivity accident.

7.1.3 Analysis of 2.8% insertion at 880 kW.

The reactivity accident considered here would take place in the following manner. Initially, the reactor is cold clean with all control rods inserted. The reactor is loaded with 4.9% δk/k excess reactivity and the pool coolant is at a temperature of 42°C. This accident requires someone deliberately violating the operating license and several interlocks and scrams.

The sequence of events leading to the postulated reactivity accident is:

a. The operator slowly withdraws all the control rods except the maximum worth rod, until all the rods are completely out and the reactor is operating at a high steady state power.

b. Upward force is applied to the maximum worth rod ejecting it (by some means impossible to conceive) from the hot operating reactor.

The consequences of the above sequence of events are:

a. Reactor power and fuel temperatures are increased by the compensated reactivity of $3.00 (that is 4.9% - 2.8% = 2.1% = $3.00) to levels of 880 kW with fuel temperatures of 380°C, peak, and 207°C, average.

b. A prompt insertion of 2.8% δk/k results in an average temperature in the core of 460°C and a peak temperature of 795°C.

c. Stresses are predicted in the clad of about 2100 psi. Even if the clad were at the maximum fuel temperature this stress is a factor of ten below the ultimate strength of the clad.

The analysis of this accident is conservative as described in the previous accident case. Equilibrium element conditions and pressure are not expected although calculations include finite reactivity insertion time, delayed neutrons and heat transfer.

It is assumed that the reactor power level is 880 kW ($3.00 of power coefficient); the average fuel temperature is (165 + 42)°C; the peak fuel temperature is (338 + 42)°C; with a pool coolant temperature of 42°C assumed. Values of the input parameters are summarized in Table 7-2.

Table 7-2
REACTIVITY TRANSIENT INPUT PARAMETERS

Reactivity insertion, $	4.0
Temperature coefficient, prompt (δk/k)/°C	-1.1×10^{-4}
delayed neutron fraction β, %	0.70
neutron lifetime l, μsec	41
Heat capacity, watt-sec/element	
fuel C_p, at 0°C	817
fuel C_p, temperature dependence	$1.6\ T_{fuel}$
water C_p, at 25°C	879
Thermal resistance, °C/MW:	
fuel to cooling channel	5.29×10^4
cooling to pool	1.42×10^3

A computer program was used to calculate the energy release in the transient. The program is a one-dimensional combined reactor kinetics heat transfer program that works extremely well for reactor transients in which detailed heat transfer analysis is not required. Delayed neutrons and finite reactivity insertion time are included in the program.

Using the parameters given above it was found that the addition of $4.00 reactivity (2.8% δk/k) from an average fuel temperature of 207°C the average fuel temperature at 880kw) produced an energy release of 32 Mw-sec in the 90 element core.

The energy density at the axial midplane of the maximum power density element, E_m, is:

$$E_m = 1.1\ P_r\ P_a\ E/n$$

where P_r = relative power in element,

P_a = axial peaking factor,

E = energy release in the transient,

n = number of elements,

and the factor of 1.1 acounts for uncertainties.

In chapter 3 the radial power distribution within a fuel element is shown. The energy deposited at radius r per unit volume is:

$$E_r = f(r)\ E_m$$

where f(r) is taken from data in chapter 3. The after pulse temperature at the radial distance r is given by:

$$T_p(r) = -C_0/C_1 + \{(C_0/C_1)^2 + 2E_r/C_1\}^{1/2}$$

where $C_0 = 8.17 \times 10^{-4}$ Mw-sec/°C

and $C_1 = 1.6 \times 10^{-6}$ Mw-sec/(°C)^2.

Calculation of the final element fuel temperature is accomplished by adding the temperature of the pulse deposited energy to the fuel element temperature prior to the pulse.

The radial temperature distribution in the fuel prior to the initiation of the transient is given by:

$$T(r)-T_s = (T_m-T_s)\ [1 - r' - r'\ln(1/r')]/r_o'$$

where $T(r)$ = temperature at radial distance from center r,

T_s = temperature at fuel surface at axial center, °C

T_m = maximum temperature in element, °C

r, r_o = radial position and radius of fuel, cm,

$r' = (r/r_o)^2$

$r_o' = [1-r"-r"\ln(1/r")]$

$r" = (r_1/r_o)^2$

and r_1 = inside fuel radius, cm.

In Figure 7-2 there is shown the before pulse and after pulse temperature in the axial misplane of the maximum power density element. As can be seen the maximum temperature occurs at the periphery of the fuel. The adiabatic value is 795°C. In Chapter 3 a plot is shown of pulse temperature distribution as a function of time. This figure shows the typical dependence of temperature as heat flows quickly toward the fuel center and toward the clad.

For a fuel temperature of 800°C the equilibrium hydrogen pressure over the fuel would be less than 15 psi and the pressure exerted by air within the element would be less than 60 psi even if it were at the maximum fuel temperature. The stress imposed on the clad by 75 psi would be about 2800 psi. The ultimate strength of the clad is over 20,000 psi at 800°C. Therefore one can conclude that the clad integrity would not be compromised as a consequence of either of these events.

A similar analysis was made in which the reactor was assumed to be operating at 1.5 Mw. In this case only $2.79 (1.95% $\delta k/k$) was available to be inserted. The peak before pulse temperature was 475°C and the reactivity insertion resulted in an energy release of almost 30 Mw-sec. The peak after pulse adiabatic temperature was 823°C which occured at the inner fuel radius because of the high initial temperature at that point.

7.2 LOSS OF REACTOR COOLANT

7.2.1 Summary

The reactor will operate at a calculated maximum power density of 18 kW/element when the reactor power is 1000 kW and there is 90 elements in the core, all of which are standard TRIGA fuel. If the coolant is lost immediately after reactor shutdown, the fuel temperature, indicated in

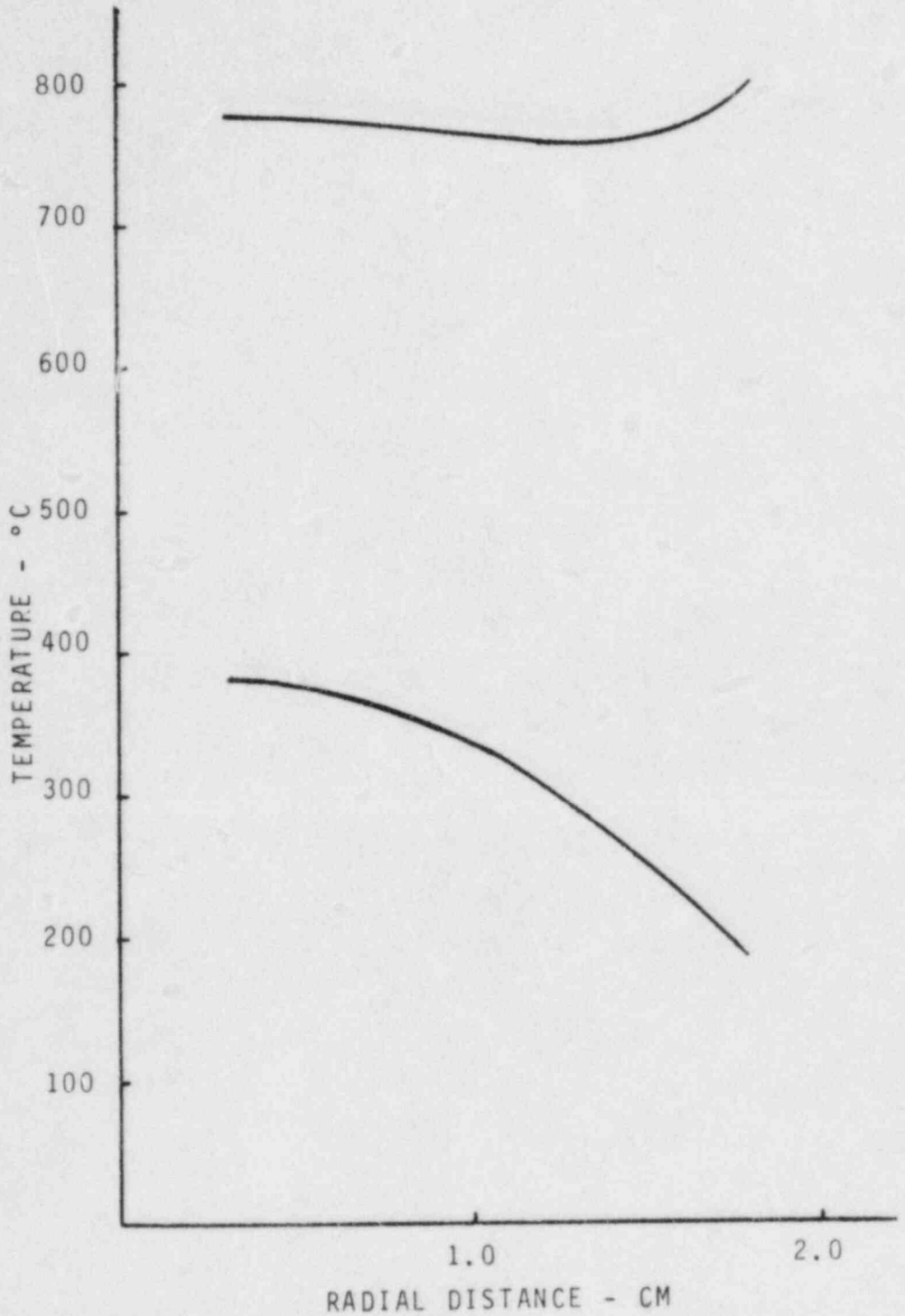

FUEL TEMPERATURE DISTRIBUTION
BEFORE AND AFTER PULSE
FIGURE 7-2

Figure 7-3, will rise to a maximum value of 750°C. The stress imposed on the fuel element clad by the internal gas pressure, presented in Figure 7-4 is about 2300 psi when the fuel and clad temperature is 750°C and the yield stress for the clad is about 19,500 psi. Therefore, it can be concluded that the postulated loss-of-coolant accident will not result in any damage to the fuel, will not result in release of fission products to the environment, and will not require emergency cooling.

If the reactor tank is drained of water, the fission product decay heat will be removed through the natural convective flow of air up through the reactor core. If the decay-heat production is sufficiently low because of a low fission product inventory or a long interval between reactor shutdown and coolant loss, the flow of air will be enough to maintain the fuel at a temperature at which the fuel elements are undamaged. The following analysis shows that:

a. The maximum temperature to which the fuel can increase is 900°C without substantial yielding of the clad or subsequent release of fission products.

b. This temperature will never be exceeded under any conditions of coolant loss if the maximum operating power density is 22 kW/element or less.

c. For maximum operating power densities greater than 22 kW/element, emergency cooling can be provided to ensure that the fuel element temperature does not exceed 900°C. The required emergency cooling time as a function of maximum operating power density is shown in Figure 7-5.

7.2.2 Fuel Temperature and Clad Integrity

The strength of the fuel element clad is a function of its temperature. The stress imposed on the clad is a function of the fuel temperature as well as the hydrogen-to-zirconium ratio, the fuel burnup, and the free gas volume within the element. In the analysis of the stresses imposed on the clad and strength of the clad the following assumptions will be made:

a. The fuel and clad are at the same temperature.

b. The hydrogen-to-zirconium ratio is 1.65.

c. The free volume within the element is represented by a space 1/8-in. high within the clad.

d. The reactor contains fuel that has experienced burnup equivalent to only about 4.5 MW-days.

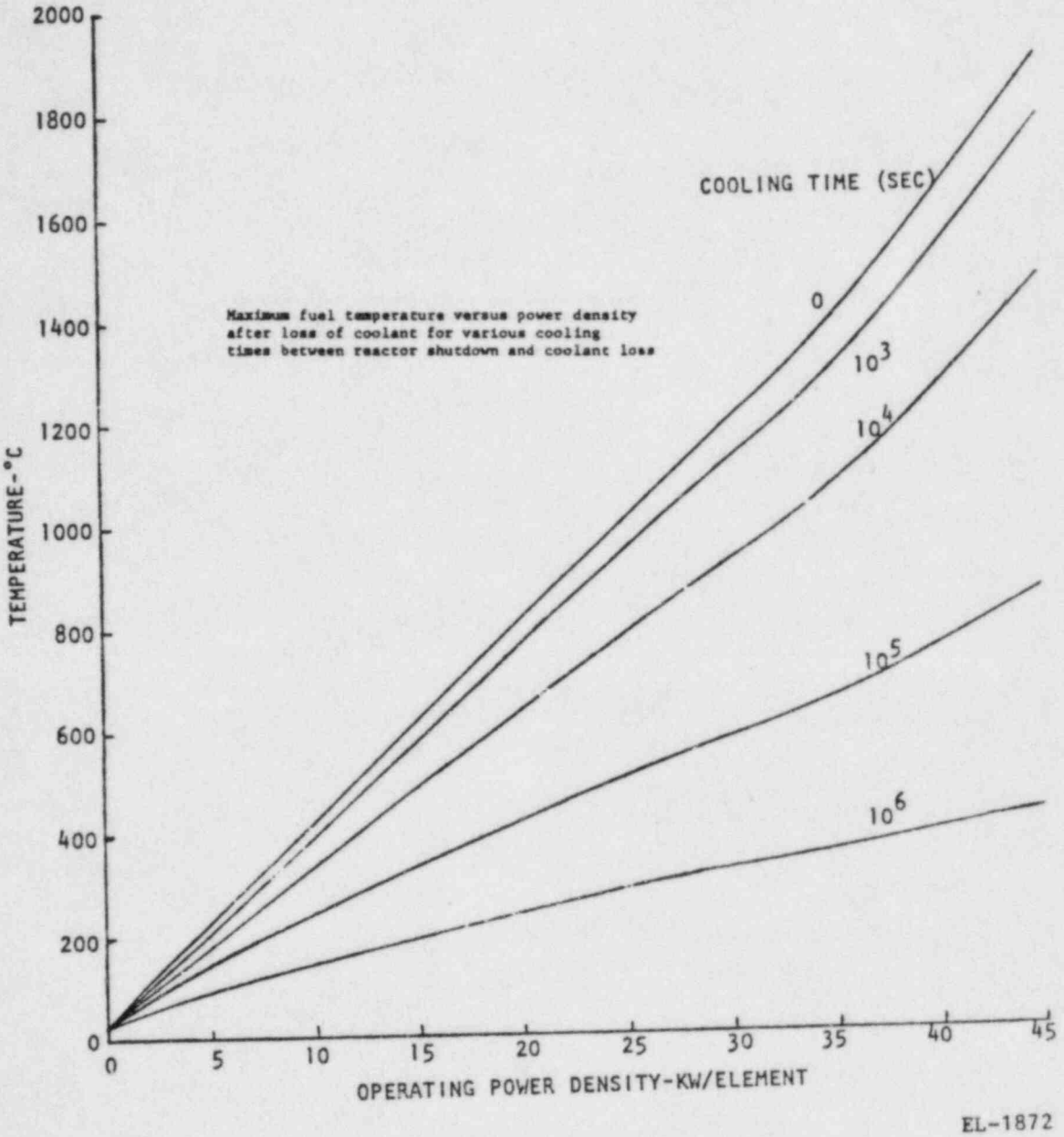

FUEL TEMPERATURE AND POWER DENSITY
FOR ELEMENT COOLING TIMES
Figure 7-3

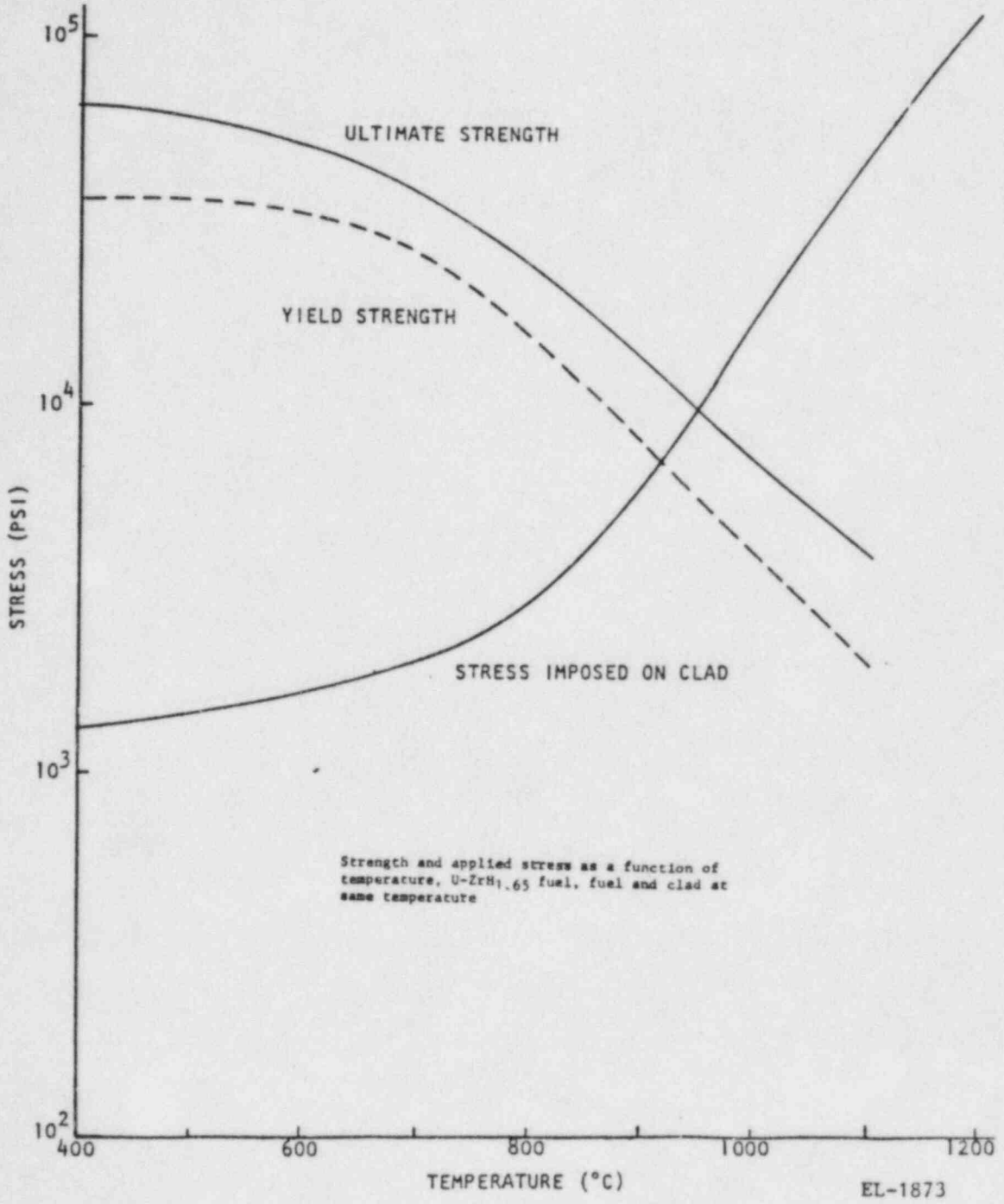

U-ZRH(1.6) STRENGTH AND STRESS
VERSUS TEMPERATURE
Figure 7-4

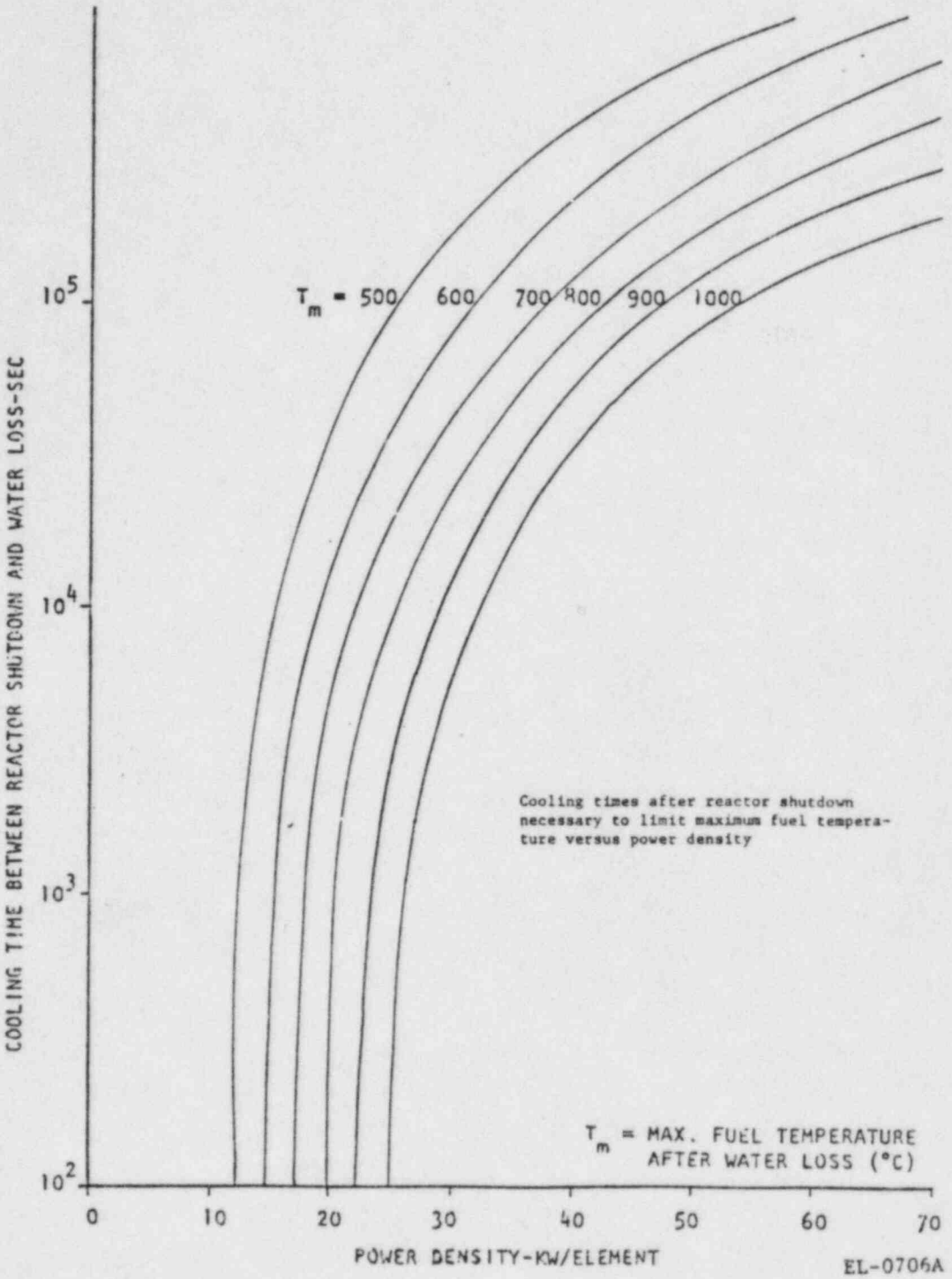

COOLING TIMES AFTER REACTOR SHUTDOWN
TO LIMIT MAXIMUM FUEL TEMPERATURE VERSUS POWER DENSITY
Figure 7-5

The fuel element internal pressure p is given by

$$P = P_h + P_{fp} + P_{air} \quad ,$$

where P_h = hydrogen pressure,

P_{fp} = pressure exerted by volatile fission products,

P_{air} = pressure exerted by trapped air.

For hydrogen-to-zirconium ratios greater than about 1.58 the equilibrium hydrogen pressure can be approximated by

$$P_h = \exp [1.767 + 10.3014x - 19740.37/(T_K)] \text{ (atmospheres)}, \qquad (26)$$

where x = ratio of hydrogen atoms to zirconium atoms, and

T_K = fuel temperature (°K).

This expression was derived from least-square fits to the data of Dee and Simnad [3]. For ZrH (H/Zr; 1.65) the hydrogen pressure becomes

$$P_h = 1.410 \times 10^8 \exp [-19740.37/(T_K)] \text{ (atmospheres)}.$$

The pressure exerted by the fission product gases is given by

$$P_{fp} = f \frac{n}{E} \frac{R}{V} T_K E \quad , \qquad (27)$$

where f = fission product release fraction,

n/E = number of moles of gas evolved per unit of energy produced, moles/MW-day,

R = gas constant, 8.206×10^{-2} liters-atmospheres/mole-°K,

V = free volume occupied by the gases, liters, and

E = total energy produced in the element, MW-day.

The fission product release fraction [4] is given by

$$f = \int_n f_n \, dn \qquad (28)$$

$$f_n = \{1.5 \times 10^{-5} + 3.6 \times 10^3 \exp [- 1.34 \times 10^4/T_n]\}$$

where T_n = fuel temperature in the differential volume of the element during normal operation, °K,

f_n = differential release fraction and

n = fuel volume normalized to 1.

The fission product gas production rate n/E is not independent of power density (neutron flux) but varies slightly with the power density. The value n/E = 0.00119 moles/MW-day is accurate to within a few percent over the range from, a few kilowatts per element to well over 40 kW/element. The free volume occupied by the gases is assumed to be a space 1/8-in. (0.3175-cm) high at the top of the fuel so that

$$V = 0.3175\ \pi r_i^2 \quad , \tag{29}$$

where r_i = inside radius of the clad (1.822 cm).

For standard TRIGA fuel the maximum burnup is about 4.5 MW-days/element. Pressure exerted by fission product gases is not significant.

The air trapped within the fuel element clad would exert a pressure

$$P_{air} = RT_K/22.4 \quad , \tag{30}$$

where it is assumed that the initial specific volume of the air (22.4 liters/moles) is present at the time of the loss of coolant. Actually, the air forms oxides and nitrides with the zirconium so that after relatively short operation the air is no longer present in the free volume inside the fuel element clad.

For ZrH (H/Zr; 1.6) fuel burned up to 4.5 MW-days/element, with a maximum operating temperature of 600°C, the internal pressure as a function of maximum fuel temperature T_K is

$$P = 1.410 \times 10^8 \exp(-19740.37/T_K) + 3.66 \times 10^{-3}\ T_K \quad \text{(atmosphere)} \tag{31}$$

or

$$P = 2.073 \times 10^9 \exp(19740.37/T_K) + 5.38 \times 10^{-2}\ T_K \ \text{(psi)}.$$

The stress imposed on the clad by the gases within the free volume inside the clad is

$$S = (r_c/t)\ p \quad , \tag{32}$$

where r_c = clad outside radius (1.873 cm),

t = clad thickness (0.051 cm).

If the previous and initial equation are combined, the stress can be rewritten as

$$S = 36.75\ p \qquad (33)$$

$$= 7.61 \times 10^{10} \exp(-19740.37/T_K) + 1.97\ T_K \quad (\text{psi}).$$

In Figure 7-4 this imposed stress is plotted as a function of maximum fuel temperatures. Also plotted are the yield and ultimate strength of the type 304 stainless steel clad. The clad ultimate strength is not exceeded if the maximum fuel temperature is maintained below about 950°C and the yield strength is not exceeded for any fuel temperatures below about 920°C, slightly below the yield point and well below the rupture point.

7.2.3 After-Heat Removal Following Coolant Loss

It is assumed that the reactor operates continuosly at a constant power density level P_o so that the maximum inventory of fission products is available to produce heat after the reactor is shut down. The power density after reactor shutdown P is given by

$$P = 0.1\ P_o\ [(t + 10)^{-0.2} - 0.87\ (t + 2 \times 10^7)^{-0.2}]$$

$$* \{1.3 \cos[2.45\ (0.26x - 0.5)]\},$$

where P_o = operating power density, W/cm^3,

t = time after reactor shutdown. sec,

x = distance from the bottom of the fuel region, cm.

At the time that the coolant is lost from the core the fuel and its surroundings are assumed to be at a temperature of 27°C. This is not necessarily true, for an accident can be postulated in which the coolant loss is the mechanism by which the reactor is shut down. (For the standard non-gapped fuel element, under normal conditions, the time to cool down from operating temperatures is a matter of one to two minutes.) Although such an accident does not appear to be conceivable, calculations indicate that: if it is assumed that the average fuel temperature at the time of coolant loss is equivalent to the operating average fuel temperature, the maximum temperature after the coolant loss is not appreciably different (2% - 4% higher) from that calculated assuming 27°C fuel initially.

The after-heat removal will be accomplished by the flow of air through the core. To determine the flow through the core the buoyant forces were equated to the friction, end, and acceleration losses in the channel as shown in the expression

$$\delta p_b = \delta p_f + \delta p_e + \delta p_i + \delta p_a \quad . \tag{35}$$

The buoyant forces are given by

$$\delta p_b = \rho_0 L - \int \rho dx = \rho_0 L - \rho_0 L_o - \bar{\rho} L_f - \rho_l L_t \tag{36}$$

where ρ_0, $\bar{\rho}$, ρ_l = the entrance, mean, and exit fluid densities, respectively,

L = the effective length of the channel ($L = L_o + L_f + L_t$),

L_o, L_f, L_t = the length of the channel adjacent to the bottom end reflector, fuel, and top end reflector plus ten channel hydraulic diameters, respectively.

The friction losses in the flow channel are given by

$$\delta p_f = \sum^{i} f_{Fi} \frac{4L_i}{D_e} \frac{w^2}{2g\rho_i A_c^2} \tag{37}$$

where the summation is over the lower unheated length, the heated length, and the upper unheated length, and

f_{Fi} = the friction factor $(23.46/R_e)$ [5] ,

D_e = the hydraulic diameter (0.0601 ft),

A_c = the flow area through the core per element (0.0058 ft^2),

$g = 4.17 \times 10^8$ ft/hr^2 .

The sum of the exit and inlet losses, using appropriate expansion coefficients, is given by

$$\delta p_e + \delta p_i = \frac{(\Sigma K)\, w^2}{2g\rho_0 A_c^2} \quad , \tag{38}$$

with

$$\Sigma K = \sum^{j} [k_j (A_c/A_j)^2] = 1.57 \quad .$$

where k_j is appropriate expansion or contraction coefficient from regions of area A_j.

The acceleration losses are given by

$$\delta p_a = (1/\rho_l - 1/\rho_0)\, (w^2/gA_c^2) \quad . \tag{39}$$

By substituting the appropriate expression in Equation 35, using the definition of the Reynolds number, and L =

2.40 ft, L_o = 0.29 ft, L_f = 1.25 ft, and L_t = 0.87 ft, one obtains

$$(0.700/\rho_1 - 0.149/\rho_0) \times 10^{-4} w^2 + \quad (40)$$

$$(0.153\mu_i/\rho_0 + 0.665\mu/\bar{\rho} + 0.153\mu_2/\rho_1 \times 10^{-2} w +$$

$$(1.25\bar{\rho} + 0.889\rho_1 - 2.139\rho_0) = 0$$

with the flow w in units of lb/hr and μ the viscosity in units of lb/hr-ft.

The properties of air for use in Equation 40 are expressed as

$$\rho_i = 40/T_i \ (lb/ft^3) \quad (41)$$

and $\mu_i = 5.739 \times 10^{-3} + 7.601 \times 10^{-5} T_i - 1.278 \times 10^{-8} T_i^2$ (lb/hr-ft),

where T_i is the appropriate temperature in °R.

The heat transfer coefficient was calculated through the relationship

$$N_u = 6.3 \qquad R_a \leq 1000 \quad (42)$$

$$= 0.806 R_a^{0.2976} \qquad Ra > 1000 \ ,$$

where N_u = the Nusselt number = $h\mathfrak{D}_e/k$,

R_a = the Rayleigh number $D_e^4 \rho^2 g\beta\delta T c_p/\mu kL$

h = the heat transfer coefficient, Btu/hr-ft^2-°F,

k = the thermal conductivity of the laminar film, Btu/hr-ft^2-°F,

β = the volumetric expansion coefficient, °F^{-1},

δT = the temperature rise over the channel length, L(°F),

c_p = the specific heat of air (Btu/lb-°F).

The expression for the Nusselt number was derived from the work of Sparrow, Loeffler, and Hubbard [6] for laminar flow between triangular arrays of heated cylinders.

The thermal conductivity and specific heat are given by

$$k = 2.377 \times 10^{-4} + 2.995 \times 10^{-5} T - 4.738 \times 10^{-9} T^2 \quad (43)$$
(Btu/hr-ft-°F)

$$\text{and } c_p = 2.413 \times 10^{-1} - 1.780 \times 10^{-6}\, T + 1.018 \times 10^{-8}\, T^2 \quad \text{(Btu/lb-°F)}, \tag{44}$$

where T is the appropriate temperature in °R.

These two expressions, as well as that given for the dynamic viscosity of air in Equation 41, are least-square fits to the data presented by Etherington [7].

TAC2D [8], a two-dimensional transient-heat transport computer code developed by GA Technologies, was used for calculating the system temperatures after the loss of tank water. The parameters derived above were programmed into the calculations.

The maximum temperatures reached by the fuel are plotted as a function of operating power density in Figure 7-3 for several cooling or delay times between reactor shutdown and loss of coolant from the core. For reactor operation with maximum power density of 18 kW/element, or less, loss of coolant water immediately upon reactor shutdown would not cause the maximum fuel temperature to exceed 750°C. Operation at maximum power densities greater than 18 kW/element will not result in fuel temperatures above 750°C, if the coolant loss occurs sometime after shutdown, or if emergency cooling is provided. (The time required between shutdown and the beginning of air cooling depends on power density.)

In Figure 7-5, the data presented in Figure 7-3 were replotted to show the time required for natural convective water cooling or emergency cooling, after reactor shutdown, to produce temperatures no greater than a given value. Thus, for example, for a reactor in which the maximum operating power density is 27 kW/element and to limit the temperature to 950°C, or less, there must be an interval of at least 3730 sec (or 1.04 hr) between reactor shutdown and either the loss of tank water from the core or the cessation of emergency cooling. The 65 minute delay time applies to the power density of a 90 element core operated at 1.5 MW but shrinks to a negligible value for the power density in a 100 element core.

7.2.4 Radiation Levels

Even though the possibility of the loss of shielding water is believed to be exceedingly remote, a calculation has been performed to evaluate the radiological hazard associated with this type of accident (see Table 7-3). Assuming that the reactor has been operating for 10 hours and 1000 hours at 1.5 MW prior to losing all of the shielding water, the radiation dose rates at two different locations are listed below. The first location (direct

radiation) is 6.4 meters above the unshielded reactor core, near the top of the reactor tank. The second is at the top of the reactor shield; this location is shielded from direct radiation but is subject to scattered radiation from a thick concrete ceiling 4.6 m above the top of the reactor shield. The assumption that there is a thick concrete ceiling maximizes the reflected radiation dose. Normal roof structures would give considerably less backscattering. Time is measured from the conclusion of operation at 1.5 MW. Dose rates assume no water in the tank.

The tabulated data show that if an individual does not expose himself directly to the core he could work for approximately 2 hours (3 hours for 1 MW) at the top of the shield tank 1 day after shutdown without receiving a dose in excess of that permitted by regulations for a calendar quarter.

Table 7-3
Calculated Radiation Dose Rates
For Loss of Shield Water

Decay Time	Direct Radiation R/hr		Scattered Radiation R/hr	
	10 hour	1000 hour	10 hour	1000 hour
1 minute	3980	4920	3.7	4.6
1 hour	929	1820	.87	1.7
1 day	87	681	.08	.64
1 week	10	281	.009	.26
1 month	2	104	.002	.10

For persons outside the building, the radiation from the unshielded core would be collimated upward by the shield structure and, therefore, would not give rise to a public hazard. The method of calculation follows.

The core, shut down and drained of water, was treated as a bare cylindrical source of 1-MeV photons of uniform strength. Its dimensions were taken to be equal to those of the active core lattice. The source strength as a function of time was determined from Way and Wigner's [9] (Equation 45) data on fission product decay. No accounting was made of sources other than fission product decay gammas (i.e., activation gammas from the steel cladding and the aluminum grid plates) or of attenuation through the fuel element end pieces and the upper grid plate. The first of these assumptions is optimistic, the second conservative; the net

effect is conservative. The conservative assumption of a uniformly distributed source of 1-MeV photons was balanced by not assuming any buildup in the core.

An approximation of the fission product energy release term is taken as:

$$\Gamma(t) = 1.26\ t^{-1.2} \quad , \tag{45}$$

where

$\Gamma(t)$ = energy release in MeV/sec-fission,

t = is the time after fission in seconds.

By integration the total core source term is

$$S(t,T) = 3.1 \times 10^{10}\ P_o \int_t^{t+T} \Gamma(\tau)\ d\tau \tag{46}$$

$$= 1.95 \times 10^{11}\ P_o \{1 - [1 + T/t]^{-0.2}\}\ t^{-0.2} \tag{47}$$

where

$S(t,T)$ = energy release in MeV/sec-watt,

P_o = reactor power, watts,

T = period of time at power.

The volumetric source of 1 MeV photons is

$$S_v = \frac{S(t,T)}{\pi r_c^2 x_c} \tag{48}$$

The direct dose rate at a point outside and on the axis of a cylindrical source is given by:

$$D_d = \frac{S_v}{K} \int_0^{x_c} \int_0^{r_c} e^{-\mu_c z}\ \frac{2\pi r\,dr\,dx}{4\pi R^2} \tag{49}$$

where

S_v = source strength in photons, 1 MeV)/cm^3-sec,

K = flux-to-dose conversion factor, 5.77×10^5 photons/cm^2-sec per rad/hr,

$2\pi r\,dr\,dx$ = cylindrical volume element, dV

r_c = core radius, 26 cm

x_c = core height, 38 cm

μ_c = core attenuation coefficient, 0.207 cm^{-1}

R = distance from volume element to receiver, cm

z = slant penetration in core = xR/(a+x), cm

a = distance from top to core to receiver, 640 cm

For distances far from the core (i.e. for a >> r_c and x_c) the above expression reduces to

$$D_d = \frac{S_v r_c^2}{4\mu_c a^2 K} \left(1 - e^{-\mu_c x_c}\right) \quad (50)$$

The scattered dose rate was calculated from

$$D_s = 6.03 \times 10^{23} \rho \frac{Z}{A} \frac{I_o C}{K(E)x^2} Q_a \quad (51)$$

where

ρ = Density of scattering material, concrete, 2.3 g/cm^3

$\frac{Z}{A}$ = Ratio of average atomic number to atomic mass of the scatterer, 0.5

and $I_o C$ = Incident current times cross section of beams, photons/sec

K = Photon current to dose rate conversion, 2.75×10^6 photons/cm^2-sec per rad/hr

E = Energy of scattered photon, Mev

x = Distance from scattering point to detector, 400 cm

$$Q_a = \frac{1}{\mu_0 + \mu_1 (\cos\theta_0/\cos\theta_1)} \frac{\delta\sigma}{\delta\Omega}$$

μ_0, μ_1 = Attenuation coefficient in scatter for incident and scattered photons, cm^{-1}, .146, .292

θ_0, θ_1 = Incident and scattered angle (measured from the normal to the scatterer), 0, 25 degrees

$\delta\sigma/\delta\Omega$ = Differential Klein-Nishina scattering cross section, cm^2/electron-steradian

It was assumed that all of the source photons that exit the top of the reactor pool were incident normally to the concrete roof (i.e., $\theta_0 = 0$) at a point directly over the core, thus

$$I_0 C = S_0 W \quad (52)$$

where $S_0 = S_v \pi r_c^2/\mu_c$ (53)

$$W = \{\sin^{-1}\left[\frac{y_0^2(r_0^2-x_0^2)+r_0^2(r_0^2+x_0^2)}{(r_0^2+x_0^2)(r_0^2+y_0^2)}\right] - \pi/2\}/2\pi$$

and r_0 = Distace from the core to the top of the pool, ~6.4 m

x_0 = Half width of the pool, ~1 m

y_0 = Half length of the pool, ~1.5 m

S_v, r_c, μ_c have already been defined.

The energy of the scattered photons is given by

$$E = \frac{E_0}{1 + E_0(1 - \cos\theta)/0.51} \quad (54)$$

where E_0 is the incident photon energy (1 Mev) and θ is the scattering angle = $\pi - (\theta_0 + \theta_1)$.

The differential scattering cross section is given by

$$\frac{\delta\sigma}{\delta\Omega} = \frac{r_e^2}{2}\left[\frac{E}{E_0} - \left(\frac{E}{E_0}\sin\theta\right)^2 + \left(\frac{E}{E_0}\right)^3\right] \quad (55)$$

where r_e is the classical electron radius = 2.818×10^{-13} cm.

7.3 FISSION PRODUCT RELEASE

In the analysis of fission product releases under accident conditions, it is assumed that a fuel element in the region of highest power density fails. The failure is assumed to occur in air after operation at full power for an extended period.

7.3.1 Fission Product Inventory

Table 7-4 gives the inventory of radioactive noble gases and halogens in the TRIGA Mark II after continuous operation at 1.5 MW for four years (i.e. 6MW-yr). The estimated inventory is conservative since actual operation after 4 years is expected to be less than 5% of 4 MW-yrs.

7.3.2 Fission Product Release Fractions

The release of fission products from U-ZrH fuel has been studied at some length. A summary report of these

studies [4] indicates that the release from the U-ZrH (H/Zr; 1.6) fuel meat at the steady-state operating temperatures is principally through recoil into the fuel-clad gap. At high temperatures (above 400°C or 500°C), the release mechanism is through a diffusion process and is temperature dependent, unlike recoil.

For the accident considered here, it is assumed that a fuel element in the region of highest power density fails in water and that the peak fuel temperature in the element is less than 400°C. At this temperature, the long-term release fraction would be less than 0.0015%. For the purpose of this analysis it is also assumed that 100% of the noble gases and 100% of the halogens are released from the highest power density fuel element in which 2.22% of the total power is generated.

Table 7-4
NOBLE GAS AND HALOGENS IN THE REACTOR

Isotope	Quantity (Ci)
Br-83	6,120
Br-84m	6,120
Br-84	12,360
Br-85	12,900
Kr-85m	12,900
Kr-85	678
Kr-87	32,400
Kr-88	46,200
Kr-89	58,500
Kr-90	65,100
Kr-91	44,100
I-131	35,700
Xe-131m	288
I-132	53,100
I-133	86,100
Xe-133m	2,100
Xe-133	86,100
I-134	96,600
I-135	80,400
Xe-135m	24,300
Xe-135	83,100
I-136	77,700
Xe-137	75,300
Xe-138	70,200
Xe-139	70,800
Xe-140	48,600

It is important to note that the release fraction in accident conditions is characteristic of the normal operating temperature and not the temperature during the accident conditions. This is because the fission products released as a result of a fuel clad failure are those that have collected in the fuel-clad gap during normal operation.

Other assumptions concerning estimated accident scenario doses are:

a. Assume an element fails in air such that all (100%) noble gases and halogens in the gap are effectively released.

b. There is no plate-out of any released fission products.

c. After the failure a ventilation rate of 10 air changes per hour occurs with no air filtration.

d. Doses are calculated assuming exposure to a semi-infinite cloud.

e. Doses are calculated for release from the total core and a single fuel element (90 element core with peak to average flux of 2.0).

f. Doses external to the building are calculated by assuming a minimum building dilution factor for releases (1.0 m/sec wind velocity with building cross section of 234 m^2).

g. Doses were also calculated for personnel in the reactor room by dumping rapidly a small fraction of the total inventory into the room such that the continuous release is equivalent to a constant concentration.

The net effect of these assumptions is that for the single element accident condition, the fraction of the noble gases released from the building is:

$$f_{NG} = 2.0 \times 10^{-5} \times 1.0 \times 2.22 \times 10^{-2}$$
$$= 4.44 \times 10^{-7} \quad , \qquad (56)$$

and of the halogens is:

$$f_{H} = 2.0 \times 10^{-5} \times 1.0 \times 2.22 \times 10^{-2}$$
$$= 4.44 \times 10^{-7} \quad , \qquad (57)$$

where a conservative release fraction of 0.002% is applied.

7.3.3 Downwind Dose Calculation

The minimum roof level dilution factor was calculated, assuming a building cross sectional area of 234 square meters. The factor is based on mixing in the lee of the building when the wind velocity is 1 m/sec. A dilution factor of 0.00854 seconds per cubic meter is applied.

The calculation of whole body gamma doses and thyroid doses downwind from the point of release was accomplished through the use of the computer code GADOSE [10]. In this code the set of differential equations describing the rate of production of an isotope through the decay of its precursors and the rate of removal through radioactive decay and removal by the ventilation system is integrated for each member of the chain. The release rate q_i to the environment for the ith isotope at time t_i in hours is:

$$q_i(t) = g_i\, Q(t)\, (\ell/V)/3600 \quad , \tag{58}$$

where $Q_i(t)$ = the release of the ith isotope in Ci,

ℓ/V = the building leakage rate in $(m^3/hr)/m^3$,

ε_i = the filter efficiency for the isotope,

$g_i = 1 - \varepsilon_i$.

The quantity $Q_i(t)$ is the amount of the ith isotope in the discharged air at the time, t. This quantity is given by

$$Q_i(t) = f_i\, Q_i(0)\, e^{-(\lambda_i + \ell/V)t} \tag{59}$$

where $Q_i(0)$ = the inventory of the ith isotope as found in Table 7-4,

λi = the decay constant for the ith isotope, and

f_i = the release fraction to the reactor hall.

The concentration downwind at a distance x for the ith isotope is calculated from

$$Q_i(t,x) = q_i(t - \tau)\, \psi(x)\, e^{-\lambda_i \tau} \quad , \tag{60}$$

where τ = the transit time from the release point to the dose point, hr,

$\psi(x)$ = the dilution factor at the distance x, sec/m^3.

The whole body gamma ray dose rate for the ith isotope, D_{wi}, at the distance x and time t is calculated, assuming a semi-infinite cloud, through the expression:

$$D_{w_i}(t,x_i) = 900\ E_i\ Q_i(t,x) \quad , \tag{61}$$

where E_i = the average gamma ray energy per disintegration, MeV, and the constant includes the attenuation coefficient for air as well as the conversion factors required. Dose rate is in units of rad/hr.

Internal dose rates, in this case the dose rate to the thyroid, are calculated by:

$$D_{th_i}(t,x) = 3600\ B\ K_i\ Q_i(t,x) \quad , \tag{62}$$

where B = the breathing rate, m^3/sec, and

K_i = the internal dose effectivity of the ith isotope, rem/Ci.

The values for the breathing rate are given in Table 7-5 and are taken from a published regulatory guide [11].

The average gamma ray energy per disintegration and the internal dose effectivity for each isotope considered are given in Table 7-6.

The decay products of these isotopes are also included in the calculation; however, their contribution to the dose rates are small and therefore the data for these isotopes were not included in the table.

7.3.4 Downwind Doses

The whole body gamma dose and thyroid dose in the lee of the building are shown in Table 7-7. These doses are acceptable relative to the conservative nature of the calculations and likelihood that an accident scenario would actually lead to these results.

Table 7-5
ASSUMED BREATHING RATES

Time (hr)	Breathing Rate (m^3/sec)
0 to 8	3.47×10^{-4}
8 to 24	1.75×10^{-4}
Over 24	2.32×10^{-4}

Table 7-6
AVERAGE GAMMA RAY ENERGY AND INTERNAL DOSE
EFFECTIVITY FOR EACH FISSION PRODUCT ISOTOPE

Isotope	E_i(MeV)	K_i(rem/Ci)
Br-83	0.92×10^{-2}	
Br-84	1.87	
I-131	0.40	1.486×10^{6}
I-132	1.96	5.288×10^{4}
I-133	0.56	3.951×10^{5}
I-134	3.02	2.538×10^{4}
I-135	1.77	1.231×10^{5}
I-136	2.91	
Kr-83m	0.8×10^{-3}	
Kr-85m	0.16	
Kr-85	0.4×10^{-2}	
Kr-87	1.07	
Kr-88	2.05	
Kr-89	2.40	
Xe-131m	0.82×10^{-2}	
Xe-133m	0.37×10^{-1}	
Xe-133	0.29×10^{-1}	
Xe-135m	0.46	
Xe-135	0.25	
Xe-137	1.22	
Xe-138	1.57	

DOSES FROM FISSION PRODUCT RELEASE

Accident Condition	Time After Release (Hr)	Dose (Rad)[1] Halogens Whole Body	Halogens Internal	Noble Gases Whole Body	Noble Gases Internal
Core Inventory Release[2] 1.5MW	0.1	0.3	5.9×10^{1}	0.19	1.0×10^{-4}
	1.0	2.1	5.8×10^{2}	1.14	5.0×10^{-3}
	8.0	8.3	4.2×10^{3}	3.57	5.7×10^{-2}
	24.0	13.8	1.1×10^{4}	4.51	1.8×10^{-1}
	720.0	31.4	8.5×10^{4}	6.37	4.3×10^{0}
Core Inventory Release[3] 1.5MW	0.1	0.019	3.8	0.013	5.6×10^{-6}
	1.0	0.028	6.0	0.017	1.7×10^{-5}
	8.0	0.028	6.0	0.017	1.7×10^{-5}
Single Element Release[2] 1.0 MW * 2.22% of energy	0.1	0.004	8.7×10^{-1}	0.002	1.5×10^{-6}
	1.0	0.031	8.6×10^{0}	0.016	7.4×10^{-5}
	8.0	0.123	6.2×10^{-1}	0.053	8.4×10^{-4}
	24.0	0.204	1.6×10^{-2}	0.067	2.7×10^{-3}
	720.0	0.465	1.3×10^{-3}	0.090	6.0×10^{-2}
Single Element Release[3] 1.0MW * 2.22% of Energy	0.1	2.8×10^{-4}	0.056	1.9×10^{-4}	8.3×10^{-8}
	1.0	4.1×10^{-4}	0.089	2.5×10^{-4}	2.5×10^{-7}
	8.0	4.1×10^{-4}	0.089	2.5×10^{-4}	2.5×10^{-7}

1.) Doses calculated assuming 4 years full power operation and release fraction of 0.002 %.

2.) Release calculated for semi-infinite cloud in room volume of 4290 m^3 with no ventilation.

3.) Release calculated at zero distance with an air change rate of ten per hour and building dilution factor of 8540 sec/cc.

Chapter 7 References

1. West G.B., W.L. Whittemore, J.R. Shoptaugh Jr., J.B. Dee, C.O. Coffer, "Kinectic Behaviour of TRIGA Reactors", General Atomic Report GA-7882, 1967.

2. Simnad, M.T., "The U-ZrH$_x$ Alloy : Its Properties and Use in TRIGA Fuels", General Atomic Report E-117-833, 1980.

3. Simnad, M.T., and J.B. Dee, "Equilibrium Dissociation Pressures and Performance of Pulsed U-ZrH Fuels at Elevated Temperatures," Gulf General Atomic Report GA-8129, 1967.

4. Foushee, F.C., and R.H. Peters, "Summary of TRIGA Fuel Fission Product Release Experiments," Gulf Energy & Environmental Systems Report Gulf-EES-A10801, 1971 p. 3.

5. Sparrow, E.M., and A.L. Loeffler, "Longitudinal Laminar Flow Between Cylinders Arranged in a Regular Array, AicleJ. 5, No. 3, 325 (1959).

6. Sparrow, E.M., A.L. Loeffler, Jr., and H.A. Hubbard, "Heat Transfer to Longitudinal Laminar Flow Between Cylinders," Trans. ASME J. of Heat Transfer, Nov. 1961, p. 415.

7. Etherington, H. (ed.), Nuclear Engineering Handbook, 1st ed., McGraw-Hill Book Co., New York 1958, p. 9-1.

8. Peterson, J.F., "TAC2D, A General Purpose, Two-Dimensional Heat-Transfer Computer Code - User's Manual," Gulf General Atomic Report GA-8869, 1969.

9. Way, K. and E.P. Wigner, "Radiation from Fission Products", Physics Review, 70 p. 115, 1946.

10. Lee, E., R.J. Mack, and D.B. Sedgeley, "GADOSE and DOSET Programs to Calculate Environmental Consequences of Radioactivity Release," Gulf General Atomic Report GA-6511 (Rev.), 1969.

11. "Programs for the Monitoring Radioactivity in the Environs of Nuclear Power Plants", U.S. NRC Regulatory Guide 4.1.

Chapter 8

FACILITY ADMINISTRATION

A TRIGA type reactor facility will be owned and operated by The University of Texas at Austin. The facility located at the Balcones Research Center is to be operated as part of the Nuclear Engineering Teaching Program, a division of the Mechanical Engineering Department in the College of Engineering. Licenses for the facility operation will include a facility specific license for operation issued by the U.S. Nuclear Regulatory Commission and a university broad license for radioactive materials issued by the State of Texas Department of Health. Additional licenses may be obtained as required for facility activities. Operation as a utilization facility will be for education, training, and the conduct of research and development activities.

8.1 ORGANIZATION

8.1.1 Structure. Figure 8-1 illustrates the organizational structure that is applied to the management and operation of the reactor facility. Responsibility for the safe operation of the reactor facility is a function of the management structure of Figure 8-1 [1]. The responsibilities include safeguarding the public and staff from undue radiation exposures and adherence to license or other operation constraints.

Facility staff is typically organized as three full time persons consisting of a supervisor, operator or technician, and researchist, and two half-time persons consisting of an operator and secretary. Faculty, researchers and students supplement the organization. Descriptions of key components of the organization follow.

8.1.2 Vice President for Research and Academic Affairs. Research and educational programs are administered through the office of the Vice President for Research and Academic Affairs with functions delegated to the Dean of the College of Engineering and Chairman of the Mechanical Engineering Department.

8.1.3 Director of Nuclear Engineering Teaching Laboratory. Nuclear Engineering Teaching Laboratory programs are directed by a faculty member of the Mechanical Engineering Department that teaches courses in nuclear engineering and performs research related to nuclear applications.

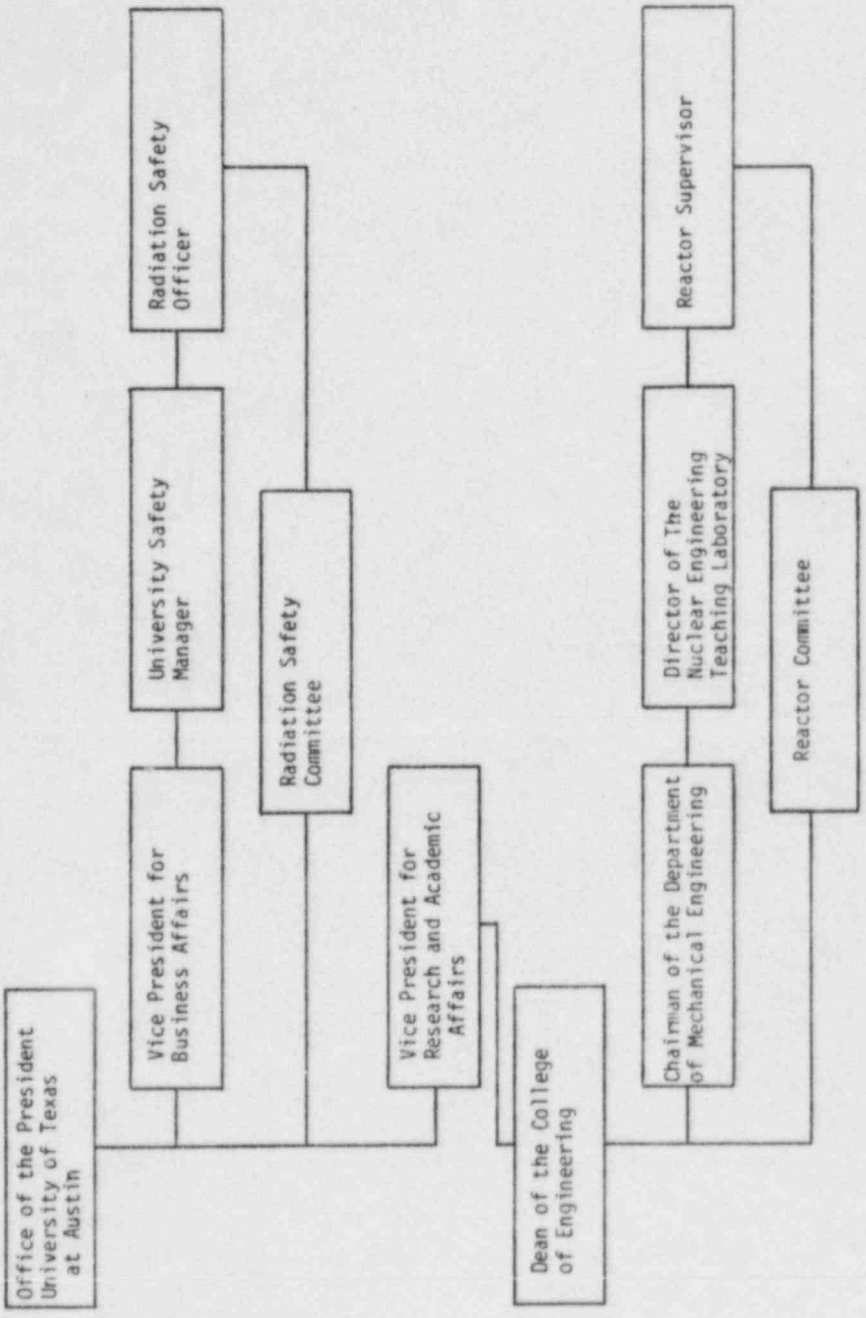

ADMINISTRATIVE STRUCTURE
Figure 8-1

8.1.4 Radiation Safety Committee. The Radiation Safety Committee is established through the Office of the President of The University of Texas at Austin. Responsibilities of the committee are broad and include all policies and practices regarding the license, purchase, shipment, use, monitoring, disposal, and transfer of radioisotopes or sources of ionizing radiation at The University of Texas at Austin.

The President shall appoint at least three members to the Committee and appoint one as Chairperson. The Committee will meet at least once each year on a called basis or as required to approve formally applications to use radioactive materials. The Radiation Safety Committee shall be consulted by the University Safety Office concerning any unusual or exceptional action that affects the administration of the Radiation Safety Program.

8.1.5 Radiation Safety Officer. A Radiation Safety Officer acts as the delegated authority of the Radiation Safety Committee in the daily implementation of policies and practices regarding the safe use of radioisotopes and sources of radiation as determined by the Radiation Safety Committee. The Radiation Safety Program is administered through the University Safety Office and University Safety Engineer. The responsibilities of the Radiation Safety Officer are outlined in The University of Texas at Austin Manual of Radiation Safety.

8.1.6 Reactor Committee. The Reactor Committee is established through the Office of the Dean of the College of Engineering of The University of Texas at Austin. Broad responsibilities of the committee include the evaluation, review, and approval of facility standards for safe operation.

The Dean shall appoint at least three members to the Committee that represent a broad spectrum of expertise appropriate to reactor technology. The committee will meet at least twice each calendar year or more frequently as circumstances warrant. The Reactor Committee shall be consulted by the Nuclear Engineering Teaching Laboratory concerning unusual or exceptional actions that affect administration of the reactor program.

8.1.7 Laboratory Supervisor. The operation of the Nuclear Engineering Teaching Laboratory is governed by a Laboratory or Reactor Supervisor, who shall be qualified as a USNRC licensed Senior Operator for The University of Texas at Austin TRIGA Reactor facility. Responsibilities of the supervisor include reactor operation, equipment maintenance, experiment operation, instruction of persons with access to laboratory areas, and development of research activities. A

UT TRIGA Operations Manual will be maintained by the Reactor Supervisor.

8.2 QUALIFICATIONS

8.2.1 General. Personnel associated with the research reactor facility shall have a combination of academic training, experience, skills, and health commensurate with the responsibility to provide reasonable assurance that decisions and actions during all normal and abnormal conditions will be such that the reactor is operated in a safe manner.

8.2.2 Academic Administration and Radiological Safety. Administrative positions not principally responsible for facility operation and staff positions of the radiological safety program are subject to qualifications standards determined by the University. Administrative qualifications depend on academic credentials appropriate to the nature of the University organization. Staff qualifications for radiological safety are subject to personnel descriptions developed for various University employment positions.

8.2.3 Facility Director. A combination of academic training and nuclear experience will fulfill the qualifications for the individual identified as the facility director. A total of six years experience will be required. Academic training in engineering or science with completion of a baccalaureate degree may account for up to four of the six years experience.

8.2.4 Reactor Supervisor. A person with special training to supervise reactor operation and related functions will be designated as the facility supervisor. The reactor supervisor will be qualified by certification as a senior operator as determined by the licensing agency. Additional academic or nuclear experience will be required as necessary for the supervisor to perform adequately the duties associated with facility activities.

8.2.5 Operators, Technicians, and others. Qualifications for operators will be determined by the certification of the licensing agency for either senior operator or operator permits. Qualifications for technicians will be determined by training and experience appropriate to the required duties to be performed. A consolidation of the duties of operator and technician may occur to better utilize staff resources. Other persons with access to the laboratory will be qualified by academic experience or by special training and instruction of persons with operator certifications.

8.3 REACTOR OPERATIONS

Operation of the reactor and activities associated with the reactor, control system, instrument system, radiation monitoring system and engineered safety features will be the function of staff personnel with the appropriate license certifications [2]. Operation will include the implementation of required procedures, execution of appropriate experiments, actions related to safety and the preparation of required reports and records.

8.3.1 Staffing. All activities that require the presence of license certified operators will also require the presence in the facility complex of a second person capable of performing prescribed written instructions. Unexpected absence of a second person for greater than two hours will be acceptable if immediate action is taken to obtain a replacement. A designated license certified senior operator will be readily available on call during all periods in which activities requiring a certified operator are being performed. The person on call will be considered available if less than 1 hour is required to initiate a call request and respond on site.

Movement of fuel or control rods and relocation of experiments with greater than one dollar reactivity worth will require the presence of a person license certified as a senior operator. Other activities such as initial startup, recovery from unscheduled shutdowns and modifications to control and instrument systems, radiation measurement equipment or engineered safety features will require concurrence and documentation of a license certified senior operator.

Operation of reactor controls, movement of reactor experiments, maintenance of control, instrument and radiation measurement systems will require the presence of a license certified operator. A license certified operator will be present in the control room whenever the reactor is not shut down by more than one dollar of reactivity or the control and instrument panel is not secured.

The staff required for performing experiments with the reactor will be determined by a classification system specified for the experiments. Requirements will range from the presence of a certified operator for some routine experiments to the presence of a senior operator and the experimenter for other less routine experiments.

Other activities that occur in the area of the reactor will require knowledge of a license certified operator but not necessarily the presence of the operator. Such activities will include maintenance, handling of radioactive materials and experiment preparation.

8.3.2 Procedures. Written procedures shall govern many of the activities associated with reactor operation. Preparation of the procedures and minor modifications of the procedures will be by certified operators. Substantive changes to procedures or major modifications, and prepared procedures will be submitted to the reactor committee for review and approval. Temporary deviations from the procedures may be made by the reactor supervisor or designated senior operator provided changes of substance are reported for review and approval.

Activities subject to written procedures will include routine startup, shutdown and operation of the reactor; fuel loading, unloading and movement within the reactor; routine maintenance of major components of systems that could have an effect on reactor safety; surveillance tests and calibrations that may effect reactor safety; administrative controls for operation and maintenance that could effect core reactivity or reactor safety; personnel radiation protection and implementation of the emergency plan.

8.3.3 Experiments. Proposed experiments will be submitted to the reactor committee for review and approval of the experiment and its safety analysis [3]. Substantive changes to approved experiments will require reapproval while insignificant changes that do not alter experiment safety may be approved by the reactor supervisor or designated senior operator. Experiments will be approved first as proposed experiments for one time application and subsequently as approved experiments for repeated applications following a review of the results and experience of the initial experiment implementation.

Each experiment will be designated as one of three classes. One class will consist of experiments such as routine reactor operation for calibration or instruction, and routine irradiations such as neutron activation analysis. This class of experiment will require only the reactor operator during the reactor operation or experiment set up. A few experiments may require the presence of both a certified operator and the experimenter and will be designated as a seperate class of experiment. Another class of experiments will be specified for experiments that require large reactivity changes such as experiment facility movement, fuel or control rod movement, or significant changes to shielding of core radiation. This class will require the supervision of a senior operator.

8.4 ACTIONS AND REPORTS

8.4.1 Operating Reports. Routine annual reports covering the activities of the reactor facility during the previous calendar year shall be submitted to licensing

authorities within three months following the end of each prescribed year. Each annual operating report shall include the following information:

(a) A narrative summary of reactor operating experience including the energy produced by the reactor or the hours the reactor was critical, or both.
(b) The unscheduled shutdowns including, where applicable, corrective action taken to preclude recurrence.
(c) Tabulation of major preventive and corrective maintenance operations having safety significance.
(d) Tabulation of major changes in the reactor facility and procedures, and tabulation of new tests or experiments, or both, that are significantly different from those performed previously, including conclusions that no unreviewed safety questions were involved.
(e) A summary of the nature and amount of radioactive effluents released or discharged to the environs beyond the effective control of the owner-operator as determined at or before the point of such release or discharge. The summary shall include to the extent practicable an estimate of individual radionuclides present in the effluent. If the estimated average release after dilution or diffusion is less than 25% of the concentration allowed or recommended, a statement to this effect is sufficient.
(f) A summarized result of environmental surveys performed outside the facility.
(g) A summary of exposures received by facility personnel and visitors where such exposures are greater than 25% of that allowed or recommended.

8.4.2 Safety Limit Violation. Actions to be taken in the case of safety limit violation shall include cessation of reactor operations until a resumption is authorized by the licensing authority, a prompt report of violation to license authorities and management, and a subsequent follow-up report reviewed by the reactor committee and submitted to the license authority. The follow-up report shall describe applicable circumstances leading to the violation including causes and contributing factors that are known, effect of the violation upon reactor facility components, systems or structures, health and safety of personnel and the public, and corrective action to prevent recurrence. Prompt reporting of the event shall be by telephone and confirmed by written correspondence within 24 hours. A written report is to be submitted within 14 days.

8.4.3 Release of Radioactivity. Actions to be taken in the case of release of radioactivity from the site above allowable limits shall include a return to normal operation

or reactor shutdown until authorized by management if necessary to correct the occurrence, a report to management and license authority, and a review of the event by the reactor committee at the next scheduled meeting. Prompt reporting of the event shall be by telephone and confirmed by written correspondence within 24 hours. A written report is to be submitted within 14 days.

8.4.4 Other Reportable Occurrences. Other events that will be considered reportable events are listed in this section. A return to normal operation or curtailed operation until authorized by management will occur. Appropriate reports shall be submitted to license authorities. (Note: Where components or systems are provided in addition to those required by the technical specifications, the failure of components or systems is not considered reportable provided that the minimum number of components or systems specified or required perform their intended reactor safety function.)

(a) Operation with actual safety-system settings for required systems less conservative than the limiting safety system settings specified in the technical specifications.
(b) Operation in violation of limiting conditions for operation established in the technical specifications unless prompt remedial action is taken.
(c) A reactor safety system component malfunction which renders or could render the reactor safety system incapable of performing its intended safety function unless the malfunction or condition is discovered during maintenance tests or periods of reactor shutdowns.
(d) Abnormal and significant degradation in reactor fuel, or cladding, or both, coolant boundary, or confinement boundary (excluding minor leaks) where applicable which could result in exceeding prescribed radiation exposure limits of personnel or environment, or both.
(e) An observed inadequacy in the implementation of administrative or procedural controls such that the inadequacy causes or could have caused the existence or development of an unsafe condition with regard to reactor operations.

8.4.5 Other Reports. A written report within 30 days to the chartering or licensing authorities of:

(a) Permanent changes in the facility organization involving Director or Supervisor.
(b) Significant changes in the transient or accident analysis as described in the Safety Analysis Report.

8.5 RECORDS

Records of the following activities shall be maintained and retained for the periods specified below [4]. The records may be in the form of logs, data sheets, or other suitable forms. The required information may be contained in single or multiple records, or a combination thereof.

8.5.1 Records to be Retained for the Lifetime of the Reactor Facility: (Note: Applicable annual reports, if they contain all of the required information, may be used as records in this section.)

(a) Gaseous and liquid radioactive effluents released to the environs.
(b) Offsite environmental monitoring surveys required by technical specifications.
(c) Radiation exposure for all personnel monitored.
(d) Updated drawings of the reactor facility.

8.5.2 Records to be Retained for a Period of at Least Five Years or for the Life of the Component Involved Whichever is Shorter.

(a) Normal reactor facility operation (supporting documents such as checklists, log sheets, etc. shall be maintained for a period of at least one year).
(b) Principal maintenance operations.
(c) Reportable occurrences.
(d) Surveillance activities required by technical specifications.
(e) Reactor facility radiation and contamination surveys where required by applicable regulations.
(f) Experiments performed with the reactor.
(g) Fuel inventories, receipts, and shipments.
(h) Approved changes in operating procedures.
(i) Records of meeting and audit reports of the review and audit group.

8.5.3 Records to be Retained for at Least One Training Cycle. Retraining and requalifications of certified operations personnel. Records of the most recent complete cycle shall be maintained at all times the individual is employed.

Chapter 8 References

1. "Standard for Administrative Controls" ANSI/ANS - 15.18 1979.

2. "Selection and Training of Personnel for Research Reactors", ANSI/ANS - 15.4 - 1970 (N380).

3 "Review of Experiments for Research Reactors", ANSI/ANS - 15.6 - 1974 (N401).

4. "Records and Reports for Research Reactors", ANSI/ANS - 15.3 - 1974 (N399).

Chapter 9

QUALITY ASSURANCE PROGRAM

Objectives of quality assurance (QA) may be divided into two major goals. First is the goal of safe operation of equipment and activities to prevent or mitigate an impact on public health and safety. Second is the reliable operation of equipment and activities associated with education and research functions of the University. The risk or potential release of radioactive materials is the primary impact on public health and safety, and may be divided into direct risks and indirect risks. Direct risks are activities such as waste disposal, fuel transport and decommissioning that introduce radioactive materials into the public domain. Indirect risks are accident conditions created by normal or abnormal operating conditions that generate the potential or actual release of radioactive materials from the controlled areas of a facility.

9.1 INTRODUCTION

Characteristics of uranium loaded zirconium hydride fuel used in the TRIGA reactor provide substantial benefits to safe reactor operation. Many accident situations are simulated by normal operation of the fuel in either pulse mode or steady state mode. Other features such as fission product retention, stainless steel cladding design, facility engineered features, and periodic schedule of operation combine with routine operation procedures to decrease the consequences of failure of any reactor components. The limited scope of application of formal quality assurance criteria is due to the fact that most parts and procedures associated with operation of the TRIGA type reactor are not relevant to public health and safety.

Safety-related identifications for quality assurance are determined from license specifications. The specifications for safe operation include design features, safety limits and limiting conditions for operation. The application of quality assurance shall be considered for those structures, systems or components in the technical specifications that are either design features or required as limiting conditions for operation. Such systems should include the control and safety system, radiation monitoring system and other support systems. Although the quality assurance program is not applied to routine reactor operations and surveillance activities, the program shall be implemented for non-routine activities determined to be

safety related in nature or effecting safety related equipment. Such activities shall include design, construction, testing, modification and maintenance of safety related items.

Two additional conditions remain, however, that are important to the application of at least portions of the quality assurance program. One is the safety to operation personnel and experimenters and the other is continuity of the operations programs. Each of these conditions must be examined objectively relative to operation procedures and program expectations. In general, the application of good industry quality assurance practices is sufficient to meet operational program goals.

The quality assurance program shall be commensurate with the TRIGA type reactor, The University of Texas administrative programs and the goals of quality assurance. This document provides requirements for establishing, managing, conducting and evaluating the QA Program. The QA Program applied to items or activities determined to be safety-related follows the guidelines of Nuclear Regulatory Guide 5.2 (77/05) [1,2].

9.1.1 Purpose. Quality assurance of certain activities associated with the University of Texas TRIGA reactor facility is important for the safe and efficient completion of tasks that are identified as safety-related. This document outlines the general elements of quality assurance applied to safety-related structures, systems or components, and activities. Requirements are documented for establishing, managing, conducting, and evaluating the QA Program. Although aspects of the QA Program may be routinely applied to many facility activities, the formal implementation of the program is limited to specific items or activities related to public health and safety.

9.1.2 Responsibility. The University of Texas at Austin as owner and operator of the TRIGA reactor facility shall be responsible for a quality assurance program. The owner-operator shall establish and implement a program consistent with the goals of quality assurance for safety-related activities, structures, systems and components. Identification of safety-related items shall be the responsibility of the owner-operator and will include a description of the item and the applicable elements of the quality assurance program. Special quality provisions, delegated functions of the program, and unresolved quality assurance problems shall also be identified by the owner-operator. Table 9-1 lists the responsibilities and key personnel participating in the University TRIGA QA Program.

Table 9.1
RESPONSIBILITIES AND KEY PERSONNEL

Responsibilities	Key University Personnel
1. Establish program Implement program Safety-related identification	Director or Supervisor of TRIGA facility
2. Unresolved issues	President or Vice President for Academic Affairs and Research
3. Delegated functions	Faculty and staff
4. Specialized functions	Specified personnel

9.1.3 Organization. The organization applied to quality assurance activities shall be part of the normal university administrative structure. The facility Supervisor shall develop and implement the quality assurance program and identify safety related items. Unresolved issues of quality assurance shall be reported to the Director of the facility and the appropriate administrative vice president of the university. Execution of specific elements of the program may be delegated to persons in the University organization or other organizations as appropriate. University persons shall include committees, faculty, researchers or staff as required for specific program applications. Non-university organizations or persons shall supplement University personnel when specialized qualifications are necessary for specific quality assurance tasks. The University organization applied to reactor safety and quality assurance is the academic administration represented by Figure 9-1.

9.1.4 Documentation. All activities affecting safety-related items subject to the quality assurance program shall be identified and documented formally. The format of Table 9-2 shall be used to identify applicable elements of the Quality Assurance Program and identify documents, procedures, reviews, inspections, tests, or other quality assurance features that are to be applied to a safety-related activity.

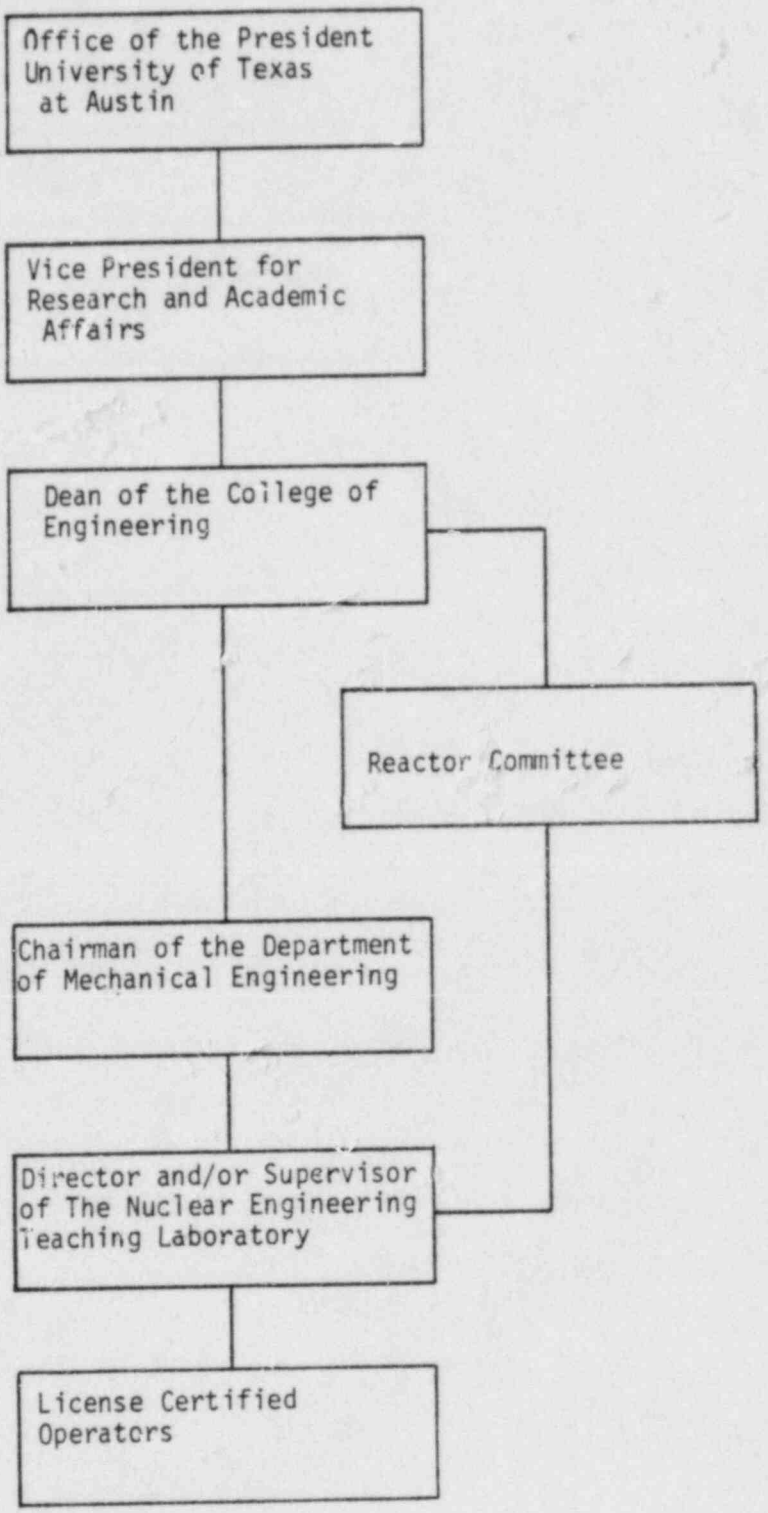

ACADEMIC ORGANIZATION
Figure 9-1

Table 9.2
FORMAT FOR SAFETY RELATED QA CHECKS

Each safety-related activity structure, system, or component will be given a letter symbol, such as A, B, C, and be appended with the following designations (for example, A1.0):

1.0 Title
Identification and description of safety-related item
1.1 Participation - supplemental organization and functions
1.2 Documents - applicable procedures or special measures

2.1 Design Control

2.1.1 Codes, standards and regulations
2.1.2 Method of verification
2.1.3 Modifications proposed

2.2 Procurement Control

2.2.1 Codes, standards and regulations
2.2.2 Quality assurance specifications
2.2.3 Proposed changes enacted
2.2.4 Procurement conformance method

2.3 Document Control

2.4 Material Control

2.4.1 Special procedures required
2.4.2 Equipment required
2.4.3 Personnel qualification

2.5 Process Control

2.5.1 Special procedures
2.5.2 Special equipment
2.5.3 Personnel qualifications

3.1 Inspection Program Description
3.2 Test Program Description
3.3 Measurement Equipment
3.4 Nonconformance Item and Disposition
3.5 Corrective Actions Instituted

4.0 Records List

9.2 QUALITY ASSURANCE CONTROLS

9.2.1 Design Controls. Design controls shall consist of design specifications, references to applicable codes, standards and regulations, design verifications and document approval. Applicable codes, standards, regulations or other quality requirements will be identified and requirements incorporated into the design documents. Design document approvals should be part of the design document. Design approval will be by a person, other than the design originator, that is knowledgeable of the design and quality requirements or knowledgeable of the designers qualifications.

Modifications of safety-related documents shall be subject to the same provisions as the original document. Approval of the design modification will be included with the design document and the modification identified.

Verification of design adequacy shall be provided by either design reviews, alternate calculation, test program or other method, determined to be appropriate. Verifications of the design should check characteristics such as compatibility of materials; suitability of application of inspection, maintenance and repair; proper interfacing of sub-systems, and proper acceptance criteria. Method of verification will be identified and documented by approval of the design document.

9.2.2 Procurement Controls. Procurement controls shall consist of procurement specifications, references to applicable codes, standards and regulations, procurement acceptance and document approval. Applicable codes, standards, regulations or other quality requirements will be identified and references incorporated into the procurement documents. Procurement document approvals shall be part of the procurement document. Procurement approval will be by a person, other than procurement originator, that is knowledgeable of the procurement and quality requirements or knowledgeable of the procurers qualifications.

Changes to safety-related procurement documents shall be subject to the same provisions as the original document. Approval of procurement changes will be included with the procurement document and the change identified.

Acceptance of procured items or services shall consist of evidence provided by the contractor, evaluation of the procurement source, inspection at the source or inspection upon receipt. Acceptance of the procurement should require measures such as quality assurance by contractor, inspection and test functions, or controls on materials processes and nonconformances. The methods of acceptance will be

identified and documented by approval of the procurement document.

9.2.3 Document Control. Document control consists of monitoring the development, revision, release and use of documents, drawings or specifications affecting safety-related activities. Document control shall include assurance that safety-related documents are identified as such, and are completed and maintained properly. The laboratory Supervisor shall provide control of safety-related documents that are specified according to the format of Table 9-2.

9.2.4 Material Control. Procedures shall be written to establish material control when special measures are necessary to assure material quality of safety-related items. Controls shall be applied to activities such as identification handling, storage, shipping, cleaning and preservation Procedures shall specify equipment and personnel required to accomplish the specified material control. Applicable codes, standards, specifications or personnel qualifications shall be documented.

9.2.5 Process Control. Procedures shall be written to establish process control when special measures are necessary to assure process quality of safety-related items. Controls shall be applied to activities such as crimping, soldering, welding, painting, cleaning and heat treating. Procedures shall specify qualifications of equipment and personnel required to perform the appropriate process control. Applicable codes, standards, specifications or personnel qualifications shall be documented.

9.3 INSPECTION AND CORRECTIVE ACTIONS

9.3.1 Inspection Program. An inspection program shall be established for safety related items or activities. The inspection program shall apply to construction, procurements, experiment equipment fabrication, and modifications that effect safety-related structures, systems, or components. Maintenance persons delegated to perform inspections shall not be the same person involved in the safety-related activity but may be from the same organization.

The inspection program will consist of written procedures that will include, as appropriate, procedures specifying characteristics to be inspected, acceptance criteria and inspection hold points.

Procedures should provide for identification of inspected, tested and non-conforming items. Procedures

shall also be written as necessary for monitoring activities.

9.3.2 Test Program. A test program shall be established for safety-related items or activities. The test program shall apply to prototype qualifications, installation proofs and functional tests. Testing shall be performed in accordance with acceptance criteria derived from design or procurement documents.

The test program will consist of written procedures that will include, as appropriate, procedures that specify acceptance criteria, monitoring requirements, equipment required, personnel qualifications, environmental conditions, data acquisition and documentation of results.

9.3.3 Measuring and Test Equipment. Measurement tools, guages, instruments, and other measuring or test devices that measure critical parameters of safety-related items shall be identified. Provisions for identified measuring and test devices shall include availability, adjustment, calibration and accuracy as required for each application. Test equipment will be identified.

9.3.4 Non-Conforming Material and Parts. Non-conforming materials and parts associated with safety-related structures, systems or components shall be identified. The disposition such as acceptance, repair, rework or rejection of parts from safety-related functions will be determined by the person responsible for document control. Repair or reworked parts will be removed or labeled until accepted. Rejected parts will be removed and labeled. Significant non-conformances and the disposition will be documented.

9.3.5 Corrective Action. Documentation of specified quality control or assurance documents shall provide evidence of quality of safety-related items. Significant deviations from acceptable quality, repeated quality problems or unresolved quality issues shall be noted and reported in writing to administrative management personnel. It should be recognized that a determination of a quality problem may be subjective and should include evaluation of the documented quality requirements relative to the impact on the safety-related nature of the item.

9.4 RECORDS AND AUDITS

9.4.1 Quality Assurance Records. Records that document quality of safety-related items or activities are identified according to Table 9-2. The records identified consist of inspection and test results, quality assurance reviews, quality assurance procedures and engineering analysis in

support of design modifications or changes. The records shall be retained with as-built drawings, manuals and other records of important facility and system information. The retention period is to be the life of the facility or system for most, if not all, safety-related items. The retention period is indicative of the expectation that items which affect safety related to a TRIGA reactor are integrally related to the reactor, instrumentation and facility design and should persist for the system or facility life.

9.4.2 Audits. An audit shall be conducted to examine the records and function of the quality assurance program. Audits will occur within two years of the QA Program activities by designated persons that were not directly responsible for the audited functions. Written procedures, Table 9-3, for the audit will be considered part of the Quality Assurance Program. A report of the audit results, actions to resolve deficiencies and evaluation of the program will be made to a facility operations committee and university administrative management, and maintained with other Quality Assurance Program documents.

Table 9-3

QUALITY ASSURANCE PROGRAM
AUDIT PROCEDURES

1.	Designate a person or persons responsible to perform the program audit.
2.	Determine the date of the previous audit.
3.	Review the Quality Assurance Program document.
4.	Examine the list of safety-related items.
5.	Note additions to the safety-related items.
6.	Identify records applicable to additional items.
7.	Determine the location of all indicated records.
8.	Review records for abnormalities and completeness.
9.	Prepare statement that evaluates functions of Quality Assurance Program.
10.	Report findings of audit and program functions to operations committee and management.

Chapter 9 References

1. "Quality Assurance Requirements for Research Reactors", Nuclear Regulatory Guide 5.2 (77/05)

2. "Quality Assurance Program Requirements for Research Reactors", ANSI/ANS - 15.8 - 1976 (N402)

Chapter 10

RADIOLOGICAL PROTECTION PROGRAM

Protection of personnel and the general public against hazards of radioactivity and fire is established through the safety programs of the University Safety Office. Implementation of safety programs at the reactor facility supplements the university programs so that appropriate safety measures are established for the special characteristics of the facility [1,2].

10.1 RADIOLOGICAL MANAGEMENT ORGANIZATION

10.1.1 Management and Policy. Radiological management policy shall include a commitment to keep occupational exposures as low as is reasonably achievable to facility personnel and the general public. Other elements of the radiological management will include:

a. instruction of personnel in awareness of the low as reasonably achievable commitment,
b. identification of radiation protection personnel and their responsibilities,
c. authority of personnel to communicate with management and modify or suspend activities for reasons of radiation protection,
d. assurance of sufficient and appropriate training of personnel in radiological safety,
e. periodic evaluations of the program to determine possibilities for lower radiation exposures.

Suggestions and recommendations for modifications to operating and maintenance procedures and to reactor equipment and facilities shall be considered by management to reduce exposure to radiation. Implementation of modifications will occur if substantial exposure reductions are possible at acceptable cost.

10.1.2 Responsibilities. Radiation protection at the reactor facility is the responsibility of the Reactor Supervisor or a designated senior operator in charge of operation activities. Responsibility shall include the authority to act on questions of radiation protection, the acquisition of appropriate training for radiation protection and the reporting to management of problems associated with radiation protection.

10.1.3 Organizational Access. The person responsible for radiation protection at the reactor facility will have access to other individuals or groups responsible for radiological safety at the University. Contact with the Radiation Safety officer will occur on an as needed basis and contac. with the Reactor Committee will occur on a periodic basis.

10.1.4 Equipment and Supplies. Equipment and supplies maintained for radiological safety management shall include:

a.) fixed area radiation monitors,
b.) air particulate monitor,
c.) gaseous effluent monitor,
d.) portable radiation monitors,
e.) detectors for contamination measurement,
f.) maintenance and calibration capability for equipment,
g.) laboratory counting and analysis equipment,
h.) supplies for storage of contaminated equipment,
i.) provisions for radioactive waste disposal,
j.) decontamination facilities,
k.) protective clothing,
l.) respiratory protection equipment,
m.) and emergency response equipment.

10.1.5 Training and Safety. Each person in the restricted area of the reactor facility shall have sufficient radiological safety training for the purpose of access to the area or be escorted by a person with the appropriate training. Training will be appropriate to the activities of persons admitted to the area and will range from simple instructions of emergency alarms and evacuation procedures to more complex implementation of the area emergency plan.

Training for facility personnel shall be specified by the Reactor Supervisor and shall provide sufficient training in radiation safety policies and procedures, and in the use of radiation safety equipment located in the facility to control exposures during normal, abnormal and emergency situations. Training will consist of:

a.) radiological safety policies, plans and procedures,
b.) radiation hazards and health risks,
c.) use of protective clothing and equipment,
d.) use of portable radiation monitoring equipment,
e.) and other documents such as the emergency plan and federal or state notices to workers.

An evaluation shall occur every two years to determine whether additional training of personnel is required and that the radiological safety program is functioning adequately.

Safety programs, with the exception of reactor operations, are operated as a function of the business administration of the University and include a radiation safety organization as presented in Figure 10-1.

10.2 RADIOACTIVE MATERIALS CONTROL

Physical control of radioactive materials shall be provided as an essential part of the radiological safety program. Control shall include identification of items or storage in identified locations. Controls such as shielding, isolation, containment and ventilation will be provided, as necessary, to control radiation exposure to the inventory of radioactive materials.

10.2.1 Reactor Fuel. Irradiated reactor fuel shall be maintained in the reactor core, reactor pool storage racks or reactor bay storage pits. Fuel elements will be removed from these facilities only for transport, measurement or experimentation. An area of the reactor facility will be designated for the storage of a few single fuel elements of unirradiated fuel before the fuel is moved to other storage areas or irradiated in the reactor.

10.2.2 Reactor Components. Each reactor component removed from the reactor pool shall be measured for activation levels and removable contamination. All components remaining in the pool shall be assumed to be radioactive. Components removed from the pool will be cleaned or covered as necessary to control radioactive contamination. Components that contain radioactive material will be labeled and stored in an area designated for such components.

10.2.3 Experiment Facilities. Experiment facilities shall consist of all tubes or penetrations into the reactor core or reflector that provide access to the reactor neutron flux for an experiment application and shall include facilities in which materials are exposed to beams originating from the reactor core. The cobalt-60 irradiator shall also be considered an experiment facility. Removal of experiment facilities from the pool or the beams originating from the reactor shall be subject to the same controls as those for reactor components.

10.2.4 Activated Samples. Materials that are inserted into reactor experiment facilities or reactor beams shall be controlled as radioactive materials until disposed as radioactive waste, transferred to an authorized user or decayed to releasable levels for non-radioactive materials.

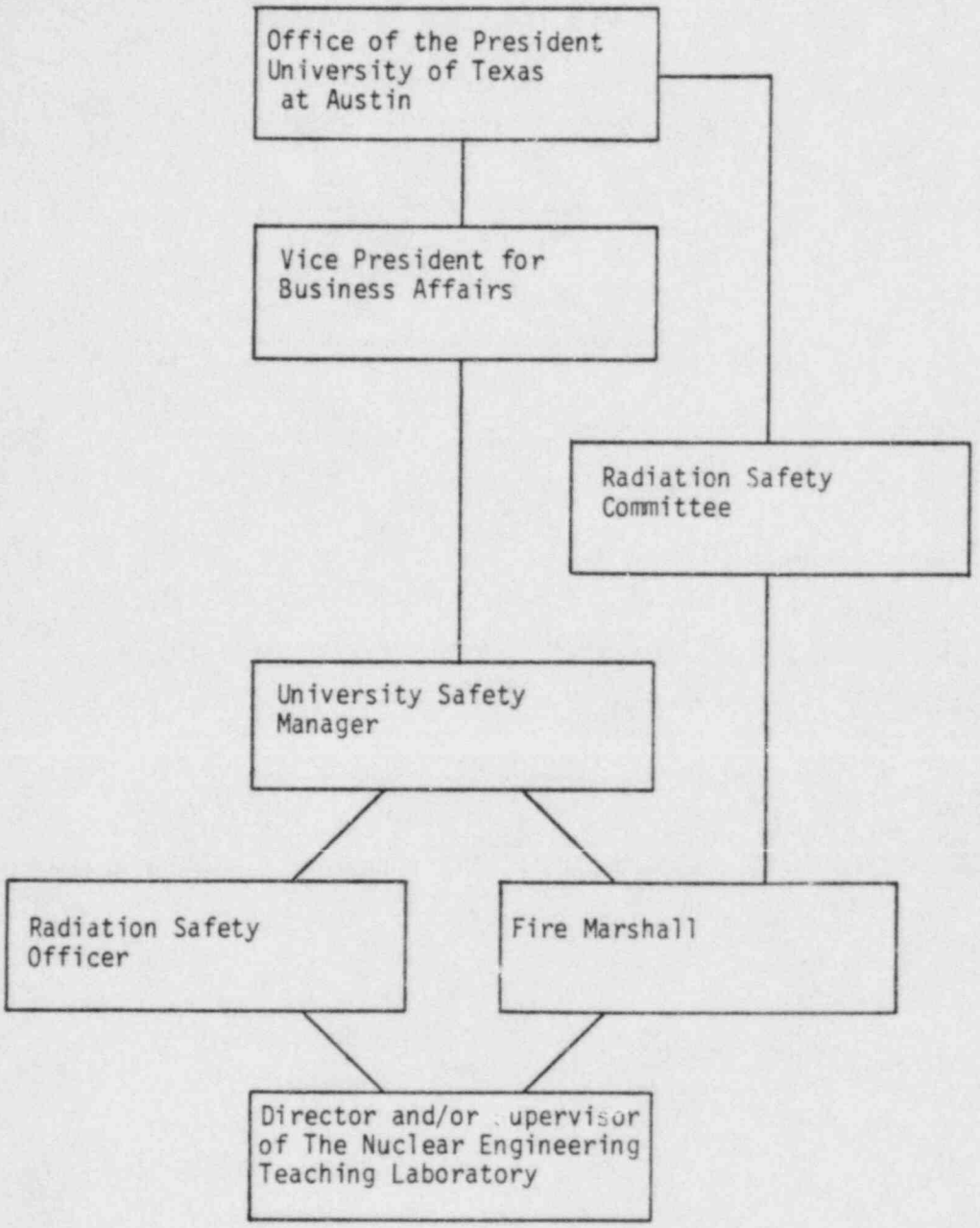

BUSINESS ADMINISTRATION
Figure 10-1

Samples exposed in the cobalt-60 irradiator will not be considered activated as radioactive materials. Specific locations that may depend on the samples analytic status shall be designated for the storage of activated samples. Locations shall be designated and labeled for storage of samples and sample encapsulations, before and after analysis. Locations should be designated for storage of sample or encapsulation materials that are decaying and that are to be

a.) analyzed,
b.) disposed,
c.) released to an authorized user,
d.) released as non-radioactive material,
e.) and retrieved for subsequent use.

10.2.5 Radioactive Waste. Canisters shall be available and labeled for radioactive waste at locations where radioactive contamination from sample processing or other activities with contaminated materials occur. A location shall be designated for storage of solid wastes that are to be released for disposal. Liquid wastes shall be maintained in a designated storage location until release criteria are determined such as decay, dilution or processing. Specific sinks and drains in the facility that are designated for radioactive materials shall be identified. Gaseous wastes are to be vented through low volume facility hoods according to allowable release criteria. Appropriate monitoring will be applied as required.

10.2.6 Other Materials. Other materials that are to be identified and controlled by identification and location are encapsulated isotopic radiation sources, radiochemical source materials and process equipment or tools possibly contaminated with radioactive materials. Activity levels of encapsulated and radiochemical sources are expected to vary widely as will the handling and storage precautions. Activity levels associated with process equipment or tools shall be identified so that appropriate handling and storage precautions can be instituted.

10.3 RADIATION MONITORING

Radiation monitoring shall consist of fixed, portable, or sampling type systems. Monitoring systems will be applied to measurement of radiation areas and high radiation areas around the reactor facility, significant contamination within and adjacent to the reactor facility and radioactive materials and their concentrations in effluents. Monitoring shall be considered for routine operations, abnormal conditions and emergency situations.

10.3.1 Minimum Procedures.

a.) Zone identification, access control and protective equipment shall be designated. Zone identification for radioactive materials and radiation areas are designated as specified by 10 CFR, part 20 (Standards for Protection Against Radiation). Access control for zones shall be to control radiation exposures and physical security of the reactor facility and its material as specified by 10 CFR parts 19 and 73, (Notices, Instructions, and Reports to Workers; Inspections and Physical Protection of Plants and Materials). Protective equipment for routine abnormal and emergency conditions shall include at least gloves, shoe covers, coveralls, half mask air purifying respirators, tape, plastic bags, and absorbent paper.

b.) Continuous monitoring or control of radiation fields in the restricted area around the reactor shall occur whenever levels greater than 100 mrem/hr are produced in accessible areas. The radiation levels may be caused by normal operation of the reactor or an experiment, deviations from normal operation, or easily changed shield configurations. Periodic measurement of accessible areas should occur in locations with significant radiation levels that do not require continuous monitoring. Personnel shall be informed of high radiation levels and care taken to prevent inadvertent increases in the levels. Continuous monitoring may be replaced by periodic monitoring for temporary conditions that do not violate applicable regulations or license constraints.

c.) Contamination areas or areas that are routinely subject to contamination shall be marked clearly and control points established to monitor for contamination of personnel or equipment that leaves the designated area. Measurements shall provide action levels for removable activities of 200 disintegrations per minute. Periodic monitoring of areas in which contamination is probable shall be of adequate frequency to reveal significant changes in contamination levels. Decontamination of personnel, equipment, and surfaces shall be appropriate to requirements for control of radiation exposure and control of radioactive material containment.

d.) Airborne radioactive monitoring shall consist of continuous sampling of air particulate activity in the reactor area. Warning levels and action levels will be determined relative to allowable maximum permissible concentrations. Measurements should be sensitive to one maximum permissible concentration change in one hour. Monitoring will occur during reactor operation or activities involving fuel, core, or experiment facilities and will provide measurements for routine, abnormal, and emergency conditions. Additional airborne monitoring equipment should

be provided for special experiment needs or locations remote to the reactor area particulate monitor.

e.) Effluent monitoring shall be provided for the discharge of the radioactive noble gas argon-41. Monitoring will consist of either the use of integrating dosimeters at a location of interest or sampling of a point in the release path. Measurements shall determine that the dose at a location of interest is either less than ten mrem per year above natural background or two percent of the allowable maximum permissible concentration for the year. Liquid effluents shall be monitored before release by sampling of gross beta-gamma activity. Specific isotopes should be identified and dilutions calculated such that released concentrations averaged over one year do not exceed 1% of the allowable maximum permissible concentrations. Other gaseous or radioactive effluents are to be examined on a case to case basis.

f.) Personnel dosimetry shall be required for access to reactor areas and some other facility activities. Monitoring devices will typically be film badges with pocket dosimeters and thermoluminescent detectors for supplemental measurements. Other personnel monitoring such as bioassays or whole body counting will be applied as determined by the activity and conditions of radiation exposure situations. Personnel shall use supplemental dosimetry during activities that deviate substantially from routine operations with supplemental dosimetry also provided for persons visiting areas with potential radiation exposures.

10.3.2 Monitoring Techniques. Implementation of radiation monitoring to maintain the goal of as low as reasonably achievable should consist of:

a.) preoperation planning,
b.) operations techniques,
c.) and post operation analysis.

10.3.3 Management Surveillance. A review by management of radiation exposures related to operations that cause significant radiations exposures compared to routine operations will be performed. The review should be applied to determine whether facility modifications or procedures should be implemented to maintain radiation exposures as low as reasonably achievable.

10.3.4 Frequency and Accuracy. Monitoring frequency and accuracy of activities will be determined by several factors related to personnel access, requirements, probability and consequences of equipment failure, contamination potential, periodicity of modifications and adequacy of current monitoring. Accepted standards for measurement sensitivity and accuracy should be appropriate to maintain radiation

exposures as low as reasonably achievable. Frequency and accuracy specifications should be specified by procedures or other documents when appropriate.

10.4 INSTRUMENTATION

Instrumentation for the evaluation of radiation exposures from routine, abnormal and emergency situations shall consist of fixed area monitors, portable survey monitors and appropriate sampling methods. The minimum instrumentation available during reactor operation shall consist of fixed area gamma dose rate monitors, continuous air particulate monitor, portable thin window GM tube survey meter, portable neutron sensitive counter and pocket dosimeters with charger. Other detection equipment that should be available includes alpha-beta proportional counter, multichannel gamma pulse height analyzer, thermoluminescent detector with reader, alpha scintillation detector, high and low range beta-gamma dose rate meters and GM tube friskers.

10.4.1 Fixed Area Monitors. Fixed area gamma monitors shall have remote readouts with audible and visual alarms at the reactor control console. Local readouts should be provided in areas with significant radiation levels and routine personnel access.

10.4.2 Airborne Radioactivity Monitors. A continuous air particulate monitor with audible and visual alarms shall be functional in the reactor vicinity during reactor operations. A gas monitor system for the noble gas effluent, argon-41, shall also be operable during operation or sufficient data available to demonstrate a calculated release quantity.

10.4.3 Laboratory Instrumentation. Portable survey monitors for alpha, beta, gamma or neutron radiation shall be maintained for area surveys of laboratory and experiment areas. Supplemental measurements should be available with alpha beta proportional counters or gamma ray pulse height analyzers.

10.4.4 Liquid Effluents. Liquid effluents shall be monitored by sampling methods to determine gross alpha-beta activity. Gamma spectral analysis should be applied for identification of isotope mixtures that require substantial dilution for disposal. Liquid effluents shall be released in batches after storage for decay and dilution determinations. Reactor coolant may be monitored for radioactivity in the coolant or purification loops as a supplemental indicator of water activity.

10.4.5 Range and Spectral Response. Instruments shall be available to measure the various types of radiation and the presence of low and high levels of radiation. Several types of detectors should be available for measurement determinations.

10.4.6 Calibrations. Calibration methods, accuracy, frequency and functional checks shall be established for radiation monitors. Two classes of monitor calibration will be applied. One class of calibration will consist of monitors applied to routine facility operation and surveys. Maintenance, calibration and functional checks will be subject to reactor operation specifications. The second class of instruments should have functional checks at annual intervals but may be calibrated infrequently or at the time of application.

10.5 RECORDS

Records are specified for maintenance of radiological data that relate to reactor operation. These records shall include:

a.) Personnel dosimetry including bioassays or other special measurements made,
b.) Radiological control surveys required by facility specifications,
c.) Gaseous and liquid radioactive effluents released to the environment,
d.) Radiation survey records,
e.) Instrument calibration records,
f.) Radioactive material receipt and transfer records,
g.) Solid radioactive waste disposal records,
h.) Leak tests of sealed sources,
i.) Data on radiological incidents.

10.6 EMERGENCY PLAN AND RADIOLOGICAL PROGRAM REVIEW

An emergency plan shall be established, maintained, and implemented by the Reactor Supervisor. The plan will exist as a separate document of the radiological safety program. A review of the radiological safety program and emergency plan should be integrally related. Some partial assessment of the radiological safety program should occur each year such that a complete assessment occurs during a two year period. The two year period shall also apply to the emergency plan.

Chapter 10 References

1. "Radiological Control at Research Reactor Facilities", ANSI/ANS - 15.11 1977 (N628)

2. "Design Objectives for and Monitoring of Systems Controlling Research Reactor Effluents", ANSI/ANS - 15.12 1977 (N647)

3. "Nuclear Regulatory Commission", Chapter 10 U.S. Code of Federal Regulations

Chapter 11

FIRE PROTECTION

The goal of fire protection shall be to provide reasonable assurance that safety-related systems perform as intended and that other defined loss criteria are met [1,2]. For the purpose of fire protection, loss criteria should include protection of safety related systems, prevention of radioactive releases, personnel protection, minimization of property damage and maintenance of operation continuity. Three components shall be applied to the fire protection objective. The three components are passive and active fire protection, and fire prevention.

11.1 FIRE PROTECTION COMPONENTS

Each of the three components of the fire protection program shall be applied to the design, operation and modification of the reactor facility and its components.

11.1.1 Passive Fire Protection Elements. Passive fire protection should provide a potential for fire safety that does not require physical operation or personal response to achieve the intended function. Passive elements to be considered should include inherent design features, building physical layout, safety-related systems layout, fire barriers and construction or component materials. Other passive elements that may be considered for special conditions will be frangible walls for overpressure relief, curbs for containment of hazardous liquids, and drainage for control of fire protection runoff water. Penetrations in fire barriers shall have fire resistant ratings compatible with the purpose of the fire barrier.

Safety-related systems shall incorporate passive fire protection features that provide protection necessary for the design functions of the system. Separation of redundant system components, if applicable, and protection of distribution systems should be examined. Materials of noncombustible or limited combustion properties should be used when practical. Materials such as sealing materials, electrical insulation, structural finishes, adhesives, and linings should be selected so as to minimize fire hazards. Material selection may consider characteristics such as calorie content, ignition properties, flame retardation and rate of heat release.

11.1.2 Active Fire Protection Elements. Active fire protection elements differ from passive elements in that active features require automatic operation, manual response, or personnel action for the intended function. Active elements to be considered should be automatic fire detection, automatic fire suppression, fire information transmission, manual fire suppression and other manual fire control or loss control measures. Automatic protection systems considered will include smoke detection, thermal detection, sprinkler action, spray or deluge and special protection such as gaseous extinguisher systems. Fire doors, dampers, ventilation control, and the inspection, maintenance and testing of equipment to assure reliability and proper operation of the equipment are also considered elements of active fire protection.

Manual protection shall consist of manual fire fighting actions and the systems necessary to support those actions such as extinguishers, pumps, valves, hoses, and the inspection, maintenance and testing of equipment to assure reliability and proper operation. Other manual actions that are elements of active fire protection shall be utility control, personnel control and evacuation. Preplanning shall be an additional element applied to active protection by training facility personnel and emergency personnel for the appropriate actions in response of fire and the possible hazards involved.

11.1.3 Fire Prevention Elements. Fire prevention shall be implemented to prevent the occurence of a fire or limit the probable severity of a fire that might occur. Elements of fire prevention shall include control of ignition sources, availability of combustible materials and locations of combustible materials. Controls should be applied as necessary on such activities as cutting, welding, other flame operations, electrical equipment and smoking.

11.2 FIRE PROTECTION CONTROLS

Management of the Nuclear Engineering Teaching Laboratory shall be knowledgeable of fire protection controls. The controls will consist of actions of equipment, actions of laboratory staff and interactions with trained University personnel.

11.2.1 Facility Fire Protection Elements. Fire protection is recognized as an important element of the safe operation of the TRIGA reactor facility. Commitment by the University to fire protection is provided by the functions of the University Safety Office.

The organization for fire protection consists of the University Fire Marshall, a member of the University Safety

Office and the Reactor Supervisor, a member of the Nuclear Engineering Teaching Laboratory. Responsibilities of the Fire Marshall are the maintenance of fire protection equipment and inspections for fire prevention. Responsibilities of the Reactor Supervisor are knowledge of potential hazards and implementation of fire protection recommendations.

Although fire protection is provided for the general safety of personnel and preservation of property, special considerations shall be provided for systems designated as safety related. Primarily special considerations are applied to protection of the reactor and shield structure, and fuel storage wells. Design features of these facility components provide a major factor of the fire protection. Fire protection for the instrumentation and control system, and radiation measurement systems are important for the initial reactor shutdown and the availability in emergency conditions. Fire protection of the reactor bay area boundary is of importance to the extent of limiting either internal conditions that would cause the release of hazardous materials or external conditions that would threaten the release of hazardous materials.

Loss criteria for decisions on fire protection at the reactor facility shall consist of preventing any injury to personnel, and minimizing the potential or actual release of radioactivity to the environment. No injury or exposure to the public should occur from the adverse effects of a fire.

Laboratory personnel, particularly certified operators, shall be instructed to observe continually conditions that might represent a risk to fire protection. Appropriate assessment of the risk should be provided by the Reactor Supervisor and will include consultation with the Fire Marshall when appropriate.

Passive fire protection elements effectively protect the reactor core, fuel elements and storage wells. Inherent design of the reactor bay and reactor tank structure, construction materials, building layout and fire barriers are all applied to the protection. Instrumentation and control systems and radiation measurement systems primarily are protected by fire detection and alarm information. These systems are important to safety only for the initial shutdown and removal of personnel. Protection of other equipment and the reactor bay boundary is accomplished in part by building design, but primarily by detection and alarm.

11.2.2 Facility Fire Protection Control. The Reactor Supervisor and the Reactor Committee shall consider the impact of major facility modifications and experiment programs on facility fire protection. The University Fire

Marshall will recommend fire protection requirements and provide for inspection and test of fire protection components.

Activities such as welding, cutting, open flames, electrical loads, or other equipment that effect fire protection shall be examined on a case by case basis by the Reactor Supervisor.

Laboratory staff shall be instructed in fire response actions and notification of response personnel. A program to familiarize response personnel with laboratory equipment, material hazards and physical layout is considered the major element for response of emergency response organizations.

11.3 FIRE SAFETY ASSURANCE

At intervals of two years the fire protection program should be examined actively by the Reactor Supervisor, University Fire Marshall and Reactor Committee. Evaluations of post inspections, tests or incidents shall be incorporated into an assessment of the fire protection evaluation. Recommendations if any should be identified and appropriate actions taken.

Chapter 11 References

1. "Standard for Fire Protection Program Criteria for Research Reactors", ANSI/ANS - 15.17 (1981).

2. Nuclear Research Reactors 1983, National Fire Protection Association, Inc., NFPA 802.

Chapter 12

TRAINING AND CERTIFICATION OF OPERATORS

This section describes the program applied to requalification and qualification of persons that are to be certified as operators by the licensing authorities [1,2]. Some features of the program are indicative of the educational nature of the University institution and the limited size of the research reactor staff.

12.1 TRAINING SUBJECTS

Instruction will be given for subject matter at the level representative of either an operator or senior operator in the following subject areas:

(a) Nuclear Theory and Principle of Operation,
(b) Design and Operating Characteristics,
(c) Facility Instrumentation and Control Systems,
(d) Facility Safety Systems and Engineered Safety Features,
(e) Normal, Abnormal, and Emergency Procedures,
(f) Radiation Control and Safety,
(g) Technical Specifications and Basis.

Instruction shall occur over a two year period and will consist of sessions scheduled for lectures, discussion or self-study. The program goal will be to cover one topic of the previously outlined subjects each calendar quarter. At least four subjects shall be covered each alternate year which allows for the repeat of one subject in a subsequent year.

Lectures may consist of facility class presentations that are scheduled or designated classes of organized university courses. Discussion or self-study sessions may replace formal lectures when three or fewer persons are participating in the qualification or requalification program.

12.2 TRAINING EXPERIENCE

Each operator or senior operator shall perform ten reactor startups or other significant reactivity manipulations of the reactor during the term prior to a new license or renewal license request. Experience for a new license shall include sufficient additional operating

experience to provide the trainee with a proficient skill and knowledge of the reactor operation for the type of license to be requested. The experience requirement for a license renewal of a senior operator shall allow directly supervised activities to substitute for direct performance.

An annual review by each operator of abnormal and emergency procedures shall occur. Changes in design procedures and licenses or technical specifications shall also be reviewed in a timely manner.

12.3 EVALUATION

Knowledge of an operator or senior operator shall be evaluated by an annual examination over the material of that years training program. Competency of an operator or senior operator shall be evaluated by annual observations of a supervisor or management. Oral questions to evaluate both knowledge and competency may also supplement the evaluation.

A written examination shall be administered to all operators or trainees and shall cover the subjects of the training program for that year. Each subject will be graded on a 100 point basis with an average of 80% as the acceptance criteria. An overall score of less than 65% shall require an immediate evaluation of continued license duties. Proficiency by retraining shall be demonstrated within 4 months or license duties shall be suspended until proficiency is demonstrated. A person that scores between 65%-80% shall retrain as necessary in those areas demonstrated by oral or written exams. The person who writes, grades, and administers the exam shall be a senior operator and shall not be required to take the exam. An accelerated program of less than two years duration will be applied to training of persons for new operator certification.

The reactor supervisor shall periodically evaluate the performance and competency of each certified operator. Evaluation shall include the individuals review of design, procedure and license changes, a review of abnormal and emergency procedures, manipulation of reactor controls, awareness of laboratory conditions and log or checklist entries. A competency evaluation shall be performed annually or as required by operator inactivity of periods greater than four months. Inactivity shall be considered an absence from all activities of reactor operation.

12.4 RECORDS

Documents shall be maintained that record results of qualifications activities [3,4]. Records shall include

tests, scores, qualification activities such as startups or equivalent reactivity changes, performance evaluation, review of design, procedure and license changes, and review of abnormal and emergency procedures.

Chapter 12 References

1. "Standard for Administrative Controls" ANSI/ANS - 15.18 1979.

2. "Selection and Training of Personnel for Research Reactors", ANSI/ANS - 15.4 - 1970 (N380).

3. "Review of Experiments for Research Reactors", ANSI/ANS 15.6 - 1974 (N401).

4. "Records and Reports for Research Reactors", ANSI/ANS - 15.3 - 1974 (N399).

Chapter 13

STARTUP PROGRAM

Startup and testing of the Balcones Research Center TRIGA facility shall be performed by personnel of The University of Texas with consultation of the reactor manufacturer GA Technologies. The University of Texas has accumulated more than 20 years operation experience with a TRIGA reactor prior to the new facility proposal. More than twenty TRIGA type reactors, eleven in the U.S., with power levels of one megawatt or more have been produced by GA Technologies.

Training of university personnel associated with startup activities at the new facility is expected to consist of the relicensing of at least two licensed operators from the current facility that have certified senior operator permits. Training of an additional operator or retraining of a current operator by GA Technologies should occur to provide an effective transfer of the manufacturer's experience to the owner-operator. One or more of the certified operators shall have a bachelors or advanced degree in a field of engineering.

The startup program is to consist of five phases beginning with the storage of nuclear fuel on site to the reporting of observed reactor parameters. At each phase written procedures, check lists or other documents shall be developed for activities or measurements that will have significant importance to safety or operation. Documentation shall include information required by the various programs to be implemented at the facility such as operator qualifications, radiological protection, fire protection and quality assurance plus operating procedures and other requirements of license authorizations. The startup program is to be divided into the following phases:

a.) Storage of fuel and acquisition of components,
b.) Tests of systems before core loading,
c.) Fuel loading and core criticality,
d.) Tests subsequent to core criticality and
e.) Acceptance of core operation.

13.1 STORAGE OF FUEL AND ACQUISITION OF COMPONENTS

Provisions for the storage fuel and components for the reactor facility at the completion of the facility construction shall require the limited implementation of

administrative controls. A license authorization for the possession and storage of special nuclear materials and other radioactive components, such as the cobalt-60 irradiator will be obtained and materials relocated to the facility. Storage of non-radioactive components, storage of other reactor components and instrumentation, and assembly of facility systems will be performed in the initial startup phase.

13.2 TESTS OF SYSTEMS BEFORE CORE LOADING

Facility systems, auxiliary systems and reactor systems or physical parameters shall be tested for the appropriate operating conditions prior to fuel transfer into the reactor core. Fuel may be loaded into the pool during this phase. Systems shall be tested according to designated specifications, when applicable, and acceptable operation shall be established before core loading proceeds. Facility systems to be tested should include security, fire, communication and ventilation systems. Auxiliary systems to be tested should include radiation monitoring, pool coolant, alarm and interlock systems. Reactor systems to be tested will include the instrument and control system and verification of physical specifications for assembly and operation of reactor components. Some systems or components that do not meet specifications and are not required for operation may be deferred for acceptance to a later startup program phase.

13.3 CORE LOAD FOR INITIAL CRITICALITY

Continuous operation of coolant system, insertion of the neutron source, installation of the cobalt-60 irradiator, and movement of fuel into the core will begin the core load startup program phase. Certain verifications of instrumentation and control system functions will be completed before initialization of an approach to critical experiment by standard reciprocal source multiplication factor measurements. Rod worth values shall be estimated from the core loading procedures.

13.4 TESTS SUBSEQUENT TO CORE CRITICALITY

Rod calibration shall be determined by positive period measurements before reactor operation at power levels effected by the power coefficient. Next an intermediate power calibration shall be made and evaluation of the fuel temperature as measured by an instrumented fuel element. Last, the fuel loading of the core should be adjusted for full power operation, and operation of the cooling system verified at power. Any variation of core parameters

significantly different than predicted by calculations or experience shall be resolved during this startup program phase.

13.5 ACCEPTANCE FOR OPERATION

The final startup program phase shall consist of the resolution of all deviations from specifications. Deviations should be resolved as specified for quality assurance or other methods determined to be acceptable. Three months after completion of requisite initial startup and power-escalation testing of the reactor, or nine months after initial criticality, a written report shall be submitted to licensing authorities. The report shall include a summary of the following:

(a) Description of measured values of operating conditions or characteristics obtained and comparison of these values with design predictions or specifications.
(b) Description of major corrective actions taken to obtain satisfactory operation.
(c) Re-evaluation of safety analysis where measured values indicate substantial variance from those values used in the Safety Analysis Report.

Results of the startup program shall become a supplement to this chapter of The University of Texas TRIGA Safety Analysis Report.